

ESL-TH-94/12-01

**AN IMPROVED PROCEDURE FOR DEVELOPING A CALIBRATED
HOURLY SIMULATION MODEL OF AN ELECTRICALLY HEATED AND
COOLED COMMERCIAL BUILDING**

A Thesis

by

TAREK EDMOND BOU-SAADA

Submitted to the Office of Graduate Studies of
Texas A&M University
in partial fulfillment of the requirements for the degree of

MASTER OF SCIENCE

December 1994

Major Subject: Mechanical Engineering

**AN IMPROVED PROCEDURE FOR DEVELOPING A CALIBRATED
HOURLY SIMULATION MODEL OF AN ELECTRICALLY HEATED AND
COOLED COMMERCIAL BUILDING**

A Thesis

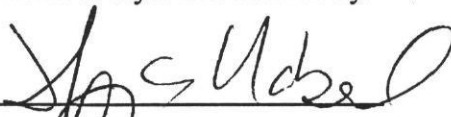
by

TAREK EDMOND BOU-SAADA

Submitted to Texas A&M University
in partial fulfillment of the requirements
for the degree of

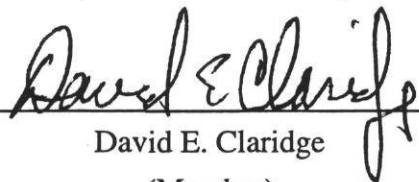
MASTER OF SCIENCE

Approved as to style and content by:



Jeff S. Haberl

(Chair of Committee)



David E. Claridge

(Member)



Namir F. Saman

(Member)



Larry O. Degelman

(Member)



George P. Peterson

(Head of Department)

December 1994

Major Subject: Mechanical Engineering

ABSTRACT

An Improved Procedure for Developing a Calibrated Hourly Simulation Model of an Electrically Heated and Cooled Commercial Building. (December 1994)

Tarek Edmond Bou-Saada, B.S., Texas A&M University

Chair of Advisory Committee: Dr. Jeff S. Haberl

With the increased use of building energy simulation programs, calibration of simulated data to measured data has been recognized as an important factor in substantiating how well the model fits a real building. Model calibration to measured monthly utility data has been utilized for many years. Recently, efforts have reported calibrated models at the hourly level. Most of the previous methods have relied on very simple comparisons including bar charts, monthly percent difference time-series graphs, and x-y scatter plots. A few advanced methods have been proposed as well which include carpet plots and comparative 3-D time-series plots. Unfortunately, at hourly levels of calibration, many of the traditional graphical calibration techniques become overwhelmed with data and suffer from data overlap.

In order to improve upon previously established techniques, this thesis presents new calibration methods including temperature binned box-whisker-mean analysis to improve x-y scatter plots, 24-hour weather-daytype box-whisker-mean graphs to show

hourly temperature-dependent energy use profiles, and 52-week box-whisker-mean plots to display long-term trends. In addition to the graphical calibration techniques, other methods are also used including indoor temperature calibration to improve thermostat schedules and architectural rendering as a means of verifying the building envelope dimensions and shading placement. Several statistical methods are also reviewed for their appropriateness including percent difference, mean bias error (MBE), and the coefficient of variation of the root mean squared error.

Results are presented using a case study building located in Washington, D.C. In the case study building, nine months of hourly whole-building electricity data and site-specific weather data were measured and used with the DOE-2.1D building simulation program to test the new techniques. Use of the new calibration procedures were able to produce a MBE of -0.7% and a CV(RMSE) of 23.1% which compare favorably with the most accurate hourly neural network models.

ACKNOWLEDGEMENTS

I would like to express my gratitude to all those who have granted me support in the pursuit of my degree. Special thanks go to Dr. Jeff Haberl for his patient guidance as committee chair and for providing me the opportunity to work with him from beginning to the end of this thesis. Thanks to Dr. David Claridge for his thoughtful review of my thesis and committee service. Also, I would like to thank Dr. Namir Saman for his careful examination of my thesis while serving on my committee as well as his helpful advice on DOE-2 building modeling. Finally, I appreciate Professor Larry Degelman's analysis as committee member and valuable opinions.

The highest appreciation goes to my parents for their unending support, encouragement, and love throughout my life. The path would have been much rougher without them.

The Energy Systems Laboratory staff deserves a special thank you. Thanks go to Dr. Agami Reddy for helping me develop the solar radiation conversion routine. I deeply appreciate Mr. Mustafa Abbas' and Ms. Anna Baranowski's help with the many hours spent helping me develop the graphical indices for this thesis. The computer staff's help (Mr. Robert Sparks, Mr. Dean Willis, Mr. Ron Chambers, Mr. Chris Cunningham, Mr. Gary Ratterree, Mr. Jeff Rife, Mr. John Steele, and Mr. Mike Johnson), was invaluable.

Support for this project was provided by the United States Department of Energy through Sandia National Laboratory under contract number AK-8010. Mr. E. James Vajda, Mr. Mark Ginsberg, Mr. Roger Hill, and Mr. Richard King deserve special appreciation for making the project possible. Mr. Louis D'Angelo, Mr. Mike Shincovich, and the General Services Administration Project Execution Branch were especially helpful in providing information and are gratefully acknowledged.

TABLE OF CONTENTS

CHAPTER	Page
I. INTRODUCTION.....	1
1.1 Background.....	1
1.2 Purpose and Objective	4
1.2.1 Organization of the Thesis.....	4
II. LITERATURE REVIEW.....	7
2.1 Calibration Time Periods	8
2.2 Guidelines for Calibration.....	13
2.3 Sensitivity Analysis.....	18
2.4 Indoor Temperature Calibration.....	22
2.5 Daytyping.....	24
2.6 Retrofit Evaluation and Verification.....	27
2.7 Summary	34
III. METHODOLOGY.....	39
3.1 Collect and Prepare Hourly Measured Data.....	41
3.1.1 Packing Site-specific Weather Data	42
3.1.2 Hourly Measured Energy Data	44
3.2 The DOE-2 Building Simulation Program.....	45
3.2.1 LOADS Sub-program.....	47

CHAPTER	Page
3.2.2 SYSTEMS Sub-program	49
3.2.3 PLANT Sub-program	51
3.2.4 ECONOMICS Sub-program	52
3.2.5 DOE-2 Required Information	53
3.3 Calibration Tools and Statistical Graphics	58
3.3.1 Architectural Rendering	58
3.3.2 New Calibration Graphing Methods	60
3.3.3 Indoor Temperature Calibration	69
3.3.4 Load Disaggregation From Whole-building Electricity	69
3.3.5 Calibration Calculation Methods.....	70
3.4 Summary	74
IV. CALIBRATING DOE-2 TO THE CASE STUDY BUILDING.....	76
4.1 Case Study Building Description	76
4.2 LOADS Sub-program	83
4.2.1 Building Construction	83
4.2.2 Building Lighting and Equipment	89
4.2.3 Building Schedules.....	93
4.3 Systems Sub-program	93
4.3.1 Building Systems.....	94
4.4 PLANT Sub-program.....	97
4.5 Data Collection and Processing	98

CHAPTER	Page
4.6 Solar Weather Data Formatting	111
4.6.1 Database Solar Radiation Data.....	112
4.6.2 Synthetic Solar Data.....	113
4.6.3 Measured Solar Data Conversion.....	119
4.7 Summary	127
V. APPLICATION OF THE CALIBRATION TECHNIQUES TO THE CASE STUDY BUILDING	129
5.1 Architectural Rendering.....	129
5.1.1 Solar Radiation and Shading Effects.....	134
5.2 Graphical Tuning With Statistical Graphics	136
5.2.1 Traditional Calibration Plotting Techniques	137
5.2.2 Comparative Three-dimensional Surface Calibration Plots	143
5.2.3 Temperature Bin Calibration Plots.....	149
5.2.4 Juxtaposed 52-Week Bin and Three-dimensional Calibration Surface Plots	157
5.2.5 Weather Dependent 24-Hour Daytype Calibration Plots	163
5.3 Indoor Temperature Calibration.....	179
5.4 Load Disaggregation From Whole-building Electricity.....	187
5.4.1 Weekend Representative Day.....	189
5.4.2 Weekday Representative Day.....	192
5.4.3 Heating and Cooling Disaggregation	195
5.5 Statistical Results of the Calibrated Model.....	197

CHAPTER	Page
5.5.1 Model Fine Tuning Progress	198
5.5.2 Monthly Statistical Results.....	203
5.6 Summary	209
VI. USING THE CALIBRATED MODEL TO PREDICT RETROFIT SAVINGS .	211
6.1 Methodology	213
6.2 Energy Efficient Lighting.....	217
6.3 Photovoltaic System.....	218
6.4 Energy Management and Control System.....	219
6.5 Lighting Controls	220
6.6 Envelope Enhancement.....	220
6.7 Clerestory Windows.....	221
6.8 High Efficiency Heat Pumps.....	222
6.9 Solar Domestic Hot Water System	222
6.10 All ECO's Combined.....	223
6.11 Results and Conclusion.....	224
VII. SUMMARY AND RECOMMENDATIONS.....	226
7.1 Summary of the Methodology	226
7.1.1 Architectural Rendering	227
7.1.2 Residual Plots.....	228
7.1.3 Temperature Binned Box-whisker-mean Plots	228
7.1.4 24-Hour Weather Daytype Statistical Plots.....	229

CHAPTER	Page
7.1.5 Comparative Three-dimensional Plots	230
7.1.6 The CV(RMSE) and the MBE Statistical Parameters	230
7.1.7 Comparison of the DOE-2 Simulated and Measured Indoor Temperatures.....	231
7.1.8 Disaggregation of Whole-building Data Into End-use Data.....	232
7.1.9 Use of the Calibrated Simulation to Verify Individual ECO Savings .	233
7.2 Findings From the New Features	234
7.3 Recommendations and Future Directions	235
7.3.1 Calibration Procedure	235
7.3.2 Recommendations to Improve Simulations.....	237
REFERENCES	241
VITA	255

LIST OF TABLES

Table	Page
4.1	Federal Holidays Observed during the 1993 Simulation Period.....83
4.2	Indoor and Outdoor Lighting Summary90
4.3	Interior Equipment and Appliance List.....91
4.4	HVAC Equipment List94
5.1	DOE-2 Models Run with Shading, without Shading, and without Beam Radiation.....135
5.2	Weekday Temperature Bin Calibration Mean Statistics151
5.3	Weekend Temperature Bin Calibration Mean Statistics157
5.4	52-Week Bin Mean Statistics.....160
5.5	Weekday 24-Hour Weather Daytype Calibration Mean Statistics.....166
5.6	Weekend 24-Hour Weather Daytype Calibration Mean Statistics.....177
5.7	Previous DOE-2 Calibration Results198
5.8	DOE-2 Input Deck Changes with Each Run.....200
5.9	Total Period Statistics Summary204
5.10	Weekday Occupied Period Statistics Summary206
5.11	Weekday Unoccupied Period Statistics Summary207
5.12	Weekend Period Statistics Summary208
6.1	Baseline and Standard Energy Conservation Options212
6.2	Comparison of Energy Conservation Options to Predictions214

LIST OF FIGURES

Figure	Page
2.1	33
3.1	46
3.2	48
3.3	50
3.4	52
3.5	53
3.6	54
3.7	57
3.8	59
3.9	61
3.10	63
3.11	65
3.12	67
3.13	68
4.1	77
4.2	78
4.3	80
4.4	81

Figure	Page
4.5	Daycare Center Layout.....82
4.6	Construction Sections85
4.7	Daycare Center.....86
4.8	Sun Angle Calculator and Altitude Measurement Device87
4.9	Photovoltaic and Domestic Hot Water Solar Panels.....92
4.10	Heating, Ventilating, and Air-conditioning System and Controls95
4.11	Measured Ambient Weather Data.....100
4.12	Thermal and Electrical Monitoring Diagrams101
4.13	Forrestal Complex and Logger Locations.....103
4.14	Data and Graphical Processing Flowchart104
4.15a	National Weather Service Weather Data Gathering Process107
4.15b	LoanSTAR Data Processing Sequence108
4.16	Kt and Percent Possible Sunshine Flowchart.....114
4.17	Daily Solar Radiation and Daily Minutes of Sunshine115
4.18	Sky Clearness and Daily Percent Possible Sunshine116
4.19	Hourly Photovoltaic Electricity and Hourly Solar Radiation.....118
4.20	Solar Data Example121
5.1a	Example of a Commercial Building Using Equivalent Thermal Surfaces.....130
5.1b	Zachry Engineering Center (South Corner)130
5.2	Child Development Center DOE-2 Model as Displayed with DrawBDL Software132

Figure	Page
5.3	Time-series Plots of CDC Electricity Use: April - June 1993138
5.4	Time-series Plots of CDC Electricity Use: July - September 1993139
5.5	Time-series Plots of CDC Electricity Use: October - December 1993.....140
5.6	Comparative Three-dimensional Plots.....144
5.7	Rotated Three-dimensional Plots148
5.8	Weekday Temperature Bin Calibration Plots150
5.9	Weekday Occupied Temperature Bin Calibration Plots152
5.10	Weekday Unoccupied Temperature Bin Calibration Plots154
5.11	Weekend Temperature Bin Calibration Plots156
5.12	52-Week Box-whisker-mean Plots158
5.13	Three-dimensional Plots159
5.14	Weekday 24-Hour Weather Daytype Scatter Plot.....164
5.15	Weekday 24-Hour Weather Daytype Box-whisker-mean Plot165
5.16	Weekday Occupied 24-Hour Weather Daytype Scatter Plot170
5.17	Weekday Occupied 24-Hour Weather Daytype Box-whisker-mean Plot171
5.18	Weekday Unoccupied 24-Hour Weather Daytype Scatter Plot172
5.19	Weekday Unoccupied 24-Hour Weather Daytype Box-whisker-mean Plot173
5.20	Weekend 24-Hour Weather Daytype Scatter Plot.....175
5.21	Weekend 24-Hour Weather Daytype Box-whisker-mean Plot176
5.22	Measured Solar Radiation Scatter and Box-whisker-mean Plot.....178

Figure		Page
5.23	Measured Dry Bulb Temperature Scatter and Box-whisker-mean Plot	180
5.24	Indoor Temperature Chart Recorder Locations	182
5.25	Indoor Measured and Simulated Temperatures, Outdoor Temperatures, and Solar Radiation.....	184
5.26	Weekend Measured Data	190
5.27	Weekend DOE-2 Simulated Data	191
5.28	Weekday Measured Data	193
5.29	Weekday DOE-2 Simulated Data	194
5.30	Electricity End-use Comparisom	196
5.31	Calibration Progress with Each Model Modification	199
5.32	Total Period Graphical Summary	205
5.33	Weekday Occupied Period Graphical Summary.....	206
5.34	Weekday Unoccupied Period Graphical Summary.....	207
5.35	Weekend Period Graphical Summary	208
6.1	ECO Savings Comparisons.....	216

CHAPTER I

INTRODUCTION

1.1 Background

Computers and programmable calculators have been used extensively during the past two decades as effective heating, ventilating, and air-conditioning (HVAC) design tools to supplement tedious manual energy calculations. Initially, super mini-computers or mainframe computers were required which restricted access to research organizations supported by public funding, large consulting firms and manufacturers, and a relatively few academic research institutions as a result of large expenses incurred for hardware, and the limited availability of both software and computer personnel. As computing technology has become affordable, engineers and architects have begun to take advantage of hourly desktop personal computer (PC) programs that can inexpensively and quickly perform load calculations (ASHRAE 1991).

With the advancements made in computer technology, shifting the main focus from simple hand calculations to computer utilization in the building energy field was the next logical step. Computers provide engineers and architects access to more powerful methods in completing tedious load calculations which in most cases would otherwise be impossible to complete and still be cost effective. A dramatic

advancement in the HVAC field was the development of various building simulation packages designed to calculate dynamic thermal loads. Initially, these programs were used as design and research tools to replace tedious hand calculations. Eventually, the simulation packages began to be used for retrofit evaluation in existing buildings and required calibration to measured data. Modeling programs such as DOE-2 (LBL 1989), BLAST (BLAST 1993), and micro-AXCESS (EPRI 1992) have been specifically developed to perform annual load calculations. They have evolved into sophisticated programs that can accurately model dynamic thermal loads and simulate multiple energy conservation options for an individual building by performing parametric studies of individual components.

At first, DOE-2, the main simulation tool sponsored by the United States Department of Energy (USDOE), was used primarily for design simulations of new construction. Simulation programs also began to be used to evaluate the impact of energy conservation retrofits to an existing building. This was accomplished by developing a simulation model of an existing building and "tuning" the simulation inputs until it adequately represented the existing building. The effects of the retrofits were then calculated by changing specific simulation input parameters that correspond to the intended retrofit. Savings were then calculated by subtracting the simulation results from the baseline simulation and reporting the results as savings.

Calibrating computer models to actual metered data is not a new practice. Various methods have been proposed for "tuning" the simulation programs to measured data from an existing building. Some researchers and engineers have attempted to compile "how to" manuals and methods in order to simplify this task; however, the end result typically falls short of a complete procedure (Hsieh 1988; Kaplan et al. 1992; Bronson et al. 1992). To date, no consensus standards have been published on calibration procedures and methods that can generically be used on a wide variety of buildings. Historically, actual calibration has been an art form that inevitably relies heavily on user knowledge, past experience, engineering judgment, and trial and error.

Calibrating a model to measured daily or hourly data can be a time consuming task in any building computer simulation project. Once the user is certain that differences between the simulation and actual data are within acceptable tolerances (typically user accuracy for electricity is approximately 5% per month), the model is considered "calibrated." The major problem with reporting simulation accuracy rests with the calculation procedures which vary with different computer simulation programs. Typically, when a model is established as being calibrated, the author does not reveal the techniques used. Hourly or daily error values are seldomly reported. Even in cases when error estimates are presented, the methods used in obtaining the comparisons are not.

1.2 Purpose and Objective

This research develops new procedures for calibrating simulation programs including architectural rendering and new techniques for non-weather dependent and weather dependent calibrations, and interior temperature calibration. The research also includes new techniques for estimating end-use data when only whole-building data are available.

1.2.1 Organization of the Thesis

This thesis is organized in the following manner: first, a literature review of past work and related work is presented to provide a detailed background of previous calibrated simulation work as well as a stepping stone for this thesis. Previous works are discussed and analyzed to provide a basis for evaluating the significance of the current calibration procedures.

A calibration methodology in this thesis includes the data collection process, the site-specific weather tape preparation procedure, an overall framework of the DOE-2 simulation procedure, and the information required to successfully model a building with DOE-2. The methodology then proceeds to describe the new calibration tools developed for this thesis. The new tools developed for this thesis include the use of architectural rendering, indoor temperature comparisons, and statistical plots including temperature-binned box-whisker-mean graphs, 52-week binned time-series plots, and 24-hour binned box-whisker-mean daytype graphs.

Next, the work for this thesis is thoroughly demonstrated using a case study 8,100 sq. ft. daycare building located in Washington, D.C. The building is described in detail including location, surroundings, and construction. Each DOE-2 sub-program description is combined with its corresponding case study building components. For example, the LOADS sub-program is linked with the case study building construction and internal loads. The SYSTEM sub-program is described by the secondary HVAC details, and the PLANT sub-program is illustrated with the building's primary HVAC systems. This chapter also details the special procedures and correlations developed to convert the solar radiation data measured at South-facing 18° tilt into global horizontal solar radiation and then split into beam and diffuse radiation (Bronson 1992) before it was added to a weather tape. Alternative solar data sources are also reviewed as possible substitutes for the measured data and a final selection rationale presented.

The resultant calibrated simulation is then discussed in the next chapter as it applies to the case study building. This chapter illustrates the use of each of the calibration techniques with greater detail and discusses resulting ramifications. The effectiveness of the architectural rendering software is discussed as well as indoor temperature comparisons. An end-use electricity estimation from a whole-building signal is also presented for the case study building. Characteristics of each new

method and previously established calibration methods are reported so that the reader will have a clear understanding of all the developments introduced in this thesis.

The next chapter deals with using DOE-2 as an energy conservation retrofit verification tool. In this chapter the case study building is simulated with and without energy saving features including: energy efficient lighting, energy efficient heat pumps, a photovoltaic system, envelope measures, and a solar domestic water heating system. To accomplish this, a DOE-2 baseline model was calibrated to the measured hourly data and compared to a building model constructed with standard features (i.e. without the retrofits). Annual energy savings were then calculated and compared to the architect's original estimates.

Finally, the concluding chapter summarizes all of the improved calibration developments introduced in this thesis. It then recommends techniques that may be implemented in prospective research and offers advice concerning future directions.

CHAPTER II

LITERATURE REVIEW

This literature review summarizes research accomplishments in the field of building energy computer simulation and calibration guidelines. Various researchers have advanced the field of calibrated building energy simulation. The most popular method thus far has been to calibrate a simulation to easily obtainable monthly utility billing data (Diamond and Hunn 1981; Haberl and Claridge 1985; McLain et al. 1993). Calibrations to daily data have also been reported, but not as often (Hsieh et al. 1988; Hinchey 1991). Hourly data is by far the most difficult to calibrate against, but yields the most accurate model (Bronson 1992).

Until recently, a limited number of reports utilized hourly calibration with the most progress being made by long-term, funded research projects in the academic field and research laboratories. The academic institutions include Texas A&M University (Torres-Nunci 1989; Hinchey 1991; Bronson 1992), the University of Texas at Austin (Reddy 1993), Princeton University (Hsieh 1988), and The University of Colorado at Boulder (Haberl 1988a). The research laboratories involve Lawrence Berkeley Laboratory (LBL) (Diamond et al. 1992), Los Alamos National Laboratory (LANL) (Diamond and Hunn 1981), Oak Ridge National Laboratory (ORNL) (McLain et al. 1993), Bonneville Power Administration (BPA) (Kaplan et al. 1990a), Pacific Northwest Laboratory (PNL) (Schliesing and Crawley 1990), and the National

Renewable Energy Laboratory¹ (NREL) (Judkoff 1988). Limited research and publications were contributed by private organizations (Bahel et al. 1989).

Internationally funded efforts include those funded by the International Energy Association (IEA) (Clarke et al. 1993).

This literature on calibrated building simulation research studies is arranged in the following topical areas: papers involving calibration time periods; guidelines and methods for calibrating a computer model; simulations involving sensitivity analysis; calibrations including indoor zone temperature; calibrations using different forms of daytyping; and retrofit evaluations and verifications. The majority of the reports were published in such journals as the ASHRAE Transactions, the ACEEE proceedings, the ASME Journal, the ASHRAE Journal, the IBPSA proceedings, and several academic theses.

2.1 Calibration Time Periods

The first section of this review discusses varying time periods for performing calibrations. Kaplan et al. (1990a) pursued the confirmation of energy conservation options by proposing short-term building monitoring and calibrating to a DOE-2 model. Subbarao et al. (1990) and Balcomb et al. (1993; 1994) also proposed short-term monitoring. However, these studies were geared to the STEM/PSTAR method

¹ Previously the Solar Energy Research Institute (SERI).

which used computer simulation to establish a base-case run and PSTAR as a calibrated follow-up. STEM and PSTAR are described with more detail later in this section. Koran et al. (1992) analyzed the effects of DOE-2 simulations using short-term monitoring and long-term monitoring.

One well documented program, the Energy Edge Program (Diamond et al. 1992), was developed to determine the effectiveness and feasibility of energy conservation options in the Pacific Northwest (Kaplan et al. 1990a). This study used calibrated DOE-2.1C simulations to measure retrofit savings by varying parameters in the calibrated simulation program. According to Kaplan, long-term tests involve large expenses which require installation of a logger along with electrical and thermal monitoring of selected equipment. Therefore, the short-term test method provides a cost efficient alternative to analyzing building energy performance. An important point to note here is that three calibration periods were used to tune the models: a cold weather month, a hot weather month, and a moderate weather month. Kaplan proposed that two periods, one short cold weather period and one short hot weather tuning period, were sufficient to meet the needs intended to calibrate models since the heating, ventilating, and air conditioning (HVAC) operation schedules were more predictable when weather patterns are more stable.

Site weather data and monitored consumption data recorded by Energy Edge stations were used extensively to verify the calibrated model. Tuning periods were

chosen according to data completeness, accuracy, and fan operating time. Once a model was produced, Kaplan used numerous iterations until HVAC end-use peak electric consumption was within a monthly percent difference tolerance. For period total and profile, the results were $\pm 15\%$ and $\pm 25\%$ respectively. One of the most significant aspects of this study is that the authors made a thoughtful effort to publish a step-by-step guide to calibrating a generic building. Adjustments to the model with each iteration were documented and effects were reported in graphical form. Another significant contribution to the literature that this study made was that small buildings are not necessarily simple buildings to calibrate. This is due to inconsistent daily schedules causing changes in equipment operation. The schedule changes tend to have a profound impact on end-use data in small buildings. Since most HVAC systems in small buildings are not controlled by an energy management and control system (EMCS) but rather locally controlled by the occupants via thermostats, energy use predictability becomes difficult.

Although a good attempt was made, Kaplan did not publish a precise series of tuning steps applicable to generic models. According to Kaplan, energy use during a moderate weather month was more difficult to accurately predict since either heating or cooling may be used from day-to-day depending on changing weather conditions. A final conclusion was the recommendation of a need for more monitored data in order to achieve a higher degree of accuracy in the measurement of energy conservation options (ECO) savings. The current research improves on Kaplan's work

by using long-term hourly data including the three weather periods used by Kaplan with a short moderate weather period being used for developing schedules. It also improves calibration techniques in graphical form by documenting changes to the model and providing improved comparisons.

A second study using short-term data was performed as part of the Short Term Energy Monitoring (STEM) method (Subbarao et al. 1990; Balcomb et al. 1993; 1994). The STEM method begins with an initial hourly simulation of a building that is based on audit findings. The model is then calibrated based on short-term data by extensively monitoring a building for three days to represent the building in an "as-built" state. STEM calculates all heat flows by using a frequency domain analysis that identifies primary and secondary terms and reconciles the output to selected measured data. The Primary and Secondary Terms Analysis and Reconciliation (PSTAR) computes hourly energy balance for a zone to determine predefined primary and secondary term adjustments. Primary terms (energy flow) are typically calculated by an audit description. They are then renormalized and used for calibration by their corresponding secondary parameters (correction factors) to achieve an energy balance.

The importance of PSTAR's capabilities is that it allows one to separately determine the building loss coefficient, the building mass, and the solar gain area without one factor interfering with the other. By measuring heat flows during

consecutive 24-hour periods, PSTAR allows a user to isolate terms since different heat flows are dominant during different parts of the day.

The PSTAR analysis does not provide a means of detecting differences in daily energy use patterns nor does it easily allow for the simulation of a building's performance using different HVAC systems. A simulation program is used after normalization to extrapolate data if seasonal infiltration dependency, ground heat flow, and solar gains are of interest. Since PSTAR is based on a frequency domain analysis and DOE-2 relies on a transfer function analysis, it is difficult to compare both to the same measured data. While a limited amount of short-term time periods were used in certain areas of the simulation performed for this thesis, no significant portions of the STEM or PSTAR methods were implemented.

In a third study, Koran et al. (1992) compared short-term calibration tests to Monthly Consumption Tuning (MCT) tests for two small credit union buildings using DOE-2.1C. The short-term test applied the STEM method of monitoring specific test points to determine building thermal conductance, building thermal capacitance, building solar gains, infiltration, and HVAC efficiency. The short-term test calibration was then compared to a long-term MCT method based on both monthly data and seasonal trends. A limited amount of hourly data including end-use energy data, zone temperatures, and fan duty cycles were used to determine hourly schedules and daytypes. The resulting difference between twelve monthly HVAC values using the

short- and long-term calibration methods was within 11% which was consistent with the preset tolerance.

While initially overshadowed by the small 11% difference, it was found that a considerable difference existed between short- and long-term monitoring when investigating their respective model inputs. The model inputs included factors such as building conductance, infiltration, and supply air heat loss. Only then do the two methods reveal discrepancies when determining system performance and annual energy consumption of individual ECOs.

The importance of Koran's study demonstrates the problems associated with using short-term tuning periods to simulate long-term models. According to the authors, weather dependent variations are difficult to predict on an hourly level. Koran recommends that certain short-term hourly data be investigated in greater detail to compare different model assumptions. The information from Koran's publication that benefits this thesis includes using long-term hourly data to calibrate a more realistic weather dependent simulation.

2.2 Guidelines for Calibration

This section describes the limited simulation guidelines that have been published. The studies included in this section are the most extensive to date in the field of calibrated simulation programs surveyed in the field of calibrated simulation

programs and include works by Hsieh et al. (1989), Kaplan et al. (1992), Carroll et al. (1993), and Clarke et al. (1993). Hsieh's study is also included in Section 2.3 because it also contributed heavily to the sensitivity analysis. Hsieh et al. (1989) and Kaplan et al. (1992) published specific details for calibrating DOE-2 which may also be used for other simulation programs. Carroll et al. (1993) presented a method of computer energy analysis that utilized interactive pull-down menus and an automated iterative calibration method. Finally, the PASSYS method, demonstrated by Clarke et al. (1993), utilized an experimental test cell to develop a methodology for calibration with empirical data and a residual analysis.

Hsieh et al. (1989) published a study that included specific calibration procedures which significantly contribute to improving DOE-2 simulations. This study compared DOE-2.1C design simulations with measured data from two buildings located in central New Jersey. The analysis showed that the design runs under-predicted actual building energy use by a margin of 3 to 1. Because this was such a large difference, specific causes for the under-prediction were sought in order to improve future calibrations. These causes may be viewed as a procedure to calibrate DOE-2 by placing a greater emphasis on eliminating them as potential sources of error.

Occupant use of lighting and equipment contributed to the highest amount of error (45% and 56% for two buildings). The second highest source of error was

determined to be inaccurate HVAC operation schedule settings. The use of DOE-2 default values further added to simulation error when compared to measured data since actual system variables and default values did not match. Occupant effects were the major sources of discrepancy between the measured and simulated data for this thesis as well. Since this thesis presents improved methods to calibrate DOE-2 to measured data, focusing on the variables shown in Hsieh's procedure helped reduce a large amount of error.

Another important aspect of Kaplan's work involved a research project that took place under the Energy Edge program which pursued a publication of guidelines and methods for modeling buildings (Kaplan et al. 1992). The importance of Kaplan's guideline approach extends further than most publications by presenting more details to aid DOE-2 users in calibrating a model. The guidelines included computer simulation capabilities, simulation reliability improvement, differences between predicted and actual ECO savings, and a description of how modeling errors can be avoided by concentrating on inputs. Computer modeling was found to be most appropriate when different internal systems interact with the HVAC system since simple hand calculations cannot be used in these situations.

Kaplan's guidelines are targeted at first time users and point out obvious problems to look for when choosing to simulate a building. Certain specific details such as zoning, system selection and controls, and error checking are covered. In

order to improve upon Kaplan's guidelines, this thesis will emphasize new methods such as statistical binned box-whisker-mean plots, 24-hour weather daytype box-whisker-mean plots, and load disaggregation from a whole-building electricity signal to show how well a simulation is calibrated using a case study approach.

The Retrofit Energy Savings Estimation Model (RESEM) is an approach that uses numerical optimization methods to minimize a function of individually weighted differential terms (Carroll et al. 1993). Implementation is carried out by automating building computer simulations to match monthly utility data. The importance of RESEM is that it presents iterative mathematical adjustments to a model that are continuously calculated and fed back into the original simulation. Carroll's study gives a brief description of an optimization technique and mostly describes an interactive computer program (RESEM) that allows a user to easily change different model variables and iterate until an acceptable monthly solution is reached.

RESEM begins by specifying a prototypical building modeled after an actual building. Numerous default values are used such as building construction components, occupancy schedules, and equipment schedules. After a building is modeled, an initial simulation pass is made and the results are reported. From the results, the user may then choose and adjust any number of "tuning characteristics" including variables such as window area, infiltration rates, chiller COP, and occupancy levels. Each primary tuning characteristic has a list of secondary parameters

associated with it that are automatically adjusted during tuning. The user is then prompted by the program to decide whether the latest tuning pass is within acceptable tolerances or continue with another iteration. The procedure may be repeated until a satisfactory goal is achieved. Although a RESEM-like optimization can be used with DOE-2 and other simulation programs, very little of this process can be directly adapted to this thesis because RESEM is not an 8,760 hourly simulation program, but rather a monthly program based on the modified bin method.

In another study on guidelines and methods, the PASSYS project demonstrated a model validation and calibration technique based on empirical adjustments (Clarke et al. 1993). An IEA sponsored test cell was used as the basis for studying the development of a methodology for model validation, calibration, and scaling/replication. The cell was comprised of little chambers located outdoors with a window, a heating and cooling system, and data logging equipment. Clarke's method relies on simulating a building and following up with a residual analysis to refine the calibration. Residual analysis is most helpful when a need exists for pinpointing over- and under-simulation of long-term trends.

The important point that stands out in this investigation is that PASSYS makes a strong effort to empirically provide a logical outline for calibrating a model that is useful for a variety of simulations including DOE-2. The residual analysis used in Clarke's study is based on statistical indices following a methodology proposed by

Palomo et al. (1991). It used the autocorrelation function and power spectrum to define a residual mean and variance allowing a computer simulation user to identify general over- or under-estimation trends. This study contributes significantly to the need and use of a residual analysis and a goodness-of-fit analysis utilizing a coefficient of variation-root mean square error (CV(RMSE)) and mean bias error (MBE). These statistical indices are discussed in Chapter III.

2.3 Sensitivity Analysis

Another method useful to DOE-2 calibration incorporates a sensitivity analysis. A sensitivity analysis helps determine which building and HVAC system components have the greatest influence on energy use. To identify certain characteristics, a general model is first run to establish a base case reference point. Input values on both extreme ends of each parameter scale are then assigned for certain relevant DOE-2 inputs and a simulation is run for each. The first study included in this section was published by Hsieh et al. (1989) in order to determine why an initial simulation was not accurate. Hsieh's guide for calibrating DOE-2 included a detailed sensitivity analysis. Mahone et al. (1992) utilized a DOE-2 sensitivity analysis to develop energy standards for different climatic regions. The final publication included in this section was presented by Griffiths and Anderson (1994). Their analysis applied DOE-2 to rank the input values in order from the most sensitive to the least sensitive in an office building and a grocery store.

A procedure by Hsieh et al. (1989) that includes a comprehensive guide for calibrating a DOE-2 simulation, shown in Section 2.2, certainly can also be considered a sensitivity analysis. The significance of this work extends far beyond most publications by providing detailed explanations of certain DOE-2 operations and a calibration methodology. In an attempt to eliminate as many unknown elements as possible, the format embodied three broad categories based on the decreasing energy impacts on a building. The first category included building tenant energy consumption while the second contained HVAC schedules. The last category was related to HVAC equipment and building shell performance. Hsieh et al. also showed that it was important to measure such factors as occupant use of lights and equipment, HVAC schedules and thermostat settings, HVAC and building shell performance, and fan curves.

In Hsieh's study it was discovered that tenant use was the most difficult to simulate due to unpredictable daily habits; for example opening or closing window blinds which have a direct impact on solar gains, or the inconsistent use of lights and office equipment. Tenant influence was also observed in Kaplan et al. (1990a) as reported in Section 2.1. Hsieh proposed a method to overcome this problem by direct measurement of electricity consumption in offices for one week to develop a daily energy use pattern or daytype. The publication lists a useful specific guide for future calibration work and important factors to consider when utilizing DOE-2 models. Several aspects of Hsieh's et al. publication were encountered during this research

such as tenant unpredictability and inconsistent HVAC schedules. Details such as fan curves and chiller performance were not included in this thesis, however, different methods of statistically presenting the calibration in graphical form are introduced in the following chapters.

Another sensitivity analysis was performed by Mahone et al. (1992) for the California Energy Commission (CEC). The CEC used the results to develop nonresidential building energy standards for 1991. Using five case study buildings in different climatic regions, the analysis considered the effects of varying design illumination, thermostat ramp, sizing ratios, economizers, and internal heat gains using DOE-2.1D. The intent was to determine the effects of the variable sensitivities on annual energy consumption estimates. Mahone et al. indicates by way of graphical results that it is difficult to establish across-the-board standards for DOE-2 inputs. Since climatic regions have a definite impact on certain system functions such as the use of economizers, it is difficult to predict how one input will react in one climate versus the other. A conclusion that may be made based on reviewing this study is that it is possible to establish standards to be used for typical climate zones. The results of Mahone's analysis as well as this thesis are useful to future simulation by cautioning users to be wary of using blind sensitivity information unless the conditions being tested and simulated are similar to the published conditions.

Griffiths and Anderson (1994) performed a sensitivity analysis on a 34,000 square foot commercial office building and a 26,000 square foot grocery store building using DOE-2.1D. The most sensitive input values were varied when initial gross model adjustment was needed while the less sensitive values were useful later for model fine tuning. The significant aspect of their analysis lies in determining which DOE-2 input values have the higher impact on simulated energy use. In the grocery store, the refrigeration auxiliary capacity and the refrigeration zone load had the highest impact while the roof insulation and defrost control had the lowest. The variables with the highest sensitivity in the office building were the equipment capacity and lighting capacity while the variables with the lowest were infiltration rate and glazing orientation. Sensitivities similar to the office building were observed during the calibration procedure used for this thesis. Specifically, it was found that lighting schedules were the most sensitive.

The results of the Griffiths and Anderson study were used to help guide calibration efforts for this thesis by realizing which input variables warranted more attention. Another important use for input variable sensitivity analysis may be applied to individual building component monitoring for future studies. With the knowledge of which input variables are the most sensitive, the user may then proceed to cost effectively monitor the most significant components. Since monitoring and simulation budgets typically govern project directions, the results from sensitivity analysis studies definitely should not be ignored.

2.4 Indoor Temperature Calibration

Most DOE-2 calibration studies typically only consider monthly simulated data. Very few of these previous publications have elected to do hourly calibrations and even fewer have attempted to match indoor DOE-2 simulated temperatures to measured indoor temperatures. In the first study, Hsieh (1988) compared DOE-2 predicted temperatures with measured temperatures in order to help identify the discrepancy encountered between the simulation and the actual building energy use data. Clarke et al. (1993) predicted indoor temperature with a simulation model under the PASSYS program. Finally, Haberl and Komor (1990) utilized minimum and maximum zone temperatures to verify HVAC system operation.

In the next category proposed here for calibration, Hsieh (1988) considered indoor temperature calibrations by recording indoor temperatures and comparing to DOE-2 simulated temperatures. In Hsieh's study, simulated temperatures reported by DOE-2 SYSTEM outputs during a particular summer week were consistently higher during morning HVAC operation and lower during afternoon and evening shut-down when compared directly to measured temperatures. Hsieh noted that more research was needed in order to provide an adequate explanation. During one winter night setback period, DOE-2 simulated temperatures oscillated frequently while daytime DOE-2 temperatures were in phase with measured data but over-predicted actual data. This same effect was also observed in this thesis.

A positive note may be added here concerning the difference between using measured interior temperatures to set the DOE-2 thermostat rather than purely specifying an average thermostat setpoint. When Hsieh used measured thermostat values in the input file instead of using an average setpoint, the simulation produced an improved comparison. Based on Hsieh's finding, using the measured data provided an 11% better monthly difference in heating energy. This reaffirms the conclusion presented earlier in Hsieh et al. (1989) to eliminate as many unknown variables as possible by including measured values in the input file.

One may conclude from this study that it is more important for the simulated temperature data to be in phase with measured temperature data than having the amplitudes match. Depending on how well a building is calibrated, indoor temperature comparisons may in some cases agree and in some cases totally disagree despite having favorable energy end-use comparisons. An indoor temperature analysis was used for this research and is detailed in Chapter V.

As part of the PASSYS project introduced earlier in Section 2.2, Clarke et al. (1993) also performed comparisons of measured versus simulated indoor temperature. To judge the fit of the predicted temperature data, Clarke et al. utilized a differential sensitivity analysis (DSA) and a Monte Carlo sensitivity analysis (MCSA) to obtain uncertainty bands. Although Clarke's method does not incorporate the use of the

DOE-2 program, it is important to note that the results were slightly affected by ambient weather conditions and predicted the temperatures with good accuracy nonetheless. A similar problem occurred with the procedure used in this thesis which is described further in Section 5.3.

In a study to improve energy audits, Haberl and Komor (1990) analyzed a New Jersey mall where measured minimum and maximum zone temperatures were used as an indication of HVAC operation. The purpose of their study was to investigate how to improve an energy audit with selected metered data. While the buildings in the mall were not simulated with DOE-2, the analysis was important for correlating zone temperatures to HVAC operation and contributed significantly to the understanding of weather dependencies in utility billing data. Their study showed that the information from daily readings of min-max thermometers in each store could be used to determine if cooling or heating systems were in use. In the current research measured zone temperatures were used to compare with simulated zone temperatures to confirm if HVAC systems were being turned on and off at similar times.

2.5 Daytyping

Daytyping has become an important aspect of simulation for developing lighting and equipment schedules specified in the DOE-2 input file. Unless an audit reveals that building operations are precisely the same on a long-term basis, an alternative scheduling method must be applied. The daytyping techniques used today

vary from complex statistical data analysis to simple data sorting. This section reviews methods proposed in three publications and includes a diurnal load shape methodology introduced by Katipamula and Haberl (1991), a principle component and cluster analysis by Hadley (1993), and a regression analysis by Akbari et al. (1988).

Katipamula and Haberl (1991), as part of the Texas LoanSTAR Program described in the next section, proposed a simple daytyping methodology to identify diurnal load shapes using monitored end-use data. Their method entailed the sorting of data into weekday and weekend 24-hour profiles, comparing and grouping each point by a predetermined standard deviation limit, and developing load profiles. The resulting load shapes could then be used in DOE-2 equipment and occupancy schedules for calibration, for example in Bronson (1992). Similar daytypes were developed for this research; however, a refined method was developed that utilizes more appropriate statistical measures including mean, median, and inter-quartile range comparison. It is shown in Chapter V that the inter-quartile range is not affected by the magnitude of the mean as were Bronson's load shapes which were based on calculated hourly standard deviations proposed by Katipamula and Haberl (1991).

Another daytyping procedure proposed a combination of daytyping and data grouping as a useful method to assist DOE-2 users in developing equipment and occupancy schedules. In one study, Hadley (1993) used a principle component analysis and cluster analysis to group typical National Weather Service (NWS)

weather data into daytypes or "representative days." Although Hadley's work did not directly involve simulation, the weather-daytypes method that Hadley developed is instructive. This thesis relates to Hadley's work by grouping days with similar characteristics (cold, moderate, and hot temperatures) into daytypes segregated into relatively accurate 24-hour system operation schedules (heating only mode, no heating/no cooling mode, and cooling only mode). Although Hadley's technique has been found to be useful in developing statistically robust weather daytypes, the current research does not focus on the use of principle component analysis which was originally reported in Hadley and Tomich (1986). Instead, it sorts the data into the weather daytypes by temperature.

Another method that used weather dependent daytypes was described by Akbari et al. (1988) and includes an algorithm to disaggregate commercial whole-building hourly electricity use into end-use data. This procedure applied statistical attributes of measured hourly whole-building data and correlated them to weather dependence. The methodology made use of hourly electricity load regressions against outdoor dry bulb temperature. The regression equations segregate the data into weather dependent loads such as the HVAC system requirements and non-weather dependent loads including lighting and equipment loads. Since the weather dependent loads were statistically identified, the non-weather dependent loads could then be distinguished by incorporating information from energy audits into the simulation.

Once a proportion of the whole-building data was assigned to each variable, the simulated total was then compared to the measured data and adjusted as necessary.

The end-use results were plotted on weather dependent daytype graphs, one for a winter profile, and one for a summer profile. The importance of this work can be immediately realized when costs of extensively monitoring a wide array of building energy consuming components is prohibitive. A similar situation was encountered in simulating the DOE-2 model for this thesis whereby only a whole-building signal was available. Chapter V describes the weather dependent daytype plots and whole-building data disaggregation methodology. Three daytype profiles were developed for this thesis which not only provide a heating and cooling period profile, but also a non-heating/non-cooling period profile. The daytype plots are further improved by using a box-whisker-mean format, unlike the averaged time-series format used by Akbari et al. (1988).

2.6 Retrofit Evaluation and Verification

In an important follow-up to building systems retrofits, several researchers have performed DOE-2 evaluations to justify and verify building operations. Included among the many studies is a study by Reichmuth and Fish (1994) who simulated a building with DOE-2 to verify HVAC, lighting, and glazing retrofits. Torres-Nunci (1989) and Hinchey (1991) also used DOE-2 to model a large commercial building for the purpose of verifying retrofit savings; each with a higher level of understanding.

Bronson (1992), as described later in this section with more detail, used DOE-2 to evaluate extensive parametric studies of retrofits on a large commercial building.

In an analysis to verify ECO savings in a 311,000 square foot office building located in the Pacific Northwest, Reichmuth and Fish (1994) used DOE-2 to model the building both with and without an upgraded HVAC system, lighting retrofit, and energy efficient glazing. An extensive monitoring and control system was installed including the addition of more than 3,500 digital sensors. It is important to note from this study that a post-retrofit simulation model was calibrated to measured data and a pre-retrofit model was extrapolated based on standard building systems. A similar methodology was used for this thesis on a building that was built with the energy efficient features installed. To accomplish the comparison, a model was calibrated to the existing "efficient" building and then changed to inefficient building systems that are typically installed as "standard" features. Details on the methodology and ECO specifications can be found in Chapter VI.

In the Texas LoanSTAR Program, retrofit savings are measured primarily with hourly pre-post whole-building thermal and electricity data often by submetering the motor control center. Data acquisition systems installed in the buildings provide a method of verifying savings and improving energy conservation retrofits (Claridge et al. 1991). The LoanSTAR program reports data collected on an hourly basis in weekly time-series plots for each channel of data and cross-plots as a function of

ambient temperature data to ensure data quality (Claridge et al. 1992). In the 24 buildings reporting savings as of May 1993, it was found that daily empirical linear, change-point linear, and multi-variable regression models were adequate at describing the building energy use in 75% of the cases (Turner et al. 1993). In certain buildings where limited pre-retrofit data exist, empirical models were not used. In these cases, alternative methods that include calibrated simulation models were used to calculate savings.

The first LoanSTAR study to verify retrofit savings with DOE-2 was a simulation of a laboratory/classroom building. Several subsequent studies made use of the same building, each progressing to a higher level of understanding of more efficient techniques to calibrate the DOE-2 simulation model (Torres-Nunci 1989; Hinchey 1991; Bronson 1992). In the first study of the building Torres-Nunci (1989) used ten weeks of measured hourly energy consumption data. Routines were developed to more efficiently extract hourly data from the DOE-2.1C reports into a usable format for analysis. This simple study made extensive use of two-dimensional and three-dimensional time-series, and scatter plots as a means of visually guiding the DOE-2 calibration.

In the second LoanSTAR DOE-2 study, Hinchey (1991) improved on Torres-Nunci's calibration by using three-dimensional time-series plots showing "residuals", or differences between hourly monitored data and simulated data. Three-dimensional

plots had previously been shown to be effective tools in displaying large amounts of hourly data in a simple and concise plot (Haberl et al. 1988b; Haberl and Vajda 1988c; Haberl and Komor 1990). Haberl et al. (1988b) was the first to use the three-dimensional plots on DOE-2 data. Haberl and Vajda (1988c) utilized three-dimensional plots to segregate whole-building electricity data into weekday, weekend, and occupied/unoccupied periods. Haberl and Komor (1990) compared measured data to a base-level model by plotting three-dimensional positive-only residuals.

Hinchey (1991) showed that problems with simulation inputs and assumptions usually can be determined more efficiently by comparing side-by-side three-dimensional plots of the entire dataset. Hourly, daily, and monthly graphs were also plotted side-by-side to illustrate the difference in simulation methodology and the resulting accuracy ultimately achievable. This, the most significant part of Hinchey's work demonstrated that the analysis of monthly data cannot typically identify hourly data bias. Daily data was shown to be the most useful for quick comparisons because it provided more data points than monthly data, but did not detect hourly schedule variations. For this case, only hourly data, with a finer resolution, displayed enough data and showed that, perhaps, the model might not fit the measured data as well as the monthly and even daily plots would indicate. In addition, Hinchey used a larger six month dataset to model the building and compare the impact of using a single thermal zone with multiple thermal zones. Hinchey showed that simulations of large internally

load driven commercial buildings show less sensitivity than smaller buildings to varying numbers of thermal zones.

Bronson (1992) continued the study of the engineering center and substantially modified the calibrated model to include several parametric studies of retrofits. Bronson's work was the first at Texas A&M to use site-monitored weather data that was overlaid, or packed, onto a Test Reference Year (TRY) weather file (TRY 1983). TRY was used instead of a Typical Meteorological Year (TMY) weather tape (TMY 1988) because TMY weather files are recorded in solar time whereas TRY files are recorded in standard time. This can cause a problem with scheduling when local weather data are recorded using standard time because the longitude and equation of time need to be included to match DOE-2 TMY weather. A substantial amount of time was dedicated in attempting to overlay recorded weather data onto a TMY file without success due the preprocessing routine's inability in passing data into DOE-2 in a usable format. Since both TRY and TMY weather files are based on long-term average data, the importance of using site monitored weather data can easily be seen especially when severe weather is part of the measurement period as was the case during the winter used in Bronson's model.

Along with packing site-monitored weather data into TRY format, the most significant part of Bronson's work included the development of more efficient routines to extract hourly data from DOE-2 reports using the AWK programming language

(FSF 1989; Dumortier 1989). Furthermore, two-dimensional and comparative three-dimensional residual plots were presented allowing in-depth calibration data analysis. Calibration of non-weather dependent loads employed a statistical daytyping method (Katipamula and Haberl 1991) and comparative three-dimensional graphs (Hinchey 1991). Calibration of weather dependent loads against measured data was done by trial and error. In addition, Bronson developed "carpet plots", a series of nine comprehensive graphs on one page, to display the effects of different ambient weather conditions on the hourly end-use energy consumption for measured data, simulated data, and daytypes. Figure 2.1 shows an example of the carpet plot. This research makes use of several routines developed by Hinchey and Bronson and develops new techniques for visualizing both the simulated and measured data.

In an analysis similar to Bronson's, Haberl et al. (1994) demonstrated the value of packing site-specific data onto a TRY weather tape. A DOE-2 simulation using packed TRY data was compared to a simulation performed with a standard TMY weather tape and actual measured energy use data. The packed TRY weather tape improved the cooling energy use prediction over TMY from +12.4% to +9.0% and improved the peak cooling load prediction from +29.4% to +21.0%. A few problems were evident in the heating load comparison due to the manner in which the building

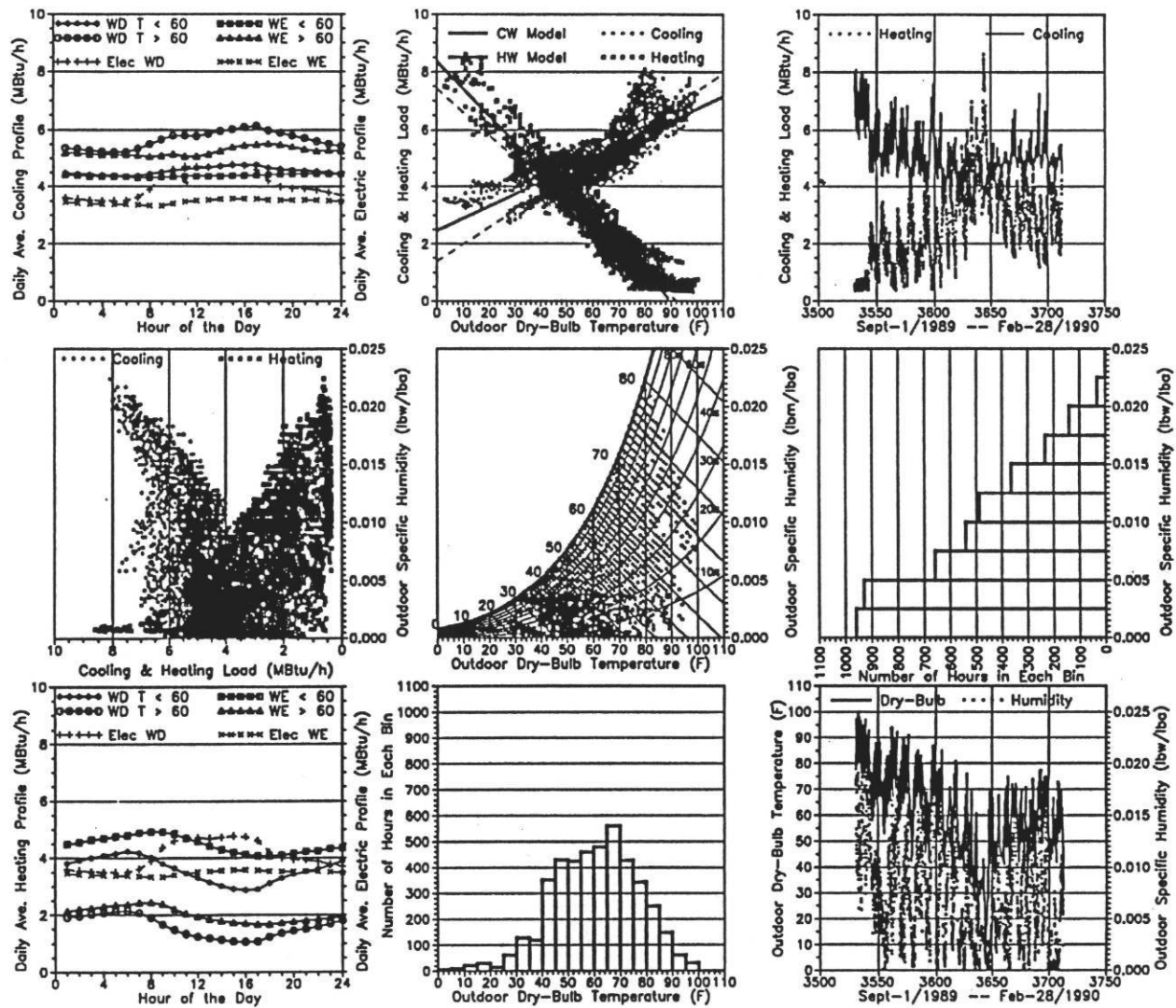


Figure 2.1 Nine Graph Carpet Plot Example (Bronson 1992).

was operated during the simulation period. Furthermore, the weather conditions during the winter caused a few simulation problems with the DOE-2 input file humidification parameter. Since the electricity load in this building is largely unaffected by weather variation, the TRY/TMY comparison produced similar results. According to the cooling load comparison, this study makes a good case for using measured weather data whenever possible to achieve the highest quality calibration possible. The simulation used in this thesis makes use of measured ambient weather data including dry bulb temperature, relative humidity, wind speed, and solar radiation.

2.7 Summary

This literature review presented a collection of studies performed by various organizations in the field of building energy simulation and model calibration. The first aspect investigated was the comparison of short calibration periods to long calibration periods where it was concluded that longer calibrations are more accurate, but also more expensive and time consuming. Kaplan et al. (1990a) verified the effectiveness of energy conservation options using DOE-2 with three short calibration periods. This study helped to reinforce the need for long-term measured data periods. Subbarao et al. (1990) and Balcomb et al. (1993; 1994) utilized the STEM/PSTAR method of separating individual heat flows to and from a building for simulation. This method was researched, but not used as part of this thesis. Finally, Koran et al. (1992) compared the STEM method to the MCT method using DOE-2. The findings

included the need to further research short-term calibration periods with more detail in order to more accurately simulate a building.

The second topic covered in this literature survey included guidelines on how to calibrate a DOE-2 model. Hsieh et al. (1989) determined the cause for DOE-2 design run under-simulation and published an extensive procedure to improve simulations. Kaplan et al. (1992) included simulation hints targeted at project managers and offered reasonable expectations from DOE-2 modeling as well as information on when computer simulation is appropriate. A study published by Carroll et al. (1993) included the RESEM simulation tool that automatically optimized model input parameters until acceptable tolerances were achieved. Clarke et al. (1993) investigated the PASSYS method for performing advanced residual analysis that were used when appropriate for this thesis.

A sensitivity analysis survey was the next portion of the literature search and included a study by Hsieh et al. (1989) which determined the cause for DOE-2's under-prediction of actual building energy use. Individual input parameters were investigated and accounted for in detail. Unpredictable tenant behavior was clearly determined to be one of the major causes of Hsieh's calibration discrepancy. Mahone et al. (1992) utilized a sensitivity analysis to develop building energy standards for different climatic regions. Griffiths and Anderson (1994) attempted to determine which DOE-2 input variables had the largest impact on the end-use energy

consumption. The information learned from these studies was beneficial to this research by recommending which input file commands such as lighting and equipment inputs to concentrate on so that the final result could be obtained more quickly.

The fourth category considered for this thesis explored the comparison of DOE-2 simulated indoor temperatures to measured indoor temperatures. Hsieh (1988) attempted to explain why DOE-2 simulated temperatures differed from measured temperatures. Also from a related study by Haberl and Komor (1990), it was learned that on/off switching of HVAC systems can be confirmed by comparing simulated to measured temperatures. This thesis utilized indoor temperature comparisons to verify HVAC system operation.

Daytyping techniques developed by Katipamula and Haberl (1991), Hadley (1993), and Akbari et al. (1988) were detailed in the next section, from which it was concluded that weather daytypes appear to hold the most promise for specifying DOE-2 lighting and equipment schedules when only whole-building electricity is available. The daytypes reviewed were based on various statistical methodologies including diurnal loads shapes, principle component analysis, and linear regression. Improved DOE-2 weather daytype graphics are presented in this thesis that are based on a statistically-based goodness-of-fit analysis which allow the DOE-2 user to simulate a building more efficiently.

Verifying energy conservation retrofits have always been a concern to engineers and building owners alike. In this final category considered for this literature review, several publications were considered that attempted to use DOE-2 to verify building energy retrofits. Reichmuth and Fish (1994), Torres-Nunci (1989), Hinchey (1991), and Bronson (1992) used DOE-2 to simulate an existing building and then modeled the same building without the efficient measures. The two most significant studies used for this thesis included the work accomplished by Hinchey (1991) and Bronson (1992). Hinchey demonstrated the added value of daily and hourly comparison as opposed to monthly comparison. Bronson advanced DOE-2 calibration techniques by developing the carpet plot. This new plot displayed end-use energy consumption comparisons to ambient weather conditions as well as statistical building load shapes. Bronson also developed a method to overlay site specific weather data onto a TRY weather file.

The literature presented here played an important role in this thesis. A significant portion of this research makes use of the information learned from the previous work. Previous graphical methods were enhanced by adding new statistically-based tools. The new tools are neither adversely affected by data overlap problems associated with graphing large datasets (Bronson 1992) nor by standard deviation value problems (Katipamula and Haberl 1991) encountered in previous daytyping routines. In the next Chapter, the methodologies used in this thesis are

described, including those borrowed from the previous work and the new methods developed for this thesis.

CHAPTER III

METHODOLOGY

In Chapter II the previous literature was reviewed as a foundation to develop the new procedures for calibrating building energy simulation programs to measured data from existing buildings. Hinchey (1991) and Bronson (1992) presented significant advancements in the art of calibration as part of the LoanSTAR Program. Hinchey used comparative three-dimensional residual plots to compare simulated data to measured data in a side-by-side format. Also, Hinchey compared monthly, daily, and hourly plotting formats of the same simulated data and showed that daily and hourly formats are more useful. These plots effectively demonstrated how subtle differences between simulated data and measured data could easily be overlooked when only using a monthly comparison analysis. This thesis improves on Hinchey's previous work by expanding the graphical analysis of time-series data to include 52-week box-whisker-mean plots. The residual plots are also presented in this thesis both as a function of hour-of-the-day and day-of-the-year perspectives. The results are then reported with statistical significance on a monthly basis.

Bronson improved upon Hinchey's work by developing DOE-2 hourly report extraction routines which were used extensively for this research. Furthermore, Bronson's research refined the calibration process by introducing "carpet plots"

consisting of time-series plots, scatter plots, and schedule profiles (Bronson 1992). Several problems were inherent to these plots including the difficulty encountered when long-term data is plotted. For example, in three of the plots in Figure 2.1 presented in Chapter II, the data points became indistinguishable in dense impenetrable clouds. This can cause a problem during the final analysis stages when one is trying to discern fine differences in black clouds (i.e. data clouds that suffer from severe data overlap problems). The desire to improve the carpet plot calibration technique is one of the foundations for this thesis.

Therefore, in a major effort to rectify the obstacles encountered in the previous work, new routines were developed for this thesis. This chapter describes the new statistical tools for graphing data and the methods used to acquire data, the DOE-2 simulation procedures, and the new computer routines developed to process the data into a format usable for weather tape packing and graphical presentation. The work presented in this thesis is not affected by the graphing problems discovered in past research because it is based on a statistical perspective. An example of each new graph is presented in this chapter. In Chapters IV and V these graphs are then used to study the simulation of the energy use of a case study building where hourly data were recorded.

3.1 Collect and Prepare Hourly Measured Data

Before DOE-2 is used to simulate an existing building, the user must consider how the model is to be validated. Various options are available varying in usefulness from monthly utility billing data, to short-term end-use hourly data from on-site monitoring, or even long-term end-use hourly data. The user may choose either to employ standard weather tapes available from the National Climatic Data Center (NCDC) or to pack a site-specific weather tape such as a Test Reference Year (TRY) weather tape for a more accurate weather dependent calibration (Haberl et al. 1994). For this thesis, a TRY weather tape was packed with existing routines (Bronson 1992) using weather data that were a combination of on-site measurements and data from a nearby NWS weather station.

The TRY weather tape is one of several weather tapes that DOE-2 can use. It was developed in cooperation with ASHRAE, the National Bureau of Standards (NBS), and the National Oceanic and Atmospheric Administration (NOAA) (NREL 1992). The primary purpose was to provide engineers with a long-term dataset containing climatological data for building design utilization. The tapes were compiled from data recorded at sixty weather stations across the United States. Data from the years 1948 through 1975 were analyzed omitting years with high or low mean extremes yielding one year per site. Packing a TRY weather tape requires relative humidity, dry bulb temperature, global horizontal and beam solar radiation, and wind speed.

Another weather tape that DOE-2 can use is the Typical Meteorological Year (TMY) weather tape (see Chapter II) for 1954 through 1972. TMY data were recorded from 249 weather stations based on the NCDC SOLMET database. A TMY tape includes total horizontal radiation, mean dry bulb and dew point temperature, and the maximum and mean wind speed. A third format, the Weather Year for Energy Calculations (WYEC) tape, developed by Crow (1970), can either be used as bin data from 51 stations (Degelman 1991) or time-series data and includes interpolated solar data measured at sixteen stations from the National Weather Service (NWS) TD 1440 tapes (NREL 1992). WYEC data is in TRY format and is composed of monthly long-term mean data. WYEC2 tapes were recently developed which include improvements to the original 51 datasets as well as the addition of 26 new sites (Augustyn & Co. 1994). Since a TRY tape has been proven to be compatible with the routines already developed by Bronson (1992), it was decided that it was to be used for this simulation rather than the TMY, WYEC, or WYEC2 tapes.

3.1.1 Packing Site-specific Weather Data

As the previous section illustrated, several weather tapes are commercially available to simulate a building with DOE-2. It has been shown in the past that packing a site-specific weather tape can give far more accurate weather dependent simulations than standard tapes (Haberl et al. 1994). Since TRY weather tapes are compiled using mean weather data averaged over a long-term basis, the simulation

accuracy will vary with deviation from the weather mean conditions. If, for instance, a sudden cold front passed over the building's location, use of a standard weather tape would result in significant differences between the simulated output and the measured energy data when considering weather dependent loads. Therefore to avoid DOE-2's modeling errors by using normalized long-term weather data, it is best to measure site-specific weather data as close to the case study building as possible which requires the use of a packed weather tape.

Packing a weather tape involves merging measured hourly outdoor dry bulb temperature, outdoor relative humidity, wind speed, and global horizontal and beam solar radiation into one data file. For this thesis a weather tape was packed using a combination of measured on-site weather data and NWS data from April through December 1993. Hourly dry bulb temperature, dew point temperature, and peak wind speed data were obtained from the NWS which has a weather station located approximately five miles South of the case study building at Washington National Airport. Prior to processing, dew point temperature was converted into relative humidity using a psychrometric routine by Sparks et al. (1993). Global solar radiation was measured on-site with a Lycor LI-200SA solar sensor mounted on the building roof as part of the photovoltaic solar installation. All four parameters were then combined into one data file and processed with Bronson's (1992) LS2TRY routine that synthesized beam and diffuse solar data before passing the data to Lawrence Berkeley Laboratory's (LBL) FORTRAN weather packing program (LBL 1982).

LBL's packing routine overlays dry bulb temperature, relative humidity, and wind speed directly onto an existing TRY weather tape. The solar data requires further processing before it is over-laid on top of the weather tape.

Prior to processing, the measured solar radiation data are passed through a routine (Bronson 1992) that synthesizes horizontal beam radiation and diffuse radiation which are then over-laid onto the TRY tape. Chapter IV describes the extra processing specific to the case study building that was required to convert the tilted data into horizontal solar radiation. In addition, the weather packer calculates dew point temperature and wet bulb temperature from dry bulb temperature and relative humidity and lays them onto the tape. Any missing data is labeled as "-99.0" by the routine. When missing weather data occurs, the weather packer compensates for the missing record(s) by linear interpolation so that no abrupt changes result on the weather tape (Bronson 1992).

3.1.2 Hourly Measured Energy Data

As Hinchey (1991) has already shown, the simulation will be more accurate if evaluated with hourly measured data gathered at several monitoring points in the building. This avoids the long-term data averaging encountered with monthly simulation comparisons. Thorough monitoring can be costly when considering the purchase of electronic equipment such as the logger and current transducers as well as installation labor costs. If extensive sub-metering is not feasible even for short-term

data collection, it may be necessary to use hourly whole-building energy use data along with special routines to estimate end-use data. Chapter V describes the techniques developed as part of this thesis to disaggregate the HVAC load from the whole-building electricity load. The new tools developed for this thesis are introduced in Section 3.3. Each tool was essential to the calibration effort since only hourly whole-building electricity data was available from the case study building.

3.2 The DOE-2 Building Simulation Program

DOE-2 is actually composed of four sub-programs: LOADS, SYSTEMS, PLANT, and ECONOMICS (LBL 1981). Figure 3.1 (LBL 1980) provides an overview of the DOE-2 program and shows the three general inputs required to run the Building Description Language (BDL) processor, including weather data, a materials library, and the DOE-2 BDL input file. The weather data is used to drive the simulation program and includes ambient dry bulb temperature, relative humidity, solar radiation, and wind speed. The materials library contains a set of default values for building construction components and is used when certain construction specifications are not provided by the user. The BDL input file describes the features of the building in detail including architectural information, occupant schedules, systems, plant, and economic information. The BDL processor compiles the input file information, verifies proper syntax and forwards it to the four main sub-programs, one at a time. The four sub-programs perform successive energy use calculations and generate standard monthly reports and specific hourly reports when called for.

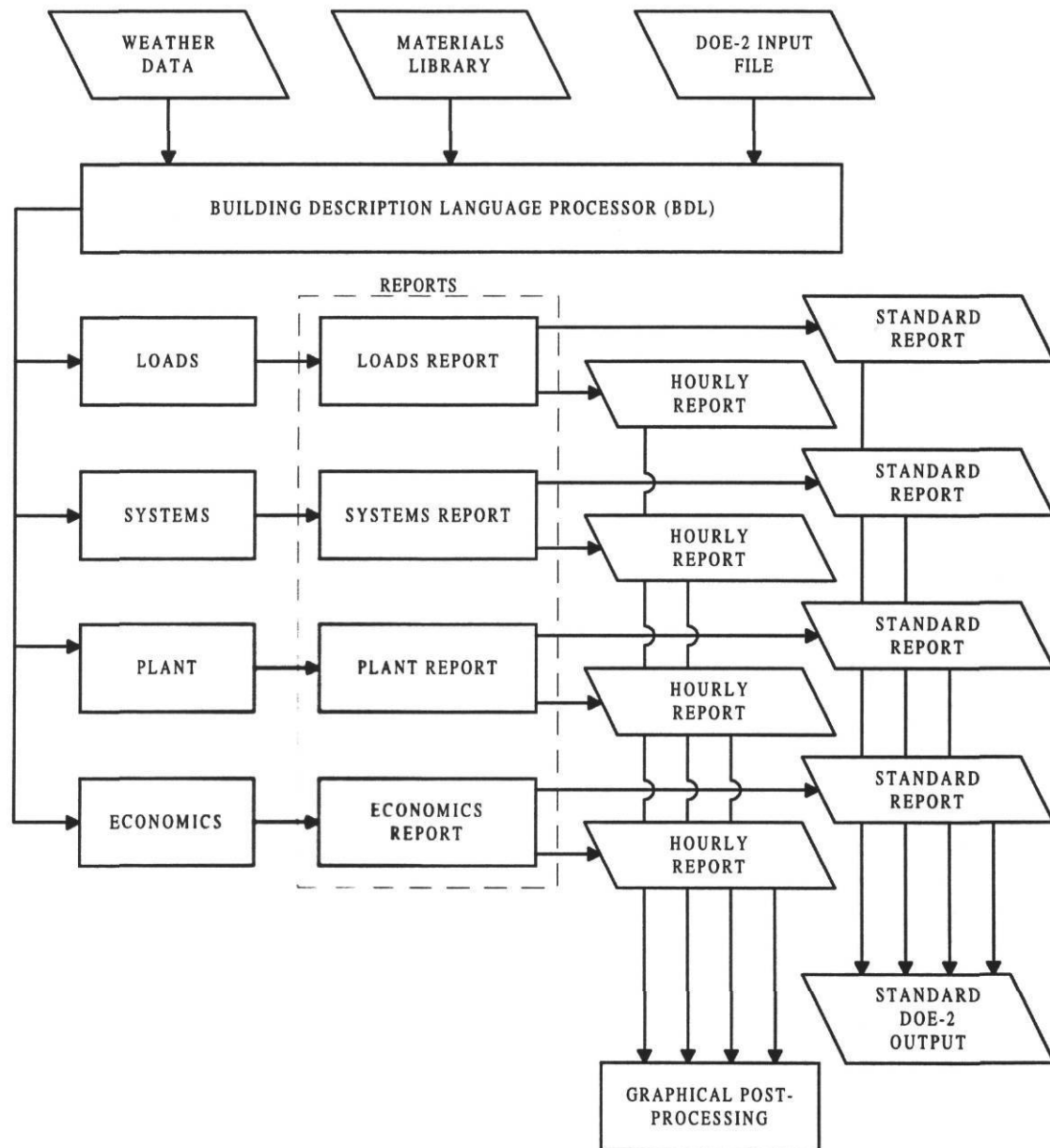


Figure 3.1 Overview of the DOE-2 Program.

3.2.1 LOADS Sub-program

The first sub-program, LOADS, calculates the heating and cooling loads imposed by the building envelope in all zones based on architectural specifications, shading surfaces, interior loads specified in the BDL, and ambient conditions from a weather tape (LBL 1981). Figure 3.2 (Haberl 1988a) provides a flow diagram for the LOADS sub-program including the hierarchy for the architectural, scheduling, equipment, and space condition information required.

The LOADS sub-program begins with the building geographical location and orientation information. As seen in Figure 3.2, occupancy, lighting, equipment, infiltration, domestic hot water, and other schedules are described for use by the SPACE-CONDITIONS command. The user then specifies building material details such as the layering and construction of the interior walls, exterior walls, roof, and floor. The window shading coefficients, glass types, and number of panes describe the window details. Then, the positioning and assembly of exterior and interior walls, the windows, the roof, and the floor details are then described by one or more SPACE commands to characterize the entire building. The BDL commands at the top and right of the figure such as END, DIAGNOSTIC, and PARAMETER provide essential operations details without which LOADS does not function properly.

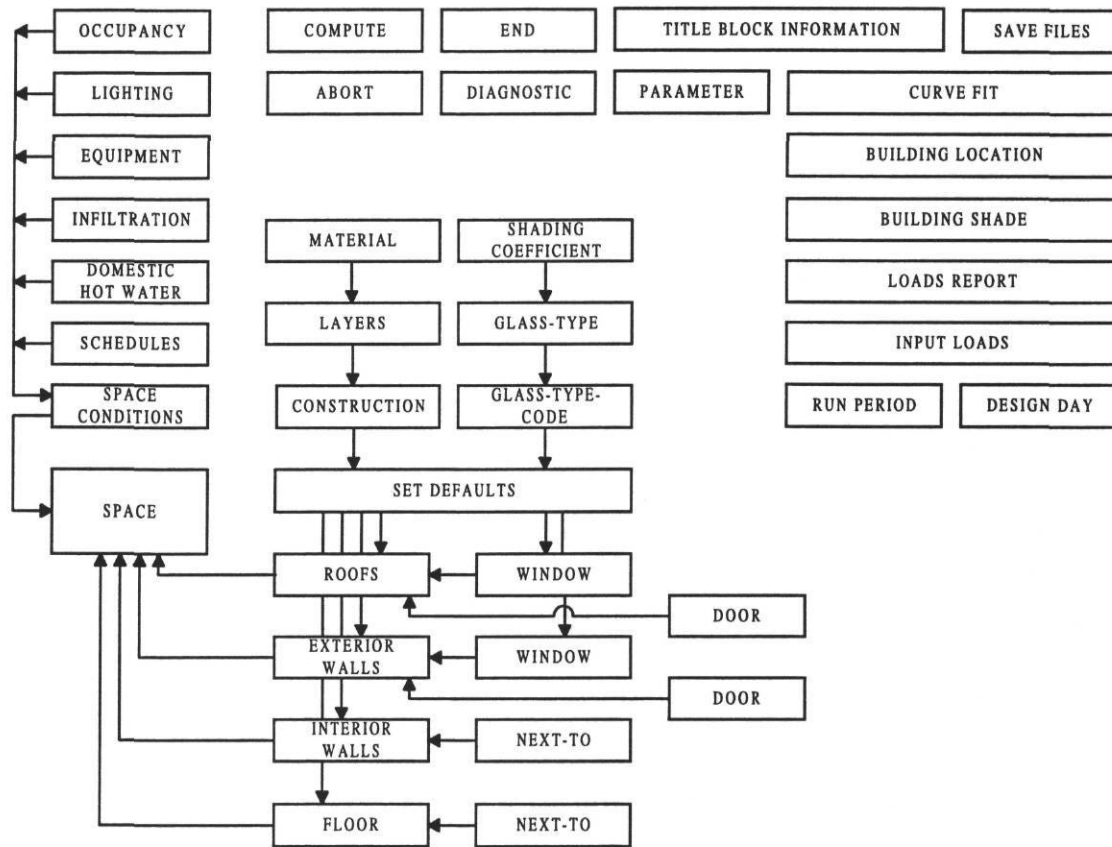


Figure 3.2 LOADS Sub-program Flow Diagram (Haberl 1988a).

LOADS utilizes the ASHRAE weighting factor method (LBL 1981) which uses z-transform techniques to solve complex dynamic heat transfer through the exterior surfaces. Latent and sensible heat gains or losses through the building envelope, internal energy use including lighting and equipment, and heat gain due to occupants are accounted for in the LOADS sub-program. LOADS performs zone

calculations based on a user specified constant space temperature to establish an initial thermal baseline profile and to reduce computation time. Once hourly loads are calculated and reports generated, the information is then passed on to the SYSTEMS sub-program. SYSTEMS estimates the energy required by the secondary HVAC systems to meet the LOADS-calculated envelope loads and ventilation loads after adjusting for thermostatic controls.

3.2.2 SYSTEMS Sub-program

With hourly information passed-on from LOADS, SYSTEMS simulates the secondary HVAC systems such as fans, coils, thermostats, and zones (LBL 1981). This sub-program uses a variety of techniques including additional weighting factors and curve-fits to correct the initial baseline calculations performed earlier at a constant reference space air temperature in the LOADS section. The system curve-fits may either be user specified or DOE-2 default equations. Some difficulty is encountered with both methods since default curves are often not the same as the building HVAC system. If a user specifies a custom system curve-fit equation based on empirical data, uncertainty still remains due to both equipment testing conditions and post-testing calculations.

Figure 3.3 (Haberl 1988a) diagrams the SYSTEMS sub-program hierarchy and shows the inputs needed for describing the secondary HVAC systems. SYSTEMS

allows the user to specify various system types such as single-duct or dual-duct systems, packaged residential systems, and/or heat pumps. Unlike the values calculated at a constant temperature in LOADS, SYSTEMS corrects the interior conditions discrepancy for temperature and relative humidity control with weighting factors (LBL 1981).

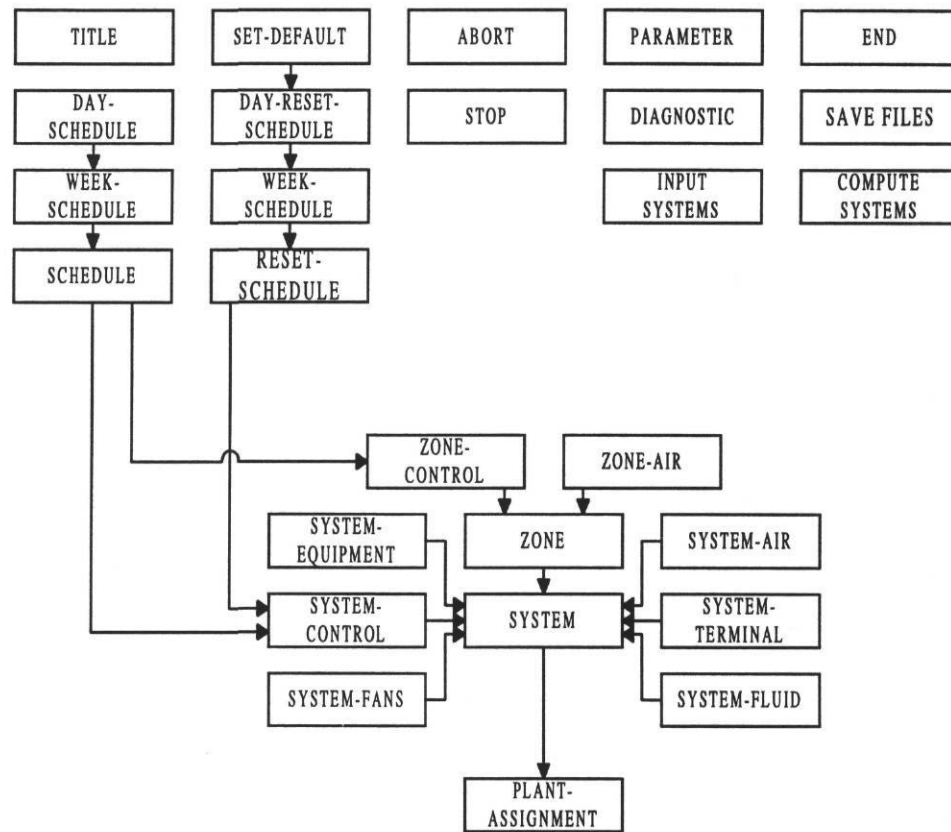


Figure 3.3 SYSTEMS Sub-program Flow Diagram (Haberl 1988a).

At this stage of the DOE-2 program, the system equipment, the system control, the system fans, and zone requirements are modeled based on specific user input information such as air flow rates, thermostat settings, equipment schedules, reset schedules, and heating and cooling capacities. When all sensible heat interaction between each zone and HVAC equipment is calculated heat and moisture calculations are performed between all the equipment, the heat exchangers, and the building.

At the top of Figure 3.3 the unattached boxes represent SYSTEMS commands that are required for verifying proper operation such as the ABORT function, which is used when an error is encountered. Verification and/or hourly reports are produced and program control is advanced to the PLANT sub-program.

3.2.3 PLANT Sub-program

After receiving the information from SYSTEMS, the PLANT sub-program then uses additional information from the BDL to simulate all primary energy-using equipment in the building such as chillers, boilers, cooling towers, and domestic water heaters (LBL 1981). Figure 3.4 (Haberl 1988a) is a flow chart of the PLANT sub-program information including operation schedules, the number and sizes of chillers, boilers, and cooling towers. The PLANT end-use energy reports provide electrical and thermal energy consumption data. The reports are commonly used to calibrate the model to the actual measured data since these data usually correspond to measurements made at the whole-building boundary.

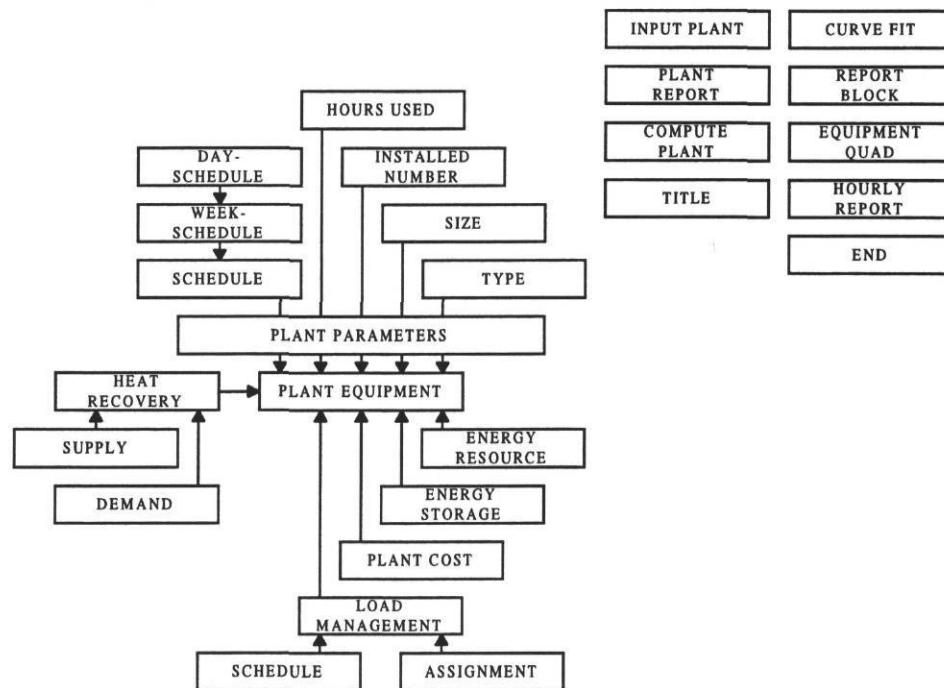


Figure 3.4 PLANT Sub-program Flow Diagram (Haberl 1988a).

3.2.4 ECONOMICS Sub-program

Finally, the ECONOMICS sub-program calculates the costs of the energy that has been calculated by the PLANT sub-program (LBL 1981). Figure 3.5 (Haberl 1988a) shows the economics functions and details. The first cost, number of units, and unit cost contribute to the overall component cost. A baseline cost is then calculated with information provided by energy cost, operational cost, replacement cost, and first cost. Energy costs are found by compiling energy escalation costs, resource costs, unit costs, and uniform costs. ECONOMICS can then provide life-

cycle cost information if required. This sub-program allows engineers to assess alternative options to determine which systems are the most economically feasible configurations for the building.

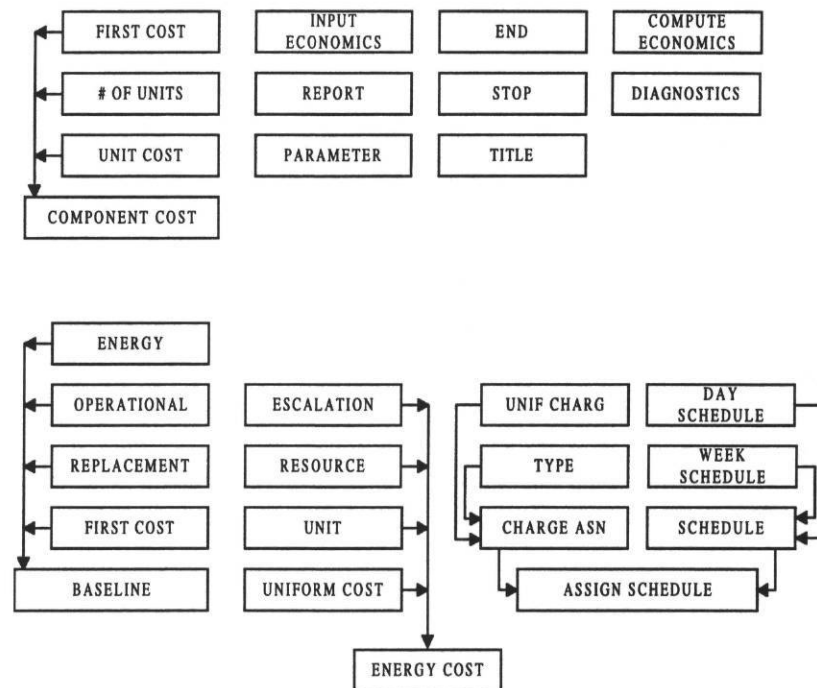


Figure 3.5 ECONOMICS Sub-program Flow Diagram (Haberl 1988a).

3.2.5 DOE-2 Required Information

Figure 3.6, adapted from Bronson (1992), presents a general overview of the calibration process used for this research. Bronson's weather tape packing routine and columnar data processing tools were both used in this research. The remainder of the calibrations in this thesis use either standard simulation practice (i.e. adjusting the input file and iteration) or new routines developed for this thesis.

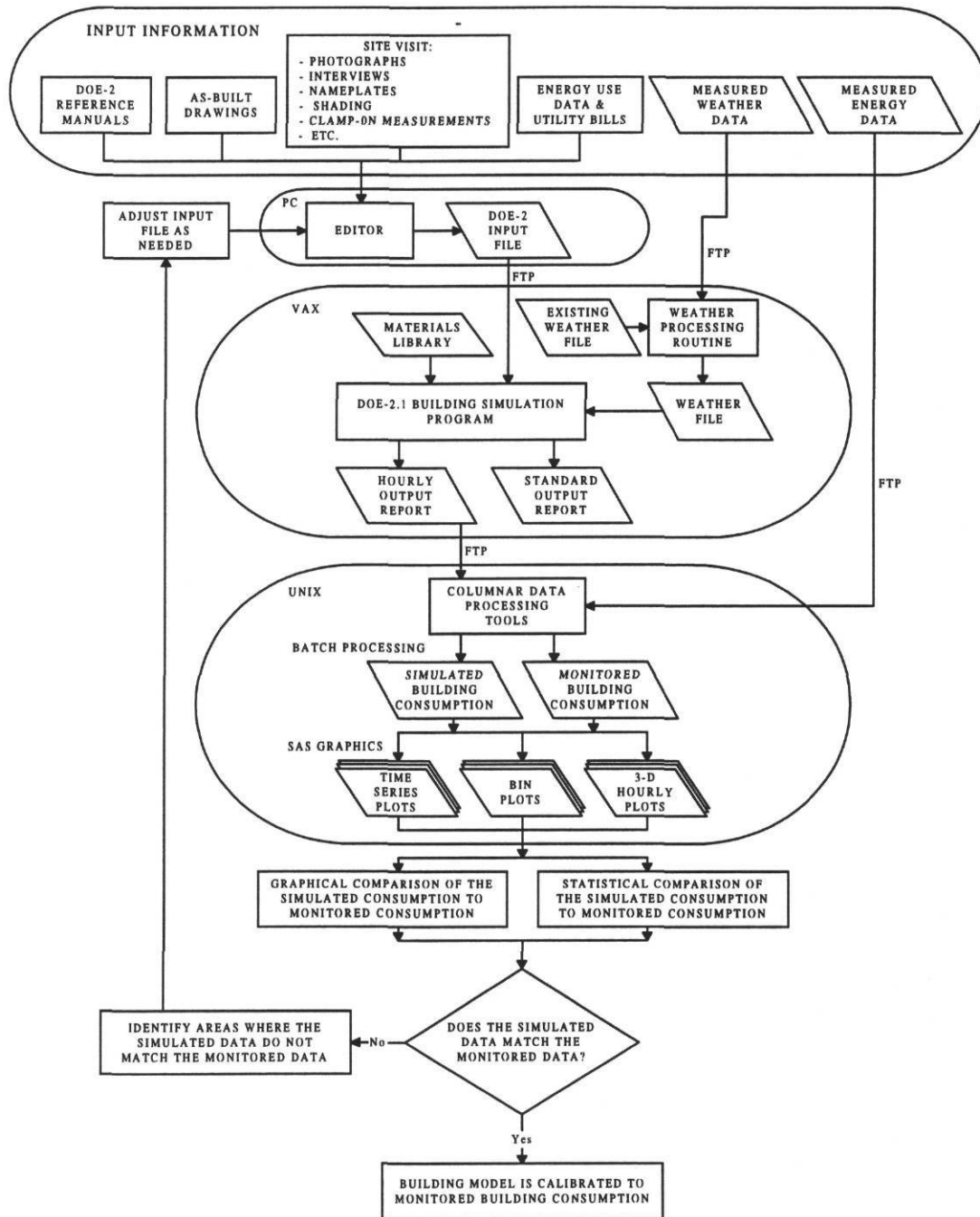


Figure 3.6 DOE-2 Calibration Procedure (Adapted from Bronson 1992).

The grouping at the top of the figure includes all the required input information to produce a DOE-2 simulation including: DOE-2 reference manuals, as-built drawings, information from site visits, utility billing data, and on-site measured data. A typical input file may be produced using any number of computerized text editors and requires detailed information. Any DOE-2 simulation usually requires a visit to the standard set of DOE-2 reference manuals to observe correct BDL syntax, the DOE-2 format, and mandatory BDL requirements (LBL 1980; 1981; 1982; 1989). As-built drawings help to correctly dimension the building and calculate lighting and equipment levels. A site visit is generally essential to verify lighting and equipment counts as well as questionable dimensions and any other miscellaneous discrepancies. The site visit should include photographs of the surroundings and the equipment and detailed interviews with occupants, engineers, architects, and building operations personnel. Also included in the site visit should be equipment nameplate inspections, shading measurements, and electric current clamp-on measurements of several key pieces of equipment.

A major part of the site visit includes the gathering of energy use data and/or monthly utility bills. Either is acceptable, but neither is a strict requirement to compile the input file. An HVAC system air balance report is also helpful when describing the zone air flow rates. On-site weather data measured for the simulation period has also been shown to be helpful by Haberl et al. (1994). In cases where no data are available, standard average weather tapes such as TRY and TMY may be purchased and used.

Finally, prior experience with the DOE-2 simulation program plays a crucial factor that can benefit the user in avoiding commonly made mistakes. Many problems with the input file may be avoided simply by having prior knowledge of program expectations as well as a thorough engineering understanding of HVAC systems and buildings in general.

The DOE-2.1D simulation program uses an input file in conjunction with a weather file and materials library to calculate building energy consumption and generate hourly and standard output reports. Figure 3.7 is an example of DOE-2's hourly report that was used for this thesis. The standard reports were also used for general input verification. Once the simulation was completed, the hourly output reports were then transferred to a UNIX system, processed into columnar data form (Bronson 1992), and merged into a single data file.

The Statistical Analysis Software (SAS 1989) program was then used to generate time-series plots, bin plots, and three-dimensional hourly plots for further analysis. This allowed for a graphical comparison of the simulated consumption to the monitored consumption. Also included in this thesis is a new technique for DOE-2 calibration that supplements the graphical comparison with a statistical comparison of the simulated and measured consumption which is described in more detail in the next section. With this information now processed, the user can then decide if the model is calibrated to an acceptable level and of equal importance where the remaining

HR-3 = HOURLY-REPORT

PAGE 1- 1

```

-----
MMDDHH  PLANT  GLOBAL
          TOTAL  AMBIENT
          ELECTRIC DRYBULB
          BTU/HR   F
          ----(10)  ----( 1)
4 1 1    31765.   51.0
4 1 2    31765.   51.0
4 1 3    31765.   51.0
4 1 4    31765.   51.0
4 1 5    31765.   51.0
4 1 6    92583.   52.0
4 1 7    88697.   54.0
4 1 8    93380.   55.0
4 1 9    84425.   58.0
4 110    82571.   59.0
4 111    76824.   65.0
4 112    72541.   63.0
4 113    65436.   64.0
4 114    60699.   69.0
4 115    58331.   68.0
4 116    63067.   64.0
4 117    65696.   62.0
4 118    65696.   60.0
4 119    68555.   58.0
4 120    31765.   58.0
4 121    31765.   55.0
4 122    31765.   55.0
4 123    31765.   54.0
4 124    31765.   53.0
0 DAILY SUMMARY (APR 1)
  MN     31765.   51.0
  MX     93380.   69.0
  SM    1356150. 1381.0
  AV     56506.   57.5

```

Figure 3.7 Example of DOE-2 Hourly Report.

mismatch may be located. This second feature is accomplished with the assistance of the calibration tools developed in this thesis. If it is determined that it is not, the areas where the simulated data do not match the measured data must be identified and adjusted in the input file. The DOE-2 program is run once again and the data processed until an acceptable calibration is reached.

3.3 Calibration Tools and Statistical Graphics

In order to improve the calibration procedures outlined by Bronson, Hinchey, and Torres-Nunci, several new computer programs and graphical tools were developed, including modifying routines originally created by Bronson (1992) and Abbas (1993) as well as routines developed specifically for this thesis. These improved calibration procedures include building architectural rendering, new graphical methods (52-week box-whisker-mean plots, 24-hour daytype box-whisker-mean plots, and binned box-whisker-mean plots), indoor temperature calibration, statistical goodness-of-fit calculations, and special routines for the case study building. These methods are discussed in the following sections.

3.3.1 Architectural Rendering

Several software programs have recently become available for purposes of architectural rendering or viewing of building simulation input files. One such program, DrawBDL (Huang 1993), was used to verify the building envelope descriptions used in the DOE-2 input file. The demonstration building shown in

Figure 3.8 shows a view of the case study building using the DrawBDL program. The software also includes such capabilities as rotating the building in a complete circle, looking at a three-dimensional view, a plan view, an elevation view, and a wire frame view. With a BDL visualization tool, each case study building envelope surface and shading surface can be inspected for proper placement, size, and orientation. This type of checking could not easily be done prior to the creation of such architectural rendering tools.

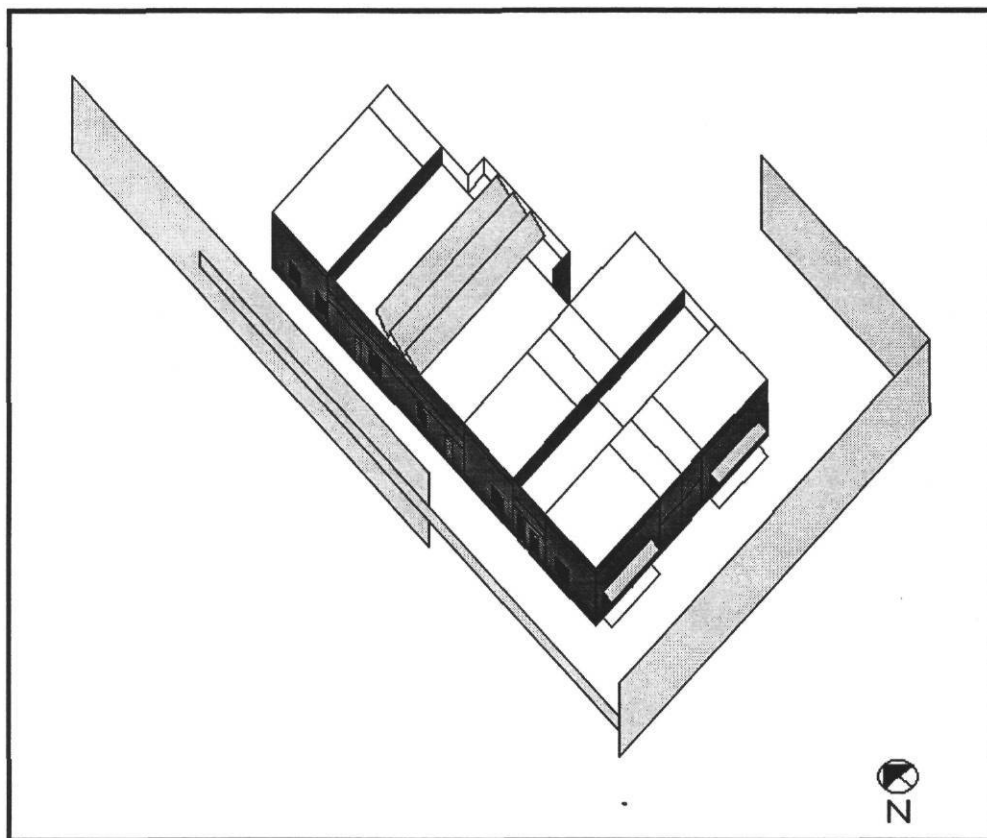


Figure 3.8 Example of DOE-2 Building Using DrawBDL.

Another personal computer software program, DOE-Plus, has been developed to increase the accuracy and to ease the use of the DOE-2 program (Byrne 1990). This program provides pull-down menus and prompting based on DOE-2 default values to allow a user to interactively prepare a DOE-2 input file. Once the building's architectural specifications are completed, the program then has the capability to draw the building with a two- or three-dimensional perspective for envelope verification and correction. This program was not used in the current work.

The ENER-WIN program (Degelman and Soebarto 1994) is a building energy performance package that was designed to perform retrofit designs, HVAC equipment specification, monthly utility estimates, and life-cycle cost analysis. The building outline, while still in the design stages, may be sketched onto a grid to allow the designer to see the basic building shape. This program was designed to run on a MS-Windows based personal computer to interface with other software routines written in FORTRAN, C, and Quickbasic. In theory, this program may be attached to DOE-2; however it does not yet have the capability to read the DOE-2 input file and translate the code into a visual image on a computer screen.

3.3.2 New Calibration Graphing Methods

Formerly, DOE-2 users were confined to using simple time-series plots (Hsieh 1988; Hunn et al. 1992; Reddy 1993) such as those shown in Figure 3.9 where simulated and actual data are superimposed upon the same graph. Although two-

dimensional time-series plots are useful for determining certain features, a special problem exists when plotting long-term time-series data. In such cases, direct comparison becomes ineffective for all practical purposes because it is very difficult to identify individual hourly measurements. It clearly can be observed from Figure 3.9 that one month of data are densely packed with significant data overlap (Cleveland 1985). As is illustrated in the graph, the problem is compounded further when plotting two data variables on the same graph. Figure 3.9 shows the difficulty a user encounters when comparing DOE-2 simulated data, represented by the dashed line, to measured data shown as a solid line. Distance between individual hourly data pairs is virtually impossible to detect. The new methods introduced in this section considerably improve a DOE-2 calibration over the use of two-dimensional time-series graphs.

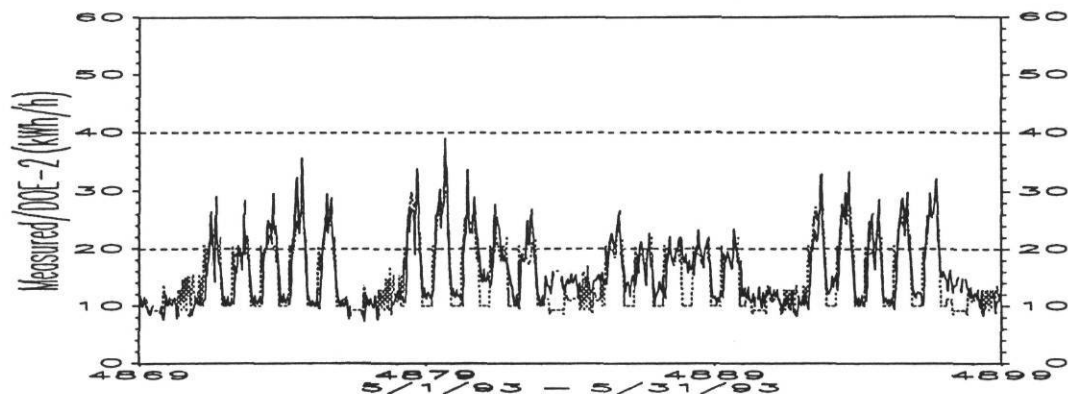
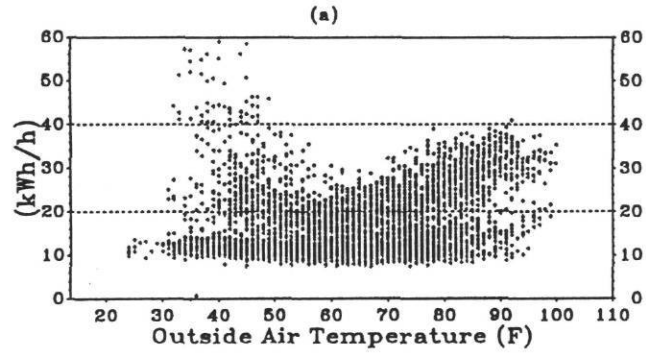


Figure 3.9 Example of Time-series Plot. Simulated Data (Dashed) and Actual Data (Solid) are Shown Superimposed on the Same Graph.

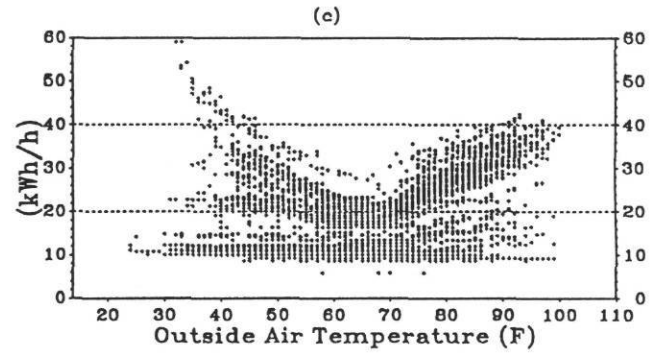
One improvement over past graphic techniques is shown in Figure 3.10 which shows an example of a binned plot that was modified for this thesis from graphs proposed by Abbas (1993). The superimposed and juxtaposed binned box-whisker-mean plots (BBWM) display the maximum, minimum, mean, median, 10th, 25th, 75th, and 90th percentile points for each data bin for a given period of data. These plots are an improvement over the scatter plots previously used by Bronson (1992) because they eliminate data overlap and allow for more accurate characterization of the dense cloud of hourly points (scatter plots are, however, useful in showing multiple operation modes). The important feature to note about this plot, and box-whisker-mean plots in general, is that the data are statistically binned by temperature. This feature allows for the bin-by-bin goodness-of-fit to be statistically calculated and compared. By using the box-whisker-mean plot combined with a scatter plot, one can visualize the data as a whole while simultaneously being able to see the effects of the outliers (Tukey 1977; Cleveland 1985; Abbas 1993).

In Figure 3.10 the entire simulation period data are plotted using a technique developed by Abbas (1993) and modified for this thesis that includes a combination of juxtapositioning, temperature-based box-whisker-mean binning, and superpositioning. In the upper left graph the hourly measured whole-building electricity use is shown plotted against hourly ambient temperature. In the upper right graph, the corresponding DOE-2 simulated data for the same period are shown. Below each

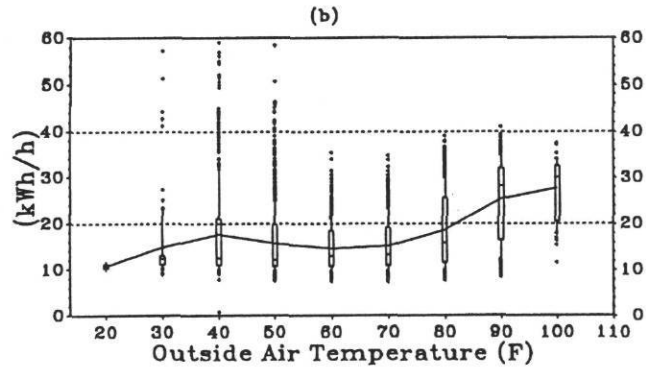
Measured Whole Building Electricity



DOE-2 Whole Building Electricity



Measured Whole Building Electricity



DOE-2 Whole Building Electricity

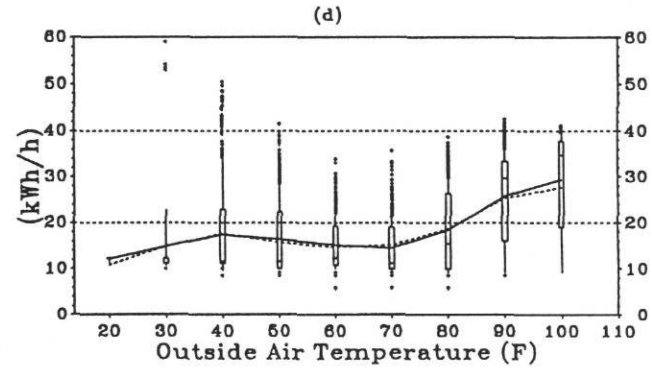


Figure 3.10 Binned Box-whisker-mean Plot.

scatter plot (parts (a) - measured and (c) - simulated) are binned box-whisker-mean plots in parts (b - measured) and (d - simulated). These plots show the whole-building electricity consumption as a function of outdoor temperature bins divided into 10° F segments. One final feature of these plots is that the mean of each measured data bin is superimposed with a dashed line onto the box-whisker-mean plot in part (d) which represents data from the calibrated DOE-2 simulation . The difference between mean lines in each bin provides a measure of how well the model is calibrated with respect to temperature. Likewise, the inter-quartile range (i.e. the distance between the 25th and 75th percentiles) represents the hourly variation in a given bin.

A new statistical plot has been developed that bins the data into 24-hour weather dependent profiles. Figure 3.11 is an example of a preliminary step that shows the whole-building electricity use versus the hour-of-the-day for both the measured data and the DOE-2 simulated data in three weather daytypes. The daytypes are divided into temperatures below 45° F, temperatures between 45° F and 75° F, and temperatures above 75° F. The original concept for this plot can be traced to the weather daytype analysis developed by Hadley (1993). The actual measured data are presented in parts (a), (c), and (e) and the simulated DOE-2 data are shown in parts (b), (d), and (f). These plots confirmed that the building's 24-hour electricity profiles are strongly influenced by the ambient temperature. The plots also provide a

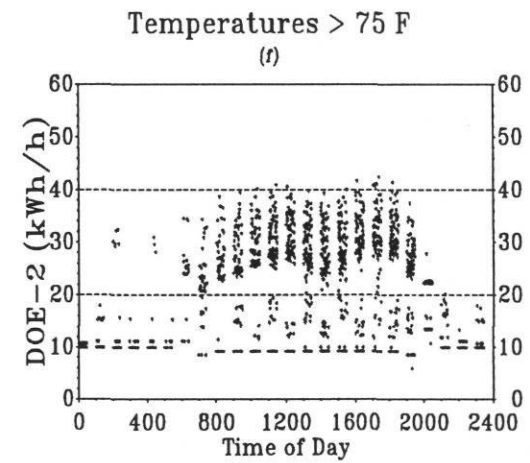
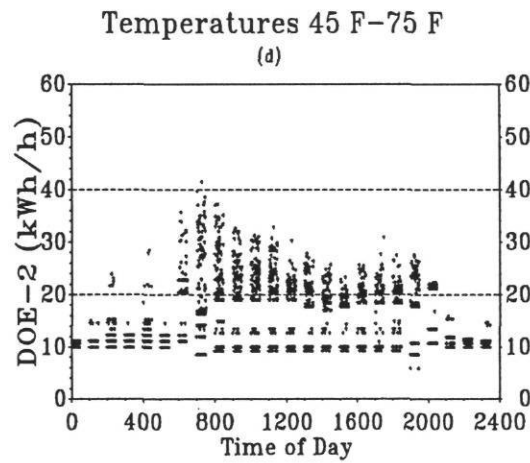
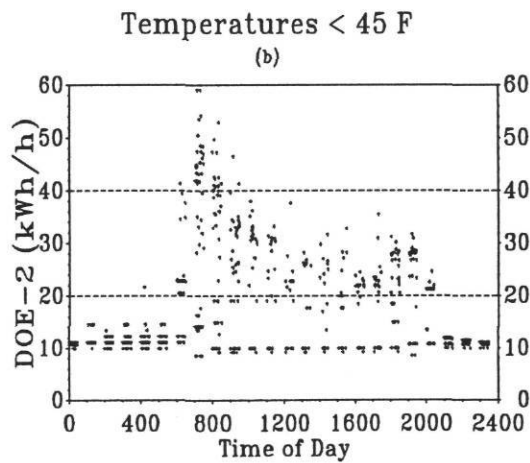
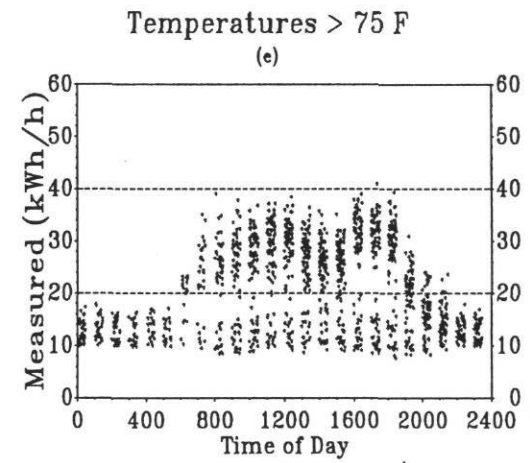
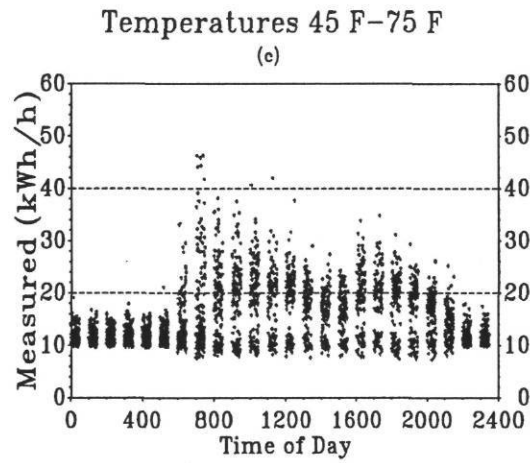
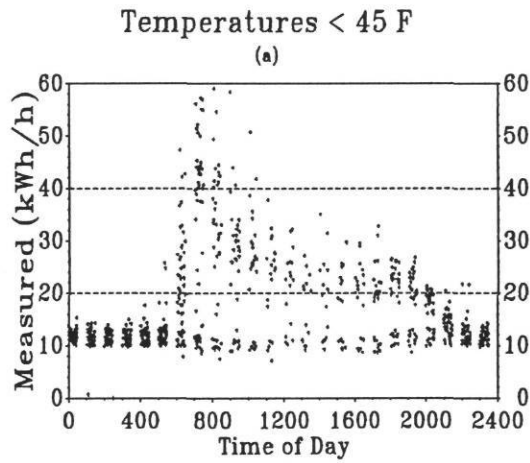


Figure 3.11 24-Hour Weather Daytype Scatter Plot.

more efficient method of viewing the data based on heating only, no heating or cooling, and cooling only modes.

One of the problems with presenting individual data points in an x-y plot (i.e. hour-of-the-day versus kWh/h, is that it is difficult to judge the density of the data at a given point on the graph because the individual data points overlap). One technique that can improve a graph which suffers from this problem is to jitter the individual data points by introducing a random noise into the variables used for the x or y axis (Cleveland 1985). Figure 3.12 demonstrates this process where part (a) shows the data without jittering and part (b) shows the data with jittering. Jittering is employed in the graphs of this thesis to improve the visibility of the data.

Figure 3.13 is a plot of the same data as shown in Figure 3.11, but displayed in a 24-hour box-whisker-mean (24H BWM) format. This additional calibration procedure allows a DOE-2 user to view and analyze the weather dependent data on an hour-by-hour basis and adjust the hourly schedules in the input file accordingly. The solid line in parts (b), (d), and (f) is the simulated mean. The dashed line is the measured mean line from parts (a), (c), and (e) that is superimposed onto the simulated data so that hour-by-hour comparisons may be made.

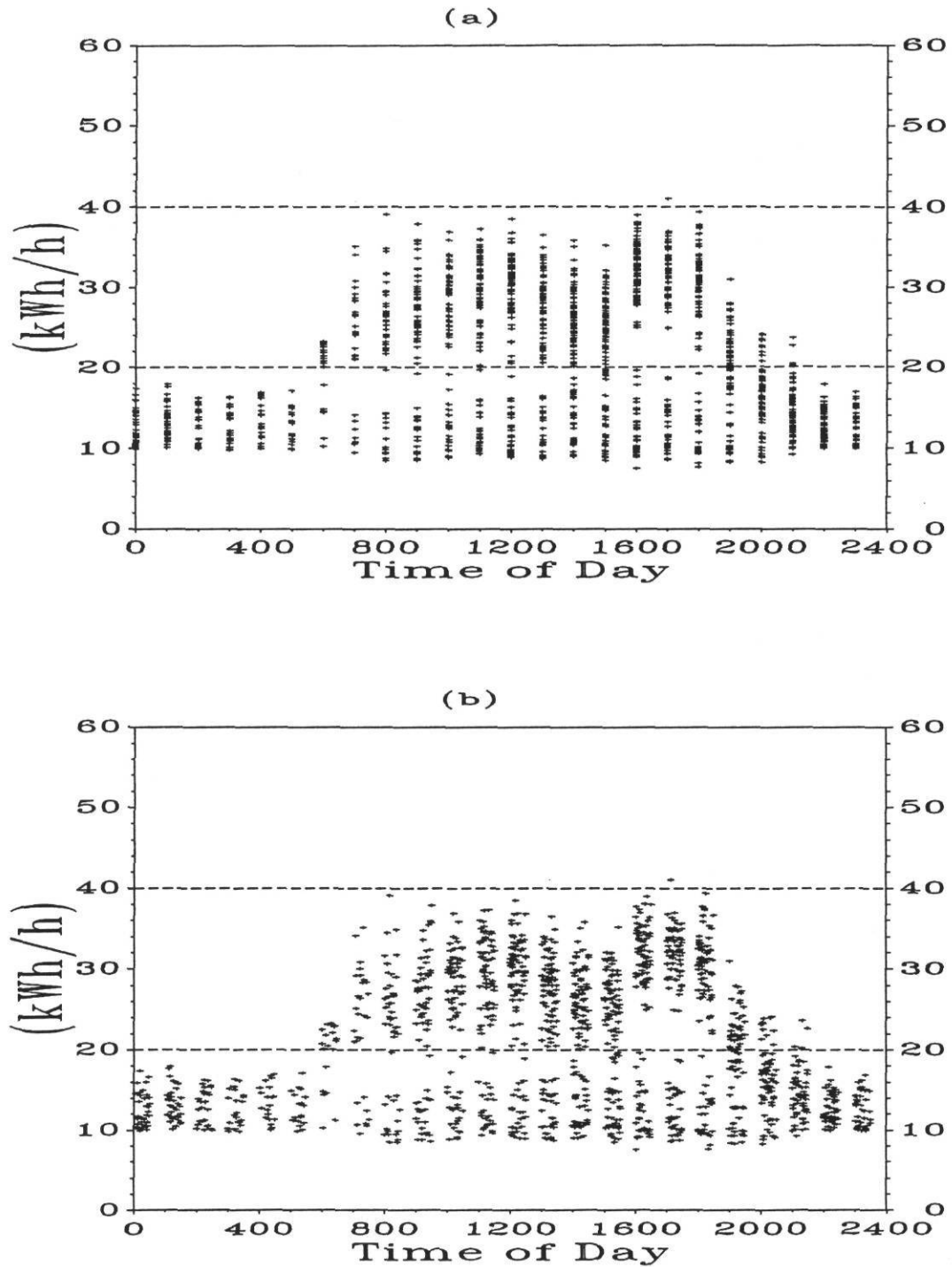


Figure 3.12 Effects of Jittering. (a) Without Jittering. (b) With Jittering.

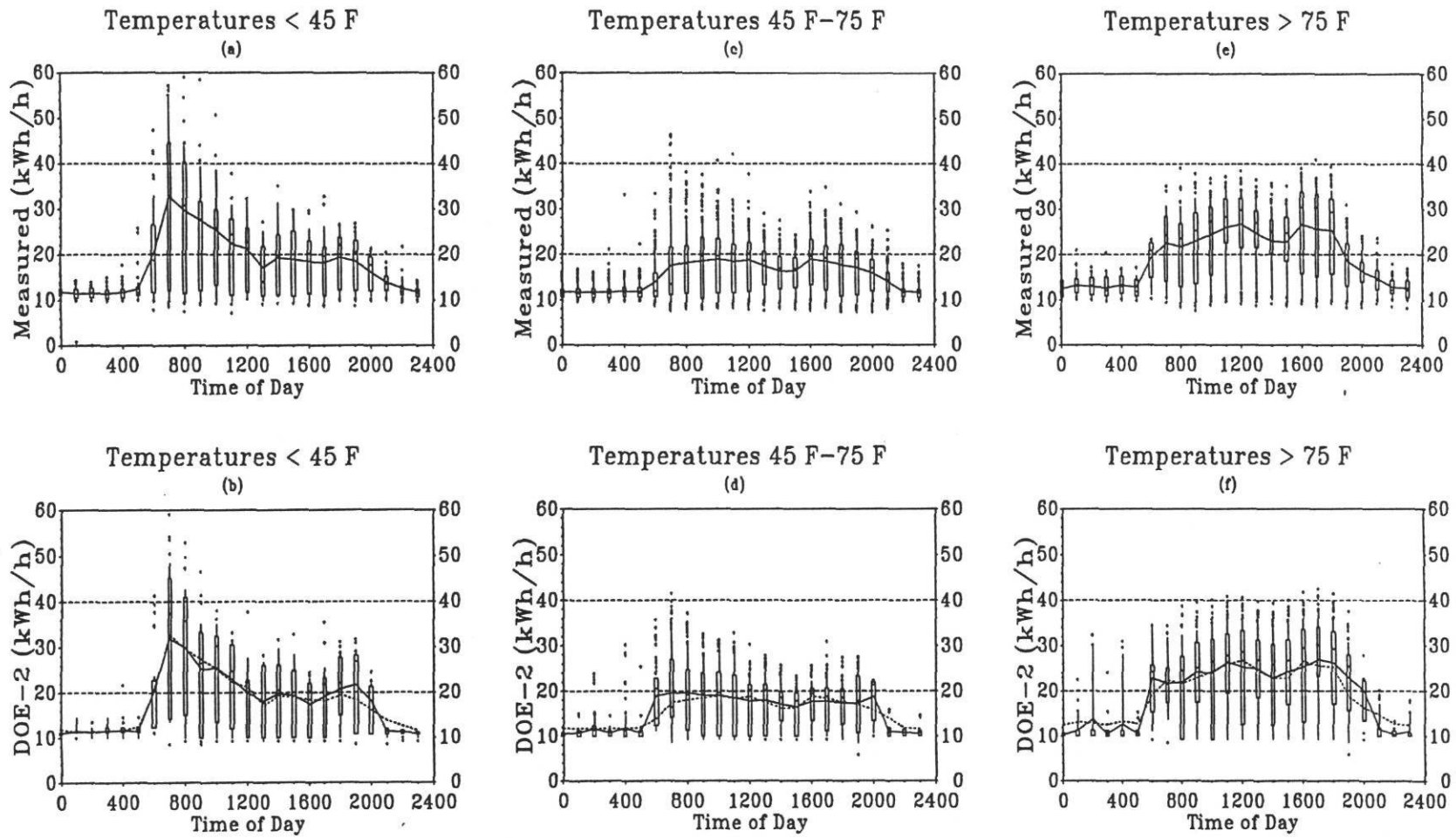


Figure 3.13 24-Hour Weather Daytype Box-whisker-mean Plot.

3.3.3 Indoor Temperature Calibration

Indoor measured temperature was recorded during both the heating and cooling seasons in order to help calibrate the DOE-2 simulation to the measured data. Two analog chart recorders were placed in the building to record the zone temperature in the north and the south section of the building. Previously, Hsieh (1988) compared DOE-2 simulated temperatures to measured temperatures, but did not attempt to calibrate the model in that fashion. In this thesis, a comparison of measured versus simulated zone temperatures is used to determine how well DOE-2 is turning the systems on or off to match what has been observed in the measured data. This technique is discussed further in Chapter V.

3.3.4 Load Disaggregation From Whole-building Electricity

Due to budget constraints, the case study building, illustrated in Chapter IV, was only monitored for whole-building electricity use. This, unfortunately, made it difficult to assign certain portions of energy consumption to individual end-use components. Therefore, a technique was developed to use two representative days, one weekday, and one weekend, to estimate the HVAC base-level energy use. Since the interior lighting, equipment, and exterior lighting levels are known from hand measurements and equipment manufacturer data, the only large-scale unknown remaining was the HVAC baseload. Chapter V describes the method used to extract the HVAC load and how it compares with the DOE-2 simulated load.

3.3.5 Calibration Calculation Methods

In the previous work, Bronson (1992) summed monthly simulation results and verified the calibration via a percent difference. Torres-Nunci (1989) and Hinchey (1991) only declared the model “calibrated” and submitted graphs to demonstrate the goodness-of-fit. Numerical differences only in the form of \pm monthly differences were provided. Therefore, in the interest of furthering the calibration procedures, several statistical calculations have been added including a monthly mean difference, and hourly mean bias error (MBE) for each month, an hourly root mean squared error (RMSE) reported monthly, and an hourly coefficient of variation-root mean squared error (CV(RMSE)) (Kreider and Haberl 1994a; 1994b). These indices have proven useful in evaluating hourly models of building hourly use. The values are tabulated for the total data as well as for each month. The statistical indices used to evaluate the models are defined below.

The percent difference is a simple calculation whereby a difference for each monthly measured and simulated energy consumption total is taken and divided by the measured monthly total consumption:

$$\text{percent difference} = \left(\frac{\sum_{i=1}^n y_{\text{pred},i} - \sum_{i=1}^n y_{\text{data},i}}{\sum_{i=1}^n y_{\text{data},i}} \right) \times 100 \quad (3.1)$$

where:

$y_{\text{pred},i}$ is the predicted monthly value for the building energy use,

$y_{data,i}$ is the measured monthly value for the building energy use, and
 n is the number of months used in the simulation.

This index is the typical value reported for most DOE-2 predictions (Diamond and Hunn 1981; Kaplan et al. 1990a; Bronson 1992; McLain et al. 1993).

The mean bias error², MBE (%) (Kreider and Haberl 1994a; 1994b), is a method with which to determine a non-dimensional bias measure (sum of errors), between the simulated data and the measured data for each individual hour. The total difference, or sum of errors, between the predicted data and the simulated data is divided by the total number of hours considered in the calculation, thus rendering a mean bias. The p value, or number of regression parameters, was arbitrarily set to be zero. The result was then divided by the measured data mean to provide a non-dimensional value reported as a percentage. This calculation may be performed on any number of data points; however, it is convenient to show results as a function of monthly or total simulation periods.

$$MBE = \frac{\sum_{i=1}^n (y_{pred,i} - y_{data,i})}{\bar{y}_{data,i}} \times 100 \quad (3.2)$$

where:

$\bar{y}_{data,i}$ is the independent variable mean value of the data set corresponding to a

² Dr. Srinivas Katipamula. 1994. Personal Communication, Richland, WA: Pacific Northwest Laboratory.

particular set of the dependent variables,

n is the number of data points in the data set, and

p is the total number of regression parameters in the model (which was assigned as 0 for the DOE-2 models).

The results of this calculation show that the MBE is in actuality the same as the percent difference calculation previously shown. However, the true definition pertains to the bias, or error, of the mean difference value between the simulated data and the measured data.

The root mean squared error, RMSE (kWh/h), is found on an hourly basis by the following equation (SAS 1990):

$$\text{RMSE} = \sqrt{\text{MSE}} \quad (3.3)$$

where:

the mean square error,

$$\text{MSE} = \frac{\text{SSE}}{n - p}, \quad p=0 \text{ and} \quad (3.3a)$$

the sum of squares error,

$$\text{SSE} = \sum_{i=1}^n (y_{\text{pred},i} - y_{\text{data},i})^2 \quad (3.3b)$$

yielding the equation:

$$\text{RMSE} = \sqrt{\frac{\sum_{i=1}^n (y_{\text{pred},i} - y_{\text{data},i})^2}{n - p}} \quad (3.3c)$$

The root mean squared error is typically referred to as a measure of variability, or how much spread exists in the data. For every hour, the error, or difference in paired data points is calculated and squared. The sum of squares errors (SSE) are then added for each month and for the total periods and divided by their respective number of points yielding the MSE; whether for each month or the total period. A square root of the result is then reported as the root mean squared error.

The coefficient of variation-root mean squared error, CV(RMSE) (%) (Draper and Smith 1981) is essentially the root mean squared error divided by the measured mean:

$$\text{CV(RMSE)} = \frac{\sqrt{\frac{\sum_{i=1}^n (y_{\text{pred},i} - y_{\text{data},i})^2}{n - p}}}{\bar{y}_{\text{data},i}} \times 100 \quad (3.4)$$

where:

$$\bar{y}_{\text{data},i} = \sum_{i=1}^n \frac{y_i}{n} \quad (3.4a)$$

It is often convenient to report a non-dimensional result. CV(RMSE) allows one to determine how well a model fits the data; the lower the CV(RMSE), the better the calibration (the model in this case is the DOE-2 predicted data). Therefore, a

CV(RMSE) is calculated for hourly data and presented on both a monthly summary and total data period.

The purpose of calculating the CV(RMSE) and comparing the results with the standard percent difference calculation is to demonstrate that a percent difference report may be misleading. Since the percent difference calculations are usually shown for total monthly simulations or even total simulation data periods, the reader is never certain if the model is a true representation of the actual building or if the \pm errors have canceled out. If one examines the hour-by-hour data results, it would be evident that each pair of points would in all likelihood be dissimilar and in some cases be significantly different, despite using measured weather data to drive the simulation model. Reporting monthly data therefore does not take into account the canceling out of individual differences observed when the simulation over-predicts during one hour and under-predicts during the next hour by approximately the same amount.

3.4 Summary

This chapter reviewed the methodology used to measure, prepare, and pack hourly weather data onto an existing TRY weather file. An overview of the DOE-2 program was discussed including the LOADS, SYSTEMS, PLANT, and ECONOMICS sub-programs. Then the new calibration tools were introduced which encompassed new graphical calibration analysis. The graphics include temperature binned box-whisker-mean plots and 24-hour daytype box-whisker-mean plots. Other

techniques shown were architectural rendering as means to verify the building envelope, indoor temperature calibration to verify HVAC run-time and thermostat schedules, whole-building electricity load disaggregation as a substitute for end-use data measurement, and improved statistical calculation methods to verify the calibration. The next chapter describes the case study building details used to analyze the new techniques.

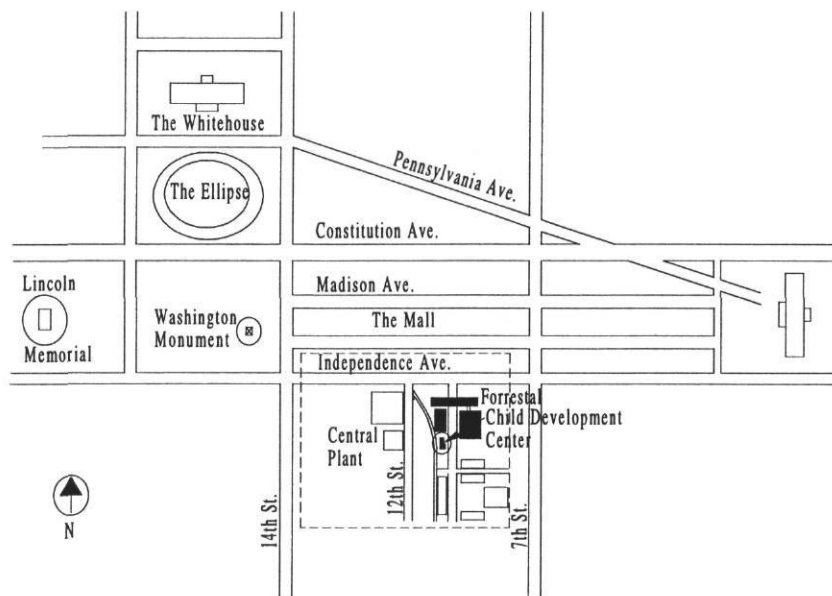
CHAPTER IV

CALIBRATING DOE-2 TO THE CASE STUDY BUILDING

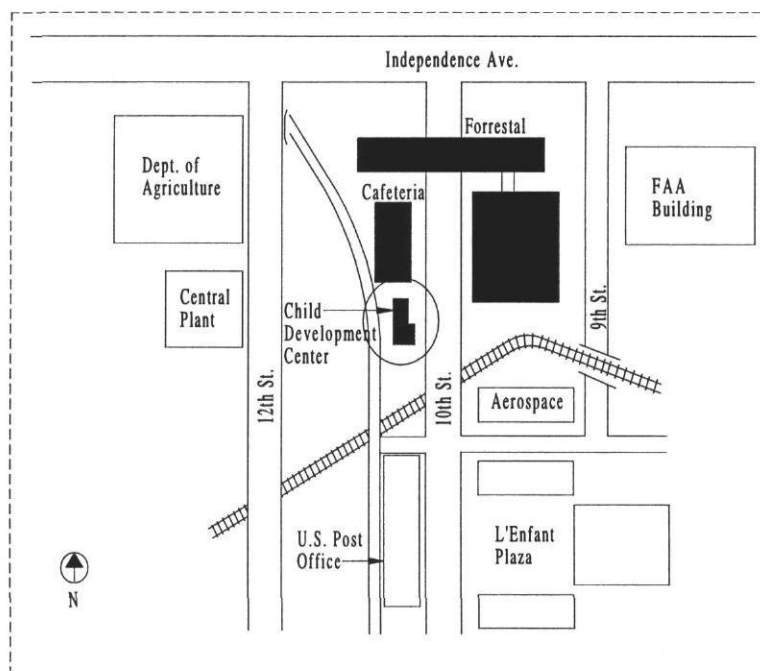
This chapter outlines the case study building used to test the new calibration tools. The HVAC systems, HVAC controls, interior equipment, and occupancy of the USDOE Forrestal Child Development Center are described in detail and how they relate to the DOE-2 input file. In addition, this chapter gives results of the calibration effort using the DOE-2.1D simulation program operating on the university's VAX 9000-210V system (CIS 1993).

4.1 Case Study Building Description

The USDOE Forrestal Child Development Center building, or daycare center, is situated directly south of the USDOE Forrestal Cafeteria building in Washington, D.C. Figure 4.1 (a) is a plan view of the Washington, D.C. area and shows the location of the USDOE complex. Figure 4.1 (b) includes a more detailed view of the area surrounding the Forrestal building and shows the daycare center, the Forrestal building, the Forrestal Cafeteria building, the U.S. Department of Agriculture, the General Services Administration central plant, and the U.S. Post Office building. The daycare center is a part of the USDOE Forrestal complex which includes a main office building, an adjacent office building, and a cafeteria building with an inter-connecting underground parking and support services area. Figure 4.2 (USDOE 1993) is a picture



(a)



(b)

Figure 4.1 Forrestal Child Development Center Location. (a) Overview of Washington, D.C. (b) USDOE Forrestal complex.

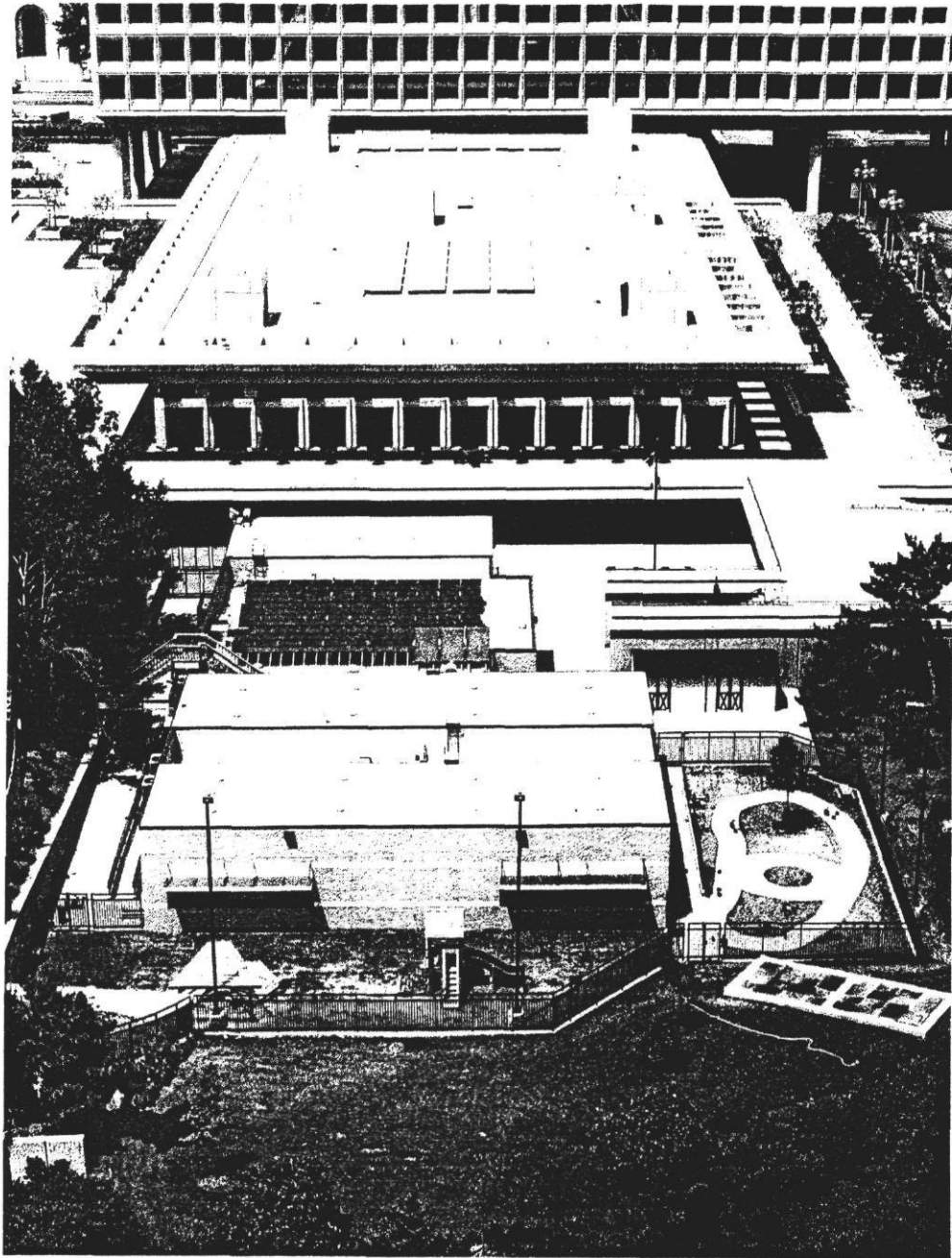


Figure 4.2 Child Development Center, Forrestal Cafeteria, and Forrestal Building.

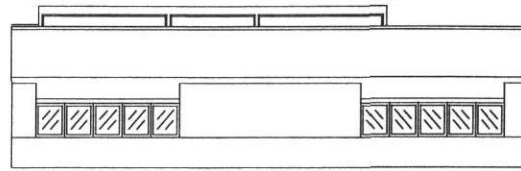
of the complex taken from the roof of the Post Office building located directly to the south. The Cafeteria and North Forrestal building can be seen at the uppermost portion (north side) of the figure. The large square building directly south of the Forrestal building is the Forrestal cafeteria building and the daycare center is the building located at the bottom of the picture. The south side daycare windows can be seen in this view with each bank being shaded by horizontal overhangs. A short time after construction, both shades were added to eliminate glare and to reduce solar heat gain during the Spring, Summer, and Fall. The left side of the daycare center building is partially bordered by tall shade trees and a short wall. A wall, staircase, and shade trees can be seen on the right side of the figure. The staircase leading to the daycare roof was temporarily added from June 1992 to March 1993 at the request of the Secretary of Energy so that visitors could tour the photovoltaic array. A small playground surrounds the east, south, and west sides of the building. Two large banks of photovoltaic solar collectors and a combination photovoltaic and DHW collector bank are located on the north side of the building roof. The three DHW collectors that can be seen on the lower right side of the first bank from the bottom of the figure. Figure 4.3 (USDOE 1993) is a picture of the daycare center showing the east side of the building with the children's playground in the foreground.

The modular daycare building was constructed in 1991 under the direction of the USDOE General Services Administration to serve as a state-of-the-art demonstration project for energy efficient design and to provide a daycare facility for

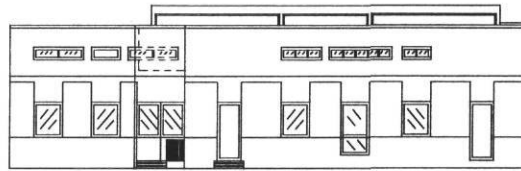


Figure 4.3 Southeast View of the Child Development Center.

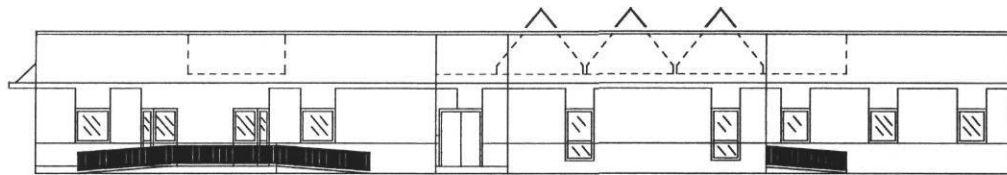
USDOE employee children. The daycare building is oriented on a North-South azimuth (the east walls face due East, the north wall faces due North, etc.) Elevation views are shown in Figure 4.4 for the four main wall sides. The building floor area consists of 8,100 sq. ft. and is divided into four conditioned zones: two main classroom zones; one kitchen/office/utilities zone; and one play area zone. An unconditioned plenum and an unconditioned crawl space are located above and below



(a)



(b)



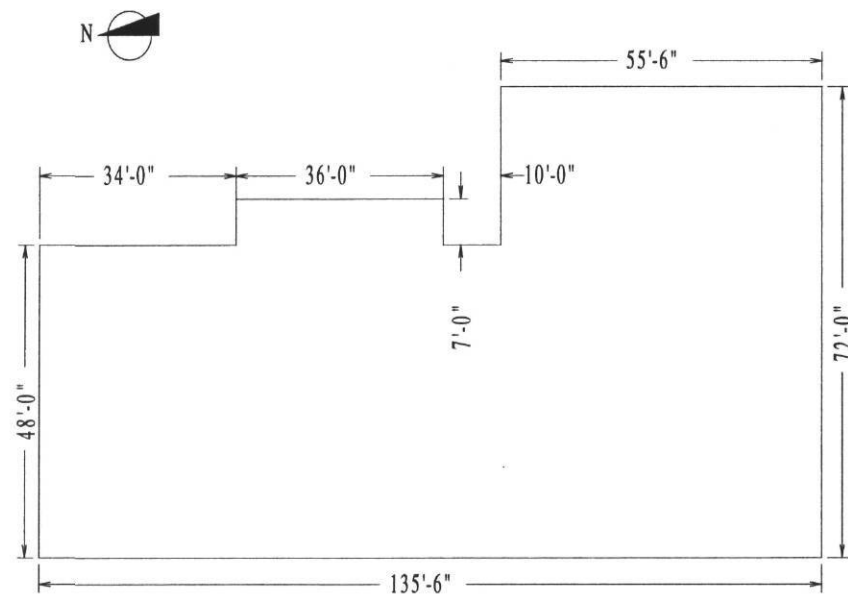
(c)



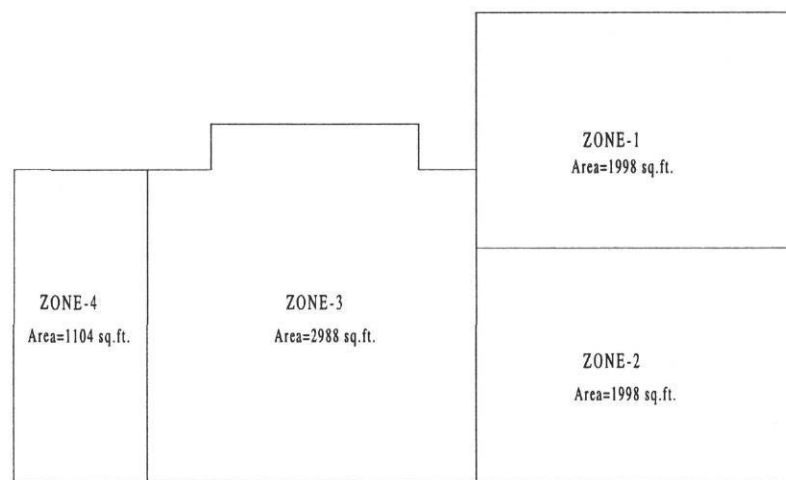
(d)

Figure 4.4 Elevation Views. (a) South. (b) North. (c) East. (d) West.

the four zones respectively. The DOE-2 model was arranged to be thermally consistent with the number of HVAC systems serving the building. Figure 4.5 (a) shows a plan view and includes the building dimensions. Figure 4.5 (b) is a plan view that locates the four zones as they were used in the input file.



(a)



(b)

Figure 4.5 Daycare Center Layout. (a) Plan and Dimensions View. (b) Planview and Zone Location.

4.2 LOADS Sub-program

The LOADS input file was modeled for the period of April 1 through December 21, 1993, which is consistent with the amount of measured energy used for the calibration. Nine months includes a sufficient amount of data to calculate loads during both the heating and cooling seasons (Fels 1986; Kissock et al. 1993). During the final week of the year, the building was not operated in a consistent manner due to the Christmas break and was therefore not simulated. The building is located at 38.85° N latitude, 77.03° W longitude, and at an altitude of 33 feet above sea level. The building operates on a schedule consistent with all federal holidays listed in Table 4.1 and is modeled as such.

Table 4.1 Federal Holidays Observed during the 1993 Simulation Period.

Day/Month	Holiday
Monday, May 31	Memorial Day
Monday, July 5	Independence Day
Monday, September 6	Labor Day
Monday, October 11	Columbus Day
Thursday, November 11	Veterans Day
Thur.-Fri., November 25-26	Thanksgiving Day

4.2.1 Building Construction

The building walls are composed of prefabricated construction materials consisting of 5/8" interior gypsum board, R-13 batt insulation and steel beam frame,

5/8" exterior gypsum board sheathing, and 1/2" light brown exterior face brick as shown in Figure 4.6 (a). The roof in Figure 4.6 (b) is constructed with a thin reflective white roofing membrane, 1-1/2" lightweight corrugated metal decking over a steel beam frame, R-30 batt insulation, and a dropped ceiling. The plenum and the main daycare space are isolated by sound insulating ceiling tiles. The floor consists of carpeting and padding, 4" mesh reinforced lightweight concrete, and R-15.4 rigid insulation over a 3' crawl space as shown in Figure 4.6 (c). The crawl space floor contains gravel on top of a polyethylene vapor barrier. Lastly, Figure 4.6 (d) shows a window section. Limited daylighting is provided by 1" tinted double pane insulated windows with venetian blinds on the ground level. The classroom side of the building has a raised ceiling with the upper north-facing walls containing 1" clerestory untinted insulated windows installed for daylighting purposes.

Figure 4.7 (a) shows the building orientation with surrounding shading surfaces provided by trees and buildings, respectively. The gray surfaces represent the trees, the wall surrounding the daycare center, and the building walls that are included in the DOE-2 input file as shading surfaces. An enlarged view of the daycare center is shown in Figure 4.7 (b) to provide a more detailed view. For shading simulation purposes, flat horizontal planes were used to represent the shading eyebrows above the south-facing windows and vertical planes represent buildings, walls, and trees. A row of trees surrounds the building on the east, south, and west sides. A wall is situated on the building west and north side. Two horizontal window shades, one above each

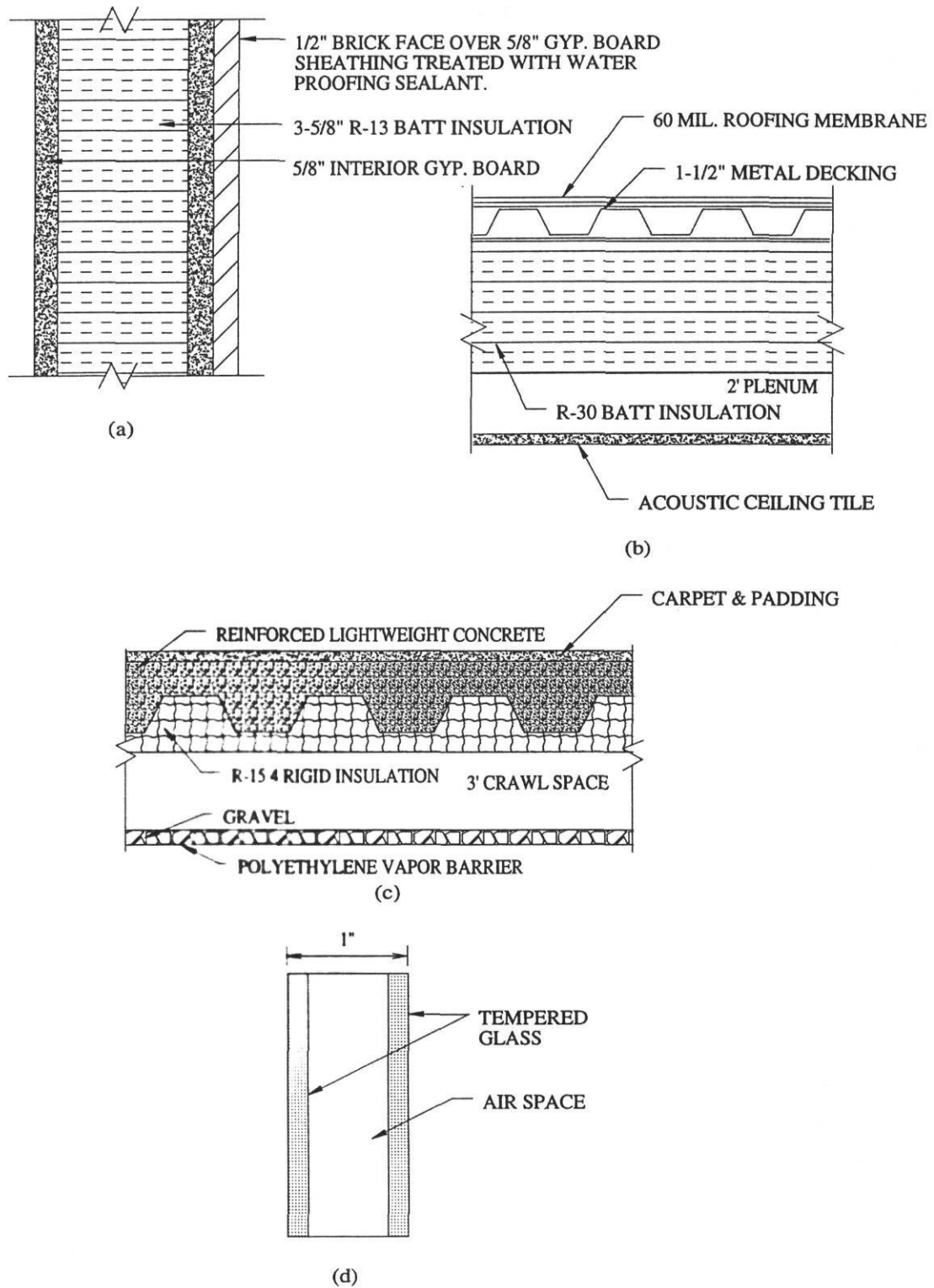
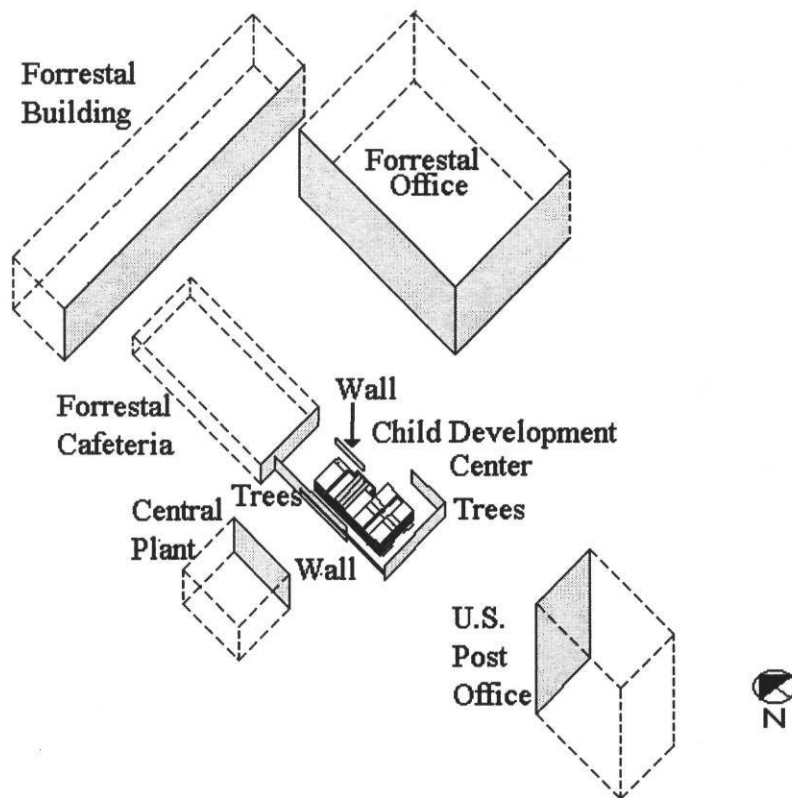
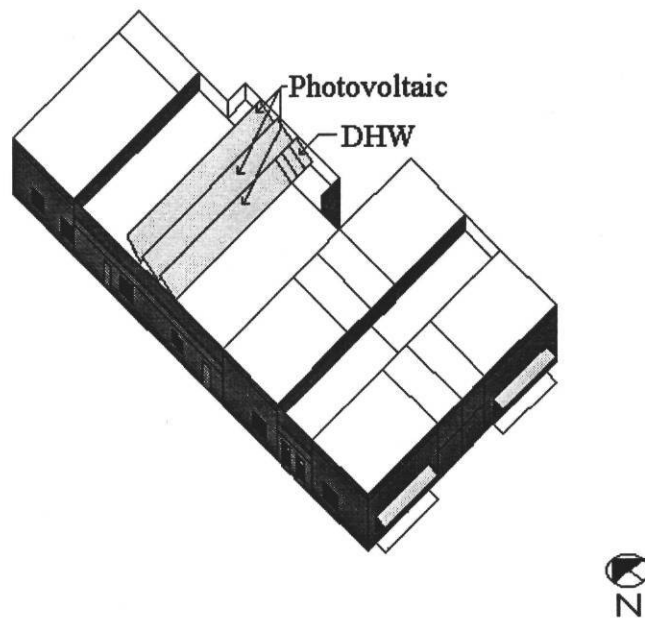


Figure 4.6 Construction Sections. (a) Wall Section. (b) Roof Section. (c) Floor Section. (d) Window Section.



(a)



(b)

Figure 4.7 Daycare Center. (a) Forrestal Complex and Surroundings. (b) Daycare Center. The Solid Planes Represent Shading From Buildings, Walls, or Trees.

bank shade the south side windows. The shading from three photovoltaic solar and DHW solar collector arrays which supplement whole-building electricity and hot water and also provide moderate shading are shown mounted on the roof.

The shading objects and dimensions are summarized in Bou-Saada (1994) as they were measured during the initial site visit. The simple, yet accurate device used to measure the shading dimensions can be seen in Figure 4.8. The tool is composed of a horizontally positioned Libbey-Owens-Ford sun angle calculator (LOF 1974; McWatters and Haberl 1994) specific to the Washington, D.C. latitude and a vertical

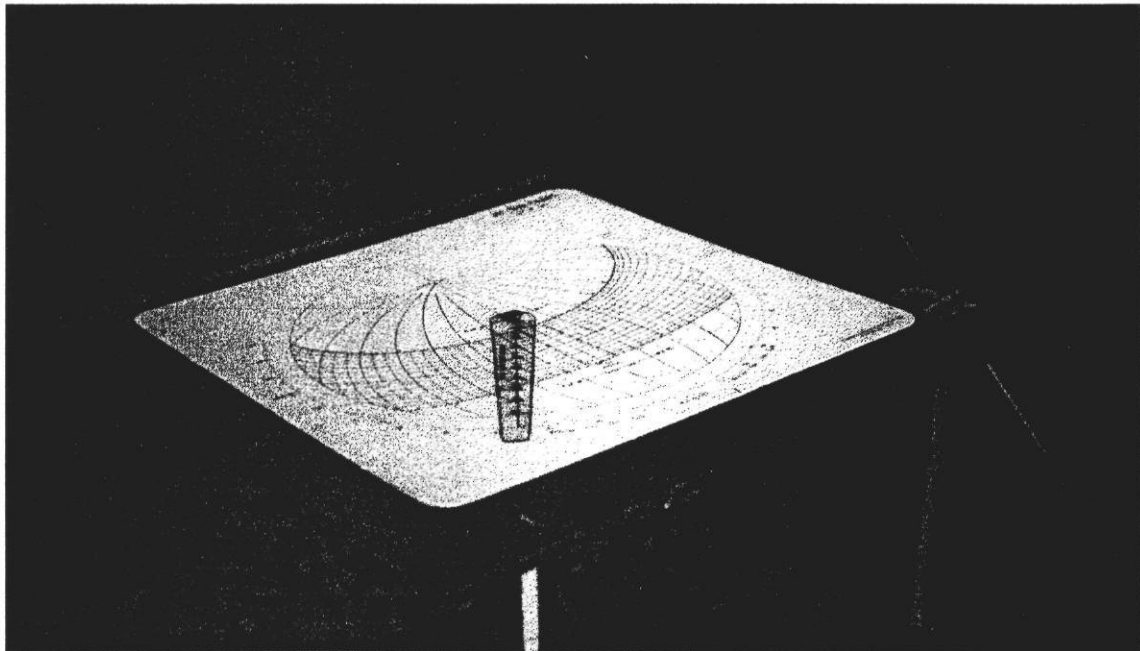


Figure 4.8 Sun Angle Calculator and Altitude Measurement Device.

protractor mounted on a tri-pod which is exactly aligned on a North-South line with a compass. It allows the user to make off-south azimuth measurements and altitude measurements by mounting it on a pre-leveled plane at eye level. The edges of each shading surface were aligned with the horizontal sun angle calculator to measure off-south azimuth angles. The shading surface height was measured by aligning the top of the surface with the base of the vertical protractor and measuring the altitude angle. Simple geometry was then used to calculate the height and width of each surface by knowing the approximate distance of each surface from the measuring device as indicated on site plans and area street maps. Ideally, measurements such as these are generally made with a transit, but unfortunately, one was not available. When using this measurement device, one must also remember to account for the device's altitude from ground level which can be critical on surfaces that are not very tall.

The actual BDL shading surface input can be found under the BUILDING-SHADE command in the DOE-2 input file. The southwest corner of the building was used as the reference point for locating each shading surface (point 0,0,0). The X, Y, and Z coordinates locate the lower left corner of a shading surface with respect to the reference point (X being the abscissa, Y the ordinate, and Z the altitude in feet). The H and W represent the shading surface height and width respectively. The AZIMUTH (AZ) command orients the direction of each surface. For example, a north facing surface has an azimuth of 0°, and a west facing surface has an azimuth of 270°. The TILT command refers to the tilt from horizontal. For instance, the horizontal solar

shades covering the south window banks have a tilt of 0° while the vertical tree surfaces have a tilt of 90° . The amount of shading may also be scheduled to account for deciduous trees. The effect of DOE-2 shading was evaluated by using the shading function in one input file and running the same input file again with no shading. Section 5.1.1 contains more details of the shading analysis performed on the building.

4.2.2 Building Lighting and Equipment

The classrooms, kitchen, hallways, and offices are illuminated with energy efficient 34 W fluorescent lights and electronic ballasts with an average of 1.5 W/ft^2 . Table 4.2 lists the indoor and outdoor lighting details. Some fixtures in the building are activated by motion sensors. Also located in several parts of the building are a variety of task and decorative lights of varying sizes. Several emergency lights and exit signs are located throughout the building that remain operational continuously. Exterior lighting is provided by four - pole-mounted 400 W and twelve - wall-mounted 175 W high intensity discharge fixtures controlled by photo sensors.

The DOE-2 BUILDING-RESOURCE feature is used to model exterior lighting and DHW energy which allows for the accounting of the energy use without contributing to interior loads. By doing so, the information by-passes the LOADS and SYSTEMS sub-programs and is directly passed into the PLANT sub-program where it is added to the hourly energy consumption report. The reason why the BUILDING-

RESOURCE was used is because the DHW system is located in an enclosed utility room in the center of the building. The heat load was assumed to be negligible due to ventilation being provided by penetrations into the plenum above for the solar DHW plumbing.

Table 4.2 Indoor and Outdoor Lighting Summary.

Number of Fixtures	Type	Number of Bulbs	Power (W)	Total Power (W)	Number of Fixtures	Type	Number of Bulbs	Power (W)	Total Power (W)
Zone 1					Zone 3				
10	A - Fluorescent	2	34	748	39	A - Fluorescent	2	34	2917
26	B - Fluorescent	2	34	1945	1	C - Fluorescent	2	34	75
2	C - Fluorescent	2	34	150	2	E - Fluorescent	2	9	40
2	H - Fluorescent	2	34	150	2	D - Fluorescent	2	9	40
2	J - Fluorescent	2	20	88	5	G - Fluorescent	2	34	374
2	X1 - Fluorescent	2	9	40	3	H - Fluorescent	2	34	224
2	R - Fluorescent	2	24	106	4	J - Fluorescent	2	20	176
			Total	3225	3	K - Incandescent	2	60	360
Zone 2					11	L - Fluorescent	2	30	726
10	A - Fluorescent	2	34	748	9	P - Fluorescent	2	34	673
26	B - Fluorescent	2	34	1945	4	X1 - Fluorescent	2	9	79
2	C - Fluorescent	2	34	150	1	X2 - Fluorescent	2	9	20
2	H - Fluorescent	2	34	150				Total	5704
3	J - Fluorescent	2	20	132	Zone 4				
2	X1 - Fluorescent	2	9	40	9	A - Fluorescent	2	34	673
7	R - Fluorescent	2	24	370	11	B - Fluorescent	2	34	823
1	X2 - Fluorescent	2	9	20	1	C - Fluorescent	2	34	75
1	S - Fluorescent	2	24	53	1	E - Fluorescent	2	9	20
			Total	3606	1	K - Incandescent	2	60	120
Outdoor					4	X1 - Fluorescent	2	9	79
12	N - HID	1	175	2415				Total	1790
4	T - HID	1	400	1840					
6	F - Incandescent	1	100	600					
			Total	4855					

The kitchen is equipped with two refrigerators, two freezers, one ice maker, a range, and other small kitchen appliances. Table 4.3 is a summary of the manufacturer specifications for the interior equipment in the kitchen. DHW is primarily supplied by a roof mounted DHW solar collection system which is capable of handling approximately 2/3 of the hot water load according to an F-CHART analysis (F-

CHART 1989). More details on the savings calculations and solar/electric DHW consumption can be found in Chapter VI. An electric DHW heater is available as a backup unit to meet the balance of the hot water load. Both the solar DHW storage tank and the electric DHW heater and tank are located in an enclosed equipment room connected to the kitchen. Since most of the hot water is used for dishwashing and clothes washing, it was assumed that sensible and latent heat gain was minimal since both of these rooms also had exhaust fans.

Table 4.3 Interior Equipment and Appliance List.

ITEM	MANUFAC.	MEAS. AMPS	VA	kW	MODEL	LOCATION
Dishwasher	G.E.	5.2 Mot/4.4 Heat	624 Mot/528 Heat		6SD700L-20	Kitchen
Toaster	Black & Decker	6	720		-	Kitchen
Toaster Oven	Black & Decker	11.5	1380		-	Kitchen
Microwave Oven	G.E.	-	-	0.4	JE1465J001	Kitchen
Blender	Osterizer	1	120		-	Kitchen
Freezer	Frigidaire	7	840		UP19N	Kitchen
Freezer	Frigidaire	7	840		UP16N	Kitchen
Refrigerator	G.E.	9	1080		TBX227	Kitchen
Refrigerator	G.E.	9	1080		TBX227	Kitchen
Ice Maker	G.E.	-	-	-	-	Kitchen
Range	G.E.	-	-	12.1	JB45090N1WH	Kitchen
Washing Machine	G.E.	-	-	-	WWA9850M	Utility
Dryer	G.E.	-	-	-	DDE9600MBLWH	Utility
Coffee Maker	Mr. Coffee	1.5	180		-	Kitchen

On the roof is a photovoltaic system, shown in Figure 4.9 (USDOE 1993), which was designed to supplement the whole-building electricity requirements by up to 6 kW at peak periods³ usually around noon on bright sunny days in the summer.

³ The actual power level never reached this value.

Two personal computers monitor the building systems - one for monitoring the photovoltaic system using a Campbell 21X datalogger and software by SWTDI⁴ and one for monitoring the Robertshaw Controls⁵ Energy Management Control System (EMCS). A building closed circuit security system is also located on the premises consisting of security monitors and roof mounted cameras.

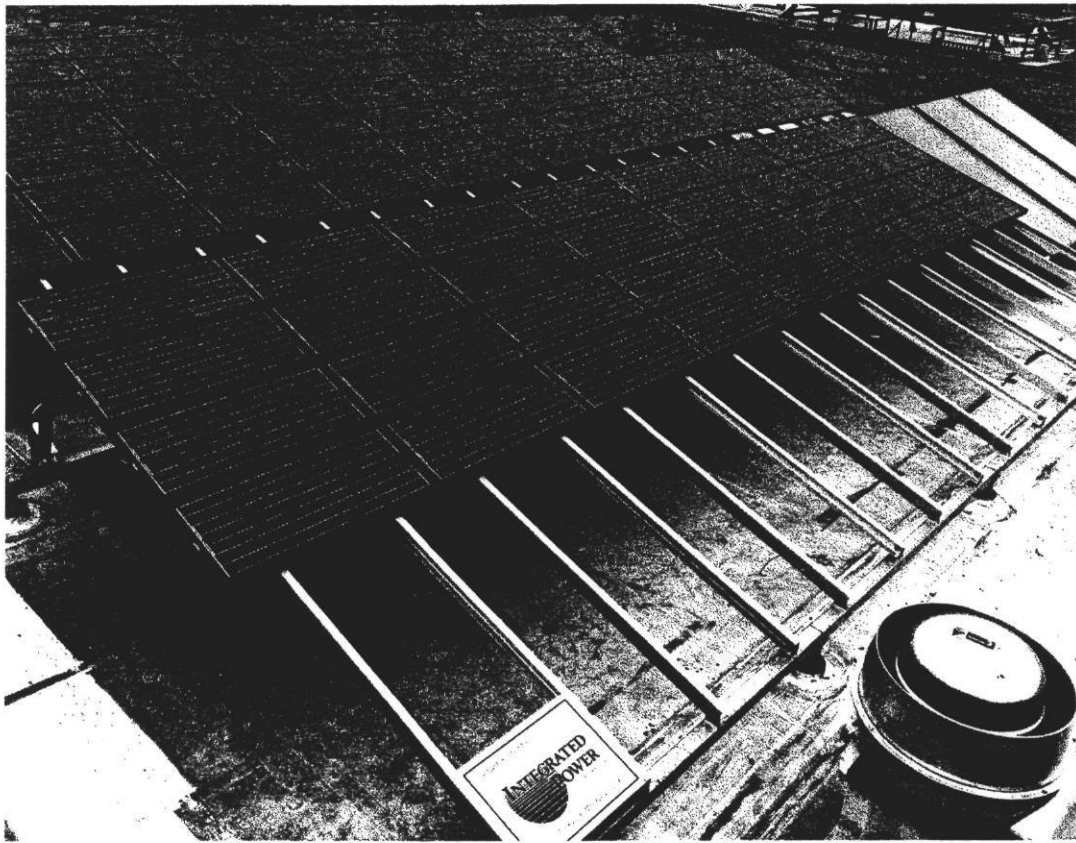


Figure 4.9 Photovoltaic and Domestic Hot Water Solar Panels.

⁴ Southwest Technology Development Institute, P.O. Box 30001, Dept. 390L, Las Cruces, NM, 88003.

⁵ Robertshaw Company, 1800 Glenside Dr., P.O. Box 27606, Richmond, VA, 23261.

4.2.3 Building Schedules

According to information obtained during the initial site visit, the building typically is occupied only on weekdays by approximately twenty staff members and about sixty children. A characteristic day begins at 7:00 a.m. and ends at 6:30 p.m., Monday through Friday. To normalize the relative smaller size of the children and their corresponding heat load, the input file NUMBER-OF-PEOPLE was preset to ten people per zone for a total of forty people. The HVAC system remains on until approximately 9 p.m. to allow for after-hours work and a nightly building inspection by maintenance crew. During afternoon hours, most classroom lights are turned-off during the children's nap time from approximately 1:00 p.m. to 3:00 p.m. This dip in electricity use is readily apparent in the statistical daytype profiles (Figure 5.15).

Hourly operation schedules were preset with estimates based on interviews and building operation schedules. However, equipment schedules, lighting schedules, and hot-water schedules were adjusted several times during the calibration procedure based on the example plots previously introduced in Chapter III and discussed again later in Chapter V with more detail.

4.3 Systems Sub-program

The building's secondary HVAC systems are presented in this section including the type of heating and cooling system, the system controls, the zone air requirements, the system fan equipment, and the equipment schedules.

4.3.1 Building Systems

The HVAC system includes four packaged single-zone high efficiency air-cooled heat pumps, one for each zone (3 - 7-½ ton units and 1 - 4 ton unit). Table 4.4 lists the HVAC equipment, function, manufacturer, motor size and location. Each heat pump (heat pump outdoor unit) is equipped with its own air-handler (heat pump indoor unit) located in one of two equipment rooms. Figure 4.10 is a model of the HVAC system showing the outdoor heat pump units, indoor units, exhaust fans, and control system.

Table 4.4 HVAC Equipment List.

ITEM	FUNCTION	MANUFAC.	SIZE	MODEL	LOCATION
HP-1	Heat Pump	Trane	7.5 Ton	TWE090A300AB	Mech/Outdoor
HP-2	Heat Pump	Trane	7.5 Ton	TWE090A300AB	Mech/Outdoor
HP-3	Heat Pump	Trane	7.5 Ton	TWE090A300AB	Mech/Outdoor
HP-4	Heat Pump	Trane	4 Ton	TWE060A400AB	Mech/Outdoor
EF-1	Exhaust Fan	Cook	1/6 hp	100C2B	Ceiling
EF-2	Exhaust Fan	Cook	1/6 hp	100C2B	Ceiling
EF-3	Exhaust Fan	Cook	1/20 hp	70C15D	Ceiling
EF-4	Exhaust Fan	Cook	1/20 hp	70C15D	Ceiling
EF-5	Exhaust Fan	Cook	1/20 hp	70C15D	Ceiling
EF-6	Exhaust Fan	Cook	1/2 hp	135VSB	Ceiling
EF-7	Exhaust Fan	Cook	1/6 hp	100C2B	Ceiling
EF-8	Exhaust Fan	Cook	1/20 hp	70C15D	Ceiling
EF-9	Exhaust Fan	Cook	1/20 hp	70C15D	Ceiling
EF-10	Exhaust Fan	Cook	frac.	GEM II	Ceiling
EF-11	Exhaust Fan	Cook	1/20 hp	70C15D	Ceiling
SF-1	Exhaust Fan	Cook	1/6 hp	ASP-9	Ceiling
RAF-1	Return Air Fan	Cook	3/4 hp	165SQ10D	Ceiling
RAF-2	Return Air Fan	Cook	3/4 hp	165SQ10D	Ceiling
RAF-3	Return Air Fan	Cook	3/4 hp	165SQ10D	Ceiling
RAF-4	Return Air Fan	Cook	1/3 hp	165SQ17D	Ceiling

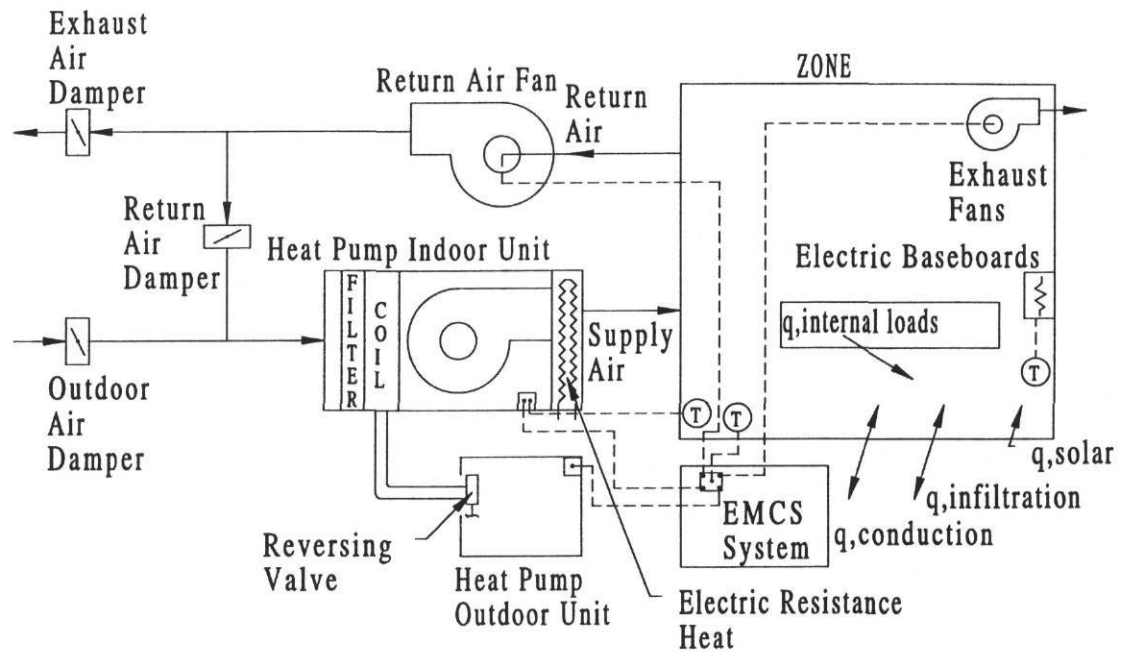


Figure 4.10 Heating, Ventilating, and Air-conditioning System and Controls.

The outdoor unit is a packaged air-cooled heat pump equipped with a reversing valve to direct the refrigerant flow depending on whether heating or cooling is needed. The heat pump indoor unit contains heat exchanger coils, an electric resistance supplemental heater, a supply air fan, and an air filter. Conditioned air is distributed by supply and return ducts located in the plenum. Four ceiling mounted return air fans, one per zone remove air from the zones, exhaust a fraction of the air volume to the building exterior, and return the balance to the indoor units. Outside air is blended with conditioned air at each air-handler. Several exhaust fans are located throughout the building to maintain an air balance. A computer-controlled EMCS controls the

heat pumps, supply air fans, and return air fans based on pre-programmed operating schedules and zone temperature night and weekend setbacks. The heat pump in the play area is supplemented with four electric baseboard heaters which are used when the heat pump reaches its maximum heating capacity. In addition to meeting heat pump capacity, it is believed that the daycare center staff turn the baseboard heaters on in the morning to provide extra heat to the children's play area, especially during the early part of the week.

According to interviews held with the building operations staff, the EMCS periodically failed to set back the thermostats. Therefore, a manual night set-back was initiated and implemented during evening lockup and morning unlock inspections. Since this is accomplishing the same thing that the EMCS night set-back was designed to do the DOE-2 simulation included the setback. An EMCS report sheet that documented all control settings was obtained during the initial site visit and used for the DOE-2 input file thermostat values and schedules. The EMCS manufacturer (Robertshaw Controls) was then contacted for information on the building's control system so that the pertinent data could be used in the input file. The values were then adjusted several times to calibrate the model according to the daytype statistical box-whisker-mean plots detailed in Chapter V.

It was also discovered that the manual zone thermostats had ultimate control capabilities over the HVAC system despite EMCS programming. Building occupants

reset the thermostats several times a day based on personal comfort. Since this made it difficult to simulate the building on a long-term basis, several assumptions were made in HVAC scheduling by both reviewing the measured data sets for trends in recorded temperatures and interviews to develop several custom daytypes. A comparison of occupied and unoccupied CV(RMSE) showed that DOE-2 was still capable of simulating the occupant effect despite the irregularities. This analysis is included in Chapter V.

The system air volume including supply air, return air, and exhaust air was set in the input file according to an air balance report⁶ obtained during the initial site visit. An overall HVAC air balance was performed by an outside contractor after building construction and was assumed to be accurate for the modeling of this building. All fan energy consumption was calculated based on clamp-on current draw measurements performed during the balancing procedure and included in the air balance report. Heating and cooling capacities were obtained from heat pump manufacturer catalog data based on the original specified heat pump model numbers (Trane Co. 1992).

4.4 PLANT Sub-program

The heat pumps were modeled as hermetic centrifugal compression chillers. The exterior lighting and DHW energy use first reported in the LOADS sub-program

⁶ Seneca Balance Inc., 8950 Rt. 108, Suite 127, Columbia, MD, 21045.

is accounted for in this section and added into the hourly total in the hourly report. All other system components were specified by the DOE-2 program default settings. The hourly report produced by the PLANT Sub-program which included whole-building electricity was primarily used as the source for the DOE-2 hourly output during calibration.

4.5 Data Collection and Processing

In order to calibrate the DOE-2 simulation to the existing building, several tasks needed to be accomplished. First, an accurate description of the building was created using the DOE-2 Building Description Language (BDL). This included a careful assessment of all architectural features and shading from nearby objects. Second, measured hourly weather data was collected and processed or "packed" into a format compatible with DOE-2 using existing routines (Bronson 1992). Next, because this building includes a photovoltaic system that is fed directly into the building's electrical system, the electricity it generates was measured and added to the measured whole-building electricity to represent actual whole-building electricity consumption. Finally, about 100 DOE-2 iterations were made to match the simulated output to the measured whole-building electricity data.

On a weekly basis, data were transferred by telephone line from two loggers and the NWS to PCs at Texas A&M University (the NWS procedure is explained later in this section). The first logger "polled" was a Campbell 21X, located in the daycare

center, which records 18° south-tilted global solar radiation, generated photovoltaic electricity, ambient temperature, and solar panel surface temperature. A Synergistics C-180 logger, located in the Forrestal office building, records the daycare center's whole-building electricity usage and other data of importance to another study at the Forrestal building (Haberl et al. 1995). For a full description of additional data channels recorded by the loggers but not used for this thesis, see Bou-Saada (1994).

Every week, the data were appended to a contiguous database (Lopez and Haberl 1992a) which allows for an analysis to be made over the entire dataset. Figure 4.11 shows a summary of the entire nine month weather dataset and includes relative humidity converted from NWS dew point temperature, ambient dry bulb temperature, peak hourly wind speed, and locally measured solar radiation from the Campbell logger. The plot shows global horizontal radiation which was processed with a conversion routine from 18° south-tilted data as will be described in Section 4.6.3.1. Thermal and electrical monitoring diagrams for the Forrestal complex Synergistics C-180 logger and the Campbell 21X logger are shown in Figure 4.12. These figures display what data channels the loggers are monitoring. Since only the daycare whole-building electricity data from one of two Synergistics C-180 loggers and solar and photovoltaic data from the Campbell 21X logger were used for this research, only they

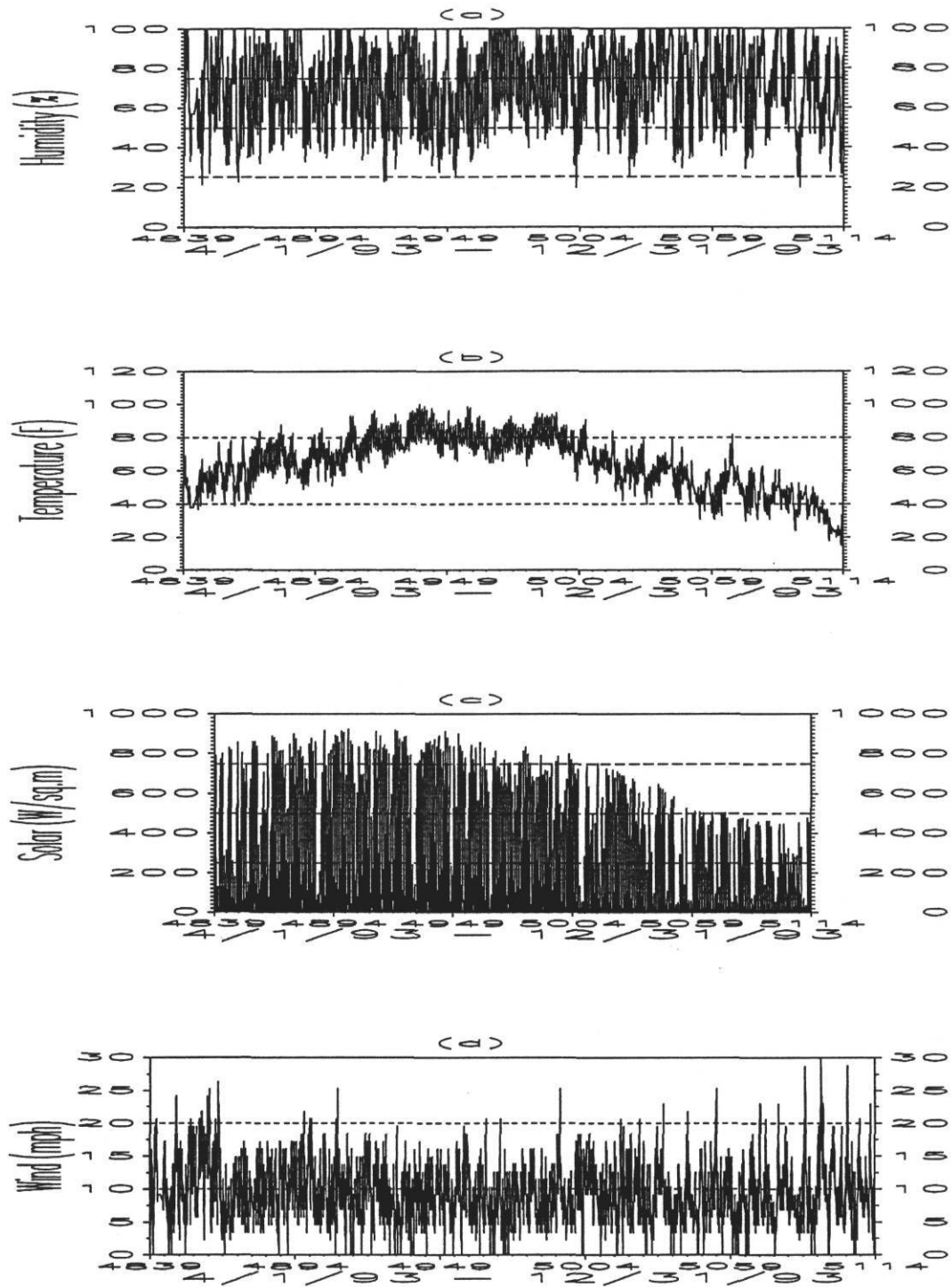
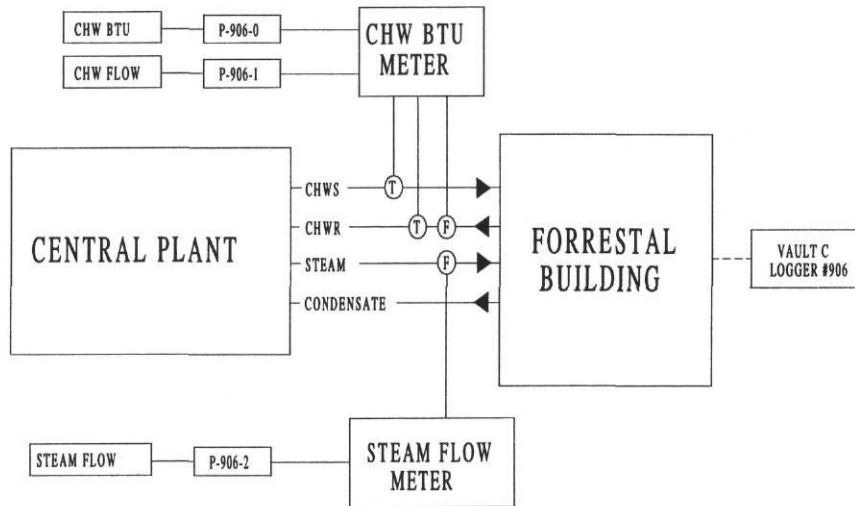


Figure 4.11 Measured Ambient Weather Data.

THERMAL MONITORING DIAGRAM



MONITORING DIAGRAM

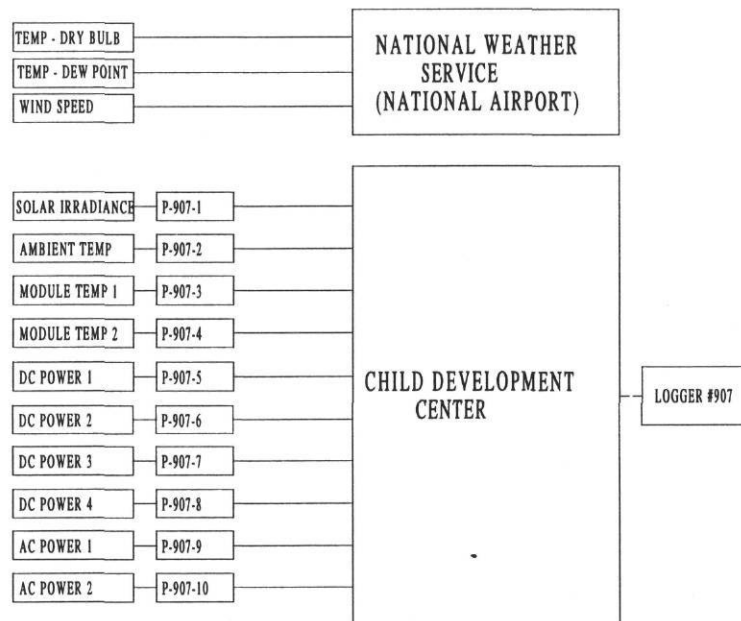


Figure 4.12 Thermal and Electrical Monitoring Diagrams.

ELECTRICAL MONITORING DIAGRAM

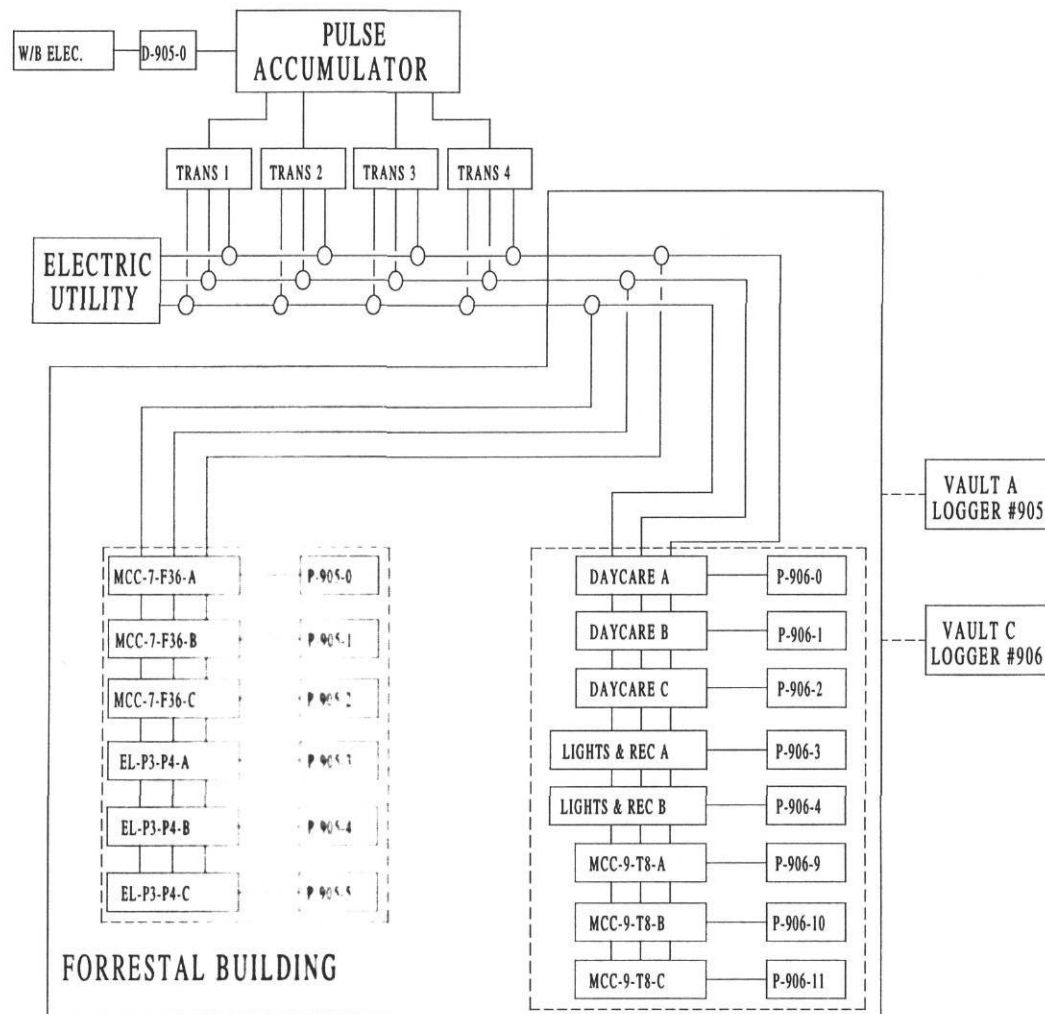


Figure 4.12 (cont'd).

are described in this chapter. Bou-Saada (1994) contains the detailed parameter sets of channel assignments for the loggers. The three loggers' approximate locations with respect to each building in the Forrestal complex are shown in Figure 4.13.

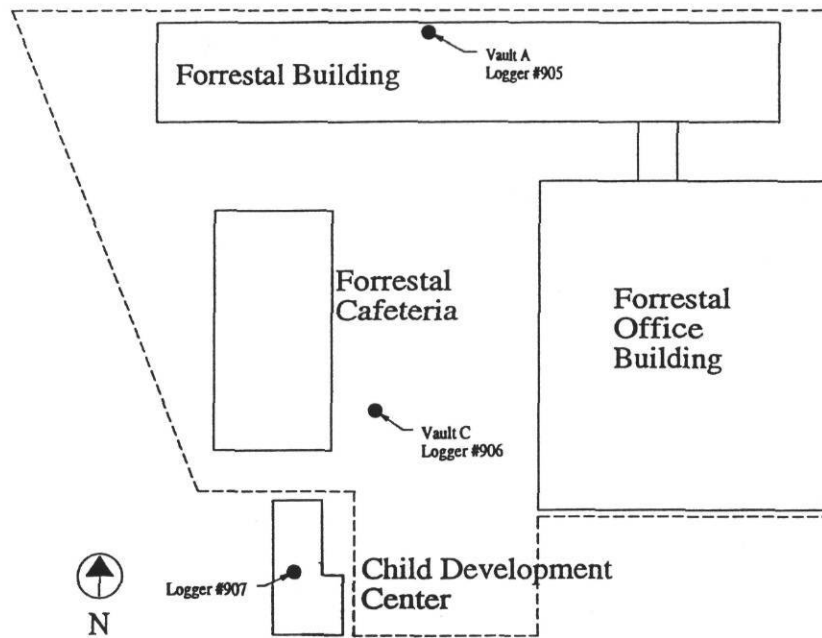


Figure 4.13 Forrestal Complex and Logger Locations.

In Figure 4.14 the flowchart details the step-by-step procedures for polling and processing the data, packing a weather tape, and generating output plots for comparison of simulated hourly data to measured data. Beginning in the upper-left corner, the first information required to develop a DOE-2 input file includes 24-hour daytype profiles, as-built drawings, and information from personal interviews. During a typical simulation session, the input file was created with a PC-based editor and transferred using the file transfer protocol (FTP) (Bhushan 1973) to the university's VAX super minicomputer cluster.

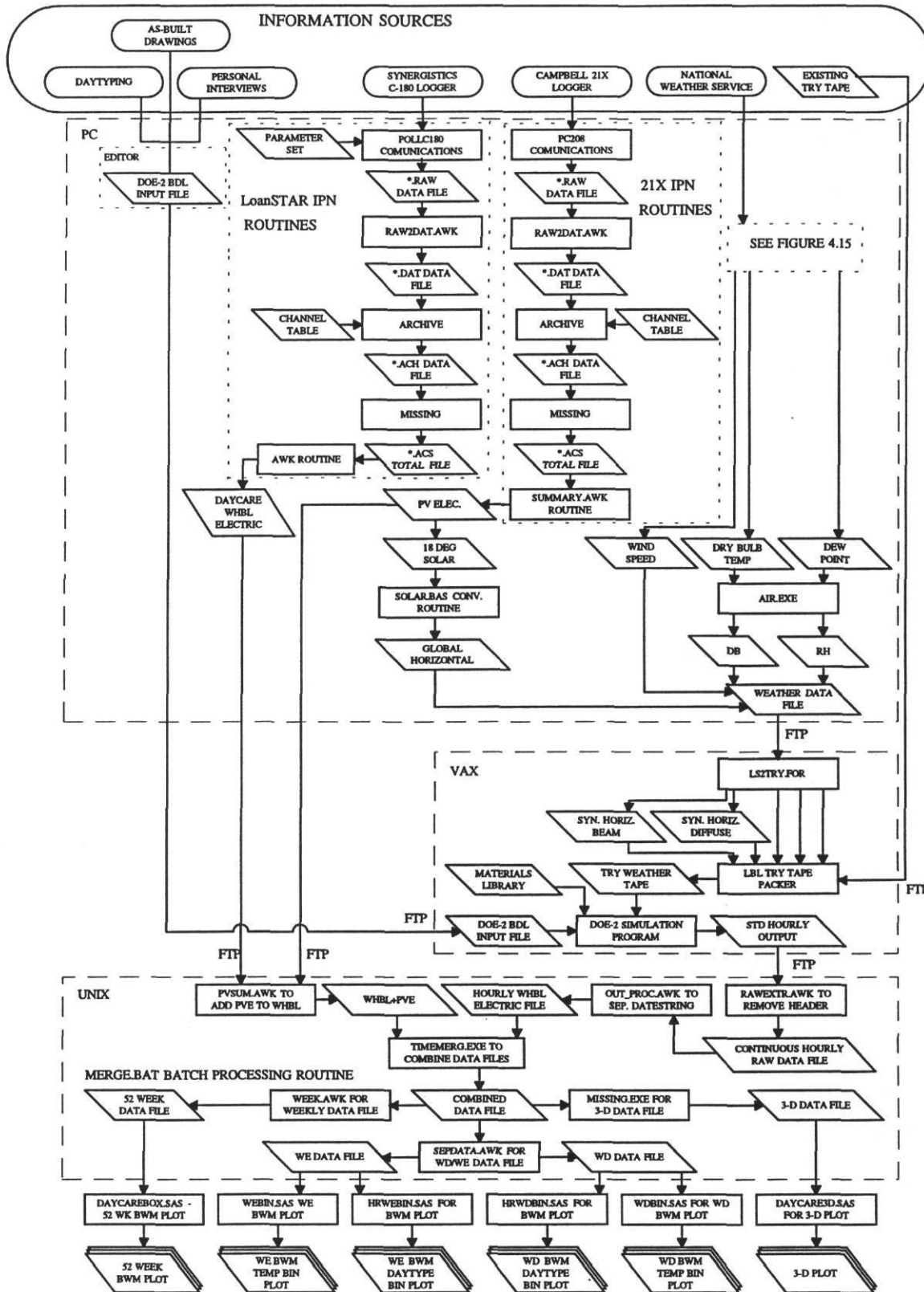


Figure 4.14 Data and Graphical Processing Flowchart.

To acquire measured data from the Forrestal building the Synergistics C-180 logger was polled weekly using the PollC180 communications package (Sparks et al. 1994) in conjunction with the Forrestal building's logger parameter set to create a raw data file. An AWK script (RAW2DAT) was used to convert the raw data file to a columnar ASCII data file and run through the ARCHIVE program (Feuermann and Kempton 1987) to process it into a format consistent with all the information in the general LoanSTAR database (Lopez and Haberl 1992b). AWK is a public domain specialized data processing language originally developed at AT&T Bell Laboratories, and was used to manipulate columnar data easily and efficiently (Aho et al. 1988; FSF 1989). A special AWK script was written for the specific task of removing the measured whole-building electricity column of data and the date stamp for calibration. This task can also be performed by several other tools including the COLS program that accompanies ARCHIVE.

The Campbell 21X logger at the daycare center was also polled weekly using the PC208 (Campbell 1993) communications package specially tailored to produce a comma delimited raw file. Bou-Saada (1994) contains instructions for polling the Campbell 21X data logger. Like the Synergistics logger data, the raw file was also converted into a columnar ASCII data file using RAW2DAT. It was then processed with ARCHIVE to produce a standardized data file that was then added to the LoanSTAR database. The AWK script, SUMMARY (Bou-Saada 1994), was used to extract the photovoltaic column, the solar radiation data measured at an 18° tilt, and

the time stamp. The photovoltaic data was then combined with the Synergistics measured whole-building electricity data via the AWK script, PVSUM (Bou-Saada 1994), into a single data file. In a different processing path, the 18° south-tilted solar radiation data was converted to global horizontal data (0° tilt) using an iterative BASIC program, SOLAR (Bou-Saada 1994), based on a correlation developed by Erbs et al. (1982). The conversion routine and equations will be discussed in Section 4.6.3.1. The Erbs correlation was also used to produce two additional data channels, synthetic horizontal beam data and synthetic horizontal diffuse data that were then packed onto a TRY weather tape using the LS2TRY (Bronson 1992) routine and the LBL TRY tape packer (LBL 1980). For more details on the TRY tape and tape packing, see Chapter III.

The dry bulb temperature, dew point temperature, and peak wind speed that were used in the analysis were recorded by the NWS. Typical NWS weather stations, such as the one located near the Washington, D.C. National Airport runway, incorporates a hygrometer sensor for dew point and ambient dry bulb temperature measurements, an anemometer sensor for wind speed and direction, a ceilometer sensor for cloud height, and an altimeter sensor for air pressure (Crowley and Haberl 1994). Figure 4.15 (a) (Crowley and Haberl 1994) outlines the general procedure followed to obtain the data and process them into a usable format. AccuWeather in State College, Pennsylvania regularly obtains data from a NOAA complete Standard Airways data file supplied by the NWS weather station at National

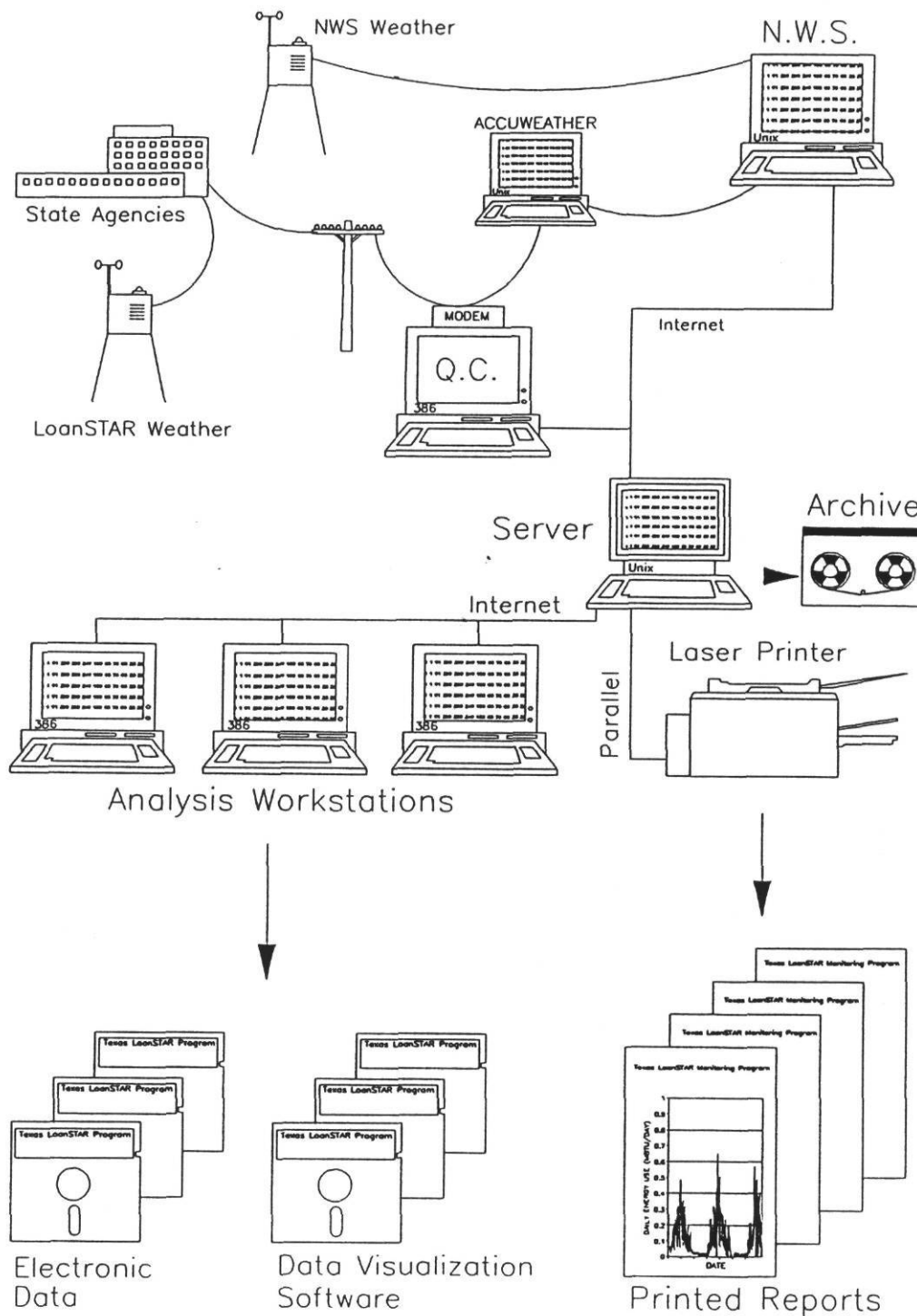


Figure 4.15a National Weather Service Weather Data Gathering Process (Crowley and Haberl 1994).

Airport and converts it into a columnar file before distribution. Once per week, a columnar data set was gathered by modem from AccuWeather which included a numbered site identification stamp, the hour of the day, dry bulb temperature, dew point temperature, and wind speed. The file was then processed with ARCHIVE to append a LoanSTAR time stamp which included the site number, month, day of the month, year, Julian data, decimal date beginning in 1980, and hour of the day. Figure 4.15 (b) (Lopez and Haberl 1992a; 1992b) illustrates the ARCHIVE results by initially combining NWS output and LoanSTAR measured data. The file was then added to the contiguous database described earlier and made ready for use with data visualization software and printed in regularly issued status reports.

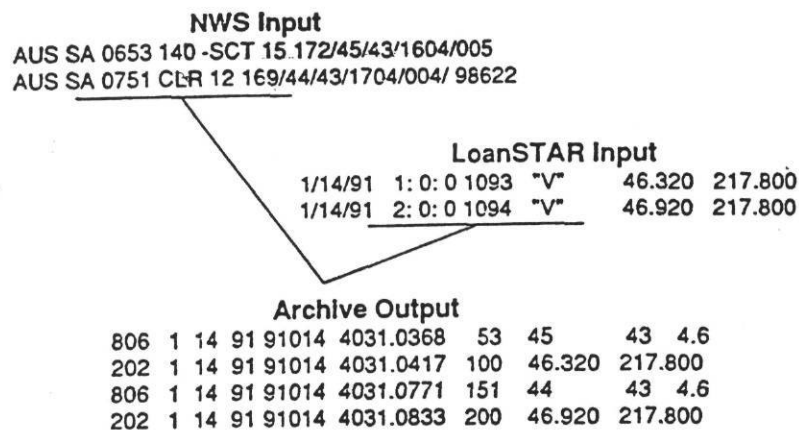


Figure 4.15b LoanSTAR Data Processing Sequence (Adapted from Lopez and Haberl 1992a; 1992b).

The NWS dew point temperature data and NWS dry bulb temperature were used to calculate relative humidity using the AIR psychrometric routines developed by Sparks et al. (1993). Dry bulb temperature, relative humidity, wind speed, synthetic horizontal beam radiation, and synthetic horizontal diffuse radiation were then transferred from the PC via FTP to the VAX main frame computer and packed onto a TRY weather tape using the LS2TRY routine (Bronson 1992) and the LBL TRY (LBL 1980) tape packer.

The DOE-2.1D simulation program was run with a BDL input file for the daycare center and the packed TRY weather tape to produce an hourly output report. The DOE-2 hourly report was then transferred via FTP link to the LoanSTAR UNIX file server for further processing. The AWK script, RAWEXTR (Bronson 1992), was used to remove the DOE-2 hourly report headers to produce an hourly raw data file that consists of sequential ASCII columnar data. Another AWK script, OUT_PROC (Bronson 1992), was then used to separate the DOE-2 report datestring by calculating a decimal date from the Gregorian date. In addition, the AWK script removes the daylight savings shift and then produces an hourly simulated whole-building electricity file. The simulated whole-building electricity file was then merged with the combined measured whole-building data and photovoltaic electricity data into a single data file using the TIMEMERG program (Sparks et al. 1992a). The combined data file was now ready to be used for the statistical analysis.

Three basic types of plots were utilized for this thesis which included the 52-week box-whisker-mean graph, the weekday/weekend box-whisker-mean graphs, and the three-dimensional graphs. Depending on which plots were required, three different processing paths were chosen. The statistical graphing routines were introduced in Chapter III and are fully described with respect to the calibration results used for this thesis in Chapter V. In regard to Figure 4.14, these routines were used in the following manner. In order to produce the 52-week box-whisker-mean plots, an AWK script, WEEK (Abbas 1993), was used to scan every row of data by counting 168 records for each week and labeling it with the week number. Then a new data file was created with the appended week number which was then used to generate a 52-week box-whisker-mean plot with the SAS routine (DAYCAREBOX) (Bou-Saada 1994).

The second processing path begins with the AWK script, SEPDATA (Bou-Saada 1994), which was used to separate the whole-building electricity data file into four files: a total weekday file, a weekday occupied file, a weekday unoccupied file, and a total weekend file. The respective files were then processed with four additional SAS scripts, each to generate temperature bin plots (WEBIN, WDBIN) (Bou-Saada 1994) and weather daytype plots (HRWEBIN, HRWDBIN) (Bou-Saada 1994). The third path is used to produce three-dimensional plots. In order to pass along the third path, a three-dimensional SAS graphics routine first required a full year of data to be properly plotted. Since DOE-2 was not used to simulate the building for an entire year, the data file was run with MISSING (Sparks et al. 1992b) to fill in "-99.0" data

for one year. DAYCARE3D (Bou-Saada 1994) was then used to generate a three-dimensional plot that compared measured and simulated whole-building electricity data.

4.6 Solar Weather Data Formatting

When simulating a building with measured weather data, solar radiation is required for the packed weather file. One obstacle frequently encountered is the need to synthesize solar data when measured site data are not available, as was the case at the beginning of this research. As the work progressed, this was no longer a problem because enough measured solar data was available for both the cooling and heating seasons. However, this can be an impediment when short-term measured data exists or when the dataset is incomplete (i.e. frequent periods containing missing data). Another problem encountered in this research was the measurement of radiation data at an 18° south facing tilt which required a special global horizontal data conversion routine. More information on this procedure is given in Section 4.6.3.1.

An accurate DOE-2 simulation should ideally have enough weather data through the cooling season period, the heating season period, and a period in between both. A few methods have been reviewed for this thesis to obtain global horizontal radiation for Washington, D.C. including a method developed by Löff et al. (1966) and the LBL method (LBL 1980). The Löff method, discussed further in Section 4.6.2, makes use of percent possible sunshine and locally derived empirical coefficients to

calculate daily total horizontal sunshine. The LBL method⁷ derives solar radiation from cloud amount and cloud type. Eventually, neither method was used since enough solar data had been measured during the time required to perform the synthesizing analysis.

Bronson's packing routine, which was employed in this thesis, converts solar radiation into beam and diffuse radiation using the method developed by Erbs et al. (1982). The LBL TRY weather packer converts the ambient weather data into units compatible with the DOE-2 weather packer.

4.6.1 Database Solar Radiation Data

Purchasing solar radiation data from existing databases was also investigated in order to pack a complete twelve month weather tape. Several difficulties were encountered with this option including an incomplete database and unreliable data. The NCDC is the prime data supplier in the United States which has a capability of providing a vast quantity of weather data. Unfortunately, the solar radiation database is severely deficient in both data quantity and data quality. A 30 year database is available for a few sites across the nation from 1951 to 1990. The NWS was the main agency responsible from 1951 through 1975 and had a network of 60 weather stations recording global horizontal solar radiation. In the beginning the data were primarily

⁷ Mr. Fred Buhl. 1994. Personal Communication, Berkeley, CA: Lawrence Berkeley Laboratory.

collected on strip charts and digitized into a database (NREL 1992). A lack of calibration is the main source of error found with these data.

In 1976, no data were collected to allow for network instrumentation upgrading. The USDOE and NOAA carried on the collection effort initiated by the NWS from 1977 through 1980 and maintained a reliable database with the support of adequate funding and reliable instrumentation. From 1981 through 1985, the data collection again deteriorated due to insufficient funding. No solar radiation data is available from 1985 through 1987 as a result of the collection breakdown. The network was then upgraded in 1988 for 29 stations and then shut down again in 1990. Therefore, no solar data were available for the measured period for the case study building. Because of this it was then decided to utilize the data collected at the 18° tilt and translated into horizontal solar radiation as will be discussed in Section 4.6.3.1.

4.6.2 Synthetic Solar Data

Another method considered to lengthen the amount of solar data was synthesizing hourly global horizontal radiation from NWS daily minutes of sunshine based on correlations developed by Löff (Kreider and Kreith 1981) and daily to hourly correlations by Collares-Pereira and Rabl (1979). Löff's methodology calculates the daily sky clearness index (K_t) and the daily percent possible sunshine (PP) from NWS measured daily minutes of sunshine (Duffie and Beckman 1991). Figure 4.16 is a flowchart detailing the methodology used to compare K_t with PP. Figure 4.17 presents

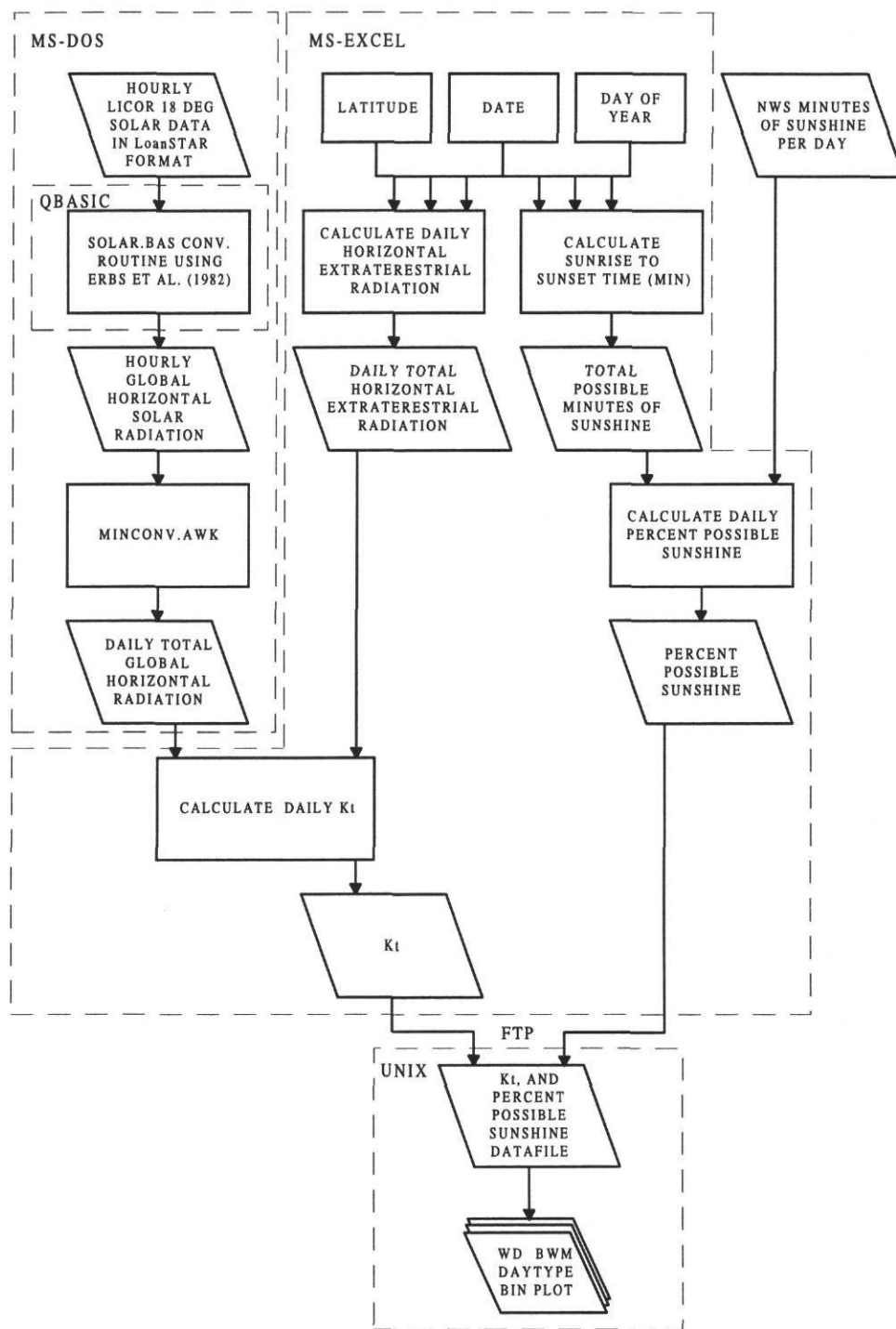


Figure 4.16 Kt and Percent Possible Sunshine Flowchart.

the measured available daily solar radiation as a function of daily minutes of sunshine. Percent possible sunshine was used with the equation developed by L f which uses the PP, empirically derived constants specific to the geographical region, and the constant extraterrestrial radiation factor to estimate daily total horizontal radiation. The daily total horizontal radiation was then used with an equation developed by Collares-Pereira and Rabl to estimate synthetic hourly horizontal radiation and complete the nine month data set.

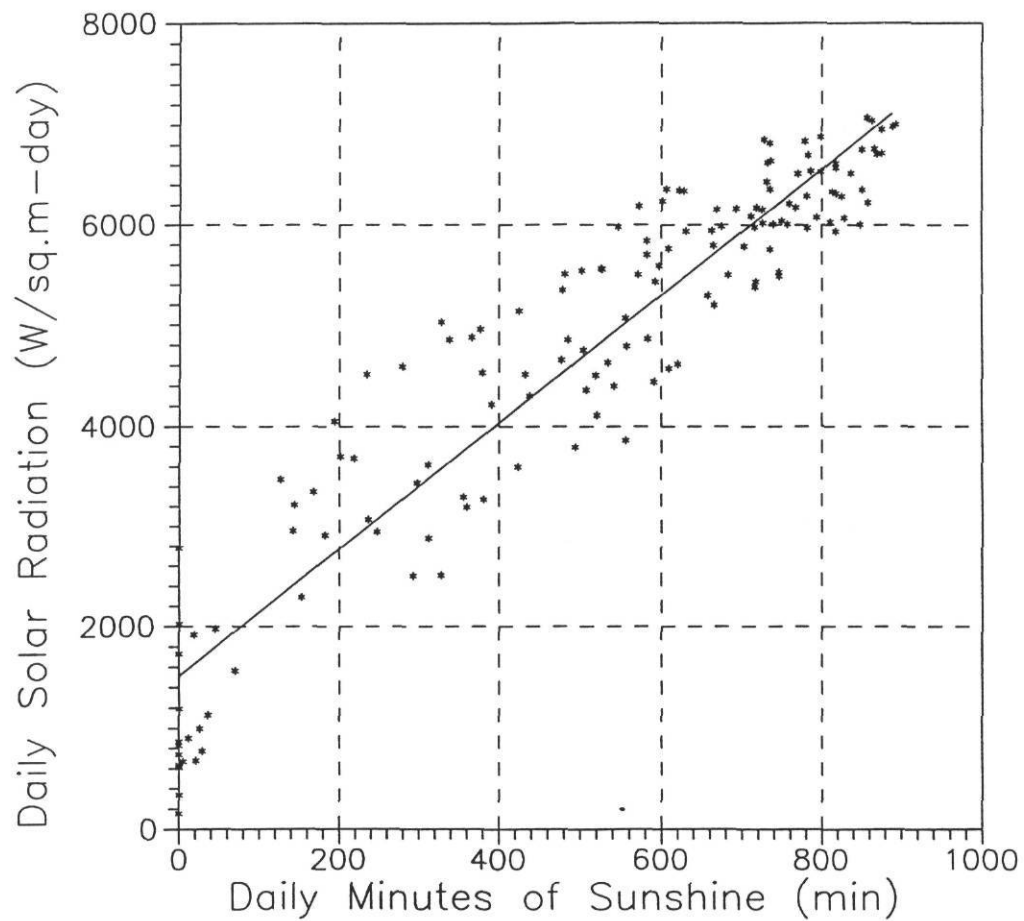


Figure 4.17 Daily Solar Radiation and Daily Minutes of Sunshine.

As Figure 4.18 shows, the clearness index, dependent on the PP, contains a significant amount of scatter. Unfortunately, an accurate calculation could not be made since the curve-fit equation was an approximation at best yielding only a 34.9% CV(RMSE). The error may be attributed to instrumentation differences encountered in the total solar radiation instrument, the pyranometer, and the NWS sunshine recorder. According to Kreider, the results “can only be expected to be accurate on the average at best.”⁸

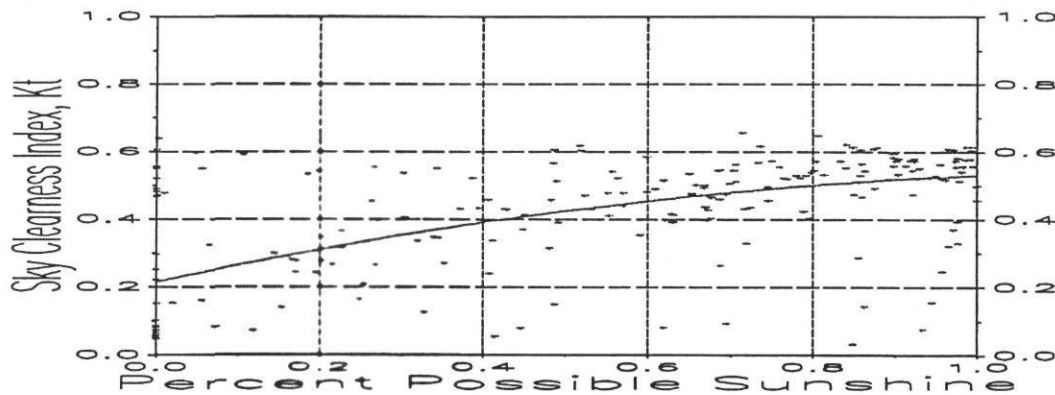


Figure 4.18 Sky Clearness and Daily Percent Possible Sunshine.

The original device used by the NWS to measure minutes of sunshine was often a Foster Sunshine Switch (Foster and Fosket 1953, ref. Duffie and Beckman 1991). The recorder is composed of two thermocouples, one shaded from beam

⁸ Kreider J.F. and F. Kreith. P. 2-70.

radiation and one not shaded. When the sun is shining, the thermocouples sense two different temperatures and record the duration of sunshine. During periods of no sunshine, the two thermocouples record identical temperatures indicating no sunshine. The amount of sunshine is continuously summed during a 24-hour period and reported as minutes of sunshine.

4.6.2.1 Synthetic Photovoltaic Data

Since the building is equipped with a photovoltaic system on the roof that had to be evaluated (see Chapter VI), twelve months of solar data was necessary to calculate annual energy savings. For the case study building, only nine months of measured data was available. Therefore, a method was required to synthesize twelve months of solar data based on available data. Figure 4.19 shows the available hourly photovoltaic data measured over nine months. In order to synthesize the photovoltaic data, the daily measured photovoltaic energy were first plotted versus daily measured global horizontal solar radiation and a best fit curve calculated as was shown in Figure 4.17. The analysis in Figure 4.17 yielded a CV(RMSE) of 12.6%. Next, hourly solar radiation was extracted from a Washington, D.C. TMY weather tape and summed to daily solar radiation data. Synthetic photovoltaic data was then calculated based on the TMY daily solar data and the curve-fit equation previously calculated. The daily photovoltaic data was then summed over entire year and used to verify the operation of the photovoltaic system as is described in Section 6.3 with more detail.

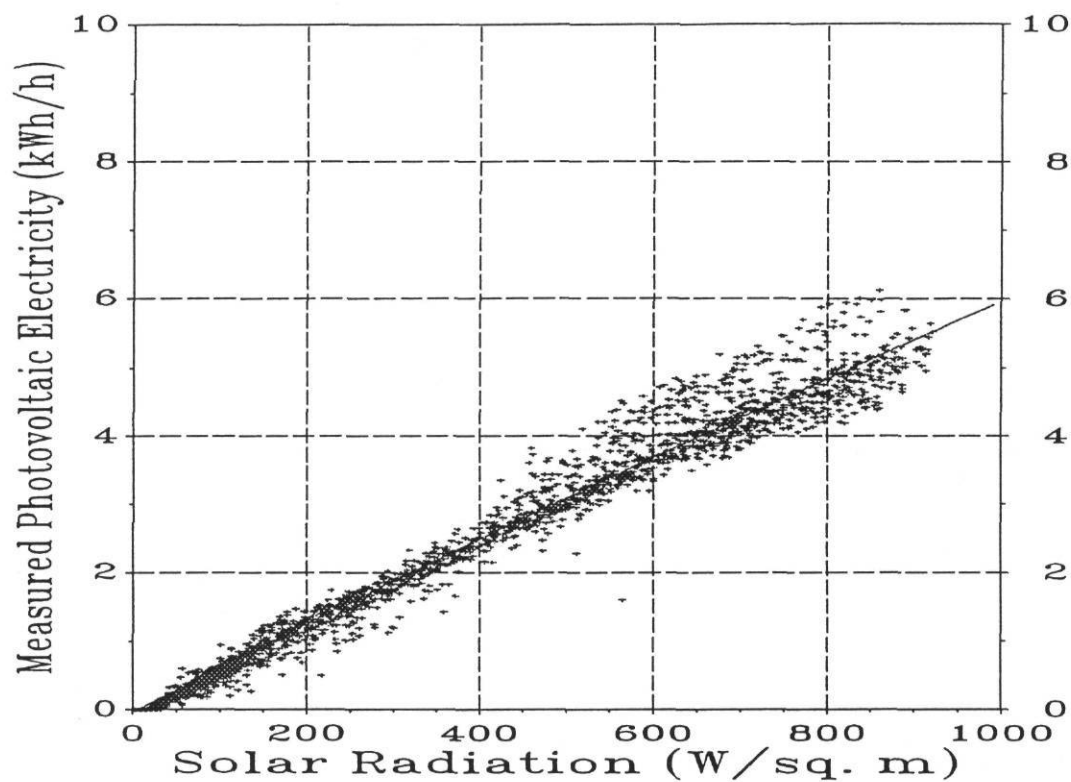


Figure 4.19 Hourly Photovoltaic Electricity and Hourly Solar Radiation.

This section has clearly demonstrated that measured solar data is difficult to substitute. The experience gained from this research indicates that certain methods of synthesizing solar data may not be reliable enough for use with DOE-2. Since the NWS has not provided solar data since 1990, DOE-2 users are either left with using standard weather tapes or measuring solar data on-site. Therefore, it is recommended to measure solar data on a horizontal surface in order to avoid the problems encountered with questionable conversions from NWS data. Although a conversion

solution was found for this thesis, this task was time consuming and can be impractical for most applications, especially in a commercial consulting environment.

4.6.3 Measured Solar Data Conversion

Due to the unavailability of reliable NCDC solar radiation data for 1993 and the severe uncertainty encountered with synthesizing hourly data from the NWS daily minutes of sunshine it was decided to collect solar radiation data on-site for use with DOE-2. For this research, global solar radiation was measured on-site at an 18° angle tilted from the horizontal toward the south, the same tilt angle of the photovoltaic solar panels located on the roof. Global horizontal solar radiation, sometimes called total solar radiation, is the sum of the beam and the diffuse radiation on a horizontal surface (Duffie and Beckman 1991). It was therefore necessary that these data be converted into global horizontal solar radiation (0° tilt) using a correlation developed by Erbs et al. (1982), given in equation 4.10 in Section 4.6.3.1, and a special conversion routine developed for this research (SOLAR)⁹.

4.6.3.1 Global Horizontal Solar Conversion Routine

The SOLAR routine begins by reading an input file containing a LoanSTAR time stamp and tilted solar radiation data. A twelve hour example of the input and output is given in Figure 4.20 (a) and 4.20 (b). The first seven columns represent the

⁹ Dr. T. Agami Reddy. 1993. Personal Communication, Energy Systems Laboratory, Texas A&M University.

LoanSTAR site and time stamp information, (i.e. site, month, day, year, julian date, decimal date, and hour). Column eight in Figure 4.20 (a) is the solar radiation recorded at the 18° tilt. In Figure 4.20 (b), column eight denotes the converted solar radiation data which were used to pack onto the TRY weather tape. The day of year (**n**) is then extracted from the Julian date by subtracting 93,000¹⁰. The day of year was then used to calculate solar declination, δ (Duffie and Beckman 1991):

$$\delta = 23.45 \cdot \sin \left(2 \cdot \pi \cdot \frac{284 + n}{365} \right) \quad (4.1)$$

$$(-23.45^\circ \leq \delta \leq 23.45^\circ)$$

(note: all equations except for those with 360° are in radians. To convert radians to degrees, multiply the angle by $\frac{180^\circ}{\pi}$.)

After solar declination is calculated, an hourly loop is used to perform calculations for each hour of the day. Since the logger is programmed to sum readings each hour to show the value at the mid point of the hour. For example, 1300 is the solar radiation recorded from the 1201 hour to the 1300 hour (12:01 p.m.-1:00 p.m.). The half hour subtraction will result in a 12:30 p.m. reading.

¹⁰ The routine must be modified for years other than 1993.

907 4 1 93 93091 4839.0417 100 -0.008
 907 4 1 93 93091 4839.0833 200 -0.010
 907 4 1 93 93091 4839.1250 300 -0.025
 907 4 1 93 93091 4839.1667 400 -0.021
 907 4 1 93 93091 4839.2083 500 -0.022
 907 4 1 93 93091 4839.2500 600 0.087
 907 4 1 93 93091 4839.2917 700 5.013
 907 4 1 93 93091 4839.3333 800 35.210
 907 4 1 93 93091 4839.3750 900 88.600
 907 4 1 93 93091 4839.4167 1000 135.700
 907 4 1 93 93091 4839.4583 1100 190.700
 907 4 1 93 93091 4839.5000 1200 407.000

(a)

907,4,1,93,93091,4839.042,100,0
 907,4,1,93,93091,4839.083,200,0
 907,4,1,93,93091,4839.125,300,0
 907,4,1,93,93091,4839.167,400,0
 907,4,1,93,93091,4839.208,500,0
 907,4,1,93,93091,4839.25,600,.087
 907,4,1,93,93091,4839.292,700,5.013
 907,4,1,93,93091,4839.333,800,35.88045
 907,4,1,93,93091,4839.375,900,90.19685
 907,4,1,93,93091,4839.417,1000,138.0671
 907,4,1,93,93091,4839.458,1100,193.9263
 907,4,1,93,93091,4839.5,1200,407.5798

(b)

Figure 4.20 Solar Data Example. (a) Global Solar Radiation Data Recorded at an 18° South Facing Tilt. (b) Global Horizontal Radiation Data After Processing with SOLAR.

To account for solar time as opposed to standard time, a solar time correction is used to correct for differences in longitude, the equation of time, and daylight savings (Duffie and Beckman 1991). Since time meridians are divided in sections of 15°, the sun is not directly overhead at 12:00 p.m. unless the collector is located exactly on a meridian (the Eastern time zone meridian is 75° W while Washington D.C. is located at 77° W). Solar time (Duffie and Beckman 1991) is found by:

$$\text{solar time} = \text{standard time} + 4(L_{st} - L_{loc}) + E \quad (4.2)$$

where L_{st} is the standard meridian, L_{loc} is the local meridian, E is the equation of time (Duffie and Beckman 1991) calculated by 11:

$$E = 229.2(0.000075 + 0.001868 \cdot \cos B - 0.032077 \cdot \sin B - 0.014615 \cdot \cos 2B - 0.04089 \cdot \sin 2B) \quad (4.3)$$

and

$$B = (n - 1) \frac{360}{365} \quad (4.3a)$$

11 Numerous equations such as eq. 4.3 have been developed that calculate the equation of time.

Photovoltaic-type solar sensors record negative nighttime radiation values since pyranometers radiate energy to the sky dome. Therefore, a check for negative radiation is then made by truncating all such values to zero. In reality, solar radiation is zero because the sun is behind the horizon. Due to limitations of the correlations, the program equates global horizontal radiation to global tilted radiation for hours occurring before 5:00 a.m. and hours after 5:30 p.m. The difference between the two is minimal during this period.

Since the Earth's rotation is 15° per hour, the hour angle (ω) must then be calculated as is shown in the next equation (Duffie and Beckman 1991):

$$\omega = (\text{solar time} - 12) \cdot 15 \quad (4.4)$$

This is accomplished by subtracting 12 from the calculated solar time and multiplying by 15. For example, 12:00 noon solar time is defined to be 0° . All hours occurring before solar noon are negative while hours occurring after solar noon are positive (10:00 a.m. is -30° , 3:00 p.m. is 45° , etc.).

Next, an hourly clearness index, k_T , is calculated which is the ratio of global horizontal radiation, I_H , to extraterrestrial radiation, I_0 . I_0 is the radiation that would be received in the absence of the atmosphere on a horizontal surface at the same

latitude, longitude, and time of the year (Duffie and Beckman 1991). It is calculated by the following equation:

$$I_o = I_{sc} \left(1 + 0.033 \cdot \cos \frac{360 \cdot n}{365}\right) \cdot (\sin \phi \cdot \sin \delta + \cos \phi \cdot \cos \delta \cdot \cos \omega); \frac{W}{m^2} \quad (4.5)$$

with the solar constant $I_{sc} = 1367 \frac{W}{m^2}$, ϕ is the latitude for Washington, D.C.

in degrees, and n is the day of the year.

The fundamental equation to calculate global radiation on a tilted surface using global horizontal radiation and diffuse radiation (Duffie and Beckman 1991) is:

$$I_T = r_{b,t}(I_H - I_D) + I_D(r_{d,t}) + I_H \cdot \rho(r_{r,t}) \quad \text{where} \quad (4.6)$$

$$r_{d,t} = \left(\frac{1 + \cos \beta}{2}\right) \quad \text{and} \quad (4.6a)$$

$$r_{r,t} = \left(\frac{1 - \cos \beta}{2}\right) \quad (4.6b)$$

where I_D is the isotropic diffuse radiation, β is the solar collector tilt angle, ρ is the ground reflectance, and $r_{b,t}$ is a tilt factor for the beam radiation which is discussed shortly. Since only I_T , the radiation measured on the tilted surface, is known and both

I_H and I_D are not known, we can solve for the ratio $\frac{I_T}{I_H}$ by rearranging the above

equation as follows:

$$\frac{I_T}{I_H} = r_{b,t} - \frac{I_D}{I_H} \left(r_{b,t} - \frac{1}{2} - \frac{\cos \beta}{2} \right) + \rho \left(\frac{1 - \cos \beta}{2} \right) \quad (4.7)$$

This equation is specifically arranged so that the Erbs equation, eq. 4.11, can be used to calculate $\frac{I_D}{I_H}$ by iteratively solving for $\frac{I_D}{I_H}$ by using guestimates of k_r . A known conversion factor, $r_{b,t}$ (Duffie and Beckman 1991), converts beam radiation from a horizontal surface to the collector plate. The $r_{b,t}$ tilt factor for beam radiation is the ratio of the cosine of the angle of incidence on the solar collector plane, $\cos \theta$, to the cosine of the angle of incidence on a horizontal surface, $\cos \theta_z$ (also known as the zenith angle), and is calculated by the following equation:

$$r_{b,t} = \frac{\cos \theta}{\cos \theta_z} \quad (4.8)$$

where $\cos \theta$ is the cosine of the angle of incidence on the south facing solar collector plane and is given by:

$$\cos \theta = \cos(\phi - \beta) \cdot \cos \delta \cdot \cos \omega + \sin \delta \cdot \sin(\phi - \beta) \quad (4.9)$$

and $\cos \theta_z$ is the cosine of the angle of incidence on a horizontal surface or zenith angle. θ_z is determined from the following equation:

$$\cos \theta_z = \cos \phi \cdot \cos \delta \cdot \cos \omega + \sin \delta \cdot \sin \phi \quad (4.10)$$

Erbs et al. (1982)¹² defined three correlations that compare diffuse fraction ($\frac{I_D}{I_H}$) to a

clearness index (k):

$$\frac{I_D}{I_H} = \begin{cases} 1.0 - 0.09 \cdot k & k \leq 0.22 \\ 0.951 - 0.164 \cdot k + 4.388 \cdot k^2 - 16.638 \cdot k^3 + 12.336 \cdot k^4 & ; 0.22 < k \leq 0.8 \\ 0.165 & k > 0.8 \end{cases} \quad (4.11)$$

Diffuse radiation, I_D , or sky radiation is scattered radiation due to the atmosphere.

Since I_D and I_H are still not known, a value for the clearness index, k_T , must be assumed to calculate $\frac{I_D}{I_H}$ above. The estimated value is labeled k_{est} in the conversion program to avoid confusion between it and the calculated clearness index k_T . The initial assumption is arbitrarily begun at 0.1 and is automatically increased by the program with a step function for values of k_{est} between 0 and 1. From this, we may now use $\frac{I_D}{I_H}$ to find $\frac{I_T}{I_H}$ from the above equations. Since I_T is known (measured), I_H

¹² Other correlations have been published as well including those by Orgill and Hollands, and Reindl-Beckman-Duffie.

may now be calculated. To verify that the initial guess of k_{est} is valid, the next step is to divide the synthesized I_H by I_0 to calculate k_T . The new value, k_T , is compared to the assumed clearness index value, k_{est} . If both are found to be within a small tolerance arbitrarily set to 0.025 (2.5%) the calculated solar radiation value, I_H , is accepted. If not, then k_{est} would increase by the step function until a maximum value of one is reached or k_{est} and k_T converge. Diffuse radiation (I_D) and beam radiation ($I_H - I_D$) are also byproducts of this calculation.

Once the synthesized hourly horizontal radiation, I_H , is calculated, the program proceeds to calculate the next hour's values until the entire data set is converted to horizontal radiation. Several assumptions were made to convert the data. First, an isotropic sky was presumed (i.e. diffuse radiation that emanates uniformly from the sky hemisphere). Second, the ground reflectance, ρ , was assumed to be a constant 0.2, roughly equal to concrete (LBL 1980). The synthesized hourly beam and diffuse radiation data were then ready to be packed onto the TRY tape and the global horizontal radiation was ready for use by the photovoltaic analysis.

4.7 Summary

Chapter IV described the case study building and how each DOE-2 sub-program input file detail related to the building. The hourly measured inputs were detailed which included whole-building electricity, relative humidity, dry bulb temperature, peak wind speed, and solar radiation. A special routine was developed to convert the

hourly solar radiation data measured at an 18° south facing tilt to hourly global horizontal radiation data. The site-specific weather data was then packed onto a TRY weather tape for use with DOE-2. Finally, the entire data analysis process was detailed beginning with initial data measurement and ending with the graphical tools developed for this thesis. Chapter V describes how the methodology discussed in Chapter III was applied to the case study building in this chapter.

CHAPTER V

APPLICATION OF THE CALIBRATION TECHNIQUES TO THE CASE STUDY BUILDING

This chapter discusses the application of the calibration techniques and the new methods developed for this thesis. The new methods include: architectural rendering, graphical tuning, schedule adjustments using indoor temperature comparisons, end-use electricity estimation, and the statistical results from the simulation.

5.1 Architectural Rendering

To improve the characterization of the building exterior envelope, a Microsoft Windows BDL visualization software package, DrawBDL (Huang 1993), was used. In the past, the DOE-2 user was compelled to rely on intense blind concentration and some guesswork to encode the physical description of a building. Often the BDL description of the building being simulated had no physical resemblance to the actual building. Figure 5.1 (a) shows a previous simulation from the Zachry Engineering Center (ZEC) (Bronson 1992) as an example of a building that was modeled without architectural rendering using equivalent thermal walls. Figure 5.1 (b) is the actual building and is included for comparison. This method suffices for DOE-2 simulations because the calculations are performed on one-dimensional walls or iso-slabs. Wall positioning is only important when shading and self-shading are taken

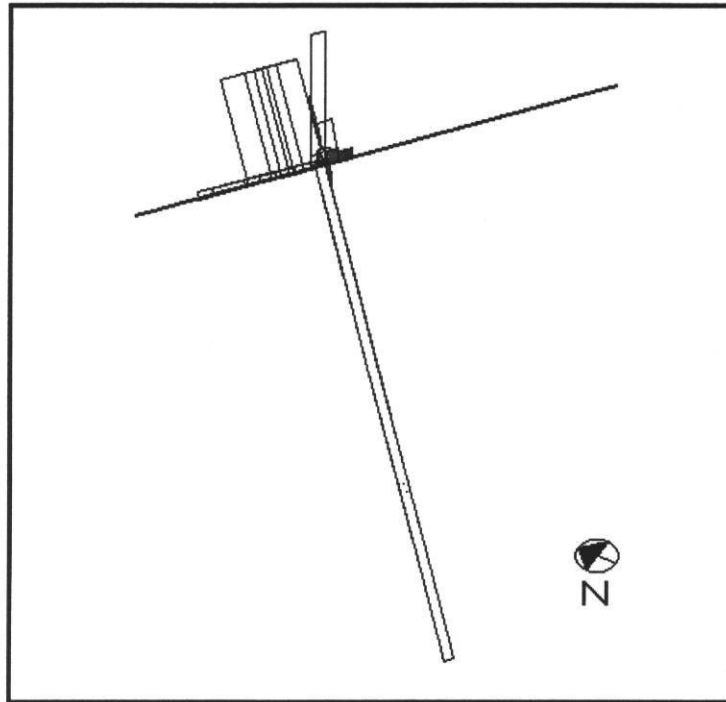


Figure 5.1a Example of a Commercial Building Using Equivalent Thermal Surfaces.

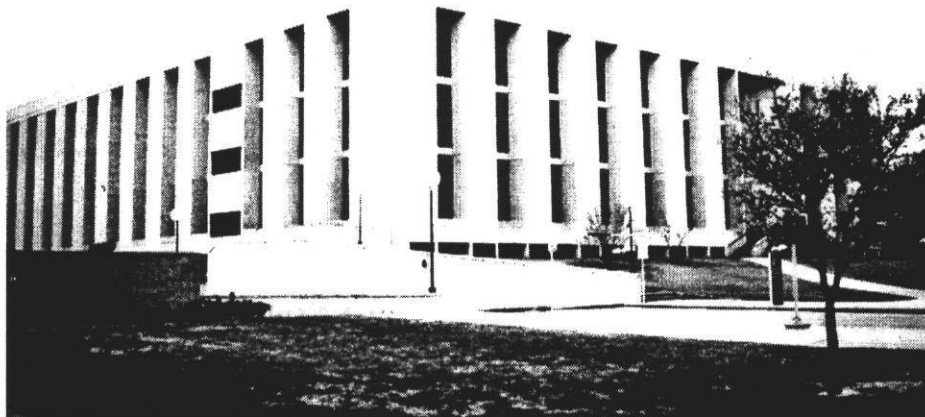


Figure 5.1b Zachry Engineering Center (south corner).

into consideration. In the case of the ZEC neither shading nor self-shading were important factors. Only the 3' set-back of the windows had a small influence.

The term shading refers to shading of beam solar radiation by other structures or trees. The self-shading term applies to the building shading itself, e.g., when a section of the building shades a window in another part of the same building. When equivalent thermal walls are used to simulate a structure, it is sometimes difficult to ensure that a building has the appropriate envelope because the user has no means of verifying the BDL input. In addition, it is difficult and may be impossible to include the effects of shading. The case study building used in this thesis was drawn using the relative wall locations. Relative wall location involves the placement of each wall, window, door, and roof section relative to one another as they actually occur on the architectural plans and eventually in the building. An example of the building and the surroundings is shown in Figure 5.2 as was drawn by the DrawBDL architectural rendering package.

The DrawBDL program recognizes the building and surface dimensions included in the DOE-2 BDL input code and uses the Microsoft Windows Graphical User Interface (GUI) to construct a three-dimensional picture of the building. The most significant portion of this viewing package provides a means to eliminate inevitable errors in coding building dimensions such as misplacement of walls or windows. This is crucial for detecting shading and self-shading orientation errors.

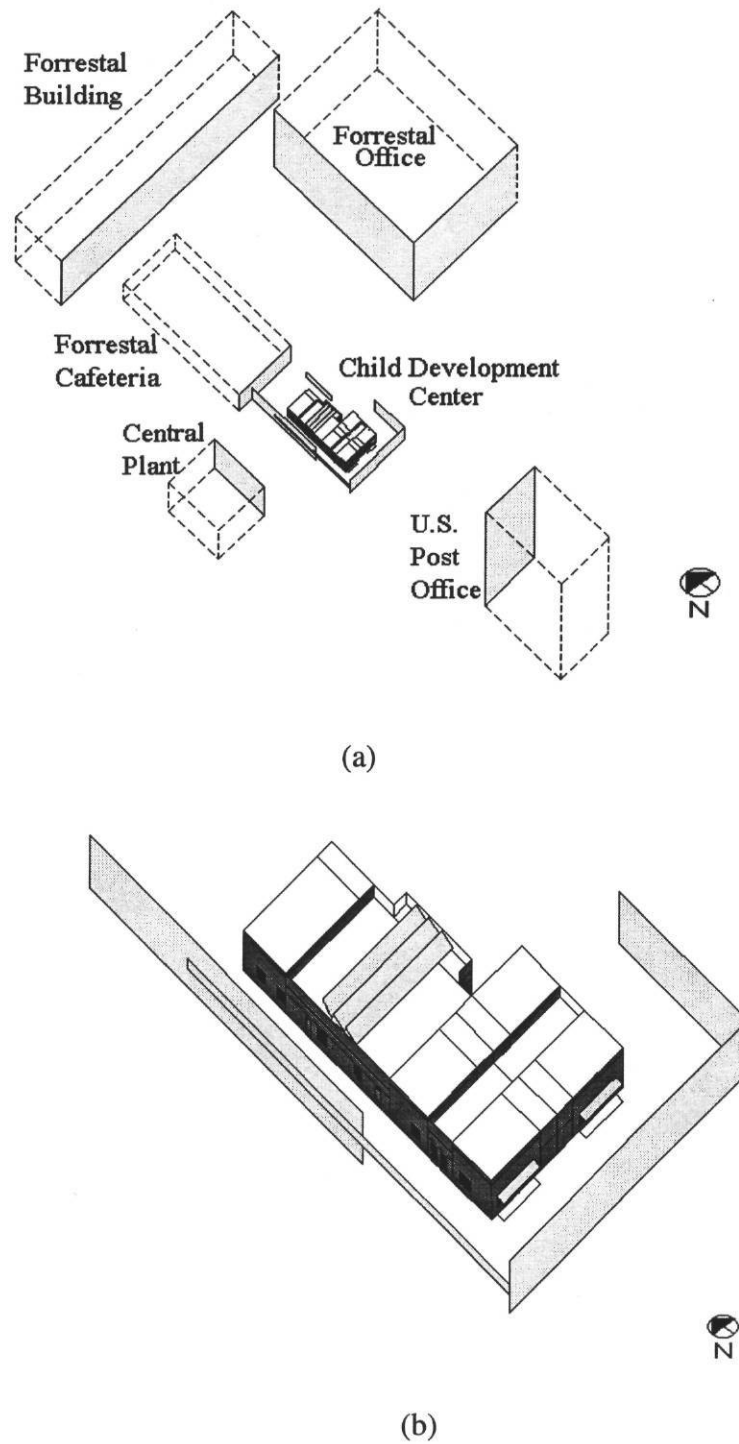


Figure 5.2 Child Development Center DOE-2 Model as Displayed with DrawBDL Software. (a) CDC and Surroundings. (b) Close-up of the CDC. The Solid Planes Represent Shading from Buildings, Walls, and Trees.

The shading effects are discussed in Section 5.1.1. A special feature of the software includes allowing the user the ability to rotate the building. Furthermore, the building may be seen in a plan view or by elevation. The DrawBDL program also has diagnostic features that allow the user to identify the offending BDL code by placing the pointer on a particular building surface and verify the dimensions.

The viewing package also provides the user with geometric information including roof area, exterior wall area, window area, door area, and skylight area. A user is able to locate any zone or surface quickly by simply choosing it from an on-screen menu. The DrawBDL program can print building surface summary reports for inspection as well as draw the building on paper using a printer. Also, building pictures may be printed and/or clipped into a document using normal Microsoft Windows clipboard features (Microsoft 1991).

The building shown in Figure 5.1 could not in reality be modeled easily with relative walls in a manner consistent with architectural drawings due to the large number of windows and BDL input file limitations. DOE-2 only allows the use of 128 exterior wall and roof surfaces, 128 windows, and 64 doors to be included per input file. Therefore, multiple input files would have been necessary to simulate the ZEC with a BDL description that was thermodynamically and architecturally similar. Two input files were actually used by Bronson to simulate the building in Figure 5.1 and the energy totals added.

The DrawBDL program requires X, Y, and Z coordinates measured from a single reference point in the DOE-2 input deck to draw each building surface as it would actually appear. Since equivalent thermal walls are not modeled with actual coordinates, the program locates all surfaces at 0,0,0 in the direction of their defined azimuths. The program also recognizes BDL commands such as LIKE, and MULTIPLIER. The command MULTIPLIER, used to specify multiple surfaces with similar characteristics, is used only to calculate the total surface area (and hence heat loss/gain) when specified.

5.1.1 Solar Radiation and Shading Effects

The effects of solar radiation were examined by comparing the calibrated DOE-2 model which includes shading by nearby buildings and trees to a model run without the shading included. The calibrated model had all the shading surfaces verified by DrawBDL to assure correct surface placement. Another comparison was then made with a model using a packed weather tape that did not contain any solar radiation data. The packed weather tape included site-specific dry bulb temperature, relative humidity, and wind speed (i.e. the same weather data that was used for calibrating the model in this thesis except for solar radiation). Table 5.1 summarizes the results from the DOE-2 models run for the calibration period (April - December 1993). The summary includes the space heating load, the space cooling load, the HVAC fan load, the lighting load, and the equipment load. In reality, the lighting and

equipment loads were not affected by the solar analysis, but were included to complete the overall total energy consumption load report.

Table 5.1 DOE-2 Models Run with Shading, without Shading, and without Beam Radiation.

DOE-2 Case Study Model	Heating MWh	Cooling MWh	HVAC Fans MWh	Lighting MWh	Equipment MWh	Total MWh
Calibrated Model With Shading	4.2	14.1	34.1	38.5	16.6	107.6
Calibrated Model Without Shading	3.8	15.2	34.5	38.5	16.6	108.7
Calibrated Model Without Solar Radiation	4.9	11.9	33.3	38.5	16.6	105.2

The model results labeled “without shading,” shown on Table 5.1, are the results from the calibrated model which had all the shading surfaces surrounding the daycare center removed. The total heating load decreased by 9.5% as would be expected due to the increased solar gain during the day normally blocked by shading surfaces. The cooling load increased by 7.8% and the HVAC fan load increased as well, but only by 1.2%. The resulting total energy load, however, only increased by 1.1% since the lighting load accounted for the majority of the total load.

This analysis did not include the effect of daylighting since the photosensors that were specified were never installed. For the model run with the solar radiation removed from the packed weather tape, the heating load increased by 16.7% while the cooling load decreased by 15.6%. The fan load decreased by 2.3% and the total energy consumption decreased by 2.2%. Although this represents a totally unrealistic

situation (i.e. no solar radiation) it helped analyze the impact of the shading on the building by defining the case for no solar radiation.

The data resulting from the DOE-2 run without solar radiation verifies that solar radiation is responsible for a significant amount of the heating and cooling loads in this building and should not be neglected. Removing the shading surfaces from the input file also affected the heating and cooling loads, but to a lesser extent than removing solar radiation. It may be concluded based on this analysis and on the negligible 3% overall case study glass area that solar radiation, although not the major source of heat gain for this building, is an important influence on its energy consumption. Despite the overall energy consumption not being largely affected, not considering solar radiation and shading for individual heating and cooling analysis proves to be a poor assumption. The use of DrawBDL, or a similar visualization tool, therefore significantly helped reduce the errors resulting from assumptions concerning misplaced shading surfaces for the case study building.

5.2 Graphical Tuning With Statistical Graphics

Over the years, graphs have played an important role in comparing measured data to simulated data (Hsieh 1988; Hunn et al. 1992; Bronson 1992; Koran 1992; McLain et al. 1993; Reddy 1993). The graphics techniques used in the previous work range from X-Y scatter plots to two-dimensional line graphs to bar charts. This section will contribute to DOE-2 calibration literature by using the previously

established methods of calibration and by introducing new statistical graphs. The established methods for the case study calibration are presented first which include two-dimensional time-series plots and three-dimensional positive residual plots. The new techniques used are binned temperature box-whisker-mean plots compared to established scatter plots and weather dependent 24-hour daytype plots. Both of the new plots advance the state-of-the-art for DOE-2 calibration by allowing for more accurate statistical comparisons of simulated versus measured data. Furthermore, they do not suffer from the indicated graphical problems such as data overlap.

5.2.1 Traditional Calibration Plotting Techniques

The most common graph still being used today is the two-dimensional time-series plot with both the measured and simulated data plotted on the ordinate (y-axis) and the time plotted on the abscissa (x-axis). Typically, simulated data and measured data comparisons were either performed by visually inspecting the graphs on a short-term basis (Hsieh 1988; Reddy 1993) or summing a particular period, one month for instance, and calculating a percent difference in the manner noted in Chapter III (Diamond and Hunn 1981; Kaplan et al. 1990a; Bronson 1992; McLain et al. 1993). Figures 5.3, 5.4, and 5.5 are two-dimensional monthly time-series plots that compare the measured data from the daycare center (solid line) to the DOE-2 simulated data (dashed line). The third line below the measured and simulated lines is the residual or difference between the measured data and simulated data. The advantages in plotting the data with this format lie with the simplicity in producing each graph, visualizing

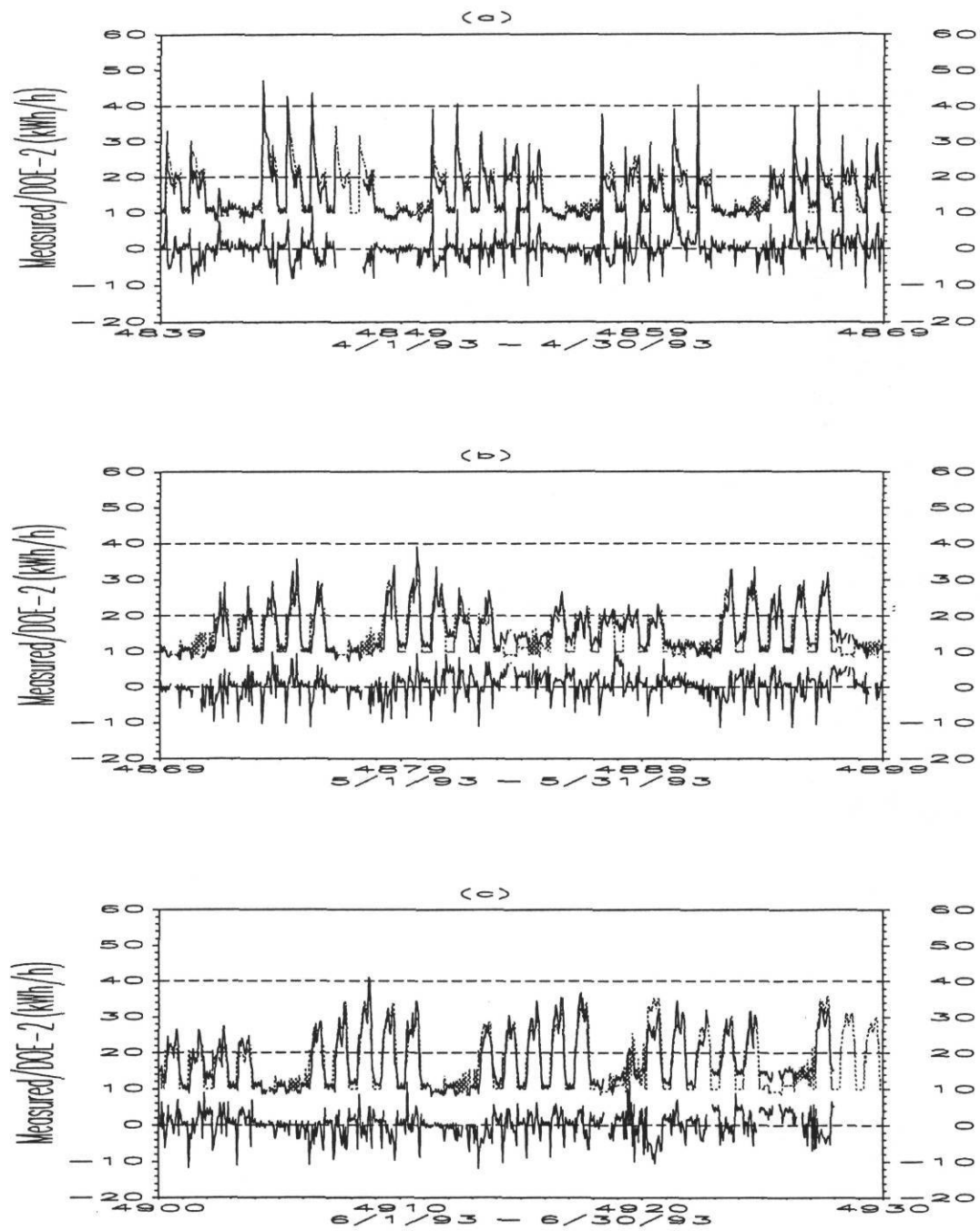


Figure 5.3 Time-series Plots of CDC Electricity Use: April - June 1993. (a) April. (b) May. (c) June. The Dashed Line is the DOE-2 Simulation. The Solid Line is the Measured Data. The Bottom Trace Represents the Residuals or the Measured - Simulated Difference.

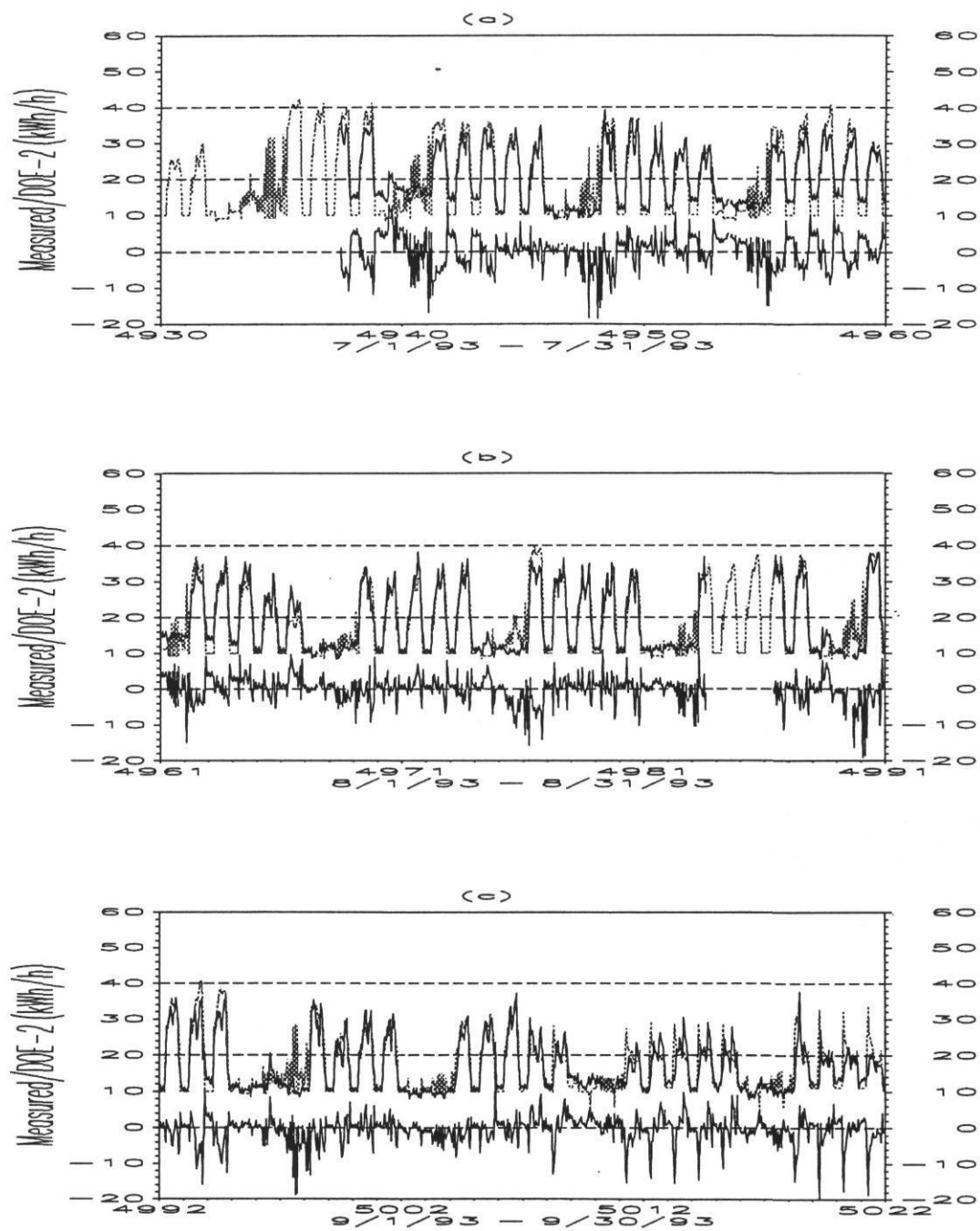


Figure 5.4 Time-series Plots of CDC Electricity Use: July - September 1993. (a) July. (b) August. (c) September. The Dashed Line is the DOE-2 Simulation. The Solid Line is the Measured Data. The Bottom Trace Represents the Residuals or the Measured - Simulated Difference.

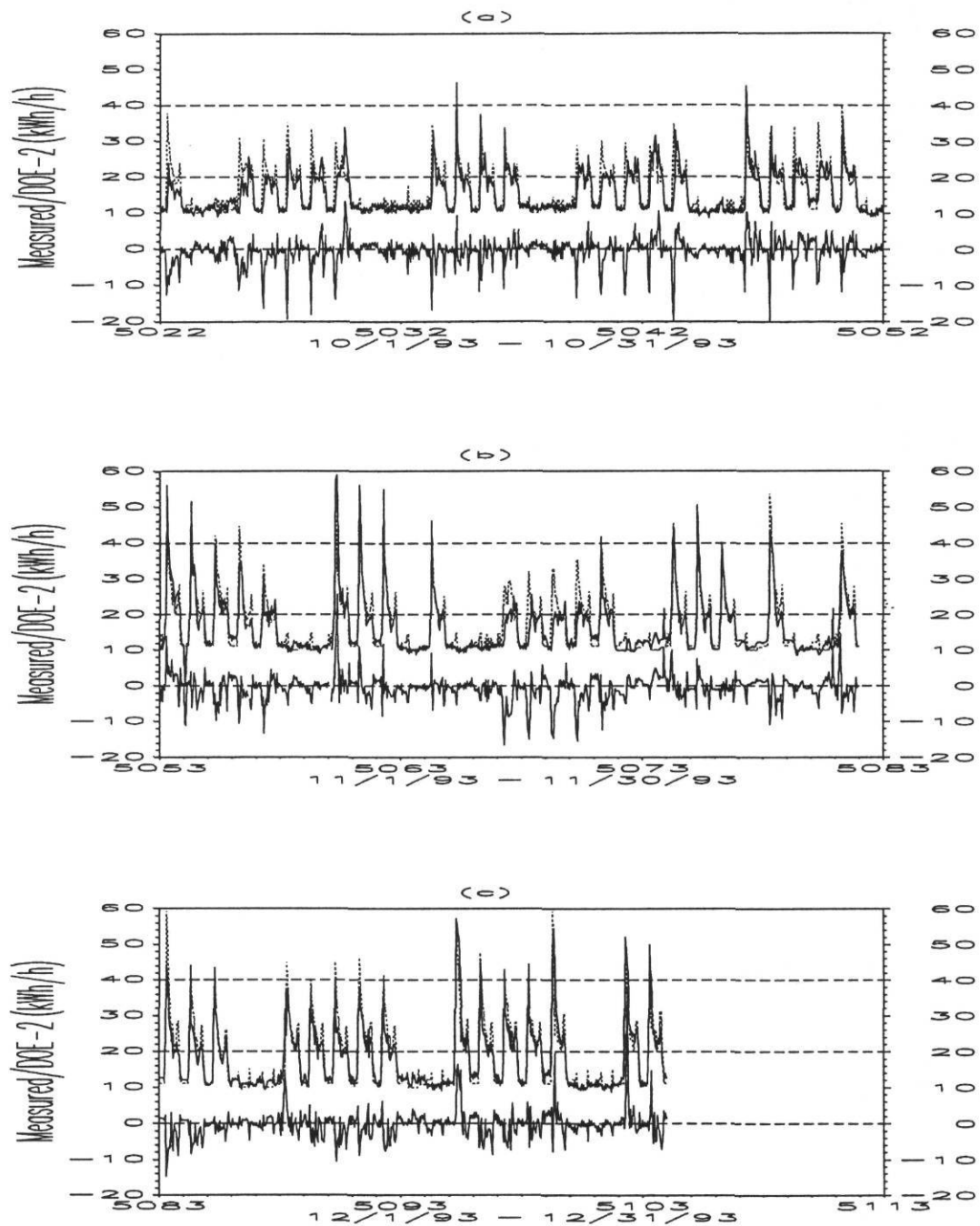


Figure 5.5 Time-series Plots of CDC Electricity Use: October - December 1993. (a) October. (b) November. (c) December. The Dashed Line is the DOE-2 Simulation. The Solid Line is the Measured Data. The Bottom Trace Represents the Residuals or the Measured - Simulated Difference.

the gross magnitude of the energy consumption, and understanding general trends and standard errors. Haberl and Claridge (1987) and Haberl and Vajda (1988c) utilized such graphs to support the advancement of a knowledge based system tested on a university Recreation Center and at the USDOE Forrestal building to provide feedback to building operators. Another important advantage of using time-series plots is the ability to observe rough trends in the data stream. A major difficulty in using this type of graph involves data overlap from hour to hour, especially if large amounts of data are used as is the case with the examples presented here. Because of the data overlap an exact hour-by-hour data comparison cannot be made using these graphs due the vast amount of densely packed data being plotted (Cleveland 1985; Abbas 1993). Also, it is difficult to tell exactly what time of day a particular feature occurs.

Figure 5.3 shows the simulated and measured data from April through June 1993. The April plot, shown in Figure 5.3 (a), shows higher early morning heating residual differences in which the measured data is consistently higher than the simulated data. This shows that the case study has a higher pick-up load than DOE-2 is simulating. In May and June, shown in Figures 5.3 (b) and (c) respectively, the residuals shift to the early afternoon periods when occupant influence was evident as inconsistent daily energy use. Most of the nighttime and weekend differences are minimal, except for two days and one weekend in late June. These differences occurred during the middle of the summer when indoor temperatures would, in all likelihood, be higher which causes the thermostat to over-ride the night setback

thermostat setting of 80° F. It would appear that the DOE-2 model did not activate the HVAC systems despite being simulated with the night setback option. Unfortunately, one of the important weeks of measured data during the setback override mode was lost due to logger malfunction making it impossible to present a more definite conclusion.

July 1993 data, shown in Figure 5.4 (a) shows a consistent morning DOE-2 over-prediction on Mondays. The reason for this could not be completely ascertained. However, it is felt that this may be caused by an improper assumption about the internal mass in the building which would cause DOE-2 to over-predict the amount of cooling required to cool-down the building after a long hot weekend. Also evident on this plot is that the building consistently consumed 2 - 5 kW more in the evenings. This was most likely due to the exhaust fans being improperly wired and operating continuously, thus pulling in hot air at night. This would also account for the April under-simulation during early morning periods because the exhaust fan operation cooled down the space. The model's fit improves during the remainder of the week and on weekends, but still does not simulate the night setback properly.

Figure 5.4 (b) is a plot of August 1993 data and shows that DOE-2 simulated August conditions more accurately than previous months with a CV(RMSE) of 21.7%. Monday morning over-simulation is still evident on two of the four weeks. Figure 5.4 (c) presents September simulation data. DOE-2 weekday night setback is more

evident here toward the end of the month. Also obvious during the last two weeks of September, is the DOE-2 early morning heating which is activated one hour before the actual building cooling activation. Information pertaining to the statistical adequacy of the model is included in Section 5.5.2.

The one hour shift returns to normal in Figure 5.5 (a) which is a plot of October data. DOE-2's early morning over-prediction problem remains throughout the month of October and into November, as is shown in Figure 5.5 (b). In November, heating is again being utilized, however compared to the early morning model over-prediction peaks, the error is not as significant as it was during the earlier part of the year when heating was used. The final graph in the time-series sequence is December data shown in Figure 5.5 (c). This month shows the smallest residuals of the entire dataset with early morning heating being predicted accurately and continuing throughout the day. Analysis of the model is hindered by the dataset's high density in each of the time-series plots. These plots are most effective when plotting short-term data such as one or two weeks at most. Long-term simulation such as this require enhanced graphing techniques such as the statistical box-whisker-mean graphs presented in Sections 5.2.3 through 5.2.5.

5.2.2 Comparative Three-dimensional Surface Calibration Plots

In Figure 5.6 comparative three-dimensional surface plots show the monitored data in part (a) and the DOE-2 simulated data in part (b) for the entire April to

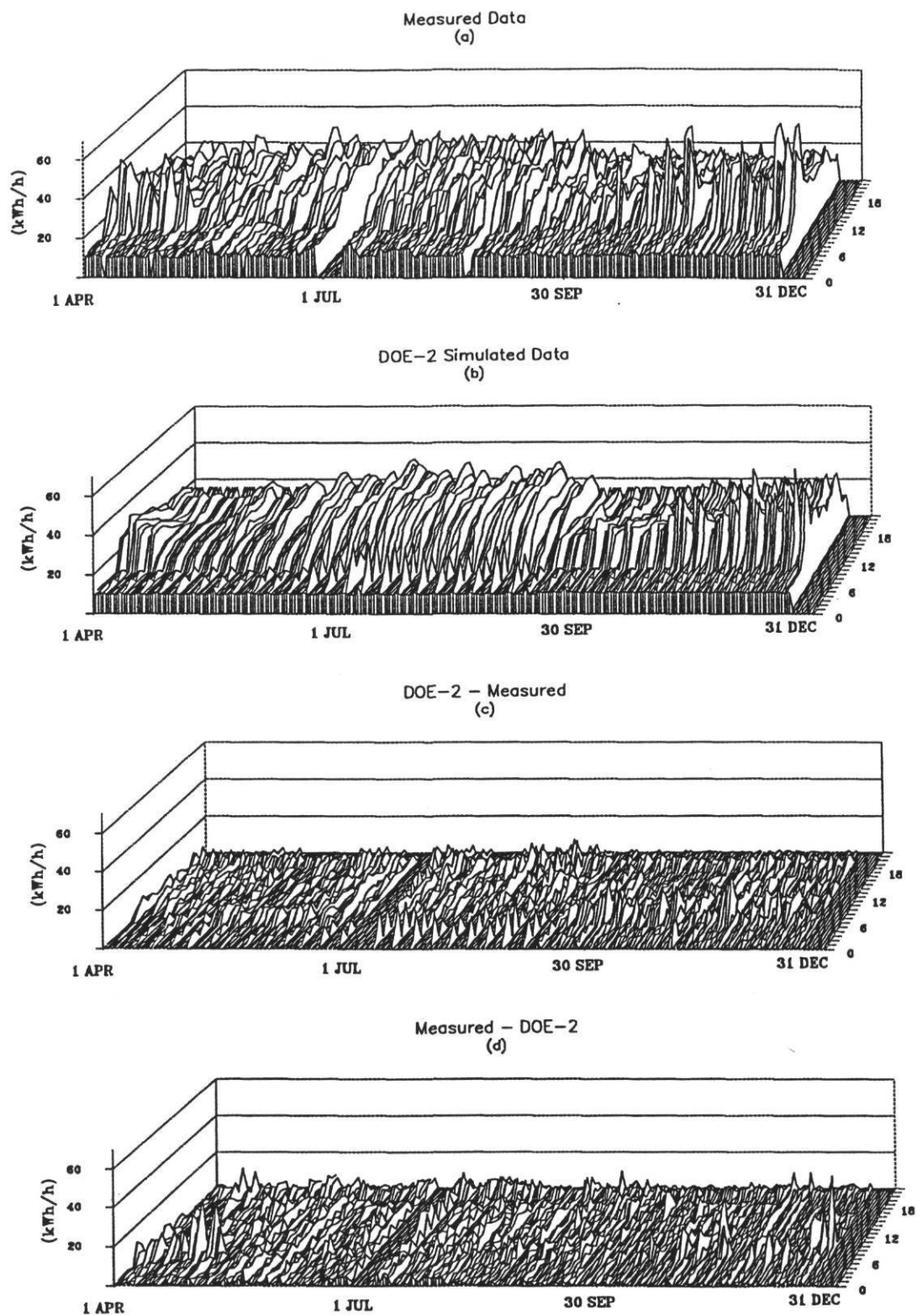


Figure 5.6 Comparative Three-dimensional Plots. (a) Measured Data. (b) DOE-2 Simulated Data. (c) DOE-2 - Measured. (d) Measured - DOE-2.

December 1993 period. Figure 5.6 (c) shows positive-only values of the measured data subtracted from the DOE-2 predicted data while Figure 5.6 (d) shows positive only values of the DOE-2 predicted data subtracted from the measured data. The bottom two plots show positive-only residuals and provide further explanation of the fine differences between the simulated and the measured data that were observed in Figures 5.3-5.5. Individual hourly differences may be visually detected over the entire April to December period allowing the user to recognize DOE-2's over-predictions in the morning and afternoon and DOE-2's under-predictions in the late evening. An immediate benefit may be recognized in the early iteration phases by identifying oversights such as a daylight savings shift or 24-hour profile misalignment of holidays (Bronson et al. 1992). One negative drawback associated with these graphs is the difficulty in viewing fine details such as the hourly differences on a specific day.

The graphs in Figure 5.6 follow the general approach used by Bronson (1992), however, they use the residual format shown by Haberl and Komor (1989). The difference between the two presentations appears in the (c) and (d) graphs. In Haberl and Komor (1989) the graph showed the measured - simulation levels. In Bronson (1992) and in Haberl et al. (1993) the measured - simulated was in the (d) plots. This can cause some confusion when labeled only with "positive" and "negative" residuals. Therefore, it is recommended that this plot should be labeled "measured-simulated" so the viewer is absolutely certain as to what is being presented.

By inspecting Figure 5.6 (d), it is clear that DOE-2 is under-predicting early morning unoccupied electricity usage in the Spring between April 1 and July 1 1993. One possible cause for this is the continuous operation of the cross-wired exhaust fans in the building that should be off, but operate continuously. This draws in cool outdoor air and activates the heating system when the temperature falls below the setback temperature of 55° F. DOE-2 will not simulate this condition properly because the program cannot account for negative pressures. Therefore, no extra heating is evident in the graph. This also probably causes the under-prediction of energy use in July as pointed out in Figure 5.4 (a).

During the month of July, the measured data is higher than the remainder of the year during early morning unoccupied periods. Further analysis of Figure 4.11 shows a higher nighttime measured outdoor temperature trend during the month of July (decimal dates 4930 through 4960). Therefore, the nighttime electricity usage may be attributed to HVAC operation since the indoor temperature most likely surpassed the thermostat setback upper limit setting of 80° F. A closer inspection of Figure 4.11 and Figure 5.6 (a) reveals that the July unoccupied electricity usage closely tracks the outdoor ambient temperature profile shown in Figure 4.11. Also, for a few early morning weekend hours, the DOE-2 model showed some HVAC usage, but only for a limited amount of time. The ragged on/off “pickets” are a characteristic of DOE-2’s hourly calculations algorithm.

The three-dimensional surface plots shown in Figure 5.7 present the same data using a perspective rotated and viewed at 90°. Although the comparative three-dimensional graphs have been previously used, this is the first time that this orientation has been shown to be effective with DOE-2 calibrations. Shown in Figure 5.7 (a) is the measured whole-building electricity data, in Figure 5.7 (b) the DOE-2 simulated whole-building electricity, in Figure 5.7 (c) the DOE-2 - measured data, and in Figure 5.7 (d) the measured - DOE-2 data. These graphs show 24-hour trends that aid in forming general hourly schedules for lights and equipment. Also, the times of various over-/under-prediction trends are clearly visible here. However, as with the graph shown in Figure 5.6 the same drawbacks are clear such as not being able to see between the lines or individual days.

The early morning DOE-2 under-prediction trend identified in the previous graph may be clearly seen in this format on an hourly basis. In Figure 5.7, this feature can also be seen to extend into other periods as well. In the later part of the simulation period shown in Figure 5.7 (a) (i.e. Nov-Dec), the actual building is using more heating energy during the day than DOE-2 simulated indicating a possibly inaccurate building mass assumption. During the afternoon, the DOE-2 graph in Figure 5.7 (b) shows a smoother trend than the actual building does. This indicates the occupant control over the thermostats. Also shown in this graph is the nighttime building shutdown indicated by DOE-2 whereas the actual building's shutdown is more scattered. Figure 5.7 (c) shows the weekend morning HVAC stepped (one hour on

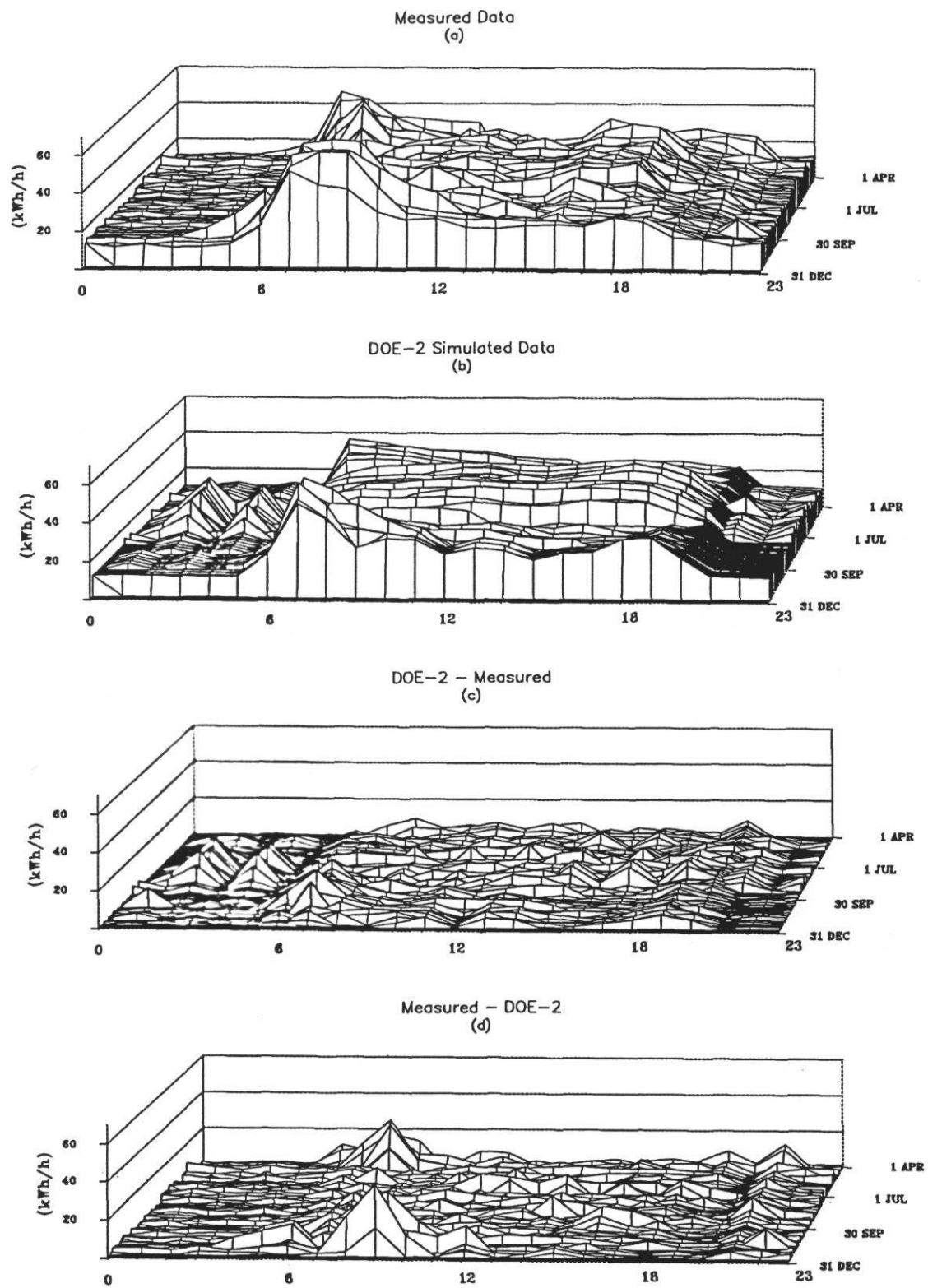


Figure 5.7 Rotated Three-dimensional Plots. (a) Measured Data. (b) DOE-2 Simulated Data. (c) DOE-2 - Measured. (d) Measured - DOE-2.

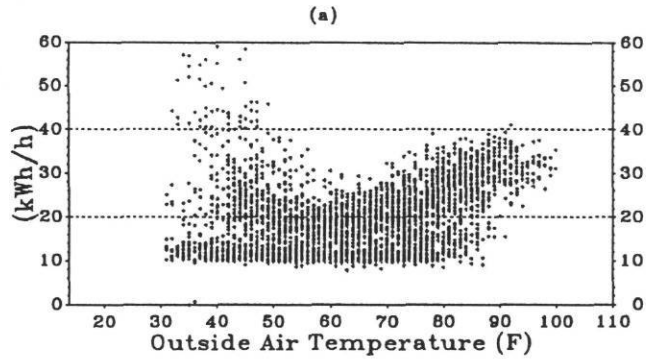
and one hour off) usage calculated by DOE-2 which is not apparent in the measured data. Overall, DOE-2 calculated a better fit during the afternoon to late evening periods for the entire simulation term.

5.2.3 Temperature Bin Calibration Plots

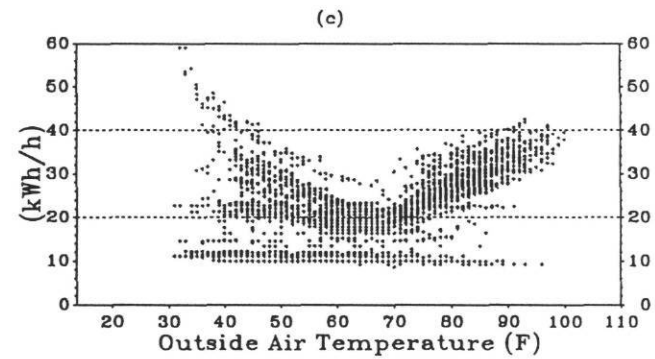
The total building weekday hourly calibration integrity versus outside air temperature is presented in Figure 5.8 for both the DOE-2 simulation and measured data. The mean statistics are listed in Table 5.2. By comparing the two mean lines in Figure 5.8 (d), the simulation follows the measured data very well. Except for a modest deviation in the 100° F bin, it may be concluded, based on the comparison of the means, that the model was well calibrated. In the 100° F bin, DOE-2 seemed to over-predict energy use during most hours and under-predict a select few nighttime hours (approximately 6-10 hours) in the 90° F and 100° F bins. The HVAC system was operational for a longer period most likely due to the negative pressure caused by the exhaust fans. Analysis of the paired bins reveals a good fit between the model and the measured data when comparing the inter-quartile range (i.e. the relative box sizes indicating the variability in bins). The predicted bin medians seem to correlate as well with the measured medians in Figure 5.8 (b).

The DOE-2 data also appears to follow the general measured data trend during both the cooling season and the heating season by comparing the scatter plots in Figures 5.8 (a) and 5.8 (c). Both figures, however, reveal the data overlap difficulties

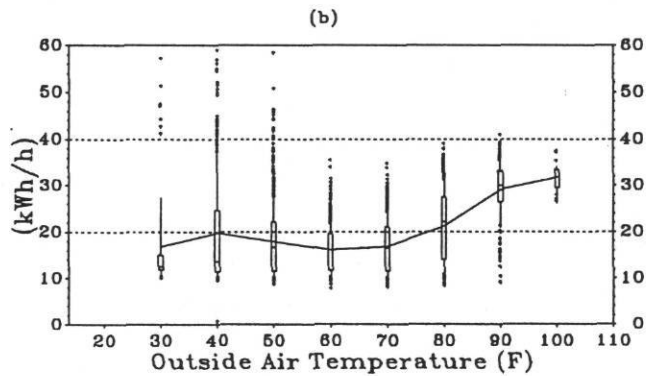
Measured Weekday Whole Building Electricity



DOE-2 Weekday Whole Building Electricity



Measured Weekday Whole Building Electricity



DOE-2 Weekday Whole Building Electricity

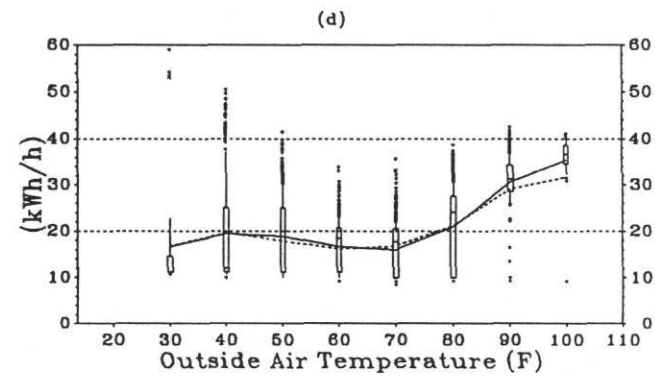


Figure 5.8 Weekday Temperature Bin Calibration Plots. (a) Measured Whole-building Scatter Plot. (b) Measured Whole-building Box-whisker-mean Plot. (c) DOE-2 Whole-building Scatter Plot. (d) DOE-2 Whole-building Box-whisker-mean Plot.

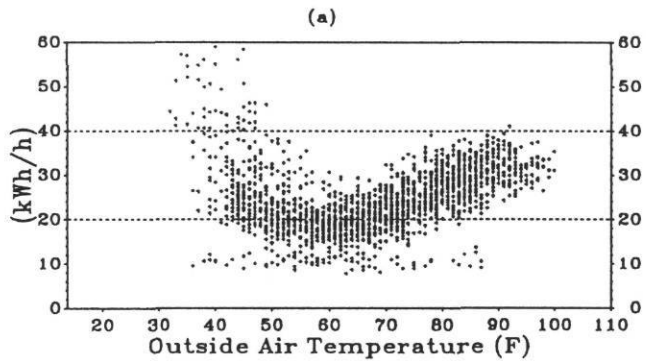
illustrated earlier in Chapter III. In the 30° F to 55° F range, the measured data are more scattered than the simulated data. This portion of the data was measured during early April when it appeared that occupants were adjusting the thermostats more frequently than usual during the early morning warm-up. Due to the unpredictable actions taken, it was decided that the building would be simulated as one thermostat schedule rather than assigning specific daily schedules.

Table 5.2 Weekday Temperature Bin Calibration Mean Statistics.

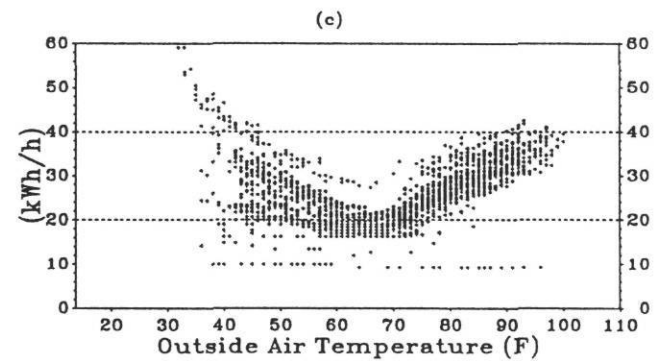
Temperature (F)	Weekday Measured (kWh)	Weekday DOE-2 (kWh)
30	16.8	16.8
40	19.1	19.7
50	18.5	17.9
60	16.5	16.1
70	15.7	16.8
80	20.9	21.3
90	30.5	29.1
100	35.3	31.6

Figure 5.9 provides a better perspective by isolating weekday occupied-only data from 7:00 a.m. to 6:00 p.m. By analyzing the juxtaposed mean lines, the measured and simulated data appear to have an adequate goodness-of-fit. Except for the boxes on each extreme side of the temperature scale, examination of the paired inter-quartile ranges shows much less variation across the data. During both the coldest and hottest bins, DOE-2 slightly over-predicted most hours of the day. Examination of the dataset revealed that most of the points in the 30° F bin appear in

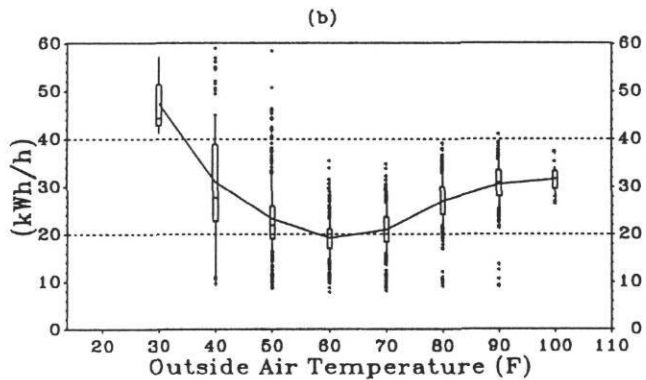
Measured Weekday Occupied Whole Building Electric



DOE-2 Weekday Occupied Whole Building Electric



Measured Weekday Occupied Whole Building Electric



DOE-2 Weekday Occupied Whole Building Electric

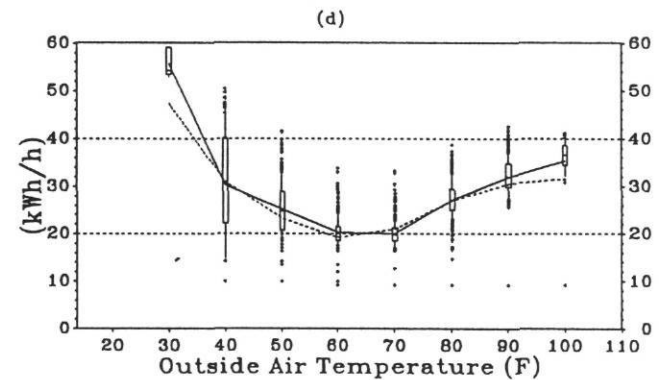


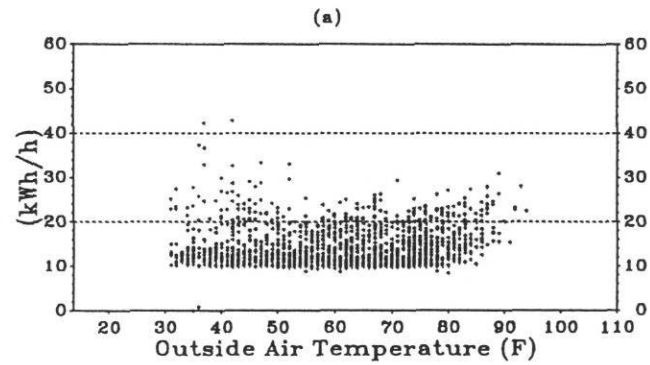
Figure 5.9 Weekday Occupied Temperature Bin Calibration Plots. (a) Measured Whole-building Scatter Plot. (b) Measured Whole-building Box-whisker-mean Plot. (c) DOE-2 Whole-building Scatter Plot. (d) DOE-2 Whole-building Box-whisker-mean Plot.

the early morning hours when the building is just beginning to be occupied. DOE-2 demonstrated some difficulty in accurately simulating the HVAC system by calculating energy use at maximum heat pump capacities for the first hour of building operation as is evident by the high points and narrow inter-quartile range. Furthermore, a closer look at the data on both ends reveals that only a small amount of points lie in the region. Therefore, even a small difference would indicate a larger error than would have otherwise occurred with a larger amount of data. According to conversations held with building personnel after graphical analysis was performed, the band of high points in the measured 40° F - 50° F bins represent the manual activation of the electric resistance baseboard heaters¹³. Since it was difficult to pinpoint the exact date and time of this activity, DOE-2 custom system schedules were not used to provide a better fit.

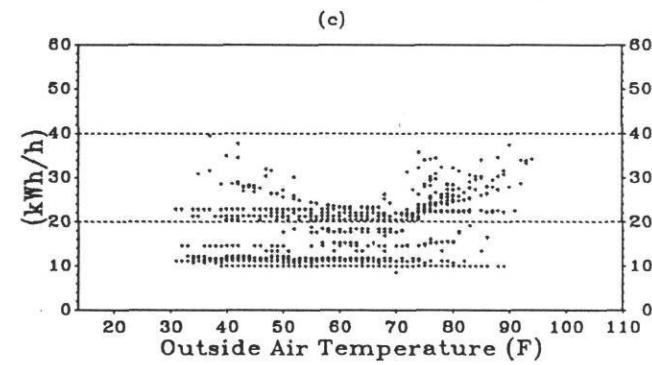
The graph shown in Figure 5.10 displays the weekday unoccupied period electricity use occurring between 7:00 p.m. and 6:00 a.m. Every paired bin except for the 90° F and 100° F bins show a close agreement between measured data bins shown in Figure 5.10 (b) and the simulated data bins in Figure 5.10 (d). The model slightly over-predicted the energy use during this period where again it would seem that DOE-2 indicated some difficulty during the setback mode. Finding a proper balance between allowing nighttime system activation and being completely off proved to be a

¹³ Mr. Mike Shincovich. 1993. Personal Communication, United States Department of Energy, Washington, D.C.

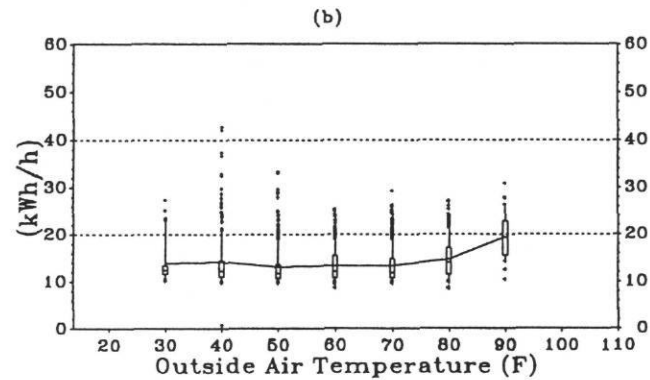
Measured Weekday Unoccupied Whole Building Electric



DOE-2 Weekday Unoccupied Whole Building Electric



Measured Weekday Unoccupied Whole Building Electric



DOE-2 Weekday Unoccupied Whole Building Electric

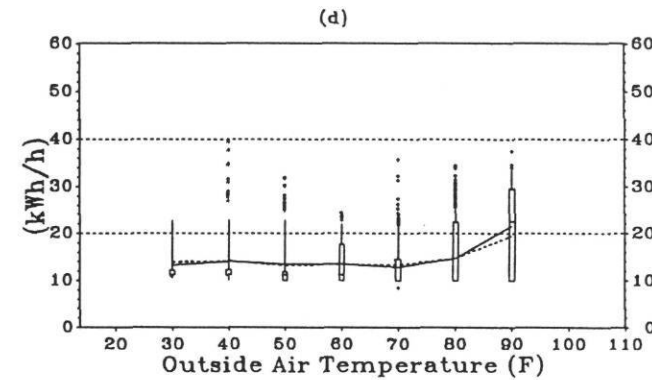
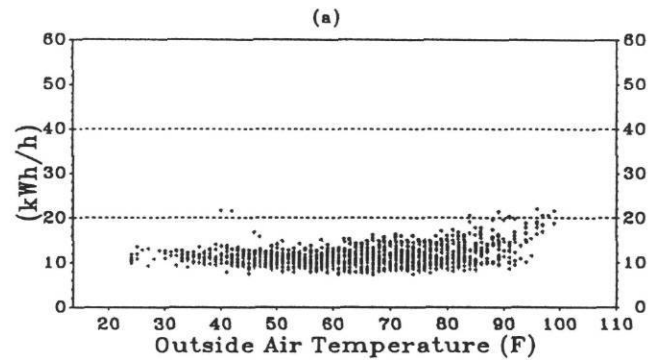


Figure 5.10 Weekday Unoccupied Temperature Bin Calibration Plots. (a) Measured Whole-building Scatter Plot. (b) Measured Whole-building Box-whisker-mean Plot. (c) DOE-2 Whole-building Scatter Plot. (d) DOE-2 Whole-building Box-whisker-mean Plot.

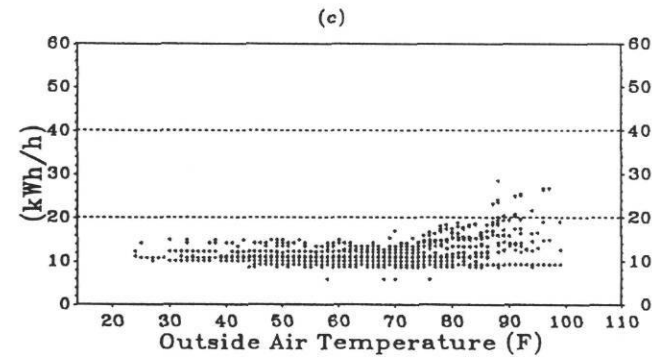
troublesome task. The DOE-2 simulator is only capable of performing hour-by-hour simulations. When the simulated fans are specified to cycle in the night setback mode, the simulator will calculate fan energy for the entire hour whereas in reality, the actual fan may not be required to operate for the full hour. The simulated data in Figure 5.10 (c) exhibits a notable gap between the 10 and 20 kWh/h range. This again is due to the one hour on and one hour off time step DOE-2 characteristic whereas the actual building data, shown in Figure 5.10 (a), can have a minute-by-minute HVAC system usage. The high outlier data points in Figure 5.10 (c) are probably indicating a possible use of the HVAC system in the evening. These points correlate with the September DOE-2 setback over-ride mode seen earlier in the time-series plots. The calibration problems presented here reinforce the definite need for the statistical graphics used in this thesis.

Weekend measured and simulated data are shown in Figure 5.11 where each paired bin except for the 100° F bin shows good agreement. The corresponding mean statistics are detailed in Table 5.3. Except for some DOE-2 scatter, unoccupied weekdays (Figure 5.10) and weekends (Figure 5.11) are almost identical. In the 100° F, DOE-2 did not predict hot weather night setback very accurately. The simulation program indicated an HVAC setback mode whereas the measured data showed an override mode. In the same bin during the day, DOE-2 over-predicted, as represented by the higher points, while during the night, it did not activate the HVAC system. Although the number of hours affected are less than twenty over a period of nine

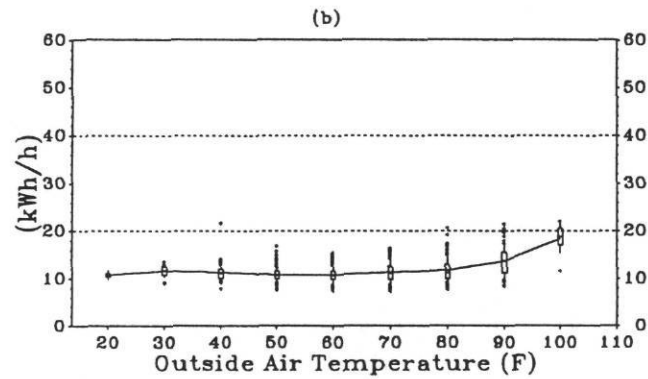
Measured Weekend Whole Building Electricity



DOE-2 Weekend Whole Building Electricity



Measured Weekend Whole Building Electricity



DOE-2 Weekend Whole Building Electricity

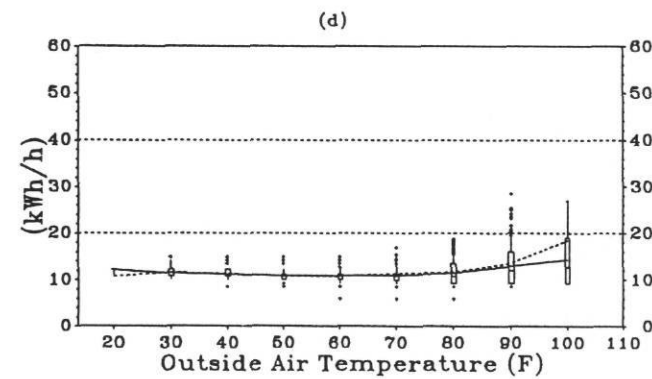


Figure 5.11 Weekend Temperature Bin Calibration Plots. (a) Measured Whole-building Scatter Plot. (b) Measured Whole-building Box-whisker-mean Plot. (c) DOE-2 Whole-building Scatter Plot. (d) DOE-2 Whole-building Box-whisker-mean Plot.

months, it is worth noting that the small spread in the 100° F bin causes the mean lines to considerably deviate from each other.

Table 5.3 Weekend Temperature Bin Calibration Mean Statistics.

Temperature (F)	Weekend Measured (kWh)	Weekend DOE-2 (kWh)
20	12.1	10.8
30	11.2	11.6
40	10.7	11.3
50	10.3	10.8
60	10.4	10.8
70	10.5	11.3
80	11.0	11.6
90	12.7	13.4
100	14.4	17.5

5.2.4 Juxtaposed 52-Week Bin and Three-dimensional Calibration Surface Plots

Figure 5.12 shows the same data as Figure 5.13, the three-dimensional graph. However, Figure 5.12 bins the energy usage using 52-week time-series box-whisker-mean graphs instead of temperature bins. Table 5.4 shows the 52-week plot's mean statistics. The measured data are shown in Figures 5.12 (a) and 5.13 (a) and the DOE-2 simulation is shown in Figures 5.12 (b) and 5.13 (b). The x-axis in Figure 5.12 is the simulation week number; for this thesis, week "0" begins on April 1. The y-axis shows the whole-building electricity use in both Figures 5.12 and 5.13. The x-axis in Figure 5.13 shows the day of the year, again beginning on April 1. The z-axis, shown as the height above the x-y plane, represents the hour-of-the-day.

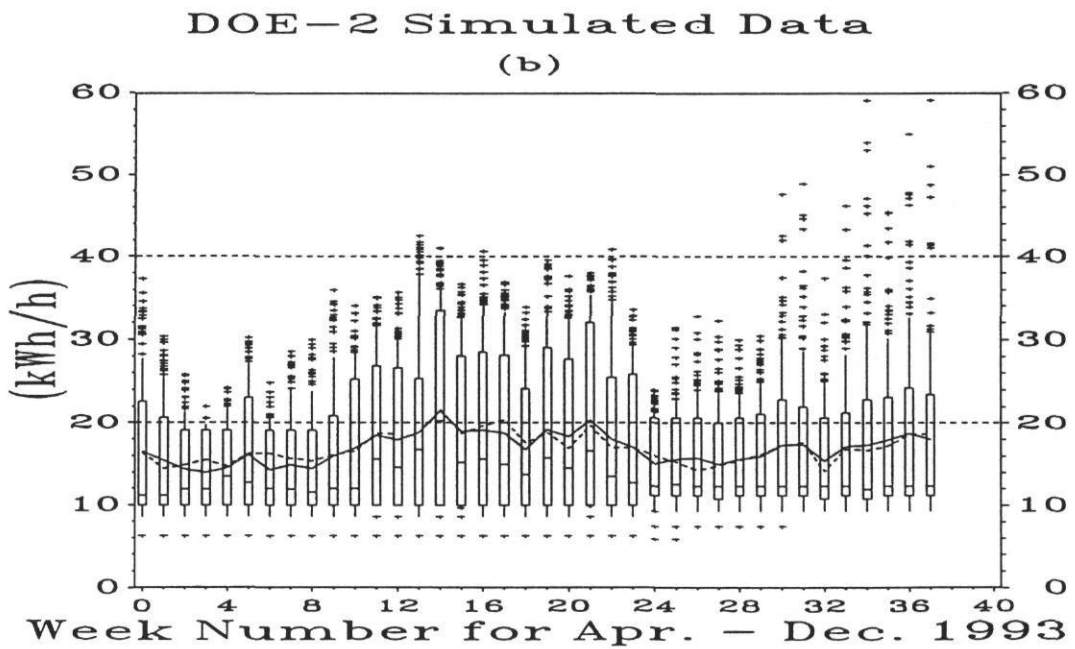
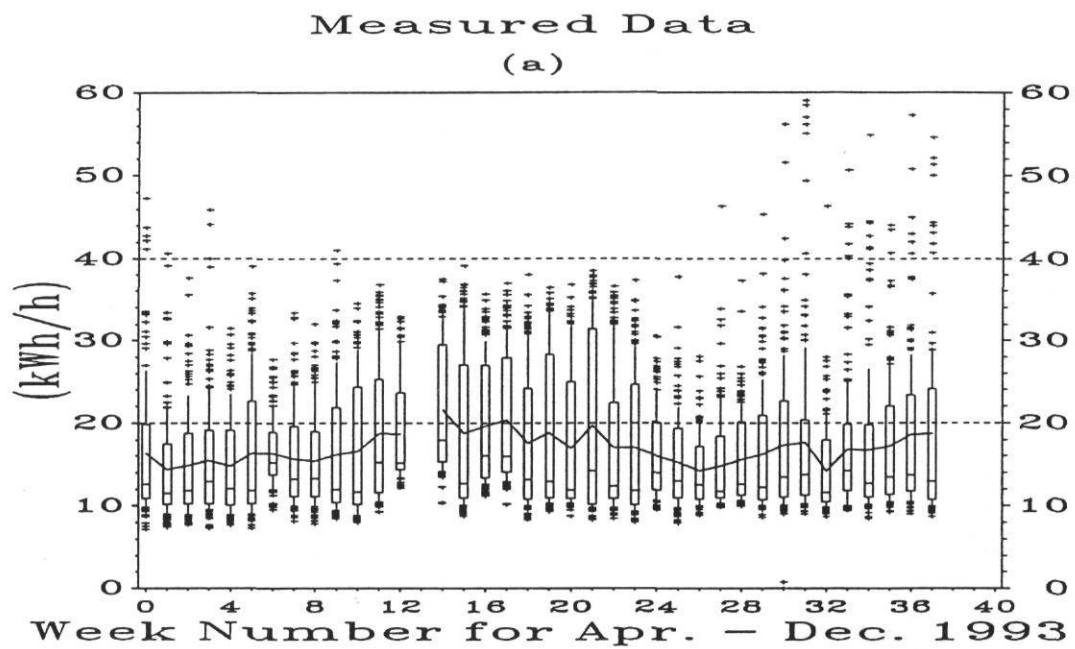


Figure 5.12 52-Week Box-whisker-mean Plots. (a) Measured Data. (b) DOE-2 Simulated Data.

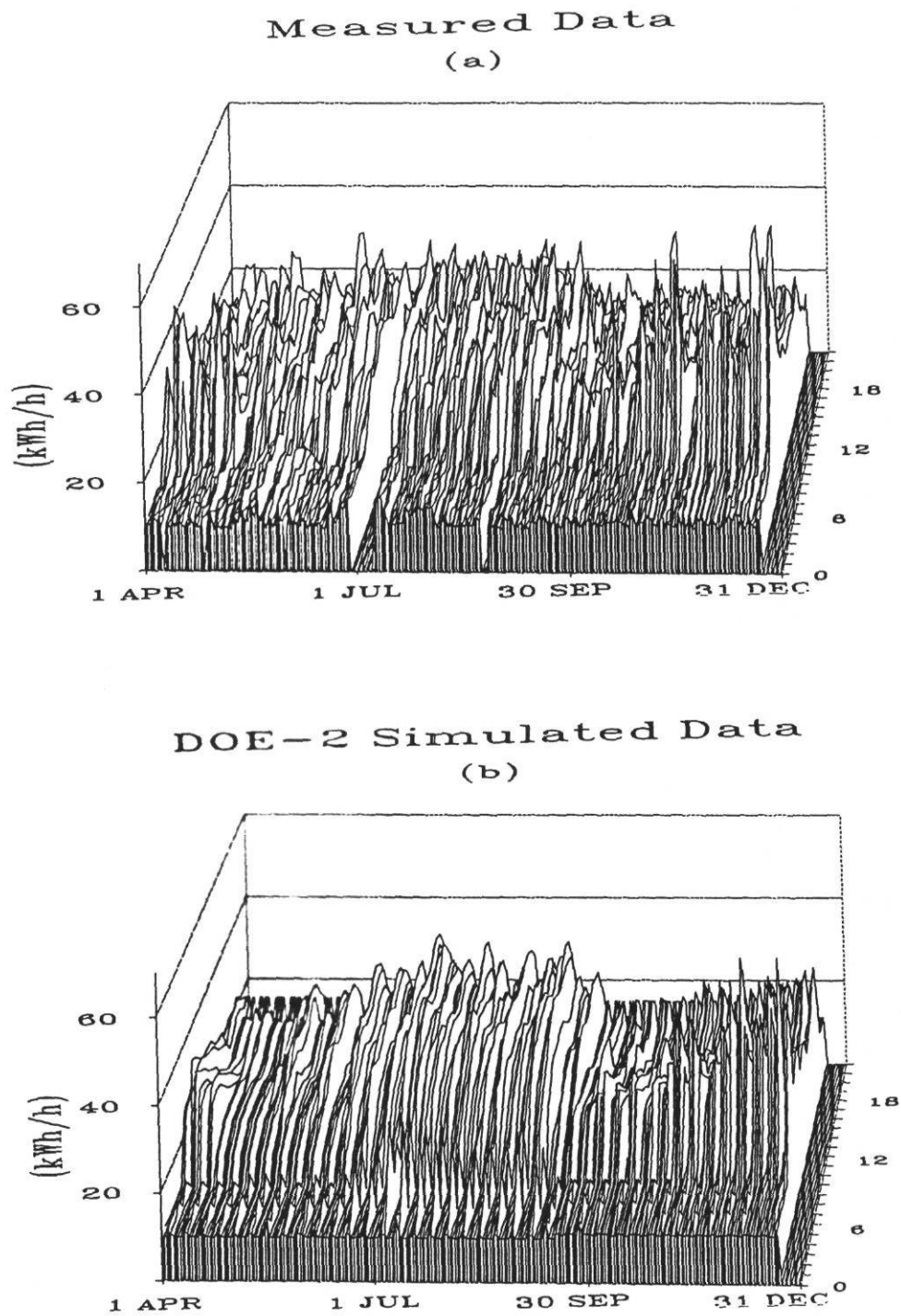


Figure 5.13 Three-dimensional Plots. (a) Measured Data. (b) DOE-2 Simulated Data.

Table 5.4 52-Week Bin Mean Statistics.

Week	Measured (kWh)	DOE-2 (kWh)	Week	Measured (kWh)	DOE-2 (kWh)
0	16.4	16.5	19	18.8	19.2
1	14.4	15.4	20	16.9	18.3
2	14.9	14.4	21	19.6	20.3
3	15.5	14.0	22	17.0	18.0
4	14.7	14.5	23	17.0	17.1
5	16.3	16.1	24	16.1	15.1
6	16.3	14.3	25	15.3	15.6
7	15.7	14.9	26	14.3	15.8
8	15.4	14.5	27	14.8	15.0
9	16.1	16.0	28	15.5	15.6
10	16.6	16.9	29	16.2	15.9
11	18.7	18.5	30	17.3	17.3
12	18.6	17.9	31	17.6	17.4
13	MISSING	18.8	32	14.2	15.3
14	21.6	21.5	33	16.8	17.1
15	18.7	19.0	34	16.7	17.3
16	19.6	19.1	35	17.2	18.0
17	20.4	18.8	36	18.6	18.7
18	17.6	16.8	37	18.7	18.0

The two plots shown use a method known as juxtapositioning on each page and juxtapositioning across pages, or juxtapaging (Abbas 1993). Juxtapositioning is a method of graph comparison whereby graphs are placed side-by-side or one next to the other using similar scales. Juxtapaging compares plots of the same data, over the same period, on two different pages as is being shown by Figures 5.12 and 5.13. These plots help to visualize long-term data trends and analyze statistical residuals. This new technique uses both a statistical analysis of weekly data and visual/comparative three-dimensional plots to judge the goodness-of-fit of the simulated data to the measured

data. Figure 5.12 also takes advantage of graphical superposition of the mean line from Figure 5.12 (a), shown as the dashed line, upon Figure 5.12 (b) to further improve the efficiency of the graph. It follows a remarkably similar path traced by the simulated data mean line represented by the solid line.

When evaluating each set of paired bins, it may be concluded that the average weekly simulated data seems to consistently track the average weekly measured data since the simulated box sizes do not deviate significantly from the measured box sizes. The minimum simulated data limits are consistently lower in the DOE-2 plot (Figure 5.12 (b)) further emphasizing the difficulties encountered in predicting the nighttime building shut down schedule. The extreme outliers shown in Figure 5.12 (a) indicate the manually operated electric resistance baseboard heaters which are not predicted by DOE-2. The exactness of the medium and minimum points seen in the winter is a characteristic of the DOE-2 scheduling. It would appear that beginning in approximately week 12 and ending in week 17, the measured nighttime HVAC setback mode was overridden due to the zone temperature exceeding the control system upper setpoint temperature limit.

Other possibilities for the night setback override would include failure to manually shut down internal equipment or kitchen refrigerators operating for longer periods due to the elevated internal temperatures. The refrigerators, in turn, add a heat load into the building causing the HVAC system to operate longer. This trend has also

been shown by Parker and Stedman (1992) who performed a study on refrigerator electricity loads by comparing older, less efficient models to newer, more efficient models. They demonstrated that seasonal variation in the published refrigerator load data shows that the daily electrical load increases beginning approximately in July and continuing through September which is consistent with what was observed with the case study building. This may also be contributing to the higher summer-time unoccupied period electricity use in the case study building, something that would be difficult to simulate with DOE-2 (i.e. an internal refrigerator load that is linked to zone temperatures).

Another finding by Parker and Stedman (1992) revealed that kitchen temperatures and door openings accounted for most of the daily variation. This trend is consistent with the measured hourly data fluctuation observed at the daycare center. The deviation in the daily time-series profiles caused by equipment cycling, especially space temperature dependent equipment, presents a problem for simulation as limitations in DOE-2 capabilities are encountered. The other factor inherent to most refrigerators produced today is the defrost cycle which according to Parker and Stedman averages 5-20 minutes for each eight hours of compressor operation. This random portion of the electrical profile is virtually impossible to predict with the DOE-2 program.

Since during daytime hours hot water is used for dishwashing, the electric domestic hot water backup system cycling is another cause for data fluctuation. This unknown factor is not easily determined since neither the hourly solar hot water contribution nor the total amount of hot water consumption were measured. Therefore, a certain amount of simulation will be seen in the analysis.

The scattered high energy use points, discussed in the temperature bin section, are also evident during weeks 0 through 5 and 27 through 37 in Figure 5.12 (a). These bins demonstrate the early morning heater use called for when building occupants manually adjusted thermostats. The measured and simulated median lines, except for a select few during the summer period, generally have similar energy use values.

5.2.5 Weather Dependent 24-Hour Daytype Calibration Plots

Examples of a new method of statistically graphing DOE-2 calibrations are shown in Figures 5.14 and 5.15. The weekday mean statistics are shown in Table 5.5. Kaplan et al. (1990b) described such daytyping as having the capability of distinguishing the daily non-HVAC loads. HVAC loads can then be shown on either side of this zone with cooling above the upper 75° F boundary and heating below the lower 45° F boundary. The graphs described in this section were motivated by the weather daytype methods developed earlier by Hadley (1993). Akbari et al. (1988) also showed daytype profiles similar to Hadley's daytypes, but Akbari used a linear regression and weighting factors whereas Hadley utilized a combination of principle

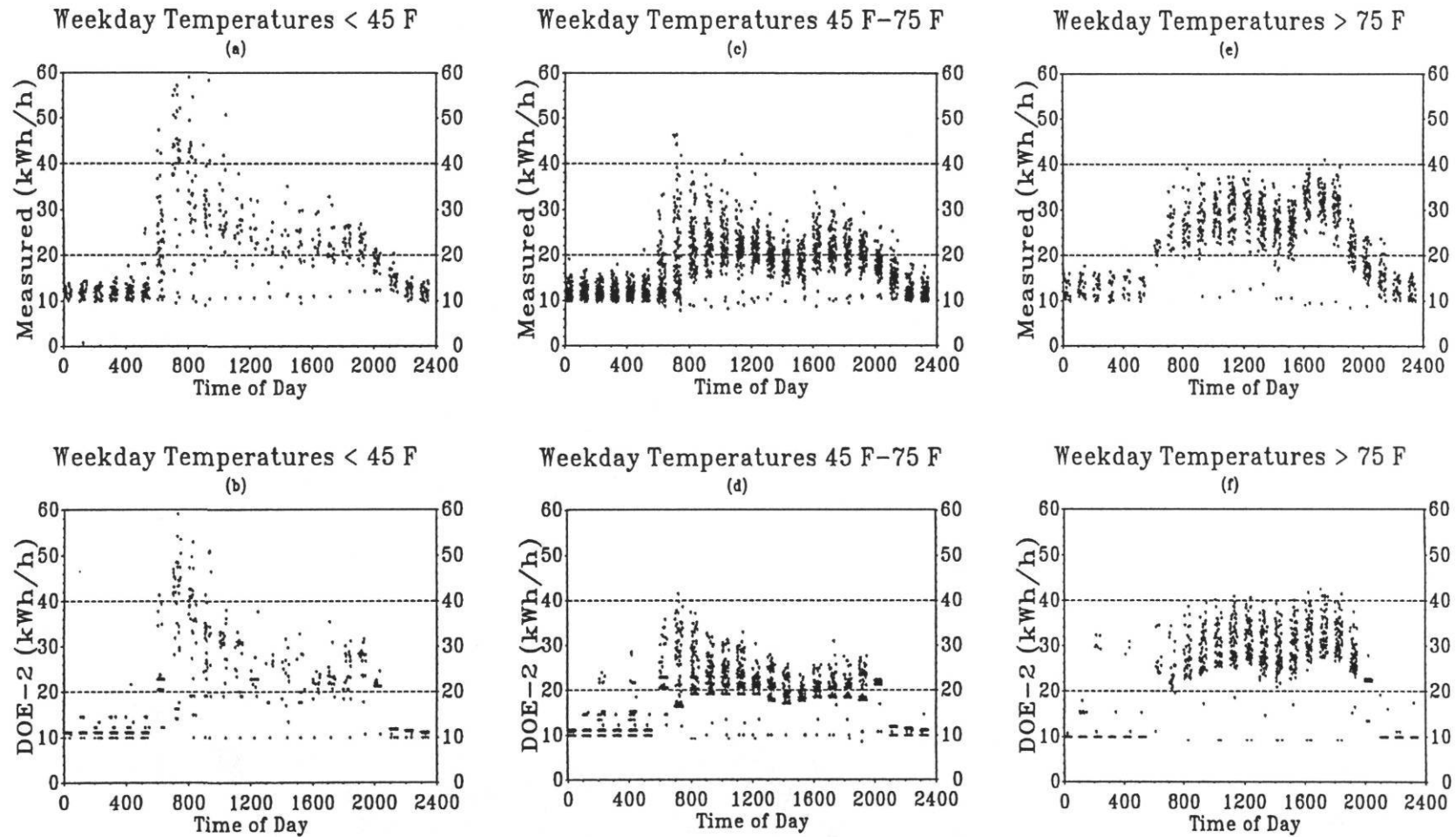


Figure 5.14 Weekday 24-Hour Weather Daytype Scatter Plot.

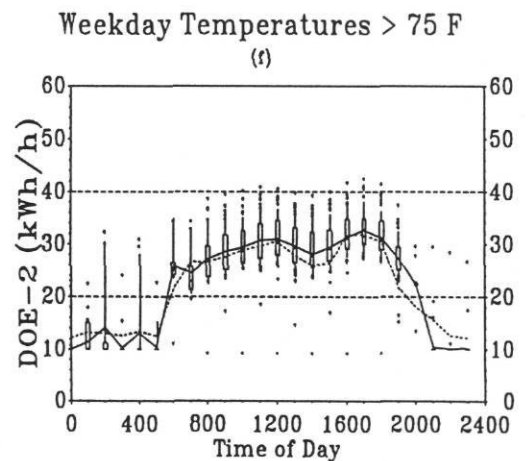
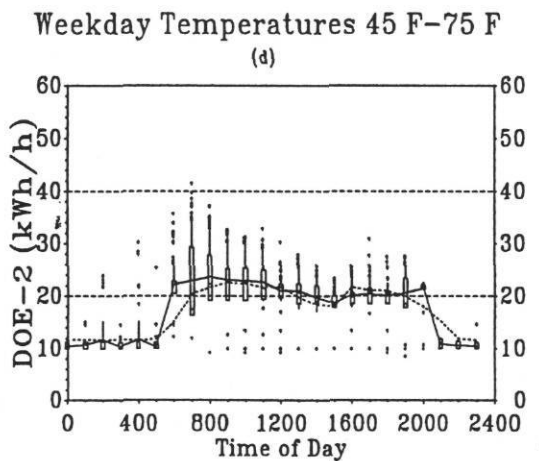
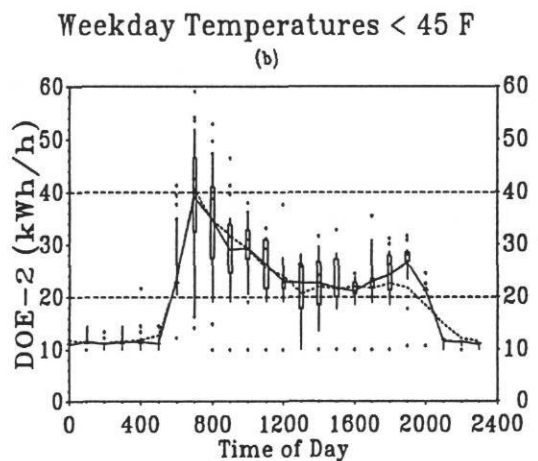
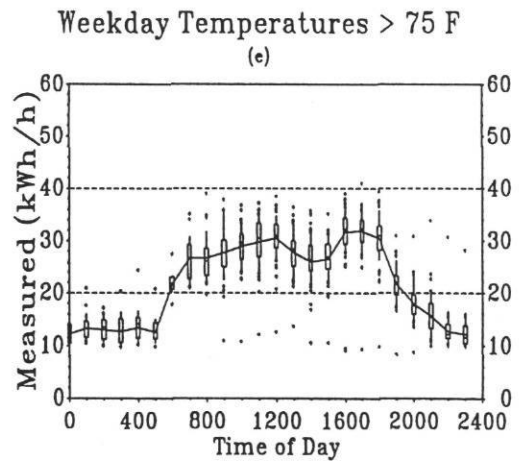
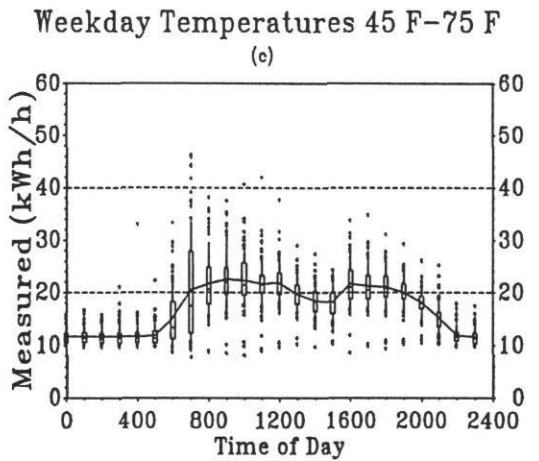
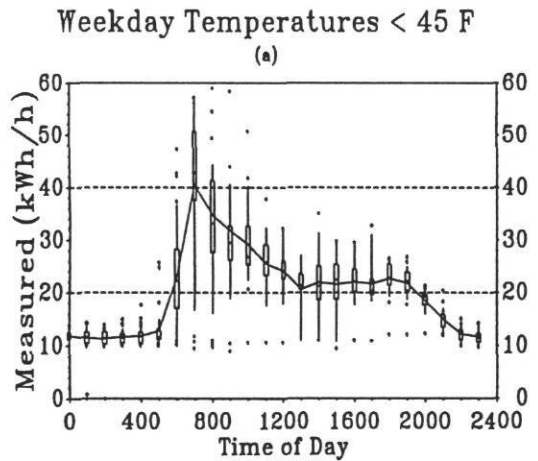


Figure 5.15 Weekday 24-Hour Weather Daytype Box-whisker-mean Plot.

component analysis and cluster analysis. The DOE-2 calibration graphs presented here simply sort the data into temperature bins and divide them into three arbitrary temperature dependent daytypes.

Table 5.5 Weekday 24-Hour Weather Daytype Calibration Mean Statistics.

TIME	Weekday Measured	Weekday DOE-2	Weekday Measured	Weekday DOE-2	Weekday Measured	Weekday DOE-2
	< 45 F (kWh)	< 45 F (kWh)	45 F-75 F (kWh)	45 F-75 F (kWh)	> 75 F (kWh)	> 75 F (kWh)
0	11.8	11.0	11.6	10.4	12.2	10.0
100	11.4	11.6	11.7	10.8	13.2	11.5
200	11.3	11.1	11.6	11.7	13.0	14.1
300	11.7	11.4	11.7	10.4	12.6	10.7
400	11.8	11.4	11.7	11.7	13.4	12.6
500	12.8	11.4	11.8	10.4	12.5	10.8
600	23.2	21.9	15.1	17.6	21.5	20.8
700	40.6	39.0	20.5	21.9	26.7	25.0
800	34.7	32.7	21.6	23.3	26.6	27.2
900	31.8	29.1	22.5	23.0	27.6	28.5
1000	29.2	29.4	22.3	22.9	28.8	29.4
1100	25.5	26.2	21.7	22.6	29.7	30.7
1200	24.0	23.0	21.8	20.9	30.5	31.0
1300	20.4	22.7	19.6	21.0	27.6	29.5
1400	22.1	22.6	18.3	19.6	25.9	28.1
1500	21.5	21.3	18.1	18.7	26.4	29.4
1600	22.1	21.0	21.7	20.2	31.6	31.3
1700	21.7	23.0	21.1	20.3	31.8	32.5
1800	22.7	24.2	21.0	20.2	30.4	31.2
1900	21.7	26.6	19.9	20.6	21.6	27.3
2000	18.4	21.1	18.0	21.4	18.0	22.3
2100	15.0	11.6	15.2	10.8	15.5	10.3
2200	12.2	11.4	12.0	10.6	12.6	10.1
2300	11.6	10.9	11.6	10.5	12.1	10.2

The three daytypes were distinctly chosen and customized to fit the weather patterns observed for the case study building. By observing long-term electricity consumption data patterns, it was observed that the daycare building is both temperature dependent and internally load driven. Therefore a general heating bin was chosen to represent all hours when temperatures were below 45° F while a cooling bin was selected for temperatures above 75° F. By analyzing the temperature bin plots, the energy use in the 45° F to 75° F range was maintained at approximately a 20 to 25 kWh/h building baseload and was defined as the intermediate zone. The non-HVAC period, as described by Kaplan et al. (1990b) is the period between the two balance temperatures (i.e. 45° F < non-HVAC < 75° F).

Figures 5.14 and 5.15 show the total weekday data in the weather dependent daytype format. From the six plots on the graph, building weather dependency is clearly discernible as varying daytype profiles. In Figure 5.14 the actual data are shown in a jittered format. In Figure 5.15 the same data are shown with 24-hour box-whisker-mean format. In the heating season which is represented by temperatures less than 45° F, the building heating system is highly active during the early to late morning hours but slowly subsides during the day when solar heating and heat from internal lights and equipment have a higher effect. The non-heating and non-cooling measured data plot (45° F to 75° F plots) indicates that the staff do not impose as large a load on the building in the early morning as DOE-2 is simulating.

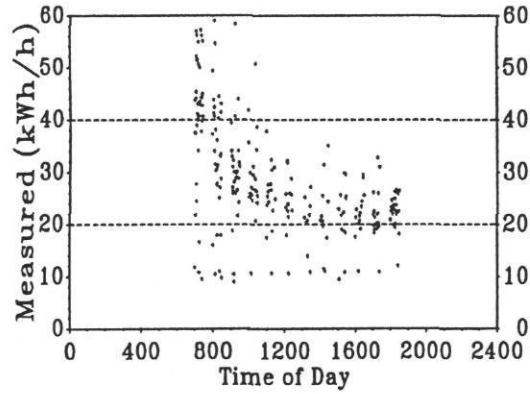
The midday to early afternoon dip in all the plots are attributable to the children's sleep period and reduced interior lighting levels. Electricity usage commences during mid afternoon to evening period when the parents arrive to take the children away. The building's energy use then reduces to a nighttime mode after 9:00 p.m. of about 10 kW and remains this way until 7:00 a.m. It would appear that the lights and equipment are shut down gradually over a two hour period at night, whereas the DOE-2 simulation schedule turned-off the systems and lights abruptly at 9:00 p.m.

The weather daytype 24-hour BWM plots in Figures 5.15 (a) through (f) show that a good daily correlation exists between the simulation and the measured data by comparing the superimposed measured mean lines (i.e. the dashed lines) in the lower graphs with the simulated mean (solid lines). These plots provide an improved insight into data patterns compared to time-series plots, scatter plots and three-dimensional plots because they show how DOE-2 is modeling the building energy use hour-by-hour under three different modes. By comparing how the measured data resembles the simulated data, one may then make adjustments to DOE-2 input schedules as required. Some knowledge of the building daily operations as well as engineering judgment is required to determine which schedule to tune. The decision is generally made based on the sensitivity analysis introduced in Chapter II and audit findings.

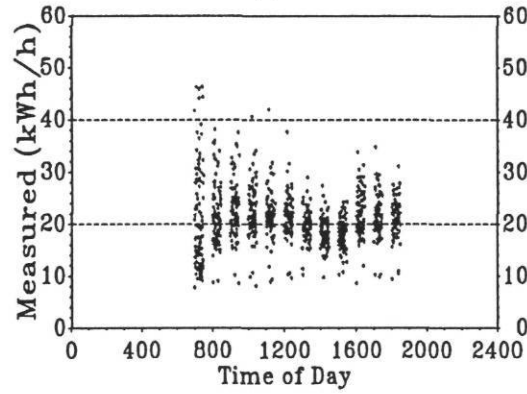
During the heating season, the peak at 7:00 p.m. shown in Figure 5.15 (b) is attributable to the exterior lights being activated. DOE-2 does not appear to robustly turn off the HVAC system to match the corresponding hour shown in Figure 5.15 (a). When comparing the mid-range temperatures in Figures 5.15 (c) and (d), it appears that DOE-2 turns the system on with a greater intensity than the actual building HVAC system as shown by the abrupt rise in consumption at 5:00 to 6:00 a.m. and the small inter-quartile range. Figures 5.15 (e) and (f) represent the weekday cooling season data which seem to reasonably well correlated. Early morning DOE-2 HVAC cycling is indicated by the jagged lines between the hours of 12:00 a.m. and 5:00 a.m. since DOE-2 simulates nighttime setback HVAC operation on a one-hour-on, one-hour-off basis (LBL 1982). Internal capacitance, as is clearly evident in these six plots, is extremely difficult to predict and would require more detailed information concerning interior furnishings so that custom weighting factors could have been specified. For more information on custom weighting factors, see Section 5.3 in this chapter.

Weekday occupied only data are shown in Figures 5.16 and 5.17 (a) through (f) and weekday unoccupied only data are located in Figures 5.18 and 5.19 (a) through (f). These plots simply divide the weekday data into their respective building operation periods and provide the reader a less distracting view of the data. Summing the statistics across the occupied versus unoccupied periods allows for a finer determination of periods in which the model's fit is better. These figures correspond to Tables 5.9 through 5.12 in Section 5.5.2. The benefits of these graphs were

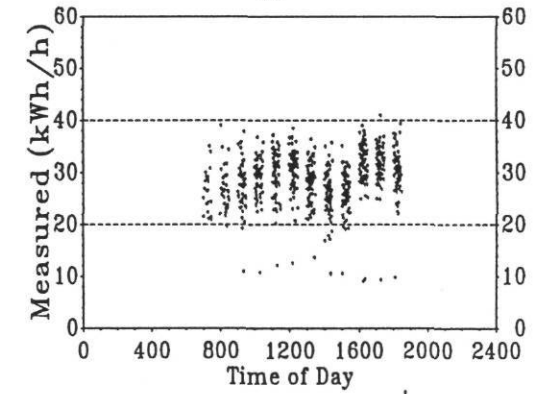
Weekday Occupied Temperatures < 45 F
(a)



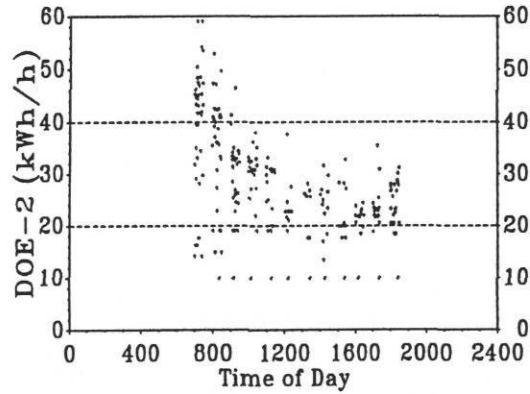
Weekday Occupied Temperatures 45 F-75 F
(c)



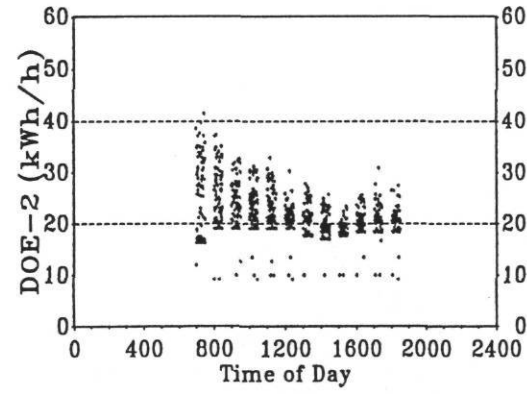
Weekday Occupied Temperatures > 75 F
(e)



Weekday Occupied Temperatures < 45 F
(b)



Weekday Occupied Temperatures 45 F-75 F
(d)



Weekday Occupied Temperatures > 75 F
(f)

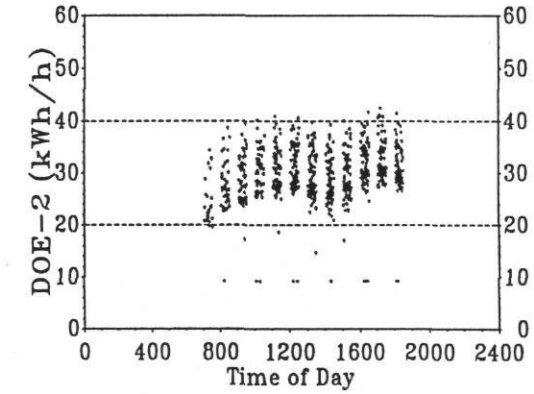
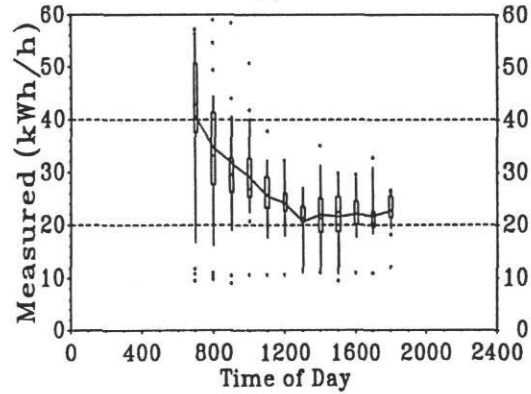
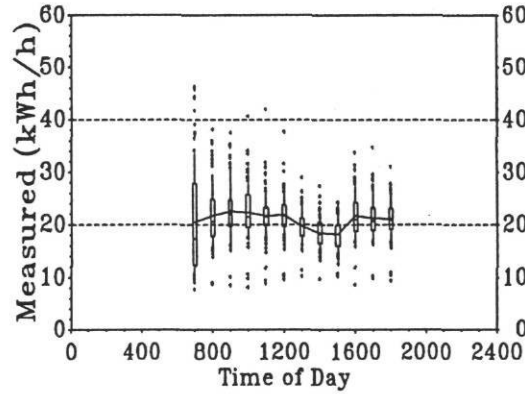


Figure 5.16 Weekday Occupied 24-Hour Weather Daytype Scatter Plot.

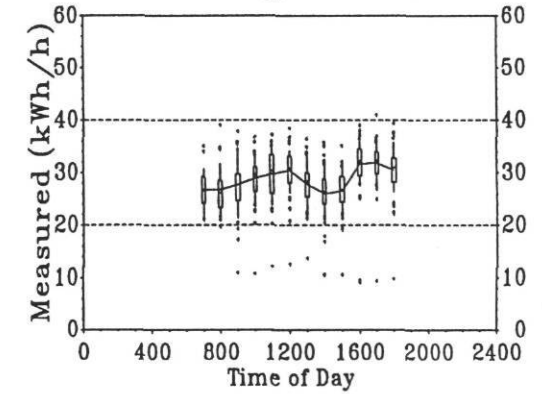
Weekday Occupied Temperatures < 45 F
(a)



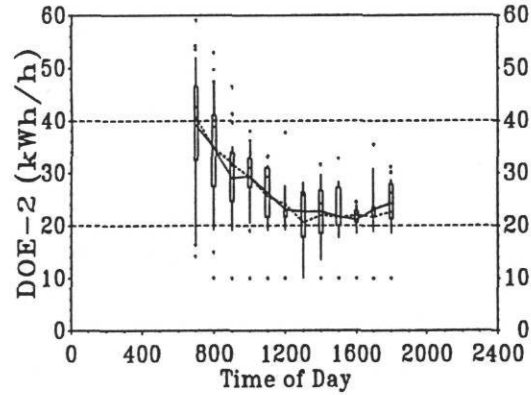
Weekday Occupied Temperatures 45 F-75 F
(c)



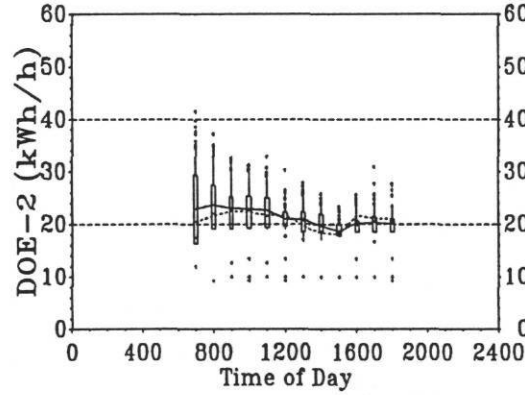
Weekday Occupied Temperatures > 75 F
(e)



Weekday Occupied Temperatures < 45 F
(b)



Weekday Occupied Temperatures 45 F-75 F
(d)



Weekday Occupied Temperatures > 75 F
(f)

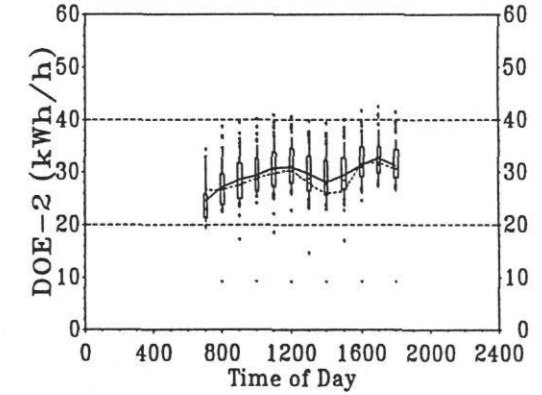
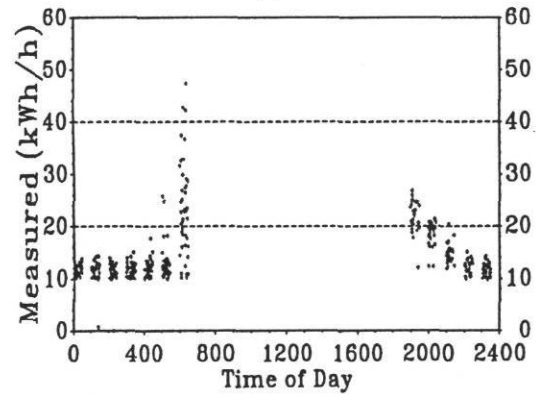
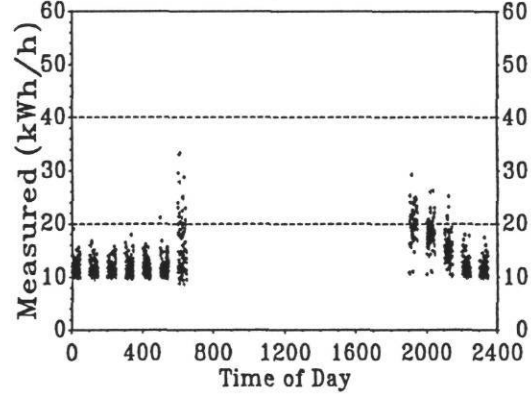


Figure 5.17 Weekday Occupied 24-Hour Weather Daytype Box-whisker-mean Plot.

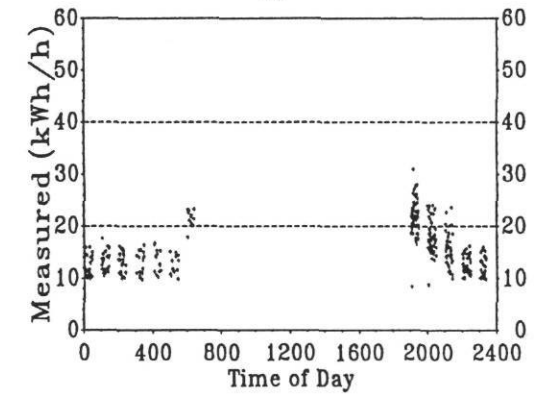
Weekday Unoccupied Temperatures < 45 F
(a)



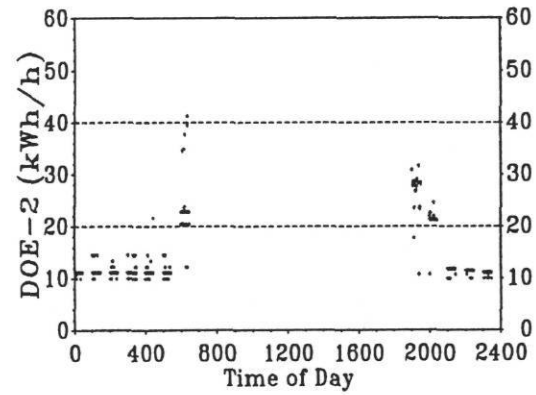
Weekday Unoccupied Temperatures 45 F-75 F
(c)



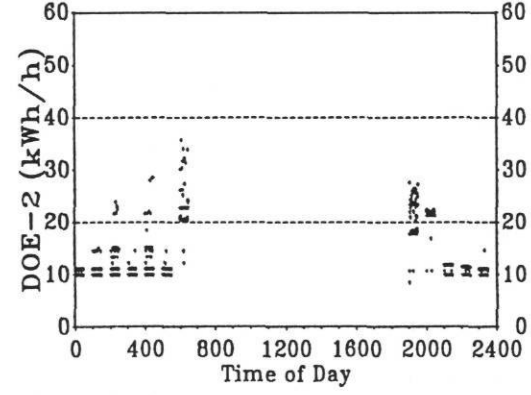
Weekday Unoccupied Temperatures > 75 F
(e)



Weekday Unoccupied Temperatures < 45 F
(b)



Weekday Unoccupied Temperatures 45 F-75 F
(d)



Weekday Unoccupied Temperatures > 75 F
(f)

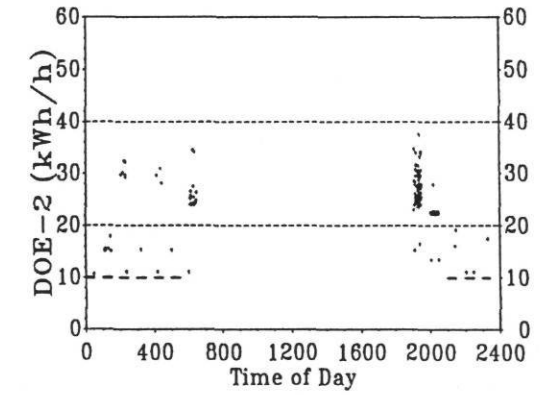
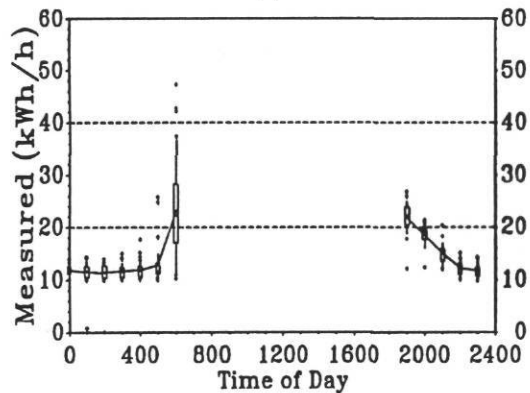
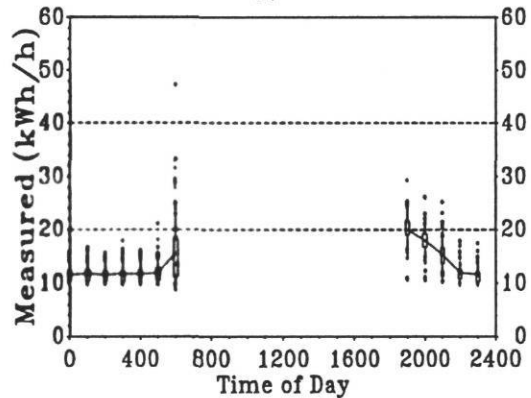


Figure 5.18 Weekday Unoccupied 24-Hour Weather Daytype Scatter Plot.

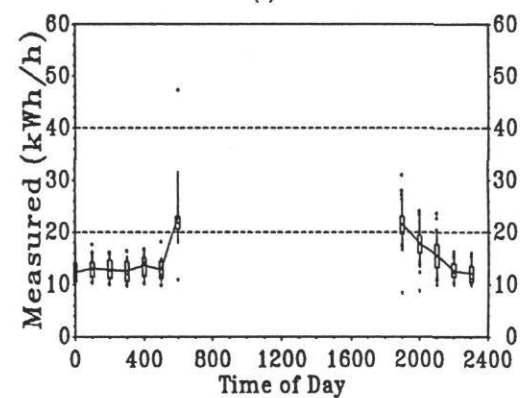
Weekday Unoccupied Temperatures < 45 F
(a)



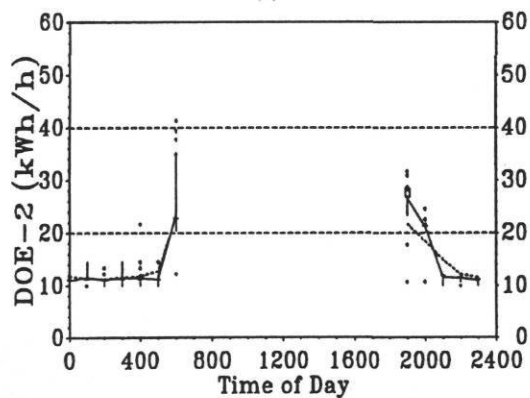
Weekday Unoccupied Temperatures 45 F-75 F
(c)



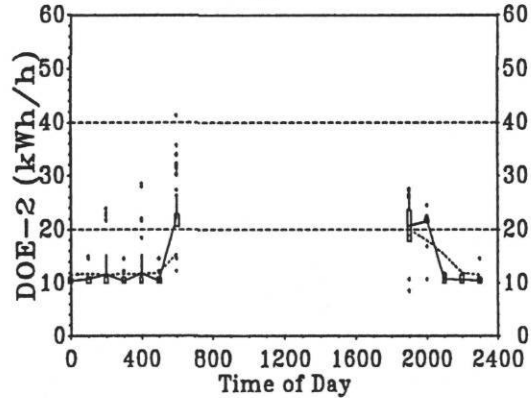
Weekday Unoccupied Temperatures > 75 F
(e)



Weekday Unoccupied Temperatures < 45 F
(b)



Weekday Unoccupied Temperatures 45 F-75 F
(d)



Weekday Unoccupied Temperatures > 75 F
(f)

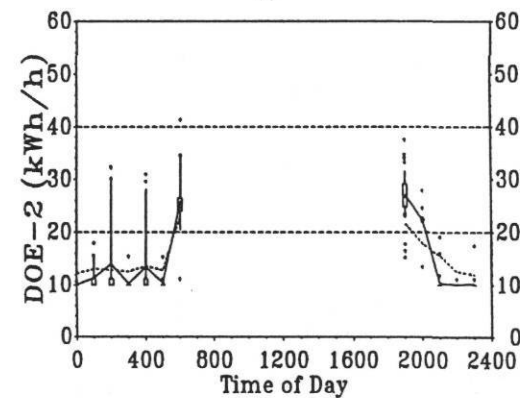


Figure 5.19 Weekday Unoccupied 24-Hour Weather Daytype Box-whisker-mean Plot.

immediately recognized as the data in the 45° F-75° F bin profiles demonstrate. The energy in the intermediate temperature (no heating or cooling) is therefore attributable to the interior lighting and equipment loads for the building excluding exterior lighting. It will be shown that data from this period can be used to disaggregate the end-use loads from the whole-building electricity load covered in Section 5.4.

In Figures 5.20 and 5.21, total weekend daytype plots are displayed including both scatter plots and box-whisker-mean plots. In Table 5.6, the weekend mean statistics are listed. Figures 5.21 (a) through (d) appear to have the best correlation with the heating season and heating to cooling season transition zone. DOE-2's nighttime HVAC cycling, as shown in the weekday plots, is denoted by the jagged line in Figure 5.21 (f). Except for a relatively few hours, the goodness-of-fit is remarkably good between Figures 5.21 (e) and 5.21 (f).

Some further exploration was performed with the weather dependent daytype plots including whether or not ambient conditions might also reveal new dependencies. Figure 5.22 shows a weather dependent daytype scatter plot and box-whisker-mean plot for the measured solar radiation data. These plots correspond to the daytypes defined in this section by indicating how most of the daily solar data are distributed. It can be seen that most of the solar data during the less than 45° F daytype are low as would be expected during cold weather days. The 45° F to 75° F daytype shows a slightly higher mean solar intensity level than is present in the 45° F

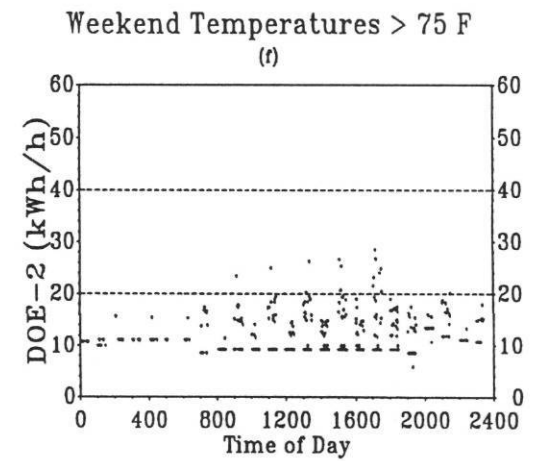
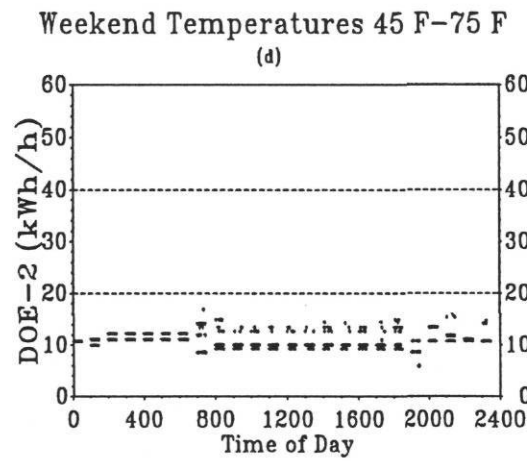
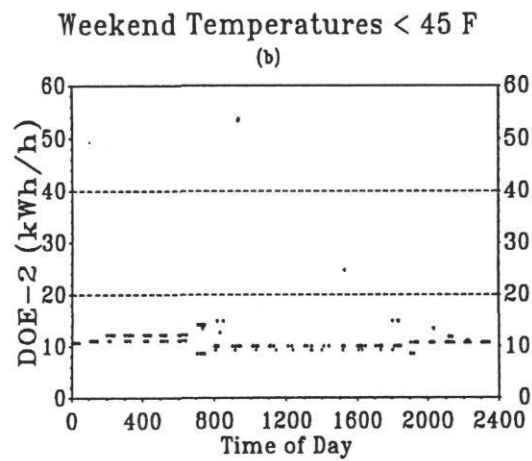
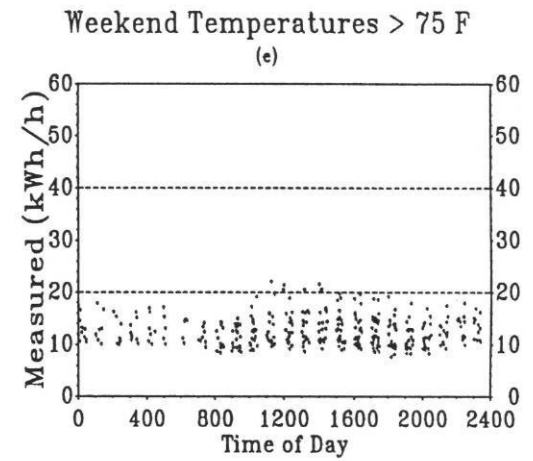
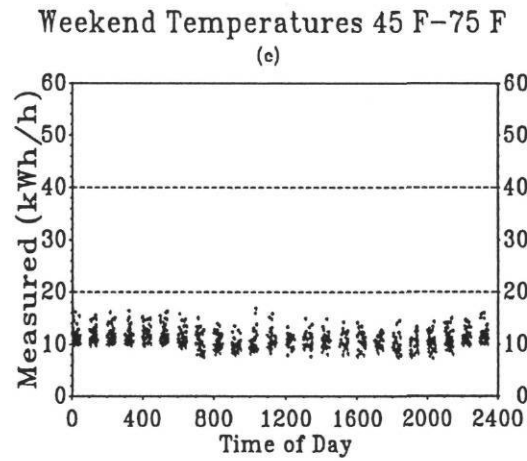
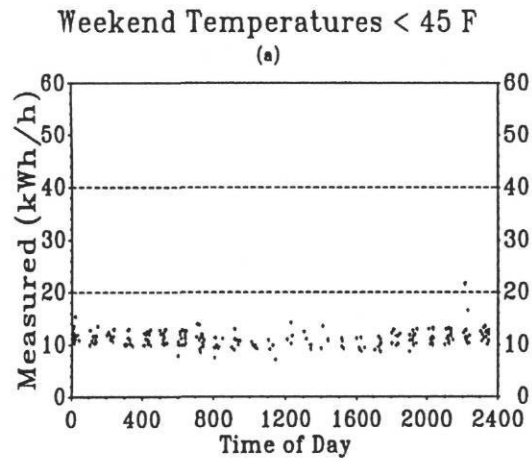


Figure 5.20 Weekend 24-Hour Weather Daytype Scatter Plot.

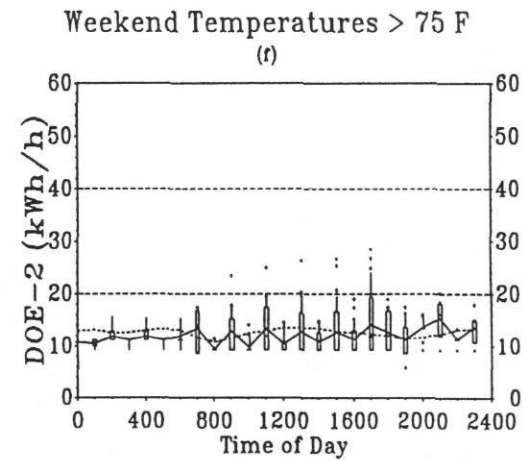
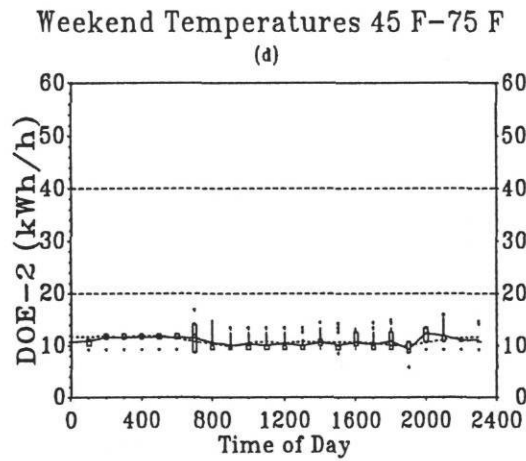
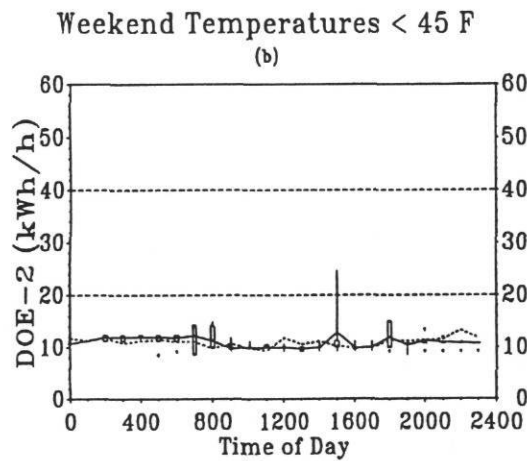
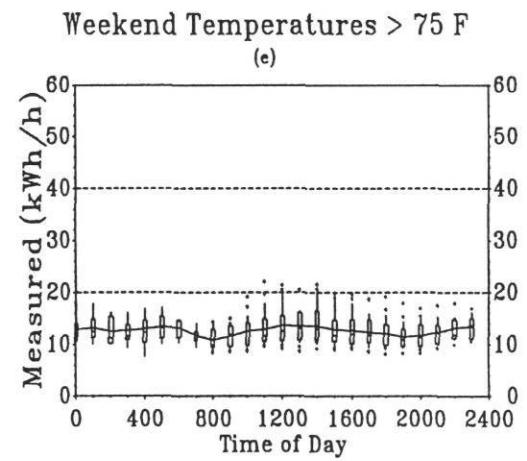
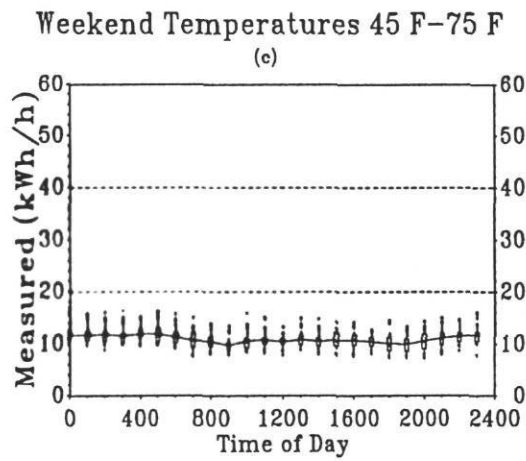
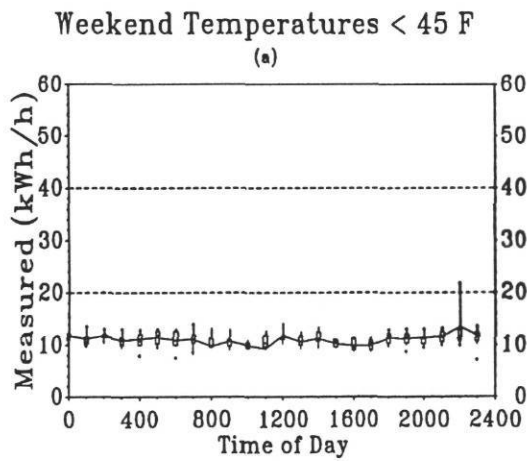


Figure 5.21 Weekend 24-Hour Weather Daytype Box-whisker-mean Plot.

daytype, however, the data are spread over a larger solar intensity range as is indicated by the large inter-quartile range when compared to the less than 45° F plot and greater than 75° F plot. In contrast, the greater than 75° F daytype shows that the majority of the data fall in the upper range with the smallest hourly inter-quartile range.

Table 5.6 Weekend 24-Hour Weather Daytype Calibration Mean Statistics.

TIME	Weekend Measured	Weekend DOE-2	Weekend Measured	Weekend DOE-2	Weekend Measured	Weekend DOE-2
	< 45 F (kWh)	< 45 F (kWh)	45 F-75 F (kWh)	45 F-75 F (kWh)	> 75 F (kWh)	> 75 F (kWh)
0	11.8	10.8	11.7	11.0	12.9	11.1
100	11.2	11.2	11.7	10.8	13.2	10.7
200	11.8	11.9	11.8	11.6	12.5	11.8
300	10.7	11.9	11.5	11.6	12.6	11.4
400	11.2	12.0	12.0	11.5	13.0	12.3
500	11.5	11.9	12.0	11.7	13.3	11.9
600	11.0	9.2	11.3	7.3	13.1	7.8
700	11.1	10.9	10.7	10.6	11.6	14.3
800	9.7	9.1	10.4	9.1	10.8	8.7
900	10.6	9.1	9.7	9.7	11.5	12.4
1000	9.8	9.2	10.4	9.3	12.6	8.8
1100	9.3	9.1	10.7	9.7	12.9	13.1
1200	11.8	9.1	10.4	9.5	12.6	8.8
1300	10.4	9.0	10.6	9.7	12.8	13.1
1400	11.2	9.1	10.6	9.5	12.9	9.4
1500	10.1	12.0	10.6	9.7	12.5	13.1
1600	9.7	9.1	10.7	9.6	12.3	10.2
1700	9.9	9.2	10.4	9.8	12.3	14.9
1800	11.3	11.2	10.0	9.7	12.0	11.2
1900	11.2	10.4	10.0	9.7	11.5	11.8
2000	11.4	11.2	10.5	12.5	11.7	13.8
2100	11.5	10.9	11.1	12.2	12.3	16.1
2200	13.3	10.9	11.6	11.0	13.1	11.4
2300	11.8	10.8	11.7	11.3	13.4	14.3

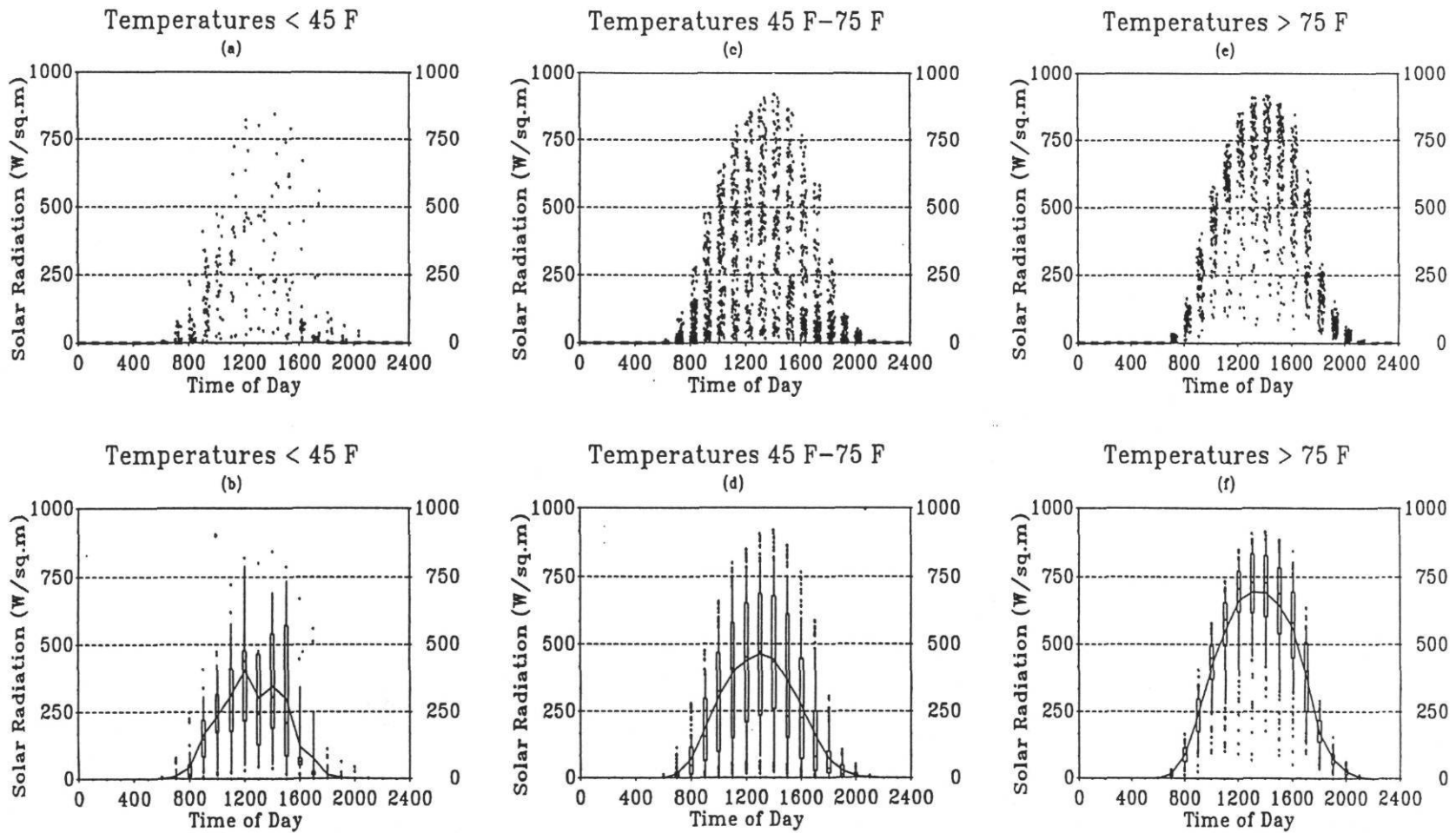


Figure 5.22 Measured Solar Radiation Scatter and Box-whisker-mean Plot.

Figure 5.23 shows the temperature data for the same daytypes as the solar data presented in the previous figure. Although plotting the temperature in a binned temperature plot may appear to be trivial, it is interesting to note that the mean in the 45° F to 75° F and less than 45° F daytypes remains constant throughout the day while in the greater than 75° F daytype, the mean peaks at approximately 2:00 - 4:00 p.m. as would be expected, during early to late afternoon indicating a 1 to 2 hour time lag in the air temperature versus solar noon. One can imagine that this is clearly contributing to the high afternoon cooling load shown in Figure 5.15.

The flat temperature profiles in Figures 5.23 (c) and (d) were quite unexpected, but not unreasonable. One can imagine that an individual day may begin with temperatures in the 45° F to 75° F bins, proceed to the greater than 75° F plot in the afternoon and drop back into the 45° F to 75° F bins in the late evening. However, what seems remarkable is that there is no statistically significant variation in the 45° F to 75° F bins whereas in the less than 45° F bins, there is a slight 5° F to 10° F curvature in the data. Clearly, in terms of temperature at this site, the binning produces a neutral temperature dependence in the 45° F to 75° F bins.

5.3 Indoor Temperature Calibration

Another technique that can be used to calibrate the DOE-2 model is to compare measured indoor zone temperatures with DOE-2 predicted temperatures. Hsieh (1988)

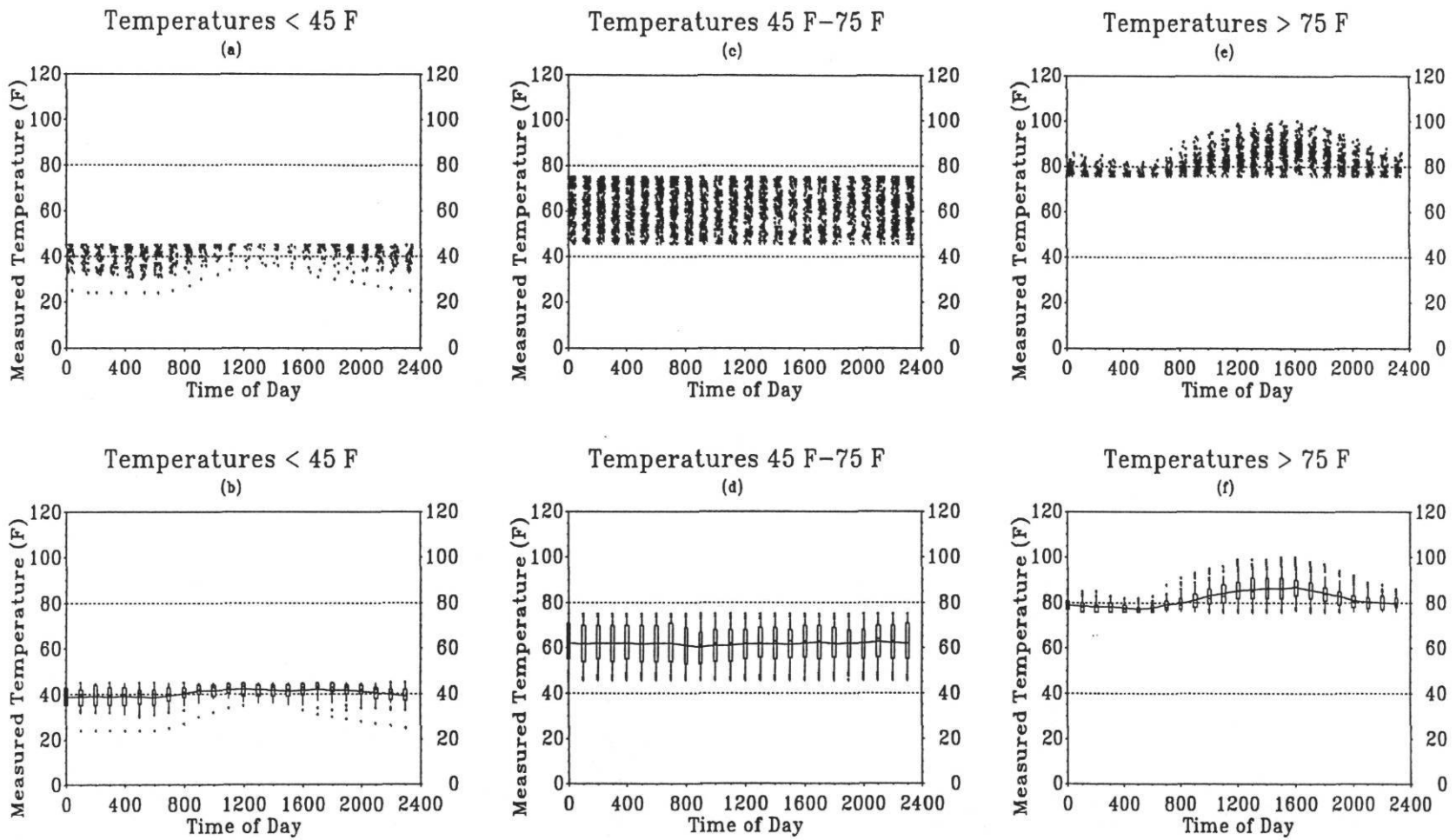


Figure 5.23 Measured Dry Bulb Temperature Scatter and Box-whisker-mean Plot.

and Kaplan et al. (1990b) performed similar research by comparing measured indoor temperature data and DOE-2 simulated indoor temperature data, but did not directly calibrate the model with this method. For this thesis, two calibrated wheel chart recorders were installed in the building, one recorder in the North zone and one recorder in one of the two South zones. Figure 5.24 shows the approximate locations of the two recorders which were hung near the ceiling away from any HVAC diffusers or windows. On a weekly basis, the charts were replaced and the data visually transcribed into a columnar ASCII format readable by graphics software. Pictures of the chart recorder and wheel chart are provided in the Appendix.

To calibrate the chart recorders, a one point calibration was performed with a NIST traceable reference thermometer. This was accomplished by placing the chart recorders near the thermometer and allowing ample time to reach equilibrium. Unfortunately, the north zone chart recorder's calibration was found to be out of adjustment when it arrived at the daycare center due to shipping. This problem was detected by a large difference between the two recorders' readings. It was then readjusted by using an electronic thermometer which, depending on how closely it was calibrated, in all likelihood added a certain amount of error to the readings. Since the same trends were observed in both zones, the data from the south zone are probably more reasonable.

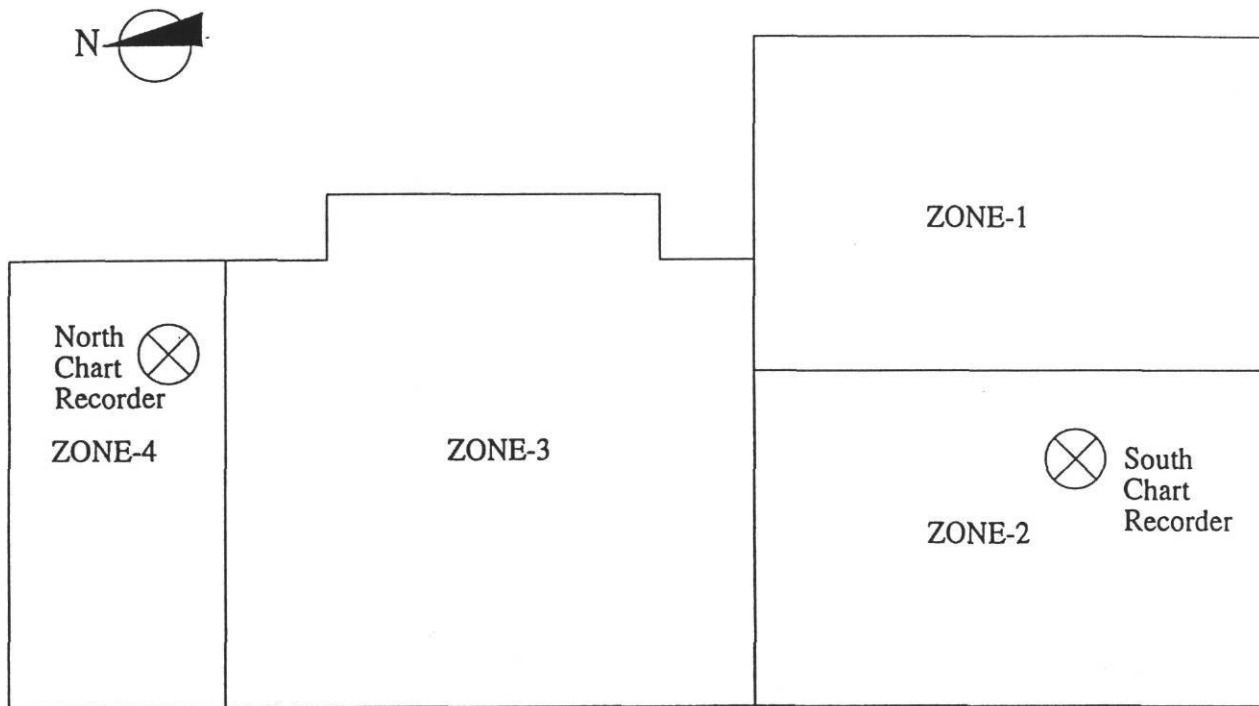


Figure 5.24 Indoor Temperature Chart Recorder Locations.

A one month period of indoor temperatures in the Summer cooling season and a one week period in the Winter heating season was recorded. Figure 5.25 shows eight graphs, the top row consisting of measured Winter indoor temperatures in the north and south zones along with outdoor measured dry bulb temperature and measured horizontal solar radiation. The bottom row is the Summer measured data from the same north and south zones with outdoor NWS dry bulb temperature and solar radiation data.

Analysis of the Summer nighttime temperatures shows the effects of the operational exhaust fans. When the nighttime outdoor temperatures were lower, as seen on the left side of the lower graphs, the indoor temperature range was larger when compared to the higher nighttime outdoor temperatures on the right side of the graphs. Since the cooler air drawn into the building did not cause a night setback override, the indoor temperatures eventually moved closer to the outdoor temperature. Conversely, the change in indoor temperature was not as high with hotter outdoor temperatures since the setback temperature was reached causing HVAC operation.

Although DOE-2 and PASSYS temperature comparisons were made in the previous research by Hsieh (1988) and Clarke et al. (1993) respectively, specific steps to accomplish model tuning were not recommended. This thesis investigated tuning the model with measured hourly zone temperatures and comparing them to measured temperature data. The intent of this study was to see how well the DOE-2 program

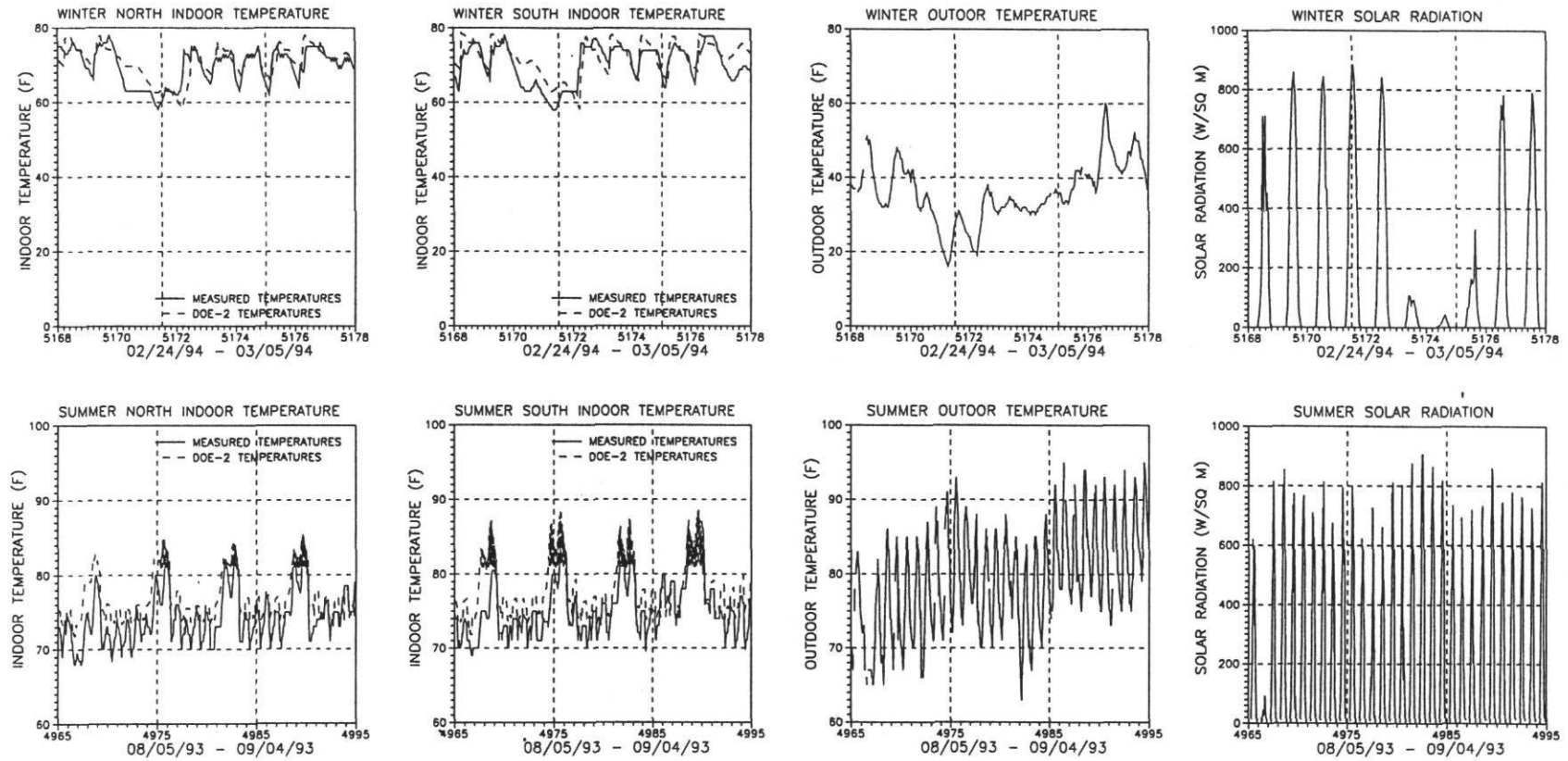


Figure 5.25 Indoor Measured and Simulated Temperatures, Outdoor Temperatures, and Solar Radiation.

simulated the indoor temperatures in two of the thermal zones of the daycare center. In a similar methodology used by Haberl and Komor (1989), measured min/max indoor temperature data were used to determine if HVAC systems were operating to maintain comfortable conditions within a space. In this study the data from the DOE-2 Systems Hourly Report was compared to the recorded data and iterations were used to tune the model.

Kaplan et al. (1990b) used a similar method by measuring indoor temperatures and developed a daytype profile for thermostat schedules. It was discovered that the average temperatures deviated from the actual thermostat especially in the deadband zone. This caused problems in simulations since the DOE-2 program uses a constant temperature for LOADS and a correction factor for temperatures in SYSTEMS. The same problems were encountered in this research and are discussed here.

An air temperature simulation begins in the LOADS sub-program where it is initially fixed by the user to provide a reference setpoint temperature value (LBL 1981). In LOADS, all heat gain calculations such as solar radiation through windows, lights, and people are based on a constant reference temperature. Heating and cooling loads are calculated based on the constant indoor temperature. Since energy in reality can be stored in the walls, the furniture, and the floor, the DOE-2 program employs weighting factors for all applicable heat gains. The weighting factors are essentially correction factors that establish the quantity and rate of energy storage and dissipation

in a zone. An overall cooling and heating load is calculated and passed to the SYSTEMS sub-program to correct for the difference between the actual conditions and the conditions calculated at the reference temperature.

In the SYSTEMS sub-program, the DOE-2 program simulates the energy required to meet the building's heating and cooling loads. The DOE-2 program then uses ASHRAE weighting factors from the program default library or custom weighting factors. When pre-calculated weighting factors are used, one must keep in mind that linear calculations are performed along with constant system properties. Unless the user specifies exact construction properties, default thermal properties are substituted from the DOE-2 library which may or may not be appropriate for all building construction components. Therefore, one should recognize that default weighting factors are only approximations which can lead to simulated temperature values which are not similar to measured values.

Custom weighting factors can improve the simulation, however a significant amount of measured data is required such as furniture and construction thermal properties which still have associated uncertainties. Also, particular attention must be given to the definitions and placement of interior walls and floors. The DOE-2 Engineers Manual (LBL 1981) recommends that custom weighting factors be used in buildings with heavy construction as well as for buildings significantly influenced by solar energy heat gains. Since the case study building is neither made of heavy

construction materials nor largely affected by solar gain, pre-calculated weighting factors were used.

Unfortunately it was discovered that during the cooling season the simulated indoor temperature did not follow the measured temperature as described earlier, but instead remained in a tight band near 75° F as can be seen in Figure 5.25. Adjusting the DOE-2 thermostat inputs, even with unrealistic test values, did not appear to have a significant impact on simulated temperatures. On the other hand the winter indoor temperatures reasonably followed the measured temperatures. The simulated building had a fairly slower response to nighttime cooling than the actual building and a more rapid response to daytime heating. The Winter temperature in the South zone appeared to be higher than in the North zone. This may be attributed to daytime solar heating which has a greater effect in the Winter due to the lower sun declination angle. The indoor temperature comparisons were found to be helpful in checking whether or not the systems were on or off, and seem to help confirm the problem with the continuous exhaust.

5.4 Load Disaggregation From Whole-building Electricity

For this research, only whole-building electricity data were available for the case study building which presented some difficulty. Ideally, a model should be calibrated to end-use data measured at several vital monitoring points such as the fans, lights, and heating/cooling equipment. Therefore as an alternative, two "representative

days" were chosen, one during the Spring and one during the Fall, to disaggregate the whole-building data into the lighting load, the equipment load, and the HVAC heating and cooling load. These disaggregated estimates were then used to further tune the model by comparing the result with non-heating/cooling HVAC electricity use as reported in BEPS.

The objective was to estimate the unknown hourly HVAC fan use by carefully choosing those weekday and weekend profiles when no heating or cooling was being used. These days were determined by weekdays and weekends when temperatures stayed between 45° F and 75° F. Once the lighting, equipment, and HVAC fan load had been determined, the heat pump heating and cooling can be extracted and the measured data compared. To accomplish this, three categories were defined, exterior lighting, interior lighting and equipment, and HVAC. The exterior lighting was a known value based on a lighting survey performed during a site visit. Interior lighting and equipment levels were determined by way of reviewing the lighting site plans and electrical hand measurements of significant pieces of equipment taken during a site visit respectively.

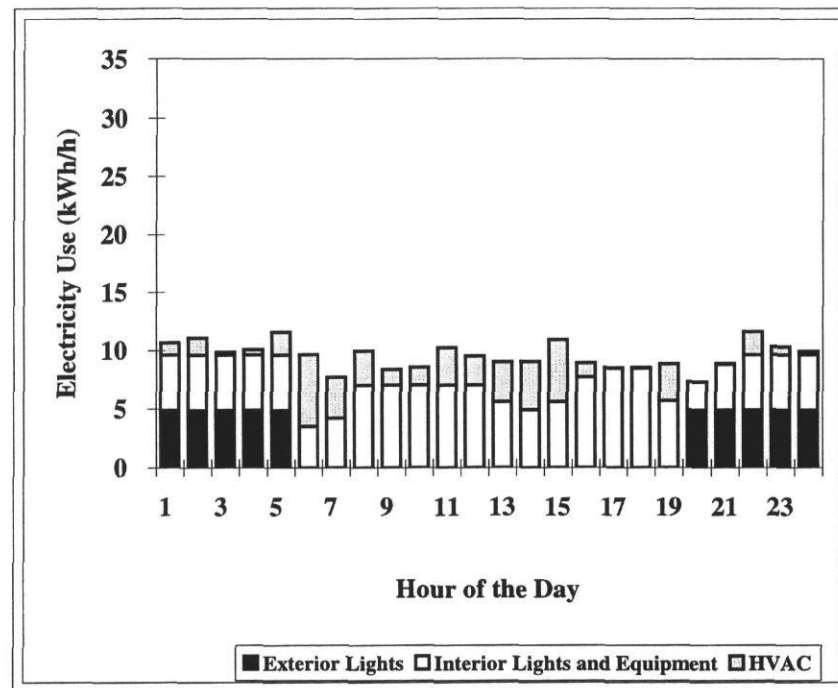
Initially, the hourly interior lighting and equipment operation load factors were estimated based on personnel interviews to establish an overall load shape. Later, the graphical tools, described in Section 5.2 and especially the daytype plots shown in Section 5.2.5, were utilized to refine the original load factor estimates as the tuning

procedure progressed. The HVAC fan electricity use was then calculated by subtracting lighting electricity use (interior and exterior) and all equipment power requirements from the whole-building electricity load. The resulting electric power was lumped into the HVAC fan category since the signature weekday and weekend days represented periods when heating and cooling were not in use.

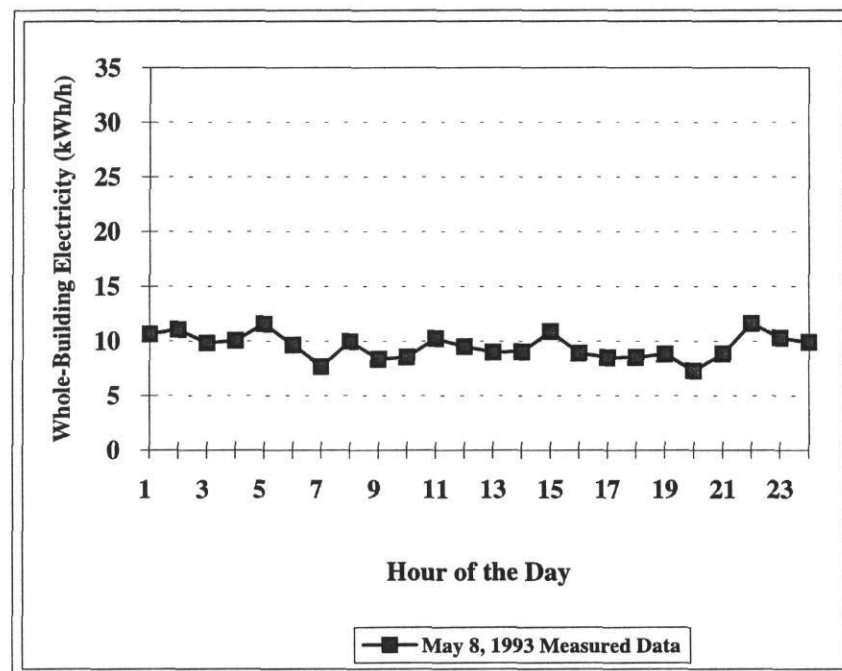
5.4.1 Weekend Representative Day

Figure 5.26, which is similar to the weekend daytype plots in Figure 5.15, shows the measured whole-building electricity data profile developed for Saturday, May 8, 1993. The bar graph illustrates the three categories used in the study. Since this day was a weekend day, theoretically, there should have been no HVAC usage. However, throughout the entire day, it would appear that a small amount of the HVAC system did operate periodically to maintain the interior temperature at the preset EMCS setback temperature. This conclusion is dependent on the assumptions concerning exterior lighting load, the interior lighting and equipment loads. For comparison to the bar graph shown in Figure 5.26 (a), the line graph in Figure 5.26 (b) shows the measured whole-building electricity level which matches each hourly bar's peak for that day.

For the same weekend day, the DOE-2 whole-building data is presented in Figure 5.27. Along with HVAC operation on this day, the measured data also indicates that a number of hours were influenced by equipment cycling. The DOE-2

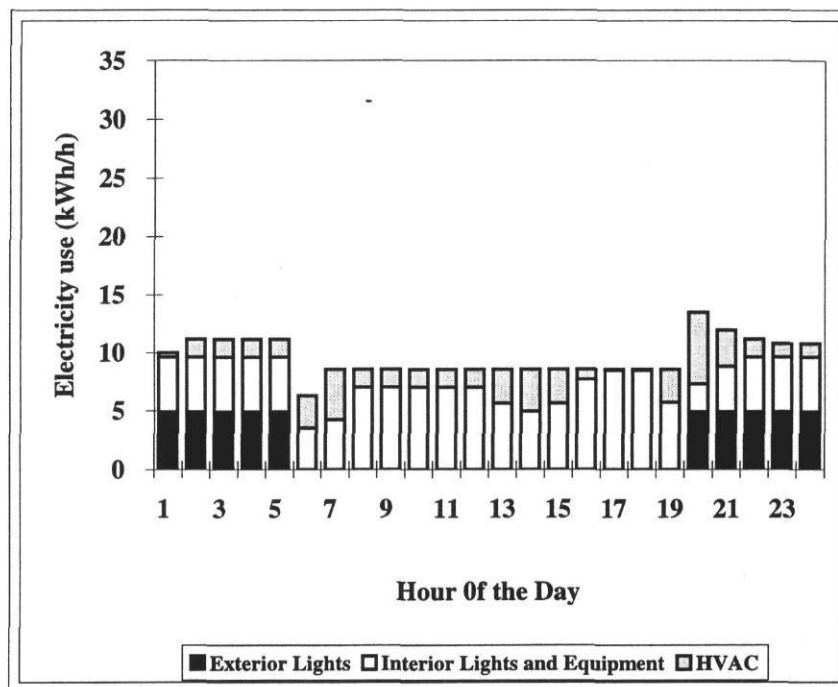


(a)

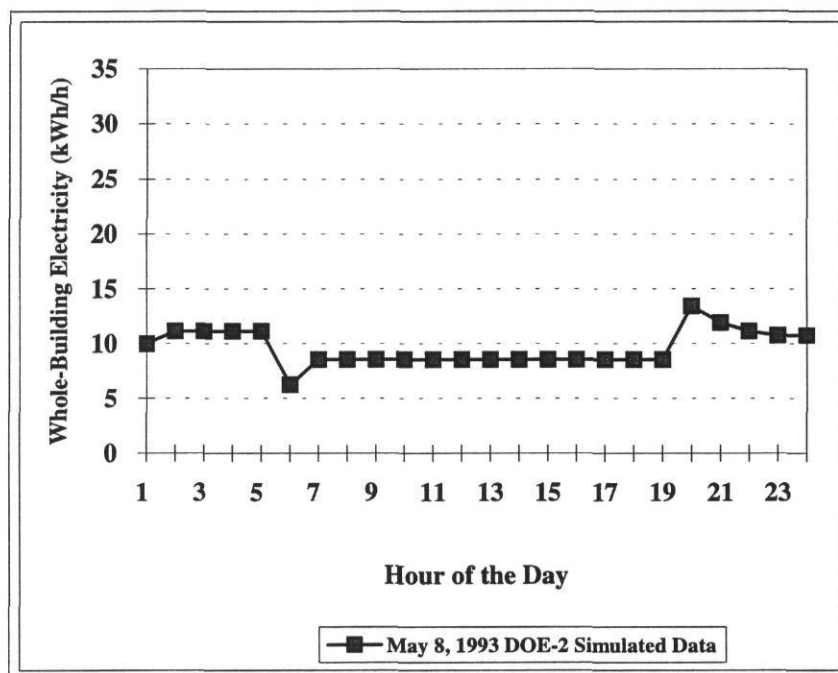


(b)

Figure 5.26 Weekend Measured Data. (a) Exterior Lights, Interior Lights and Equipment, and HVAC. (b) Time Series.



(a)



(b)

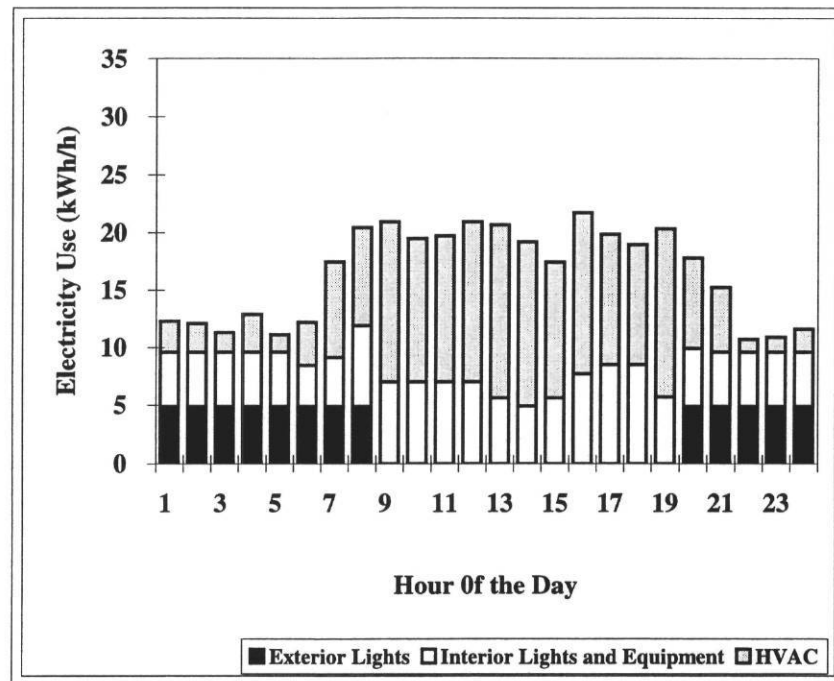
Figure 5.27 Weekend DOE-2 Simulated Data. (a) Exterior Lights, Interior Lights and Equipment, and HVAC. (b) Time Series.

simulation predicted the HVAC usage with reasonable accuracy when compared to the measured data. The measured data shows that the HVAC power level did deviate slightly from the DOE-2 model, but not significantly. This is to be expected since the model was calibrated to measured data. Since it is not possible to model random events such as interior equipment cycling with DOE-2, especially if not directly sub-metered, the remaining differences between the measured data and the DOE-2 are considered to be unavoidable error. One problem encountered with the weekend simulations was the obvious peak in the DOE-2 model for 8:00 p.m. not observed in the measured data. The peak clearly shows the effect of the exterior lighting activation. A smoother transition would have been feasible with sub-metering and more knowledge of actual system schedules.

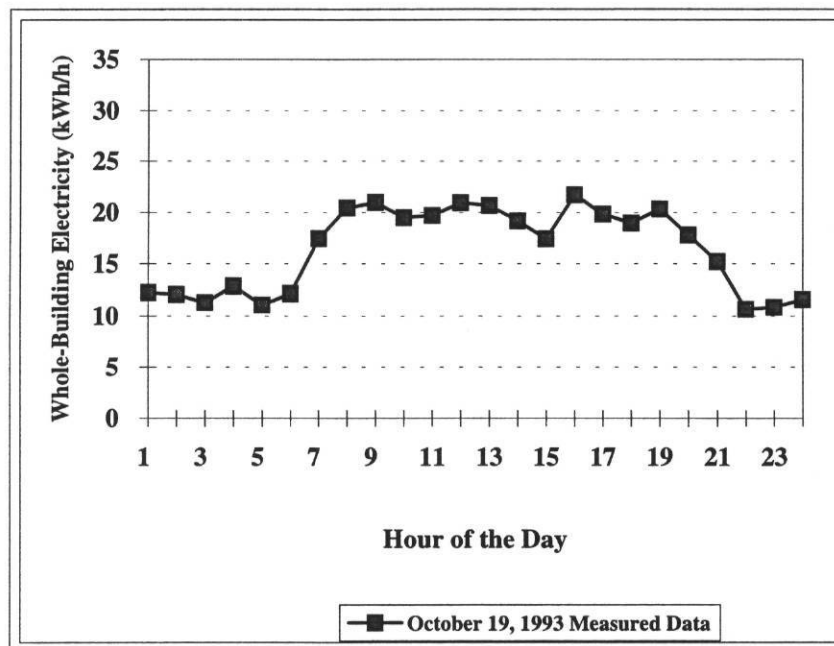
5.4.2 Weekday Representative Day

To determine the electricity loads on the building during a typical weekday, Tuesday, October 19, 1993, was chosen as the representative day and is shown in Figure 5.28. The same fundamental procedure was used for the weekday loads as for the weekend loads analysis to determine contributions by each of the three categories. Despite the DOE-2 morning over-prediction in Figure 5.29, the overall trends are better than in the weekend simulation presented in the previous section.

Iteration based on the inter-quartile range and mean from the statistical bin plots was used to adjust the schedules until the simulation was calibrated to measured

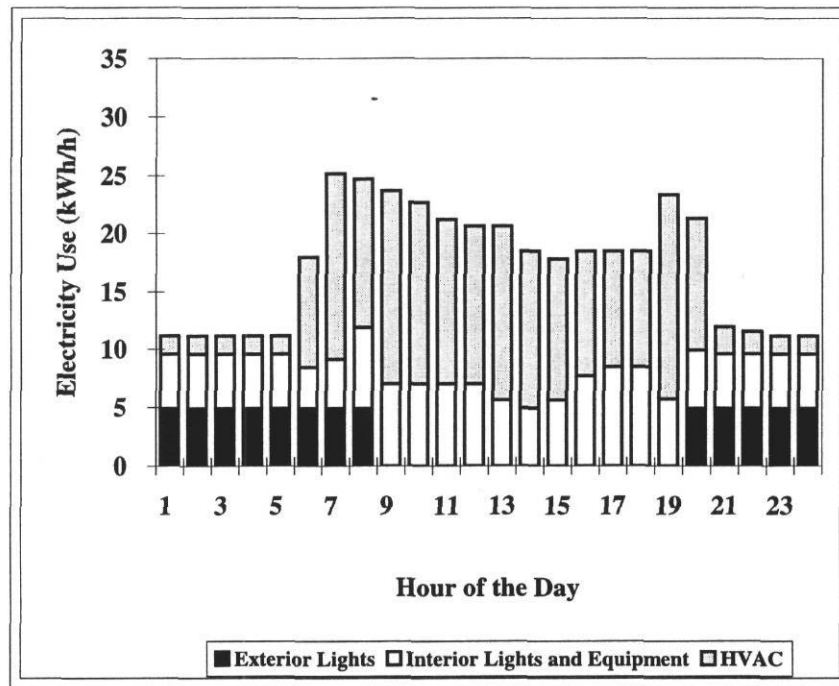


(a)

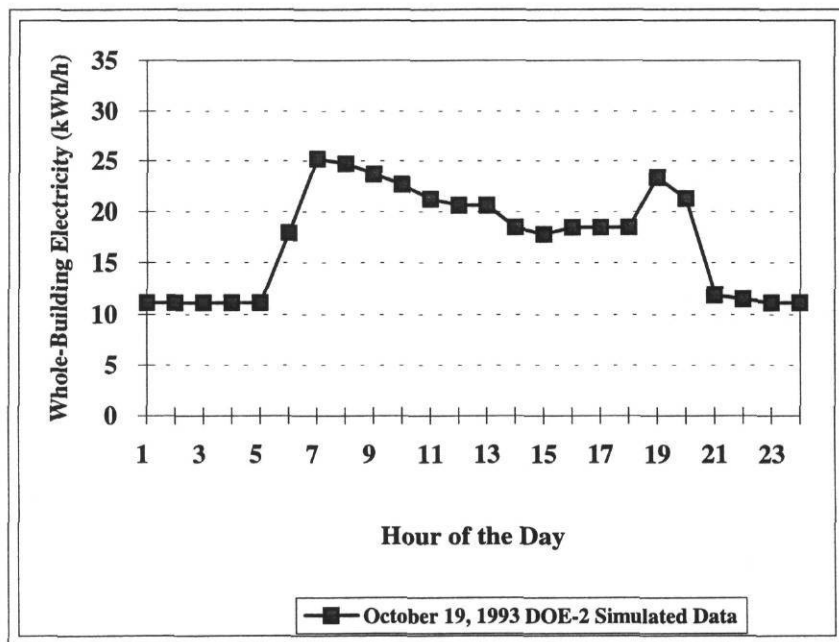


(b)

Figure 5.28 Weekday Measured Data. (a) Exterior Lights, Interior Lights and Equipment, and HVAC. (b) Time Series.



(a)



(b)

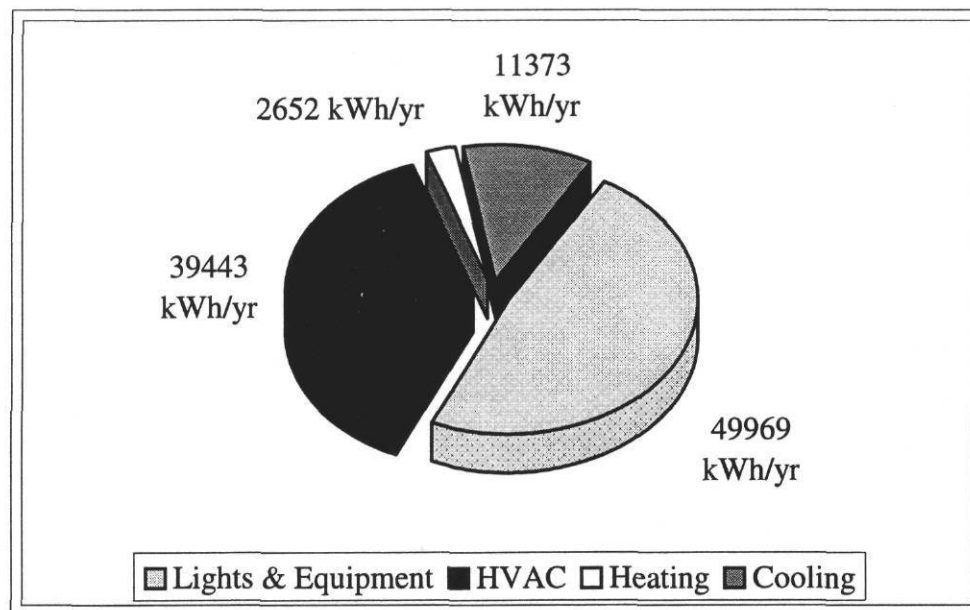
Figure 5.29 Weekday DOE-2 Simulated Data. (a) Exterior Lights, Interior Lights and Equipment, and HVAC. (b) Time Series.

data. As was detailed in previous sections, the calibration effort was hindered to a certain degree due to the daily thermostat readjustments by daycare employees. Although the “representative day” method of scheduling is not as accurate as real-time hourly end-use monitoring, it is important to note that it may be used as a general alternative to extensive and more costly individual system monitoring for developing DOE-2 schedules.

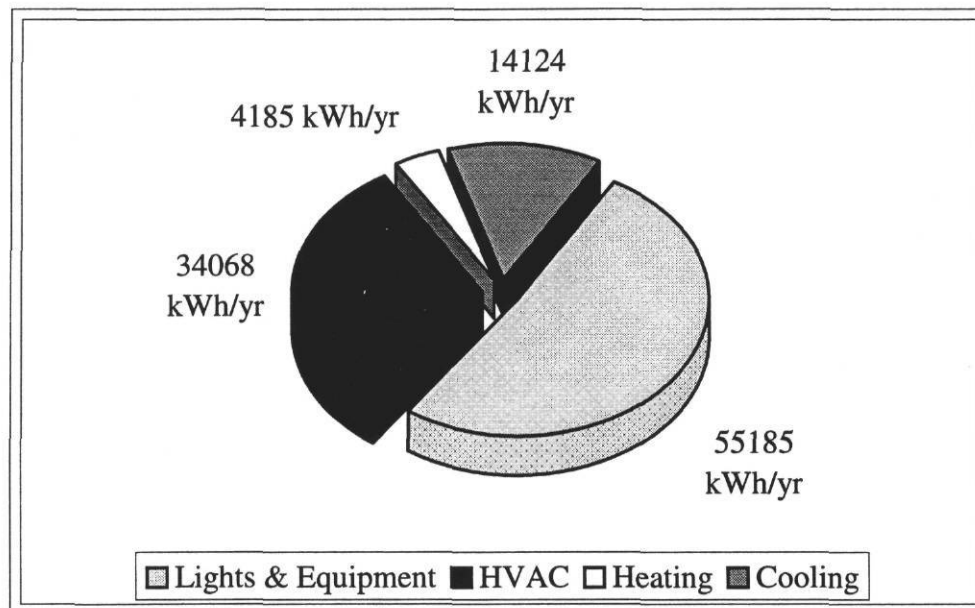
5.4.3 Heating and Cooling Disaggregation

Heating and cooling was extracted by extending the building baseload profiles determined by the disaggregation method into the heating and cooling seasons as follows: since two representative days, a weekday day and a weekend day, were chosen when no heating or cooling loads were evident, the weekday/weekend daytypes, essentially baseloads, were used to construct a data file for the nine month calibration period. By using the same weather dependent sorting methodology as was used for the three daytypes, the difference between the total electricity load and the building baseload was allocated to heating for outdoor temperatures below 45° F and to cooling for outdoor temperatures above 75° F.

Figure 5.30 shows the breakdown of energy use: lighting and equipment loads, HVAC loads, heating loads, and cooling loads in a format similar to the DOE-2 energy breakdown summary report, or BEPS report. Figure 5.30 (a) is a graph of the load disaggregation results and Figure 5.30 (b) is a graph of the DOE-2 BEPS report



(a)



(b)

Figure 5.30 Electricity End-use Comparison. (a) Load Disaggregation. (b) DOE-2 BEPS Summary Report.

(lighting and equipment are lumped). By analyzing the graphs, it can be seen that the disaggregation method is remarkably similar to the DOE-2 BEPS analysis indicating a reasonable methodology. The benefit of such a procedure is that the disaggregation of end-use data was accomplished statistically without the use of a simulated model. It is recommended for the future that this method be pursued in greater detail so that a more refined methodology can be developed.

5.5 Statistical Results of the Calibrated Model

The coefficient of variation of the root mean square error (CV(RMSE)) and the mean bias error MBE, previously defined in Chapter III, were the two main statistical indices used for this analysis. A review of the previously calibrated DOE-2 studies revealed that a monthly percent difference method was most often used to represent DOE-2's calibration accuracy. In this section it will be shown that a monthly percent difference comparison is insufficient for comparing how accurate a calibrated simulation is.

Typically, monthly percent differences often appeared to be within remarkably tight tolerances. Most researchers did not take into consideration or report the "canceling out" of peaks and troughs when long-term data comparisons were made between the hourly measured data and the DOE-2 simulated data. Therefore, hourly CV(RMSE) and MBE reported for each month are used here to illustrate the contrasts that exist between the monthly (and occasionally longer periods) percent difference

and hourly calculations. Table 5.7 shows a list of previous DOE-2 calibrations and the claimed accuracy. It will be shown here that although a percent difference may appear to be satisfactory, the goodness-of-fit calculated by the CV(RMSE) reveal a different situation.

Table 5.7 Previous DOE-2 Calibration Results.

Date	Author	Claimed Accuracy WBE	Period of Comparison	Type of Comparison
1981	Diamond & Hunn	-15% to +12% (1)	12 months	monthly % difference
1988	Hsieh et al.	4% to 5% (2)	12 months	monthly % difference
1990	Kaplan et al.	15% (3)	1 day	daily % difference
1992	Bronson	1.04%	6 months	monthly % difference
1992	Koran et al.	11%	12 months	monthly % difference
1994	McLain et al.	0.50%	1 week	weekly % difference

- (1) Performed for seven individual buildings.
- (2) Performed for two individual buildings.
- (3) Peak lighting calibration.

5.5.1 Model Fine Tuning Progress

To represent the adequacy of the DOE-2 models from an initial workable model to a final calibrated model, each major change to the input file was documented throughout the research phase. A condensed set of iterations is graphically displayed in Figure 5.31 which shows the impact of most of the major modifications made to the

model. The corresponding history of the changes is listed in Table 5.8 which details the hourly total MBE, CV(RMSE), and RMSE for each model and modifications. In reality, about 100 different iterations were run, however due to space constraints, summary groups of the runs are shown in the figure and table.

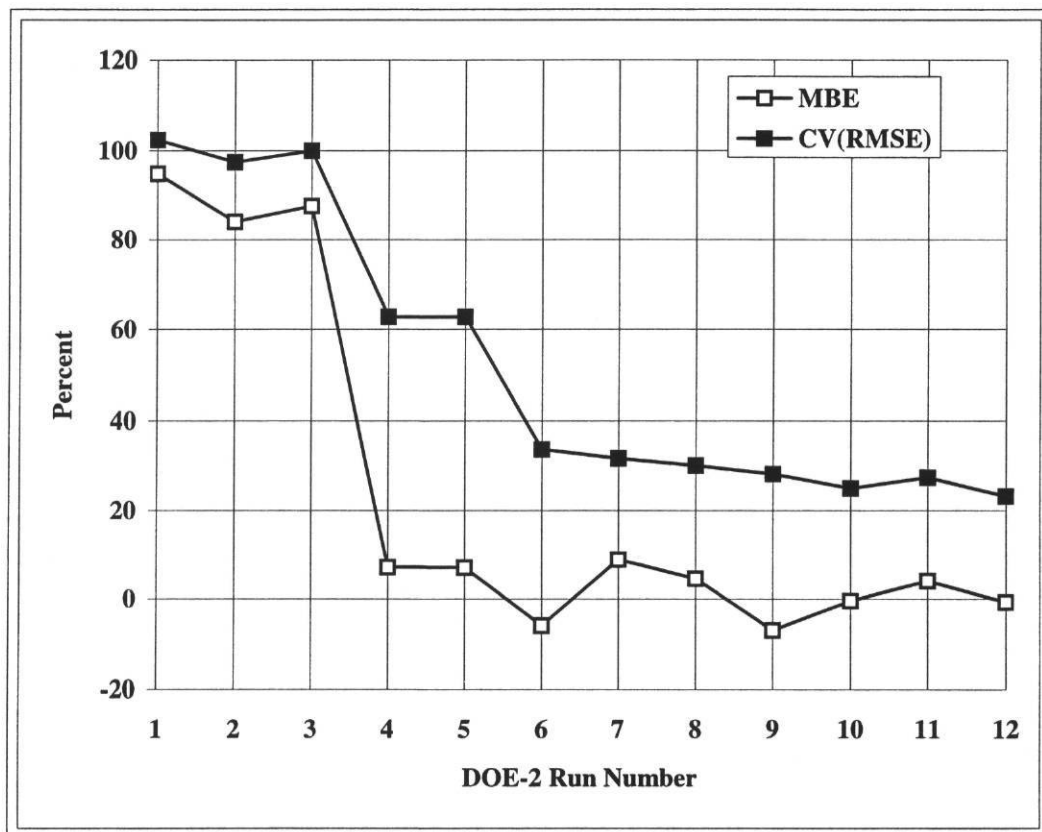


Figure 5.31 Calibration Progress with Each Model Modification.

Table 5.8 DOE-2 Input Deck Changes with Each Run.

Run	Change Made To Model	MBE (%)	CV(RMSE) (%)
1	Base model	94.8	102.4
2	Adjusted infiltration from 0 to 0.1 ACH Added PLANT sub-program to model for hrly reports Modified indoor light & indoor equipment schedules from 10% night/100% day to 35% night/100% day	84.0	97.4
3	Set correct cooling & heating capacities (as per spec.)	87.6	100.0
4	Modified indoor light & indoor equipment schedules (adjusted schedules downward)	7.2	62.8
5	Corrected walls as per DrawBDL Added sizing option -> "ADJUST-LOADS"	7.1	62.8
6	Adjusted air changes from 0.1 ACH to 0.6 ACH Set exhaust CFM as per balance report Set exhaust kW as per balance report Adjusted lighting kW in 1 zone Added surrounding building shading to input file Added ground temperatures to input file Adjusted cooling & heating schedules from 24-hour operation to off at night	-5.9	33.7
7	Adjusted indoor equipment schedules	8.9	31.7
8	Set thermostat settings as per EMCS specs. (summer:74-day, 80-night; winter:72-day, 55-night) Added baseboard heat (7504 BTUH) in north zone	4.6	30.1
9	Adjusted indoor light & indoor equipment schedules Modified HVAC schedule to winter/summer setting Added DHW schedule Adjusted fan schedule from 24-hour operation to off at night	-6.9	28.2
10	Removed two buildings from building shading (they were not close enough to affect shading) Adjusted indoor light & indoor equipment schedules Adjusted DHW schedule	-0.4	25.0
11	Adjusted indoor light & indoor equipment schedules Increased return air CFM as per balance report (this corrected an error of not simulating enough fans)	4.1	27.4
12	Added return air fan as per balance report Adjusted indoor light & indoor equipment schedules	-0.7	23.1

The first DOE-2 model to run without errors was considered Run #1 and is labeled as the base model. This run consisted of the best information that could be obtained from as-built drawings, equipment lists, audit findings, and DOE-2 default values. As Table 5.8 shows, the error is large with a 94.8% MBE and a 102.4% CV(RMSE). Run #2 showed slight improvements with the change of infiltration from 0.0 to 0.1 air changes per hour (ACH), extraction of hourly data from the PLANT sub-program instead of from the SYSTEMS sub-program, and modifications made to the indoor use of indoor lighting and equipment. Correcting the cooling and heating capacities to the manufacturer's specifications in Run #3 worsened the MBE and CV(RMSE) slightly calling for adjustments to the model elsewhere. The most significant modification to the model occurred with Run #4 when indoor lighting and equipment schedules were adjusted downward to match the measured daily profiles. Clearly, one may conclude for this building that the lighting and equipment schedules had a significant impact on the simulation. This is consistent with advice given by Hsieh (1988), Kaplan (1992), and Griffiths and Anderson (1994).

Run #5 was the first simulation to make use of the DrawBDL software to verify the envelope. As was the case with this simulation, corrections to wall locations were minor because they had been placed fairly close to where they belong in the first place. Run #5 also did not include the effects of shading at the site, thus not affecting the output significantly. Run #6 was another notable improvement in the process in which a large change in the MBE and CV(RMSE) was observed. This run

incorporated a combination of adjustments to the ventilation air changes per hour, exhaust air volume, and power level corrections as specified by the balance report, adjustment of lighting power in one zone, addition of building shading, addition of specified ground temperatures, and the adjustment of cooling and heating schedules from 24-hour operation to “off at night” schedules. The cooling and heating load adjustment would in all probability be the most influential factor of this list by reducing the PLANT load significantly in the night setback mode.

As Figure 5.31 and Table 5.8 show, the remainder of the runs were fine-tuning runs with no large scale change in either the MBE or CV(RMSE). Most of the changes made to the model included minor schedule adjustments until Run #12. By reviewing the input file, an error was detected in the original assumptions concerning the SYSTEMS input file. It was discovered that the incorrect air volume was originally specified by the inadvertent omission of the return air fan and volume. Correcting this error required a recalibration effort by adjusting the lighting and equipment schedules to compensate for the return air fan correction. Run #12, the final run, was then considered the “calibrated” version of which all the graphs in this thesis are based on. The MBE of -0.7% and an hourly CV(RMSE) of 23.2% were considered acceptable for the research. Previous work reported by Kreider and Haberl (1994a; 1994b) showed that even the very best empirical models (i.e. artificial neural networks used with a large commercial building) were only capable of producing

CV(RMSE) in the 10 to 20% range. When comparing the neural network results to the daycare center, minute in size comparison, the CV(RMSE) of 23.2% is favorable.

For this research, both CV(RMSE) and MBE did not appear to improve any further without additional major modifications to the input file such as additional schedules to account for fine differences in the occupants' behavior. The energy conservation option verification study presented in Chapter VI also used this final model.

5.5.2 Monthly Statistical Results

A major point of this thesis is presented in this section which includes a closer look at the statistical results of the final calibrated DOE-2 model. The statistical results for the DOE-2 model can be seen in Tables 5.9 through 5.12 and Figures 5.14 through 5.21. These tables show monthly and total measured kWh/h, measured mean kWh/h, total simulated kWh/h, and simulated mean kWh/h. More importantly, the tables compare the monthly and total percent difference to the hourly MBE, hourly RMSE, and hourly CV(RMSE) for each month and total period. The MBE, RMSE, and CV(RMSE) statistics are calculated for each hour and summed for each month and for the total period as explained in Chapter III, Section 3.3.5. This section will explain why the percent difference statistics typically reported in most calibrations may not be true representations of the measured data, and why the hourly CV(RMSE) calculations may be more appropriate.

Table 5.9 is a summary of the statistics for the total calibration period from April 1, 1993 through December 21, 1993. Figure 5.32 shows the CV(RMSE) and MBE graphically. The contrast between percent difference and CV(RMSE) clearly can be seen when comparing May and July. In May, a simulation under-prediction exists to the tune of 4.9% while the CV(RMSE) is a relatively low 21.8% (low as opposed to the other months in the table). July shows an under-prediction difference of 1.7% whereas the CV(RMSE) is a high 24.7%. The peak and trough canceling out effect described in Section 3.3.5 is evident here showing an overall low percent difference in July and an hourly high CV(RMSE). Despite all the months generally showing a low percent difference, the hourly CV(RMSE) consistently remained in the 21 to 27% range. This is still well within the range reported in a recent simulation competition held that compared various modeling techniques including a Bayesian non-linear modeling technique and complex neural networks (Kreider and Haberl 1994a; 1994b).

Table 5.9 Total Period Statistics Summary.

Month	Total Measured (kWh)	Mean (kWh)	Total Simulated (kWh)	Mean (kWh)	Total Difference %	Hourly MBE %	Hourly RMSE (kWh)	Hourly CV(RMSE) %
April	10,606	15.5	10,243	15.0	-3.4	-3.4	4.2	26.9
May	11,507	15.5	10,948	14.7	-4.9	-4.9	3.4	21.8
June	11,568	17.4	11,313	17.0	-2.2	-2.2	3.5	20.2
July	11,247	19.9	11,052	19.6	-1.7	-1.7	4.9	24.7
August	12,621	18.6	12,531	18.5	-0.7	-0.7	4.0	21.7
September	11,885	16.5	12,012	16.7	1.1	1.1	3.7	22.5
October	11,216	15.1	11,413	15.3	1.8	1.8	3.5	23.2
November	11,944	16.7	12,202	17.0	2.2	2.2	4.0	23.7
December	9,220	18.3	9,337	18.5	1.3	1.3	4.2	22.8
Total	101,814	16.9	101,051	16.8	-0.7	-0.7	3.9	23.1

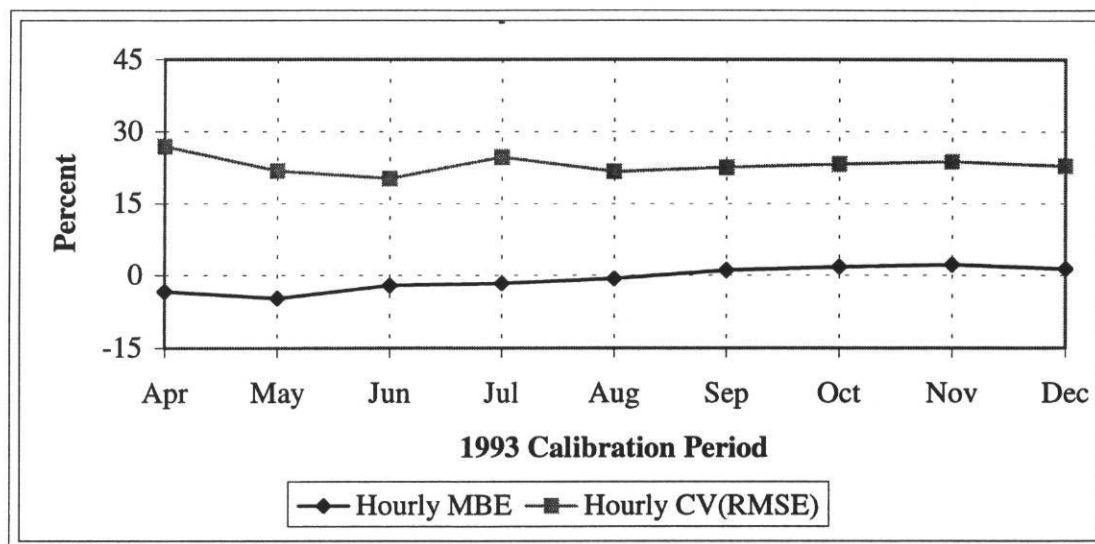


Figure 5.32 Total Period Graphical Summary.

The same effect is evident in Table 5.10 and Figure 5.33 showing the weekday occupied period. By observing June and July, the percent difference has a large range while the CV(RMSE) remains exactly the same. Tables 5.11 and 5.12 show the unoccupied periods for weekdays and weekends. When comparing unoccupied periods to occupied periods, the unoccupied periods generally have a higher CV(RMSE) and MBE. Since the unoccupied periods consume less energy than the occupied periods, any error will have an overall greater impact on the final percent difference result. The effects of the cross-wired exhaust fans can be seen with the model's under-prediction trend shown in Figures 5.34 and 5.35 for most winter and summer months, as is indicated by the mostly negative MBE values. Figure 5.33, the

weekday occupied period, is not affected by the exhaust fans since the building systems are operating as intended.

Table 5.10 Weekday Occupied Period Statistics Summary.

Month	Total Measured (kWh)	Mean (kWh)	Total Simulated (kWh)	Mean (kWh)	Total Difference %	Hourly MBE %	Hourly RMSE (kWh)	Hourly CV(RMSE) %
April	5,233	21.3	5,172	21.0	-1.2	-1.2	5.6	26.1
May	5,379	21.3	5,334	21.2	-0.8	-0.8	3.4	15.9
June	6,127	25.6	6,169	25.8	0.7	0.7	3.6	13.9
July	5,859	29.3	6,246	31.2	6.6	6.6	4.1	13.9
August	6,997	29.9	6,886	29.4	-1.6	-1.6	3.6	11.9
September	6,246	23.7	6,438	24.4	3.1	3.1	4.5	19.1
October	5,292	21.0	5,440	21.6	2.8	2.8	5.1	24.1
November	6,153	23.4	6,410	24.4	4.2	4.2	5.2	22.4
December	4,932	27.4	5,149	28.6	4.4	4.4	6.2	22.6
Total	52,217	24.5	53,244	25.0	2.0	2.0	4.6	18.9

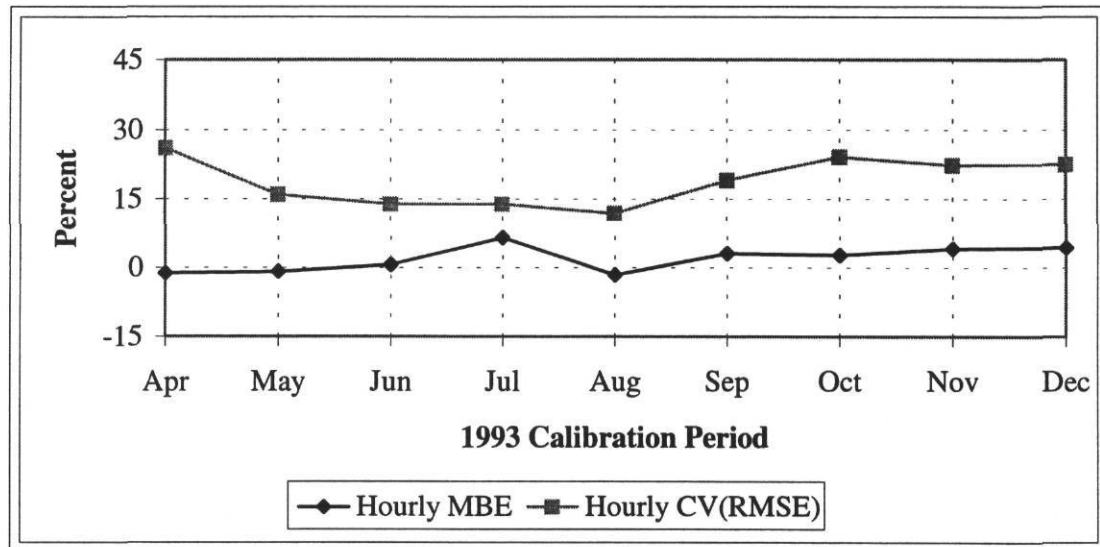


Figure 5.33 Weekday Occupied Period Graphical Summary.

Table 5.11 Weekday Unoccupied Period Statistics Summary.

Month	Total Measured (kWh)	Mean (kWh)	Total Simulated (kWh)	Mean (kWh)	Total Difference %	Hourly MBE %	Hourly RMSE (kWh)	Hourly CV(RMSE) %
April	3,486	13.9	3,210	12.8	-7.9	-7.9	3.7	26.8
May	3,404	13.5	3,140	12.5	-7.8	-7.8	3.6	26.3
June	3,168	13.5	3,037	13.0	-4.1	-4.1	3.6	26.6
July	3,133	15.8	2,807	14.2	-10.4	-10.4	5.4	33.8
August	3,128	13.8	3,147	13.9	0.6	0.6	4.5	32.3
September	3,504	13.3	3,543	13.4	1.1	1.1	3.5	26.6
October	3,285	13.0	3,463	13.7	5.4	5.4	2.8	21.4
November	3,628	13.9	3,732	14.3	2.9	2.9	3.5	24.9
December	2,695	14.9	2,633	14.6	-2.3	-2.3	2.9	19.5
Total	29,430	13.9	28,712	13.5	-2.4	-2.4	3.8	27.0

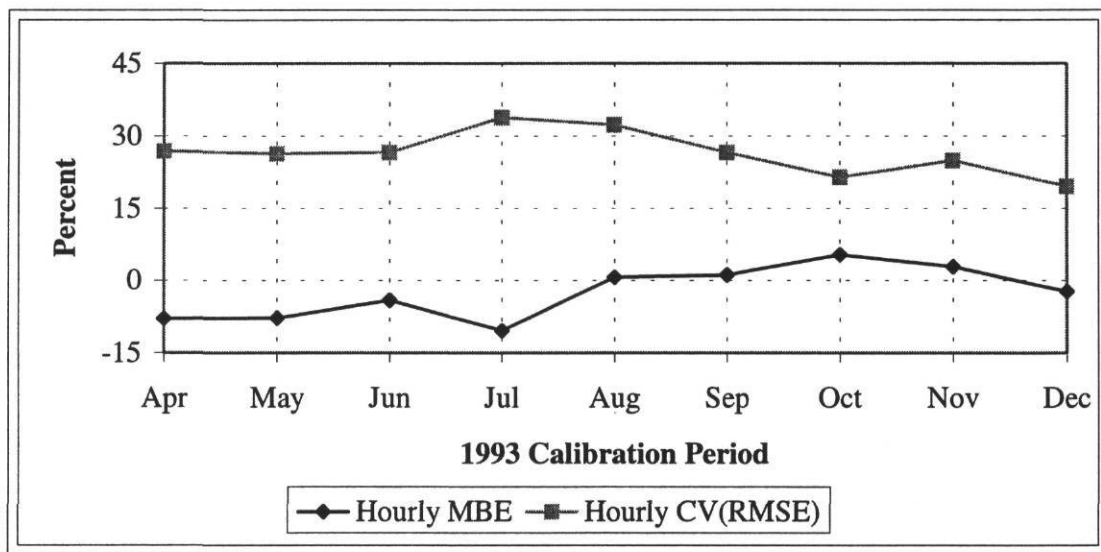
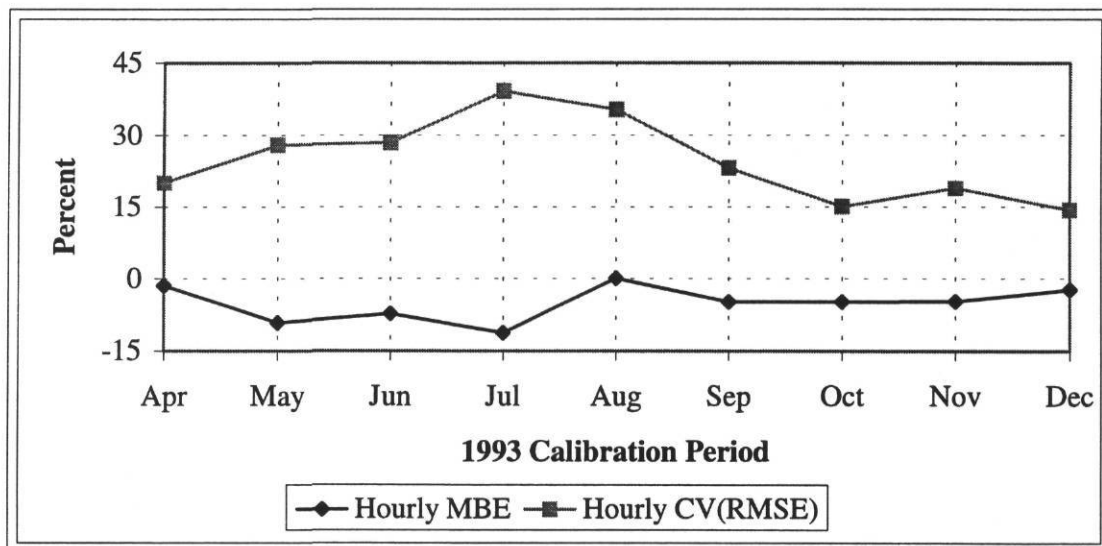


Figure 5.34 Weekday Unoccupied Period Graphical Summary.

Table 5.12 Weekend Period Statistics Summary.

Month	Total Measured (kWh)	Mean (kWh)	Total Simulated (kWh)	Mean (kWh)	Total Difference %	Hourly MBE %	Hourly RMSE (kWh)	Hourly CV(RMSE) %
April	1,887	10.0	1,860	9.8	-1.5	-1.5	2.0	20.1
May	2,725	11.4	2,474	10.3	-9.2	-9.2	3.2	27.9
June	2,272	11.8	2,106	11.0	-7.3	-7.3	3.4	28.5
July	2,255	13.5	2,000	12.0	-11.3	-11.3	5.3	39.2
August	2,496	11.5	2,497	11.5	0.0	0.0	4.1	35.4
September	2,135	11.1	2,031	10.6	-4.9	-4.9	2.6	23.2
October	2,639	11.0	2,511	10.5	-4.9	-4.9	1.7	15.0
November	2,164	11.2	2,060	10.7	-4.8	-4.8	2.1	18.9
December	1,593	11.1	1,556	10.8	-2.4	-2.4	1.6	14.3
Total	20,167	11.4	19,095	10.8	-5.3	-5.3	3.1	27.0

**Figure 5.35 Weekend Period Graphical Summary.**

Perhaps the finest example of this analysis can be seen during the month of August in Table 5.12. The percent difference is 0% while the CV(RMSE) of 35.4% is the second highest of all four tables. As it would have been traditionally reported in

other calibrations, this particular month would have been singled out as an outstanding characteristic of a well calibrated model. The CV(RMSE) of 35.4%, on the other hand, shows the problem from a different perspective. Clearly, calibrations should be performed on hourly CV(RMSE) and hourly MBE calculations rather than solely with the total percent difference calculation. These statistical indices serve to shed light on improving calibration techniques well into the future.

5.6 Summary

This chapter showed how the new calibration tools were utilized with the case study building. Each method introduced in Chapter III was described in this chapter along with the results specific to the case study building. Architectural rendering proved to be an invaluable tool for verifying the building envelope and surrounding shading. Temperature bin box-whisker-mean plots were shown to be an improvement over x-y scatter plots since they are not affected by data overlap. 52-Week bin box-whisker-mean plots were used to display long-term data trends along with previously shown comparative three-dimensional plots. Weather dependent 24-hour daytype box-whisker-mean were developed to show hourly temperature-dependent energy use profiles to help calibrate lighting and equipment schedules. They also provided the basis for the whole-building electricity load disaggregation technique used to identify specific end-uses. Indoor temperature calibration was effective in calibrating the DOE-2 thermostat schedules as well as helping to verify HVAC operation. Finally, improved statistical indices, CV(RMSE) and MBE, were used to provide a more

accurate method of verifying the calibration. For the case study building, the model was determined to have a 23.1% CV(RMSE) and a -0.7% MBE which compares well with highly accurate neural networks. Chapter VI applies the case study DOE-2 model to verify retrofit savings.

CHAPTER VI

USING THE CALIBRATED MODEL TO PREDICT RETROFIT SAVINGS

Since the case study building was initially intended to represent the state of the art in energy efficient new building construction, a methodology was needed to verify their effectiveness. The energy conservation options (ECOs) installed in the building included more efficient lighting, a photovoltaic system, an energy management and control system (EMCS), lighting controls, additional insulation in the ceiling and walls, clerestory windows, high efficiency heat pumps, and a solar domestic hot water system (DHW). Most of the installed energy conservation options in the case study building such as the lighting, the EMCS, the insulation, the clerestory windows, and the heat pumps were analyzed using a calibrated DOE-2 simulation model. The results were then compared to the initial estimates submitted by the General Services Administration (GSA) architects before the building was built. The DHW solar components were verified using the F-CHART (F-CHART 1989) solar analysis software and the system was verified using the procedures outlined in Chapter IV.

In this chapter, each ECO is described in detail as well as the specific measures taken to verify the option. Where applicable, either the DOE-2 input file change, the F-CHART calculations, or other actions taken are described to account for the particular energy conservation option in question. Table 6.1 is a list of the baseline installed ECO features provided by the GSA architect and their standard (w/o ECO)

Table 6.1 Baseline and Standard Energy Conservation Options.

ENERGY CONSERVATION OPTION	BASELINE	STANDARD W/O ECO	COMMENTS
Energy efficient lighting	Energy efficient 34 W lamps (fluorescent) architect proposed value	Standard 40 W lamps (fluorescent) PEPCO recommended baseline	1 DOE-2 run with either option
Photovoltaic	Use measured data, curve-fit to TMY weather	No photovoltaic	Verification independent of DOE-2
EMCS	Schedule heat pumps according to on/off period and temperature	Thermostat control only (fans on 24 hrs/day)	1 DOE-2 run with either option
Lighting controls	Dimmers (not installed according to DOE personnel)	No dimmers	No DOE-2 simulation performed
Insulation, airlocks, South window shading	Roof - R-30 Walls - R-13 Tight building - 0.6 ach Shading over south windows	Roof - R-18 Walls - R-11 Loose building - 1.0 ach No shading over south windows	1 DOE-2 run with options combined
Clerestory windows	Add to BDL	Replace with equivalent walls	1 DOE-2 run with either option
Heat pumps	3 @ 10.6 EER summer 1 @ 8.9 EER summer 3 @ 10.2 EER winter 1 @ 10.0 EER winter	3 @ 8.3 EER summer 1 @ 8.3 EER summer 3 @ 8.3 EER winter 1 @ 8.3 EER winter	Baseline values based on manuf. data/Stdnd values from PEPCO rebate form
Solar DHW system	Solar prediction with F-CHART	No solar; 80 gal/day	F-CHART prediction
All ECOs combined	All above features installed	No ECOs installed	1 DOE-2 run with either option

counterparts. An overall ECO combination DOE-2 run was then made and the result of each is presented throughout the chapter.

6.1 Methodology

The first model was run in order to calibrate the simulation to measured whole-building electricity consumption using the site specific TRY weather data for the nine month period of April - December 1993 as was described in Chapters III, IV, and V. This model was intended to represent the building as it is currently operating with all the ECOs installed and functioning properly. During this stage, input file errors were eliminated in order to have as accurate a simulation as was feasible by using the toolkits introduced in Chapter III. Once all the parameters were adjusted to what was determined to be as close as possible to actual building conditions, the model was declared "calibrated". As it was reported in the Chapter V simulation summary, the final DOE-2 simulation achieved an MBE of -0.7% and a CV(RMSE) of 23.2% when an overall nine month comparison was taken into account. This fit was considered accurate enough to assess the ECOs.

By using the nine month calibrated model, a base model was produced that simulated the building for an entire year instead of nine months so the energy savings estimates could be calculated on an annual basis. Since a one year site specific weather file was not available, a Washington, D.C. TMY (TMY 1988) weather tape was utilized. The annual energy consumption was extracted from the DOE-2 Building

Energy Performance Savings (BEPS) report which divided the energy use among lighting, space heating, space cooling, fans, and equipment. Table 6.2 summarizes the savings of each ECO and how each compares to the original estimates.

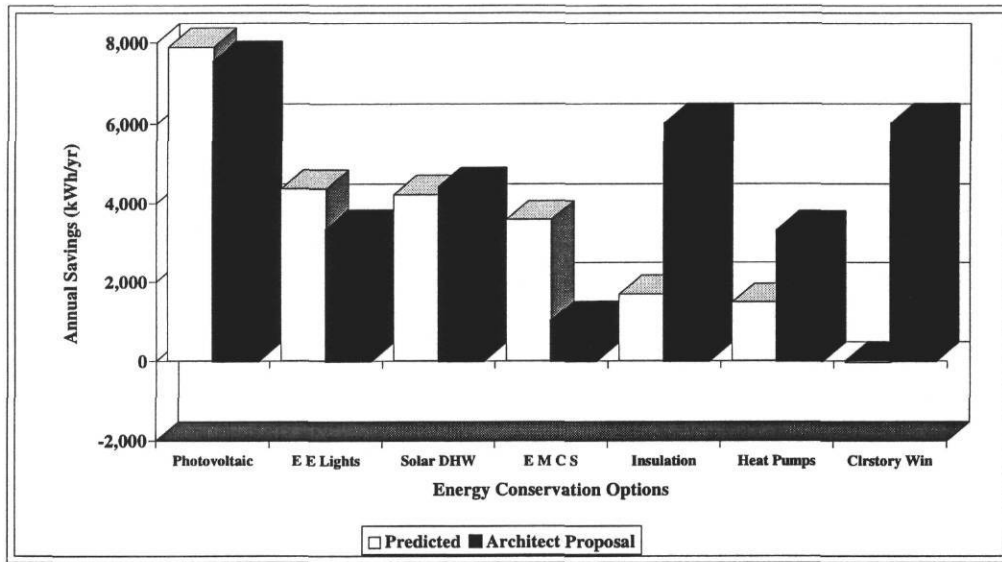
Table 6.2 Comparison of Energy Conservation Options to Predictions.

	Energy Conservation Option	DOE-2 Basemodel "as-built" (kWh)	DOE-2 Predicted w/o ECO (kWh)	DOE-2 Predicted Savings (kWh)	Architect's Proposal (kWh)	Percent Difference (7)	Difference
1.	Energy Efficient Lights	157,116	161,477	4,361	3,328	31.0%	1,033
2.	Photovoltaic Generation (1)	-7,880	0	7,880	7,530	4.6%	350
3.	Energy Management and Control System (2)	157,116	160,695	3,579	1,000 (est)	257.9%	2,579
4.	Lighting Controls & Dimmers (3)	-	-	-	-	-	-
5.	Insulation, Airlock, South Shading	157,116	158,795	1,679	6,000	-72.0%	-4,321
6.	Clerestory Windows	157,116	157,075	-41	6,000	-100.7%	-6,041
7.	Improved Heat Pumps	157,116	158,590	1,474	3,300	-55.3%	-1,826
8.	Solar Hot Water (4)	2,345	6,565	4,220	4,407 (6,033 is incorrect)	-4.2%	-187
	All ECOs Combined (5)	151,581	166,108	14,527	-	-	-
	Total (6)			23,152	31,565	-26.7%	-8,413

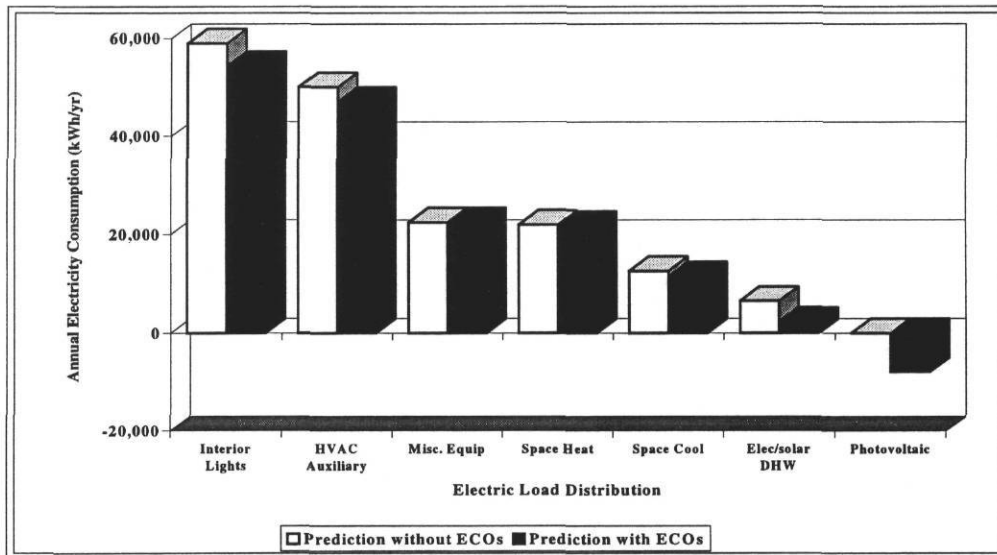
- (1) Difference was determined by a curve fit equation comparing photovoltaic generation as a function of global horizontal radiation. Global horizontal radiation was extracted from a Washington, D.C. TMY weather tape. DOE-2 was not used for this verification.
- (2) According to U.S.D.O.E. personnel, the HVAC system is manually operated each day. The 1,000 kWh savings by the GSA architect were based on engineering judgement.
- (3) According to U.S.D.O.E. personnel, the dimmers were not installed.
- (4) Savings was determined by F-CHART. The value of 6,033 as specified in the original estimate is incorrect because the calculation was based on the total DHW requirements and not the solar DHW contribution.
- (5) Not part of original ECO list. Calculated by: (Basemodel + photovoltaic + dhw)
- (6) Savings total does not include "All ECOs Combined."
- (7) The percent difference was calculated as follows: $[(\text{DOE-2 savings} - \text{architect proposal}) / \text{architect proposal}] \times 100$

Figure 6.1 (a) is a bar graph which compares the individual simulated ECO savings versus the original architectural savings estimates. It includes (in the order shown) the photovoltaic savings, the energy efficient lighting savings, the solar DHW savings, the energy management and control system savings, the envelope improvement savings (extra insulation, entrance airlock, and window shades), the heat pump savings, and the clerestory window savings. The data calculated for the DHW system savings was determined by F-CHART while the data for the photovoltaic system savings was determined by the analysis procedure described in Section 4.6.2.1. Figure 6.1 (b) shows the annual electricity end-use data taken from the DOE-2 BEPS report with and without all of the ECOs, as simulated by DOE-2. The data with all the installed ECOs was determined by the as-built calibrated model using the base-level simulation. To simulate the inefficient building, a DOE-2 model was run with all the ECOs removed.

To avoid confusion, the negative photovoltaic savings in Figure 6.1 (b) must be clarified here. The assumption that was made is that the annual electricity consumption with the installed photovoltaic ECO is negative because the photovoltaic system is producing electricity rather than consuming it. For the comparison DOE-2 run, the annual electricity consumption is zero since the system would not otherwise have been installed.



(a)



(b)

Figure 6.1 ECO Savings Comparisons. (a) Annual Electricity Savings. (b) Annual Electricity Consumption.

6.2 Energy Efficient Lighting

The first energy-efficient feature considered was the installation of 34 W energy efficient fluorescent lighting instead of standard 40 W fluorescent lighting. The 34 W lamps are located in each zone for main lighting and were simulated in the DOE-2 base model as LIGHTING-KW. The remainder of the lights throughout the building, not considered as part of this verification, were lumped into the task lighting category for simulation purposes. The fixture number was based both on the architectural plans, and verbal confirmation of which a total wattage was calculated per zone.

For the energy efficiency verification DOE-2 model, 40 W lamps using metal-core 40 W ballasts were substituted for 34 W lamps with efficient electronic ballasts to represent what the “business-as-usual” option that would normally have been installed. As is true with most commercial buildings, interior lights account for a major portion of the whole-building electricity consumption and are excellent candidates for energy savings retrofits. According to Figure 6.1(a), the lights are the second largest contributors to energy savings. Figure 6.1(b) verifies the lights as being the largest whole-building electricity consumers in the building. The DOE-2 simulation shows that the lights are saving 31.0% more than the published GSA estimate. This is most likely due to occupant habits.

6.3 Photovoltaic System

The next conservation measure evaluated was the installation of a photovoltaic system¹⁴ to supplement whole-building electricity usage. This savings verification did not utilize DOE-2. Instead, several processing steps were required in order to calculate the annual savings from the photovoltaic array as outlined in Section 4.6.2.1. First, hourly electricity produced by the photovoltaic array were recorded and compared to the available global horizontal solar radiation data. Then, a quadratic curve-fit was calculated as was previously shown in Figure 4.19. In a separate procedure, one year of hourly global horizontal radiation was extracted from the long-term Washington, D.C. TMY weather tape. The TMY radiation data, in turn, was used in conjunction with the curve-fit equation to synthesize photovoltaic generation for one year. The synthetic data was then summed for comparison to the proposed photovoltaic savings estimates¹⁵ and accounts for the largest portion of annual energy savings. The existing photovoltaic system, according to this procedure, saves 4.6% more than the estimates predicted.

Two interesting features were noted about the photovoltaic system. First, prior to March 1993, one-half of the photovoltaic system's electricity production was not occurring because one of the breakers had tripped on the DC to AC inverters. Second,

¹⁴ Integrated Power Corporation, 7524 Standish Place, Rockville, MD, 20855.

¹⁵ Photovoltaic analysis for system design was performed by Sandia National Laboratory, P.O. Box 5800, Albuquerque, NM 87185.

shading by nearby trees decreases the output to about 4 kW during certain times of the year. This effect diminishes in the fall-when the leaves fall off of the trees. Simple problems such as these reinforce the need for real-time monitoring which is closely checked. The problems would have otherwise gone unnoticed until regularly scheduled maintenance detected them, which in some cases might not occur until major breakdowns are encountered.

6.4 Energy Management and Control System

A computerized EMCS was put in place to optimize heat pump operation and air handlers. The base model was run by specifying DOE-2 parameters such as set-point temperatures and operations schedules made available from a computer print-out from the EMCS system obtained during an audit visit. The DOE-2 standard verification run assumed that the HVAC system was allowed to operate under thermostat control at any time of the year (i.e. 24-hour-per-day operation). DOE-2 predicts that the EMCS actually saves 257.9% more than originally stated (only an annual savings estimate was available from the architect; no indication was given as to what conditions the architect assumed or how the savings were calculated).

As was disclosed in Chapter IV, the EMCS was often overridden by the building's manual thermostats. Also, it lost its programming before the calibration period began and had to be reset. Therefore, the HVAC system was manually activated and deactivated daily by maintenance personnel which assures that the night

setback occurs. In light of these circumstances, the verification run was performed nonetheless since personnel were manually performing the tasks that the EMCS would have otherwise accomplished.

6.5 Lighting Controls

The original savings calculations for the lighting controls and dimmers were based on the dimmers theoretically reducing light levels by 30 - 40%. This ECO could not be verified since DOE personnel confirmed that dimmers had not been installed. The occupancy sensors, on the other hand, have been installed in the restrooms, but could not be realistically simulated due to unpredictable zone utilization. Therefore, a DOE-2 simulation was not performed for these options since it was assumed that their contribution to the overall savings was minimal..

6.6 Envelope Enhancement

The fifth energy conservation option analyzed involved all the thermal envelope measures and consisted of the installation of additional insulation in the roof and wall, an air-lock at the main entrance, and shading devices for the south-side windows. Roof insulation, as is currently installed, is energy efficient R-30 batt insulation which was to be compared to standard R-18 batt insulation in the roof. Wall insulation was improved from standard R-11 batt insulation to more efficient R-13 batt insulation. The effect of the main entrance airlock was estimated by changing the infiltration setting of 1.0 air changes per hour in the base model to 0.6 air changes per

hour per zone representing a "tight" building (Mitchell 1983). The standard R-18 and R-11 insulation options were chosen to match the values used in the GSA architect's analysis.

To reduce glare, the south-side windows were shaded by overhangs which were accounted for in the base model with opaque shading planes. To simulate the savings, the overhangs were omitted from the input file for the non-ECO option. The savings comparison shows that these combined features save 72.0% less than savings predicted by the GSA architect. No details were provided by the GSA architect as to how these estimates were determined.

6.7 Clerestory Windows

Clerestory windows were added to the north-side raised ceiling walls above the classroom areas to provide daylighting. The base model included them as per architectural and window manufacturer specifications. They were removed from the model and replaced with equivalent R-13 insulated walls to simulate savings. The results revealed that the building actually loses energy as a result of the windows to the tune of 100.7% less than the GSA architectural calculations. One of the reasons for this large discrepancy was that the daylight lighting control sensors that were specified were never installed. Therefore, no discernible reduction in the interior lights from the clerestory windows could be justified.

6.8 High Efficiency Heat Pumps

The seventh feature examined was the installation of high efficiency air-cooled heat pumps with a higher EER than standard heat pumps. Manufacturer catalogs were obtained to verify EER values (Trane 1992). For the cooling season, EER values of 10.6 for the 7-½ ton units and 8.9 for the 4 ton unit were specified compared to a standard 8.3 EER value for all four heat pumps. In the heating season, EER values of 10.2 for the 7-½ ton units and 10.0 for the 4 ton unit were modeled instead of a standard 8.3 EER model. For the standard comparison model, the standard EER reference values were provided by the GSA architect who used data available from the Potomac Electric Power Company (PEPCO)¹⁶, the local utility company. The difference shows that the installed higher efficiency heat pumps save 55.3% less than originally calculated. One possibility for the discrepancy might be the excessive use of the electric resistance baseboard heaters.

6.9 Solar Domestic Hot Water System

The solar DHW system savings were verified using the F-CHART program (F-CHART 1989) instead of DOE-2. By applying the solar DHW system manufacturer specifications¹⁷, the program estimated annual DHW energy consumption as well as annual solar system contribution. This was then compared to the original estimated

¹⁶ PEPCO Commercial Energy Services Department, 1900 Pennsylvania Ave., N.W., Washington, D.C. 20068.

¹⁷ American Energy Technology, model AE-32, P.O. Box 1865, Green Cove Springs, FL, 32043.

savings calculated by the National Renewable Energy Laboratory's (NREL) F-CHART analysis which was used by GSA.

The initial GSA savings estimate was inaccurate because an incorrect value was extracted from NREL's F-CHART analysis and published as potential savings, specifically, the original estimate incorrectly used the total DHW requirements, 6,033 kWh, in place of the corrected solar system contribution of 4,407 kWh. This was discovered when an independent F-CHART verification was performed. Therefore, the value was used for comparison and tabulated. The results (when compared to the corrected F-CHART run) were quite good with the solar system actually providing only 4.2% less than originally predicted. The original F-CHART run was based on a collector tilt angle of 30° while the actual collectors are mounted at 25°. The verification F-CHART run was based on the actual tilt angle as well as the actual manufacturer collector performance data. The operation of the solar DHW was confirmed by the DOE personnel and a site inspection by the solar DHW maintenance contractor¹⁸.

6.10 All ECO's Combined

Finally, the base model was compared to a run made with all the ECOs removed in the same model to simulate the total. The analysis revealed that the

¹⁸ Mr. Peter Lowenthal, 4707 Elmhurst, Bethesda, MD, 20814-3954.

existing building saves 26.7% less than originally anticipated (i.e. it saves 73.3% of the audit estimated savings).

6.11 Results and Conclusion

With the exceptions of the photovoltaic and solar DHW systems, a calibrated DOE-2 simulation, long-term weather tape data, and F-CHART were used to test each individual ECO over a one year period using a Washington, D.C. TMY weather tape and compared to original architectural savings estimates. A one year model was run and used as a baseline energy consumption reference point. This model used the same input file that was calibrated to the nine months of measured data. In effect, the calibrated model represents the "as-built" building.

The DOE-2 input file was then modified, one ECO at a time, to determine what the energy use would have been had the ECOs not been installed. For each comparison, the ECO parameter in question was changed to the standard ECO value provided by either the architect, or the PEPCO reference value. The annual energy consumption was then measured against the base model and the difference compared to the original estimates. A percent difference was then calculated and tabulated in Table 6.2. Based on this analysis it can be concluded that the daycare center is working within 73.3% of what was designed. If more accurate estimates had been

made concerning the envelope measures (ECO #5) and the clerestory windows (ECO #6), the building would be performing within 90%¹⁹ of what was estimated.

¹⁹ The percent difference was found by removing ECOs # 5 and #6 and recalculating.

CHAPTER VII

SUMMARY AND RECOMMENDATIONS

This thesis has investigated techniques for calibrating computer building energy simulation methods and has presented several new techniques for improved calibration. The review of the previous literature defined the problems associated with past calibration techniques. Several improved calibration approaches were then proposed which included new graphical procedures and statistical goodness-of-fit parameters for quantitatively comparing simulated data to measured data. A four zone, single story electrically heated and cooled case study building was simulated with DOE-2.1D and calibrated using hourly measured whole-building electricity data and ambient weather conditions to demonstrate the new techniques. New routines were also developed for disaggregating whole-building electricity into its end-use components (i.e. heating, cooling, fans, and lights and equipment) which were then compared to similar values from DOE-2. The calibrated simulation was then used to determine the effectiveness of efficient HVAC measures incorporated into the design of the case study building.

7.1 Summary of the Methodology

Site specific measured hourly weather data were used in this research to improve the calibration. Ambient weather data were measured for nine months, and processed with special routines developed for this thesis that build on routines used in previous

research (Bronson 1992). The data collection procedures included merging data from two dataloggers made by different manufacturers and the NWS. Weather data included dry bulb temperature, relative humidity, and peak wind speed gathered from the nearby NWS weather station and global solar radiation data measured on-site. A special routine was developed to convert global solar radiation measured at an 18° south facing tilt into global horizontal beam and diffuse solar radiation. The weather data were then assembled into a single datafile and packed onto a TRY weather tape for use with the DOE-2 energy simulation program. The new routines to improve the calibration procedure are included in this section

7.1.1 Architectural Rendering

In order to ensure that the building envelope was correctly specified in the input file, a commercially available architectural rendering tool (Huang 1993) was used in this thesis. The software directly interpreted the DOE-2 input file and graphically reproduced the building envelope in three dimensions. A comparison to a previously calibrated model was made to demonstrate differences between architecturally rendered and thermodynamically similar building simulation. By being presented with the opportunity to inspect every surface of the building's envelope from all directions, the DOE-2 user is now able to simulate a building with the complete knowledge that no placement errors were made which could effect the solar shading.

7.1.2 Residual Plots

New graphical visualization tools were used as the foundation of this thesis. Although developed in past research for different applications (Abbas 1993), the first graph presented for DOE-2 calibration in this thesis was the time-series residual plot. This plot consisted of monthly data summaries of the simulated and measured data with a residual comparison to show the difference. This, perhaps the simplest plot of the series, allowed general visualization of data trends. The data overlap problems associated with plotting hourly data were recognized and rectified with the new box-whisker-mean plots employed for the DOE-2 calibration in this thesis.

7.1.3 Temperature Binned Box-whisker-mean Plots

The next set of graphs introduced were temperature binned box-whisker-mean plots (Abbas 1993). These plots consisted of four juxtaposed plots, two assigned to the measured data and two allocated to the simulated data. The measured data and simulated data were plotted on the same page as juxtaposed scatter plots and box-whisker-mean plots binned by temperature. The data overlap problem in the hourly scatter plots were significantly improved with the box-whisker-mean plots. The statistical box-whisker-mean analysis allowed accurate comparisons of two clouds of hourly data. One of the important features of these plots is the inter-quartile range which allows one to judge the overall grouping of the data.

Use of the inter-quartile range is an improvement over the standard deviation because the inter-quartile range is not sensitive to one or more outliers. A large inter-quartile range can also be indicating the need for additional data sorting (i.e. weekday/weekend). In addition, the measured mean of the actual data was superimposed onto the simulated plot to allow direct comparison. Temperature-bin plots were further enhanced to show a weekday/weekend format which segregated the occupied/unoccupied period of operation.

7.1.4 24-Hour Weather Daytype Statistical Plots

New 24-hour weather daytype statistical plots, developed for this thesis, also were shown to be extremely useful. These plots were developed to demonstrate the weather dependent and schedule dependent influences on the building's HVAC related energy use and helped fine tune the lighting and equipment schedules. Six graphs were divided into three weather daytype pairs for measured data and simulated data; a cooling season daytype, a heating season daytype, and a non-cooling/non-heating season daytype. The superposition of the mean lines was also utilized. These plots were instrumental in pinpointing hourly effects of changes made to the DOE-2 input file schedules. They proved to be extremely sensitive to input file schedule changes by graphically showing the effects on an hour-by-hour basis across heating, cooling, and intermediate periods. Like the temperature binned box-whisker-mean plots, these plots also were then further divided into a weekday/weekend format and occupied/unoccupied formats to facilitate comparisons of specific simulation periods.

7.1.5 Comparative Three-dimensional Plots

Comparative three-dimensional plots presented in earlier research (Haberl and Komor 1989; Hinchey 1991; Bronson 1992; Haberl et al. 1993) were also utilized for calibration purposes in this thesis. To enhance the use of these plots a new graph was adopted from Abbas (1993) that consists of a 52-week box-whisker-mean plot that bins the data by individual weeks. It allows for a weekly comparison of simulated data to measured data and does not suffer from the data problems encountered in the three-dimensional plot such as crowding of the 24-hour daily profiles. For this research, the data were plotted for the 37-week calibration period beginning in April 1993 and running through December 1993. The 52-week binned plots showed the measured data and the simulated data for the same period along with the mean from the measured data superimposed onto the simulated data plot. This allowed for a close week-by-week comparison of the means between the two datasets.

7.1.6 The CV(RMSE) and the MBE Statistical Parameters

Two additional contributions to DOE-2 calibration projects made by this research effort were the utilization of the CV(RMSE) and the MBE statistical parameters. The CV(RMSE) provided a vastly improved measure of model goodness-of-fit by comparing hourly difference between the actual data and the simulation rather than the traditionally used monthly percent difference comparisons. The MBE statistic is a percent difference that compares the simulated hourly data to the measured hourly data

calculated for each hour and reported monthly. For this thesis, the hourly CV(RMSE) for the total calibration thesis was 23.1%, the MBE was -0.7%, and the average monthly percent difference, as is typically reported was -0.7%. As is apparent, there is a large discrepancy between the CV(RMSE) and the percent difference statistics which makes a case for the use of the more rigorous CV(RMSE) statistics. The MBE yields the same result as the monthly percent difference.

7.1.7 Comparison of the DOE-2 Simulated and Measured Indoor Temperatures

A comparison of the DOE-2 simulated and measured indoor temperatures for summer and winter conditions also proved to be useful. Although this method was not a new practice, this thesis showed that the comparison could be used to calibrate DOE-2's thermostat by matching the data to measured indoor temperatures recorded by a chart recorder. The most beneficial aspect of the indoor temperatures allowed for the verification of system on/off switching. It was found that the winter simulated temperatures followed the measured temperatures closely with a 5.5% CV(RMSE) in the south zone and a 5.2% CV(RMSE) in the north zone.

The summer simulated indoor temperatures remained in phase with the measured temperatures but tracked the measured temperatures with a slightly lower accuracy. The CV(RMSE) in the south zone was 5.6% and 6.0% in the north zone. Additional measured temperatures over a longer period using an electronic datalogger would be required to obtain a better understanding of this problem.

7.1.8 Disaggregation of Whole-building Data Into End-use Data

Since the building was only monitored for whole-building electricity data and only limited measurements were available from infrequent site visits, calibration was more difficult than it would have been if end-use data had been monitored. As a solution, the HVAC fan load was disaggregated from the whole-building electricity data by subtracting the known exterior and interior lighting and interior equipment loads from the whole-building hourly data during special signature days. These signature days represented weekday/weekend periods when the building did not require heating or cooling. The hourly lighting load was calculated by multiplying the number of fixtures times the fixture's rated load. The diversity was determined from conversations with the daycare personnel and verified with measured data. The equipment load was determined by clamp-on measurements and/or by inspecting the equipment nameplates.

To compare the estimated HVAC end-use loads to the DOE-2 simulated HVAC end-use load, estimates of the lighting and equipment loads were fed into the DOE-2 input. DOE-2 was then allowed to calculate the HVAC load. The resultant differences agreed well with the lighting and equipment loads being within 10% of the DOE-2 results, the HVAC load being within 16%, the heating load being within 37%, the cooling load being within 20% and the total load being within 4%.

7.1.9 Use of the Calibrated Simulation to Verify Individual ECO Savings

The case study building was initially designed with energy efficient features at the time of construction. A reliable method such as a calibrated simulation was therefore needed to evaluate the features and compare them to the original savings estimates proposed by the building designers. The advantage of a calibrated simulation becomes clear in an exercise such as this because of its ability to evaluate the energy use of numerous changes to the building and its equipment. To accomplish this by using the simulation program, each ECO (except for the solar DHW system and the photovoltaic system) was replaced by the standard inefficient feature on which the initial design savings estimates were based and a separate DOE-2 simulation performed. The difference of each feature was then calculated and ranked from the most effective to the least effective. A total combined difference for all calculations was also determined.

Comparisons of the original savings predictions were then made to the DOE-2 predicted energy savings. When all ECOs were combined, they saved 73.3% of what was originally anticipated by the GSA designers. A closer evaluation of the individual measures revealed that by removing the two ECOs with the largest discrepancy, the DOE-2 predicted savings compared to within 90% of what was initially estimated (i.e. 1949 kWh/yr).

7.2 Findings From the New Features

The important new calibration features that were developed and demonstrated in this thesis include:

1. The use of architectural rendering software allows for visual verification of size and placement of the building's exterior surfaces and shading surfaces to those of the actual building.
2. The use of statistical analysis and data displays for assessing the progress of non-weather dependent data calibrations.
3. The use of statistical analysis and data displays for assessing weather dependent data calibrations.
4. The development of new weather daytype statistical analysis for assessing weather and schedule dependent loads.
5. The use of 52-week, binned box-whisker-mean time-series plots that allow for a statistical evaluation of the three-dimensional plots introduced in prior research.
6. The use of a DOE-2 zone temperature comparison to measured indoor temperature to confirm simulated HVAC schedules.
7. The development of a new method for estimating end-use electricity loads using "signature days" and the comparison of these end-use loads to DOE-2's predicted loads.

8. The use of solar beam and diffuse data synthesized from on-site measured global solar radiation data tilted at 18° toward the south. Development of routines for converting 18° tilted global solar data into global horizontal solar data.

These new techniques significantly improved the previous DOE-2 calibration methods. The long-term goal of this type of research is to eventually lead to an easier to use calibration procedure that could be used on a wide variety of buildings. The next section provides additional details concerning recommendations for future work.

7.3 Recommendations and Future Directions

During this research effort, many valuable lessons were learned by refining the simulation. As a guide to future DOE-2 users, recommendations are provided so that calibration efforts can be improved.

7.3.1 Calibration Procedure

The first step to simulating a building should include a site visit to acquire the following building information:

- A complete set of as-built drawings (architectural, mechanical, and electrical).

Information gathered from as-built drawings includes envelope description and placement, HVAC zoning, lighting loads, and control specifications

- An HVAC air balance report including supply and return air temperature measurements.

- Information concerning actual thermostat settings including daytime and night setback. If an EMCS is installed, a printout of the programming settings is helpful.
- Measure indoor temperature in each zone during normal operations and nighttime for heating, cooling, and intermediate seasons.
- Hourly HVAC schedules, hourly interior/exterior lighting schedules, hourly occupancy schedules, and hourly equipment schedules. Note the general operation schedule for miscellaneous activity such as dishwashing frequency, etc.
- Perform a blower door test to determine infiltration rates. (Not used in this thesis).
- An evaluation of exterior shading surrounding the building including relative distance from building off-south orientation, height and angle of each shading objectobject.
- Measurements of seven to nine months of hourly whole-building electricity, cooling, heating, and major equipment end-uses are recommended.
- For smaller electrical equipment such as appliances and small motors, clamp-on RMS Watt measurements for 24-hours should be made.
- Survey all equipment and copy nameplate specifications.
- An accurate light fixture count is imperative and should include tube size and ballast power level. Note how many lamps are typically off for extended periods and verify power consumption with clamp-on RMS Watt meter.
- Measure hourly weather data including relative humidity, dry bulb temperature, wind speed, and global horizontal solar radiation. An alternative would include

the NWS, preferably with a weather station as close to the site as is possible.

However, NWS solar data are not very useful for similar purposes.

- Photograph the building's exterior, interior, equipment, and surrounding area.
- Contact HVAC equipment and internal equipment representatives to obtain specifications for the building systems.

Then create the DOE-2 simulation input file by matching the building HVAC system to the nearest fixed schematic HVAC system in the DOE-2 reference manual. It is imperative to use as many measured details as possible. All DOE-2 default values should be investigated for appropriateness.

Use data from the DOE-2 hourly reports corresponding to the measured data from the building. Process the data into a single ASCII columnar datafile compatible with the comparative graphical routines presented in this thesis. Finally, use the tools developed in this thesis and those previously developed to compare the simulated energy use to the measured energy use. Iterate until the measured data matches the simulated data to a suitable level.

7.3.2 Recommendations to Improve Simulations

Need for monitoring:

1. Measure hourly data from a case study building and include at a minimum whole-building electricity, heating, and cooling loads.

2. If the case study building is equipped with an electric and solar domestic hot water system, measure the electricity directly to determine the DHW usage and profile.
3. When measuring solar radiation data for weather tape packing, it is important to mount the pyranometer horizontally for more accurate measurements. Although a routine was developed in this thesis that converted south 18° tilted data to horizontal data, a certain amount of error still existed since the routine is based on correlations. On-site measurement of hourly beam and diffuse solar data can significantly improve the calibration of simulations on buildings with a large amount of solar gain.
4. Approach equipment scheduling with a methodology based on empirical data rather than personal interviews. Sub-metering on an hourly basis for at least one to two weeks to improve the understanding of equipment cycling. This information can be used to improve DOE-2's scheduling assumptions.
5. During a building audit, an important contribution to the input file consists of direct RMS electrical measurement of all significant equipment. This allows one to properly size large pieces of equipment without relying on architectural schedules and/or manufacturer rated information which can deviate substantially from actual installations and at best only indicate estimated loads.
6. Perform an in-depth indoor temperature analysis using long-term hourly indoor measured temperature data recorded by an electronic datalogger. Data should be measured during the cooling season, the heating season and the non-cooling/non-heating season. Additional temperature measurements including the supply air

temperatures, return air temperatures, and temperatures of plenums and unconditioned spaces are helpful as well.

7. Use measured average hourly wind data instead of NWS peak hourly gusts.
8. Measuring ground temperatures will provide a more accurate simulation than using ground temperatures from the TMY or TRY weather tapes. At a minimum, the F-CHART manual provides monthly average water main temperatures that are an improvement over the ground temperatures in the standard TMY or TRY tapes.
9. If a building is equipped with renewable energy systems such as photovoltaic and solar DHW systems, they must be monitored for proper operation. In its simplest form, the monitored system could consist of a kWh meter on the photovoltaic system that could be read in the same fashion as the utility meter. Data recorded in such a manner could then be compared to predicted power. In the case of the daycare center, this alerted the staff to the fact that one of the breakers had tripped. The solar DHW system could also be simply monitored with a Btu meter that displays a cumulative odometer-type reading that could also be read monthly. With systems such as these, proper operation could be maintained at full capacity to recover the taxpayer's investment.

Improvements to the methodology:

10. Determine a more accurate and inexpensive method for deriving hourly solar beam and diffuse measurements from commonly available NWS data, or use beam and

diffuse data from a multipyranometer array (MPA) sensor (Curtiss 1993; Munger and Haberl 1994).

11. Improve DOE-2 to assist with calibrated simulations by including such features as:
 - a) component-based system simulations (ASHRAE 1991) (versus DOE-2's fixed schematic systems) for easier modifications, b) 8,760 scheduled data inputs, and c) easier access to hourly data values (i.e. not having to rely on printed hourly reports with headers and footers).

Calibration development:

12. Extend this type of super-calibrated work to other building simulation programs including BLAST, TRACE, ESP, etc.
13. Develop and distribute public domain software for directly and easily converting NWS weather data into TRY or TMY format and/or columnar format for easier processing.
14. Develop an improved method for capturing site shading including a possible photographic method for capturing shading information and converting into geometrical coordinates.

REFERENCES

- Abbas, M. 1993. Development of graphical indices for building energy data. Master's Thesis, Texas A&M University, College Station, TX, Energy Systems Laboratory Report No. ESL-TH-93/12-02.
- Aho, A.V., B.W. Kernighan, and P.J. Weinberger. 1988. *The AWK programming language*. Addison-Wesley Publishing Company. Reading, MA.
- Akbari, H., K.E. Heinemeier, P. LeConiac, and D.L. Flora. 1988. An algorithm to disaggregate commercial whole-building hourly electrical load into end uses. *Proceedings from the ACEEE 1988 Summer Study on Energy Efficiency in Buildings*, Vol. 10, pp. 10.14-10.26. Washington, DC: American Council for an Energy-Efficient Economy.
- ASHRAE. 1991. *ASHRAE handbook: 1991 HVAC applications volume*. American Society of Heating, Refrigerating, and Air-Conditioning Engineers, Inc., Atlanta, GA.
- Augustyn and Company. 1994. WYEC2 user's manual and toolkit. Augustyn and Company report, Albany, CA.
- Bahel, V., S. Said, and M. Abdelrahmen. 1989. Validation of DOE-2.1A and a microcomputer base hourly energy analysis computer program for a residential building. *Energy*, 14(4): 215-221.

- Balcomb, J.D., J.D. Burch, and K. Subbarao. 1993. Short-term energy monitoring of residences. *ASHRAE Transactions*. 99(2): 935-944.
- Balcomb, J.D., J.D. Burch, R.D. Westby, K. Subbarao, and C.E. Hancock. 1994. Short-term energy monitoring for commercial buildings. *Proceedings from the ACEEE 1994 Summer Study on Energy Efficiency in Buildings*, Vol. 5, pp. 5.1-5.11. Washington, DC: American Council for an Energy-Efficient Economy.
- Bhushan, A.K. 1973. *FTP and network mail system*. Internet Request for Comments 475. March.
- BLAST. 1993. BLAST users manual. BLAST Support Office, University of Illinois Urbana-Champaign.
- Bou-Saada, T.E. 1994. Advanced DOE-2 calibration procedures: A technical reference manual. Energy Systems Laboratory Report No. ESL-TR-94/12-01, Texas A&M University, College Station, TX.
- Bronson, D.J., S.B. Hinchey, J.S. Haberl, and D.L. O'Neal. 1992. A procedure for calibrating the DOE-2 simulation program to non-weather-dependent measured loads. *ASHRAE Transactions*. 98(1): 636-652. Energy Systems Laboratory Report No. ESL-PA-91/05-01, Texas A&M University, College Station, TX.
- Bronson, J.D. 1992. Calibrating DOE-2 to weather and non-weather dependent loads for a commercial building. Master's Thesis, Texas A&M University, College Station, TX, Energy Systems laboratory Report No. ESL-TH-92/04-01.
- Byrne, S. 1990. DOE-Plus: An interactive pre- and post-processor for DOE-2. *DOE-2 User News Letter*. 11(4): 4-13.

- Campbell Scientific, Inc. 1993. PC208 datalogger support software instruction manual. Campbell Scientific, Inc. P.O. Box 551, Logan, UT, 84321.
- Carroll, W.L. and R.J. Hitchcock. 1993. Tuning simulated building descriptions to match actual utility data: Methods and implementation. *ASHRAE Transactions*. 99(2): 928-934.
- CIS. 1993. VAX and openVMS road map: A guide to the VMScluster and VAX help, VAX 9000-210V, Computing and Information Services, Texas A&M University, College Station, TX.
- Claridge, D., J. Haberl, W.D. Turner, D. O'Neal, W. Heffington, C. Tombari, M. Roberts, S. Jaeger. 1991. Improving energy conservation retrofits with measured savings. *ASHRAE Journal*. 33(10): 14-22.
- Claridge, D.E., J.S. Haberl, R.J. Sparks, R.E. Lopez, and K. Kissock. 1992. Monitored commercial building energy data: Reporting the results. *ASHRAE Transactions*. 98(1): 636-652.
- Clarke, J.A, P.A. Strachan, and C. Pernot. 1993. An approach to the calibration of building energy simulation models. *ASHRAE Transactions*. 99(2): 917-927.
- Cleveland, W.S. 1985. *The elements of graphing data*. Wadsworth & Brooks/Cole, Pacific Grove, CA.
- Collares-Pereira, M. and A. Rabl. 1979. The average distribution of solar radiation - correlations between diffuse and hemispherical and between daily and hourly insolation values. *Solar Energy*. 22:155-164.

- Crow, L.W. 1970. Summary description of typical year weather data, Chicago midway airport. ASHRAE Research Project RP 100. American Society of Heating, Refrigerating, and Air-Conditioning Engineers, Inc., Atlanta, GA.
- Crowley, G.D. and J.S Haberl. 1994. Use of NWS weather measurements for cross-checking local weather measurements. *Proceedings from the Ninth Symposium on Improving Building Systems in Hot and Humid Climates*. Arlington, TX. pp. 32-46.
- Curtiss, P.S. 1990. An analysis of methods for deriving the constituent insolation components from multipyranometer array measurements. Master's Thesis, University of Colorado, Boulder, CO.
- Degelman, L.O. 1991. Bin weather data for simplified energy calculations and variable base degree-day information. *ASHRAE Transactions Preprint*. 91(1).
- Degelman, L.O. and V.I. Soebarto. 1994. ENER-WIN: A visual interface model for hourly energy simulation in buildings. *Transactions from the Engineering and Architecture Symposium*. Prairie View A&M University, Prairie View, TX. 1:270-275.
- Diamond, R., M. Piette, B. Nordman, O. de Buen, J. Harris and B. Cody. 1992. The performance of the energy edge buildings: Energy use and savings. *Proceedings from the ACEEE 1992 Summer Study on Energy Efficiency in Buildings*, Vol. 3, pp. 3.47-3.60. Washington, DC: American Council for an Energy Efficient Economy.

- Diamond, S.C. and B.D.Hunn. 1981. Comparison of DOE-2 computer program simulations to metered data for seven commercial buildings. *ASHRAE Transactions*. 87(1): 1222-1231.
- Draper, N. and H. Smith. 1981. *Applied regression analysis*. 2nd. Ed. John Wiley & Sons, New York.
- Duffie, J.A. and W.A. Beckman. 1991. *Solar engineering of thermal processes*. John Wiley & Sons, New York.
- Dumortier, D. 1989. A method to quickly analyze DOE-2 outputs. *DOE-2 User News Letter*, 10(2):7-12.
- EPRI. 1992. Building energy analysis program: User's guide and technical reference manual. Electric Power Research Institute. Palo Alto, CA 94304.
- Erbs, D.G., S.A. Klein and J.A. Duffie. 1982. Estimation of diffuse radiation fraction for hourly, daily, and monthly-average global radiation. *Solar Energy*, 28(4): 293-302.
- F-CHART. 1989. F-CHART Solar System Analysis Software. IBM PC Version 5.6. 4406 Fox Bluff Rd. Middleton, WI 53562
- Fels, M. 1986. Measuring energy savings: The scorekeeping approach. *Energy and Buildings*, 9(1-2):5-18.
- Feuermann, D. and W. Kempton. 1987. ARCHIVE: Software for management of field data. The Center for Energy and Environmental Studies. Princeton University, Princeton, NJ, PU/CEES Report No. 216. (June).

- Foster N.B. and L.W. Foskett. 1953. A photoelectric sunshine recorder. *Bulletin of the American Meteorological Society*. 34: 212.
- FSF. 1989. GAWK (PC version of the UNIX-based AWK toolkit). Free Software Foundation, 675 Massachusetts Ave., Cambridge, MA 02139.
- Griffiths, D.M. and K.J. Anderson. 1994. Commercial building/system characteristics sensitivity analysis. *Proceedings from the ACEEE 1994 Summer Study on Energy Efficiency in Buildings*, Vol. 5, pp. 5.105-5.112. Washington, DC: American Council for an Energy Efficient Economy.
- Haberl, J.S. and D.E. Claridge. 1985. Retrofit energy studies of a recreation center. *ASHRAE Transactions*. 91(2b): 1421-1433.
- Haberl, J.S. and D.E. Claridge. 1987. An expert system for building energy consumption analysis: Prototype results. *ASHRAE Transactions*. 93(1): 979-998.
- Haberl, J.S. 1988a. Using the DOE-2 building energy analysis computer program; Session one, Joint Center for Energy Management, Department of Civil, Environmental, and Architectural Engineering, University of Colorado, Boulder, CO.
- Haberl, J.S., M. MacDonald, and A. Eden. 1988b. An overview of 3-D graphical analysis using DOE-2 hourly simulation data. *ASHRAE Transactions*. 94(1): 212-227.
- Haberl, J.S. and J. Vajda. 1988c. Use of metered data analysis to improve building operation and maintenance: Early results from two federal complexes.

Proceedings from the ACEEE 1988 Summer Study on Energy Efficiency in Buildings, Vol. 3, pp.3.98-3.111. Washington, DC: American Council for an Energy Efficient Economy. Energy Systems Report No. ESL-PA-88/09-01, Texas A&M University, College Station, TX.

Haberl, J.S. and P.S. Komor. 1989. Investigating an analytical basis for improving commercial energy audits: Early results from a New Jersey mall. *Thermal Performance of the Exterior Envelopes of Buildings IV*. ASHRAE. Atlanta, GA.

Haberl, J.S., J.D. Bronson, S.B. Hinchey, and D.L. O'Neal. 1993. Graphical tools to help calibrate the DOE-2-2 simulation program: Comparative 3-D surface plots improve the ability to view small differences between simulated and measured data. *ASHRAE Journal* 35(1): 27-32.

Haberl, J.S., J.D. Bronson, and D.L. O'Neal. 1994. An evaluation of the impact of using measured weather data versus TMY weather data in a DOE-2 simulation of an existing building in central Texas. Energy Systems Laboratory Report No. ESL-TR-93/09-02. College Station, TX.

Haberl, J., T. Bou-Saada, E.J. Vajda, L.A. D'Angelo, M. Shincovich, and L. Harris. 1995. The U.S.D.O.E. Forrestal building lighting retrofit: Preliminary analysis of electrical savings. Energy Systems Laboratory Report No. ESL-TR-95/09-02. College Station, TX.

Hadley, D.L. and S.D. Tomich. 1986. Multivariate statistical assesment of meteorological influences in residential space heating. *Proceedings from the ACEEE 1986 Summer Study on Energy Efficiency in Buildings*, Vol. 9, pp. 9.132-9.145, Washington, DC: American Council for an Energy Efficient Economy.

- Hadley, D.L. 1993. Daily variations in HVAC system electrical energy consumption in response to different weather conditions. *Energy and Buildings*. 19: 235-247.
- Hinchey, S.B. 1991. Influence of thermal zone assumptions on DOE-2 energy use estimations of a commercial building. Master's Thesis, Texas A&M University, College Station, TX, Energy Systems Laboratory Report No. ESL-TH-91/09-06.
- Hsieh, E.S. 1988. Calibrated computer models of commercial buildings and their role in building design and operation. Master's Thesis, Princeton University, Princeton, NJ, Center for Energy and Environmental Studies Report No. 230.
- Hsieh, E.S., L.K. Norford, R.H. Socolow, and G.V. Spadaro. 1989, Calibrated computer models to track building energy use: The role of tenant and operator decisions (Private Collection, T. Bou-Saada).
- Huang & Associates. 1993. DrawBDL user's guide. 6720 Potrero Ave., El Cerrito, CA, 94530.
- Hunn, B.D., J.A. Banks, and S.N. Reddy. 1992. Energy analysis of the Texas Capitol restoration. *The DOE-2 User News*. 13(4): 2-10.
- Judkoff, R.D. 1988. Validation of building energy analysis simulation programs at the solar energy research institute. *Energy and Buildings*. 10: 221-239.
- Kaplan, M.B., B. Jones, and J. Jansen. 1990a. DOE-2.1C model calibration with monitored end-use data. *Proceedings from the ACEEE 1990 Summer Study on Energy Efficiency in Buildings*, Vol. 10, pp. 10.115-10.125, Washington, DC: American Council for an Energy Efficient Economy.

- Kaplan, M.B., J. McFerran, J. Jansen, and R. Pratt. 1990b. Reconciliation of a DOE-2.1C model with monitored end-use data for a small office building. *ASHRAE Transactions*. 96(1): 981-993.
- Kaplan, M.B., P. Caner, and G.W. Vincent. 1992. Guidelines for energy simulation of commercial buildings. *Proceedings from the ACEEE 1992 Summer Study on Energy Efficiency in Buildings*, Vol. 1, pp. 1.137-1.147. Washington, DC: American Council for an Energy Efficient Economy.
- Katipamula, S. and J. Haberl. 1991. A methodology to identify diurnal load shapes for non-weather dependent electric end-uses. *Solar Engineering 1991: Proceedings from the Second ASME-JSES-JSME International Solar Energy Conference*: 457-467 Reno, NV (March).
- Kissock, J.K., T.A. Reddy, D. Fletcher, and D.E. Claridge. 1993. The effect of short data periods on the annual prediction accuracy of temperature-dependent regression models of commercial building energy use. *Proceedings of the ASME-ASES-SED International Solar Energy Conference*, Washington, DC, Energy Systems laboratory Report No. ESL-PA-93/04-01, Texas A&M University, College Station, TX.
- Koran, W.E., M.B. Kaplan, and T. Steele. 1992. DOE-2.1C model calibration with short-term tests versus calibration with long-term monitored data. *Proceedings from the ACEEE 1992 Summer Study on Energy Efficiency in Buildings*, Vol. 3, pp. 3.165-3.176. Washington, DC: American Council for an Energy Efficient Economy.
- Kreider J.F., and F. Kreith. 1981. *Solar energy handbook*. McGraw-Hill Book Company. New York.

- Kreider J.F. and J.S. Haberl. 1994a. Predicting hourly building energy use: The great energy predictor shootout-overview and discussion of results. *ASHRAE Transactions Preprint*. 100(2).
- Kreider J.F. and J.S. Haberl. 1994b. Predicting hourly building energy usage. *ASHRAE Journal*. 36: 72-81.
- LBL. 1980. DOE-2 User Guide, Ver. 2.1. Lawrence Berkeley Laboratory and Los Alamos National Laboratory, LBL Report No. LBL-8689 Rev. 2; DOE-2 User Coordination Office, LBL, Berkeley, CA.
- LBL. 1981. DOE-2 Engineers Manual, Ver. 2.1A, Lawrence Berkeley Laboratory and Los Alamos National Laboratory, LBL Report No. LBL-11353; DOE-2 User Coordination Office, LBL, Berkeley, CA.
- LBL. 1982. DOE-2.1 Reference Manual Rev. 2.1A. Lawrence Berkeley Laboratory and Los Alamos National Laboratory, LBL Report No. LBL-8706 Rev. 2; DOE-2 User Coordination Office, LBL, Berkeley, CA.
- LBL. 1989. DOE-2 Supplement, Ver 2.1D. Lawrence Berkeley Laboratory, LBL Report No. LBL-8706 Rev. 5 Supplement. DOE-2 User Coordination Office, LBL, Berkeley, CA.
- LOF. 1974. Libbey-Owens-Ford Company, Sun Angle Calculator. Toledo, OH.
- Löf, G.O.G., J.A. Duffie, and C.O. Smith. 1966. World distribution of solar radiation. Engineering Experiment Station Report N.o 21, University of Wisconsin, Madison, WI.

- Lopez, R. and J. Haberl. 1992a. Data management in the LoanSTAR Program. *Proceedings of the Eighth Symposium on Improving Building Systems in Hot and Humid Climates*, pp. 149-154, Dallas, TX.
- Lopez, R. and J. Haberl. 1992b. Data processing routines for monitored building energy data. *Proceedings of the 1992 ASME/JSES/KSES Solar Energy Conference*, ASME New York, pp. 329-336.
- Mahone, D.E., S. Krishnamurti, T. Alereza, and J.A. Johnson. 1992. Nonresidential energy standards and sensitivity analysis. *ASHRAE Transactions*. 92(1): 627-635.
- McLain, H.A., S.B. Leigh, and J.M. MacDonald. 1993. Analysis of savings due to multiple energy retrofits in a large office building. Oak Ridge National Laboratory, ORNL Report No. ORNL/CON-363, Oak Ridge, TN.
- McWatters, K. and J.S. Haberl. 1994. Development of procedures for the computerized plotting of a sun-path diagram, and shading mask protractor. *Proceedings from the 1994 ASME-JSES-JSEE International Solar Energy Conference*.
- Microsoft Corporation. 1991. *User's guide*. Microsoft Windows Version 3.1, Redmond, WA.
- Mitchell, J.W. 1983. *Energy engineering*. John Wiley and Sons, New York.
- Munger, B. and J.S. Haberl. 1994. An improved multipyranometer array for the measurement of direct and diffuse solar radiation. *Proceedings from the Ninth*

Symposium on Improving Building Systems in Hot and Humid Climates, pp. 125-131 Arlington, TX.

NREL 1992. User's manual: National solar radiation database (1961 - 1990).

Version 1.0. National Renewable Energy Laboratory. Golden, CO.

Palomo, E., J. Marco, and H. Madsen. 1991. Methods to compare measurements and simulations. *Proceedings of Building Simulation '91*, pp. 570-577, Nice, France

Parker D.S., and T.C. Stedman. 1992. Measured electricity savings of refrigerator replacement: Case study and analysis. *Proceedings from the ACEEE 1992 Summer Study on Energy Efficiency in Buildings*, Vol. 3, pp. 3.199-3.211, Washington, DC: American Council for an Energy Efficient Economy.

Reddy, S.N. 1993. Determination of retrofit energy savings using a calibrated hour-by-hour building energy simulation model. Master's Thesis, The University of Texas at Austin. Austin, TX.

Reichmuth, H. and Fish, K. 1994. Case study in building commissioning and savings verification applied to a 311,000 ft² office tower retrofit. *Proceedings from the ACEEE 1994 Summer Study on Energy Efficient Buildings*. Vol. 5, pp. 5.209-5.218, Washington, DC: American Council for an Energy Efficient Economy.

SAS Institute, Inc. 1989. SAS reference manual. SAS Institute, Inc., SAS Circle, P.O. Box 8000, Cary, NC, 27512-8000.

SAS Institute, Inc. 1990. SAS/STAT user's guide, version 6, 4th ed, Vol. 2. SAS Institute. Cary, NC.

- Schliesing, J.S. and D.B. Crawley. 1990. Effect of different versions of DOE-2 on building simulation results. *Proceedings from the ACEEE 1990 Summer Study on Energy Efficient Buildings*, Vol. 10, pp. 10.233-10.235, Washington, DC: American Council for an Energy Efficient Economy.
- Sparks, R., R. Chambers, R. Lopez and J. Haberl. 1992a. Documentation manual for TimeMerg version 1.1 β , Energy Systems Laboratory, Texas A&M University, College Station, TX.
- Sparks, R., J. Spadaro, K. Weber, R. Lopez and J. Haberl. 1992b. Documentation manual for Missing version 1.2 β , Energy Systems Laboratory, Texas A&M University, College Station, TX.
- Sparks, R., S. Katipamula, J. Spadaro, J. Mahoney and J. Haberl. 1993. Documentation manual Air, version 1.5 β , Energy Systems Laboratory, Texas A&M University, College Station, TX.
- Sparks, R., J. Mahoney, and J. Haberl. 1994. PolIC180, Version 1.3. Energy Systems Laboratory, Texas A&M University, College Station, TX.
- Subbarao, K., J. Burch, C.E. Hancock, A. Lekov, and J.D. Balcomb. 1990. Measuring the energy performance of buildings through short-term tests. *Proceedings from the ACEEE 1990 Summer Study on Energy Efficient Buildings*, Vol. 10, pp. 10.245-10.252, Washington, DC: American Council for an Energy Efficient Economy.
- Torres-Nunci, N. 1989. Simulation modeling energy consumption in the Zachry Engineering Center. Master's Project Report, Texas A&M University, College Station, TX.

- TMY. 1988. Typical meteorological year user's manual - TD-9734. National Climatic Data Center, Asheville, NC 28801-2696.
- Trane. 1992. Split system heat pumps. Technical Literature. The Trane Company. Clarksville, TN 37040.
- TRY. 1983. Test reference year (TRY) tape reference manual - TD-9706. National Climatic Data Center, Asheville, NC 28801-2696.
- Tukey, J.W. 1977. Exploratory data analysis. Addison-Wesley Publishing Co. Reading, MA.
- Turner, W., W. Heffington, D.L. O'Neal, D. Claridge, and J. Haberl. 1993. The monitoring and advisory review committee - Presentations. Energy Systems Laboratory Report no. ESL-TR-93/06-03. Texas A&M University, College Station, TX.
- USDOE. 1993. Printing and Graphics Division: Administrative Services of United States Department of Energy, Washington, DC.

VITA

Tarek Edmond Bou-Saada, son of Edmond and Renate Bou-Saada, graduated in 1985 from Alief Hastings High School in Houston, Texas. He received a Bachelor of Science degree in Mechanical Engineering from Texas A&M University in August of 1991. In January of 1992, he enrolled in the Master's degree program with the Mechanical Engineering department. While completing the program, he worked for the Energy Systems Laboratory as a Graduate Research Assistant with the DOE-2 building energy simulation program. His permanent address is 12211 Corona Ln., Houston, TX 77072.